Side chain decoration of Anthocyanins; Mechanisms and Effects On functionality

Kalyani Kallam

Department of Metabolic Biology

A thesis submitted to the University of East Anglia for the degree of Doctor of Philosophy

July 2012

ABSTRACT

Anthocyanins are plant pigments offering a range of colours to fruits and flowers. Many properties of anthocyanins are influenced by the degree and type of side chain modifications. Though much is known about the biosynthesis of anthocyanins and the enzymes involved in side-chain decoration, there is limited understanding of the structural features of anthocyanin acyltransferases that determine their substrate preference. Anthocyanin acyltransferases belong to the BAHD family of enzymes and are involved in acylation. Through mutagenesis I showed that an arginine positioned close to motif-1 in aliphatic anthocyanin acyltransferase determines the enzyme's specificity for malonyl transfer. Modification of arginine to phenylalanine in Ch3MAT, led to gain of acetylation property. This study thus suggests that CoA interacting residues are conserved in aliphatic acyltansferases. A phenylalanine in a similar position, close to motif 1 in aromatic anthocyanin acyltransferases is crucial for the specificity for aromatic-CoA of aromatic acyltransferases.

To understand the influence of different side-chain modifications on the formation of anthocyanic vacuolar inclusions (AVIs), I showed that coumaroylation of anthocyanins leads to AVI formation when high levels of anthocyanins are accumulating. Malonylation does not lead to the formation of AVIs, suggesting that the ability of aromatic moieties to form intra-molecular stacks can cause formation of AVIs. Neither the presence of flavonols nor light or high amounts of anthocyanins can lead to the formation of AVIs. Therefore, the type of decoration mainly aromatic acylation of anthocyanins is responsible for AVI formation.

From understanding the molecular mechanisms of acyltransferases for side chain decoration to their activity, anthocyanins can be engineered by anthocyanin acyltransferases in plants for novel functionalities. I showed that coumaroylation of anthocyanins promotes copigmentation more effectively than 5-glucosylation. 5-glucosylation, together with coumaroylation, offered stability to anthocyanins, both *in-vitro* and *in-vivo*. I also showed that flavonols copigment better than phenolics with anthocyanins, a property which could be useful for developing natural food colours. Thus, my study provided an in-depth investigation from molecular mechanisms to final applications of side chain decoration of anthocyanins.

ACKNOWLEDGEMENTS

I thank my supervisor Prof. Cathie Martin for all the scientific and moral support she had given me during the entire period. I am grateful for the opportunity she gave to work in her lab and for introducing me to a fascinating world of anthocyanins. My special thanks to Dr. David Lawson, my co-supervisor, for all the guidance and support he provided throughout the period. I am very thankful to my adviser, Dr. Stephen Bornemann for his constant support and advice. I also thank Prof. Mike Merrick for his moral support and for making me understand the importance of timekeeping.

My special thanks to Dr. Ghanasyam Rallapalli (teaching quantitative PCR analysis), Dr. Lionel Hill (teaching Mass spectrometry analysis), Ms. Baldeep Kular (teaching HPLC), Dr. Paul Needs (assisting in preparative HPLC), Dr. Shirley Fairhurst (NMR services), Ms. Kim Findley (for scanning and electron microscopy services), Dr. Clare Stevenson (teaching crystallization technique), Mr. Steve Mackay, Dr. Jie Luo and Dr. Eugenio Butelli for all the support and expertise training provided to me. I also thank many people belonging to several departments (graduate studies office, metabolite services, media kitchen, horticultural facilities and computing) at the JIC for providing excellent services.

My thanks to all the past and present members of Cathie's lab (Eugenio, Yang, Katharina, Prashanth, Qing, Daniel, Gabriel, Bulong, Anne), friends (Yamini, Kazuko, Rosalba, Ariane), yoga mates (Paola, Helen, Sarah, June) and many others in the institute (whom I have not named) for their companionship. I am grateful to my parents (Leela and Ch. Reddy), my foster parents (Basamma and Hussain Reddy) sisters and in-laws (Suni and Vijay, Anu and Satish), kids (Sohi and Sanu) and all the family members for their love, affection and support through the whole journey. I am indebted to my husband (Shyam) for all his support, love and care and without whom my life would have not been so amazing and peaceful.

A very special thanks to Plant cell support grant and Dorothy Hodgkin international student fellowship for supporting me with the funding.

TABLE OF CONTENTS

LIST OF FIGURES

LIST OF TABLES

GENERAL ABBREVIATIONS

A	absorbance
AAT	anthocyanin acyltransferase
ACN	acetonitrile
ANR	anthocyanidin reductase
ANS	anthocyanidin synthase
AOMT	anthocyanin methyltransferase
ATP	adenosine tri-phosphate
AVI	anthocyanic vacuolar inclusions
BAP	benzyl aminopurine
BCIP	5-bromo-4-chloro-3-indolyl phosphate
bHLH	basic-helix-loop-helix
bp	base pair
BSA	bovine serum albumin
4CL	4-hydroxy-cinnamoyl CoA ligase
C4H	cinnamate 4-hydroxylase
CAD	cinnamyl alcohol dehydrogenase
CaMV	cauliflower mosaic virus
CAT	chloramphenicol acetyltransferase
CCR	cinnamyl-CoA reductase
CHS	chalcone synthase
CHI	chalcone isomerase
cm	centimetre(s)
COMT	caffeic acid O-methyltransferase
COSY	homonuclear correlation spectroscopy
cDNA	complementary DNA
CoA	co-enzyme A
2,4D	2,4 –dichloro phenoxyacetic acid
dH_2O	distilled water
DPL	deep purple
DFR	dihydroflavonol reductase
DHK	dihydrokeampferol
DHM	dihydromyri cetin
DHQ	dihydroquercetin
DNA	deoxyribonucleic acid
dNTPs	deoxyribonucleotide triphosphates
DTT	dithiothreitol
E. coli	*Escherichia coli*
EDTA	ethylenediaminetetraacetic acid
F3H	flavone3-hydroxylase
F3'H	flavonoid 3'-hydroxylase
F3'5'H	flavonoid 3'5'-hydroxylase
FLS	flavonol synthase
FPLC	fast performance liquid chromatography
FVs	flavylium salts
GT	glucosyltransferase
g	gravitational acceleration
g	gram(s)
h	hour(s)
HMBC	heteronuclear multi-bond connectivity
HPLC	high performance liquid chromatography
HSQC	heteronuclear single quantum coherence
ICX1	increased chalcone synthase expression-1

kb	kilobase pair
kDa	kilo Dalton
H-NMR	proton-nuclear magnetic resonance
His	histidine
HQT	hydroxycinna-moyl CoA quinate transferase
L	litre(s)
LAR	leucoanthocyanidin reductase
LC	liquid chromatography
LDS	lithium dodecyl sulphate
LT	ligandin tranport
M	molar
MAT	malonyltransferase
MBP	maltose binding protein
MBW	Myb/bLHL/WDR40
MEOH	methanol
mg	milligram(s)
min	minute(s)
milliQ	millipore
mL	millilitre(s)
mm	millimetre(s)
mM	milli molar
MOPS	3-(N-morpholino) propanesulphonic acid
mPa	mega pascal
mRNA	messenger RNA
N	normality
NAA	1-naphthalene acetic acid
NBT	4-nitroblue tetrazolium chloride
ng	nanogram(s)
Ni-NTA	nickel nitrilo triacetic acid
NOESY	nuclear overhauser effect spectroscopy
nt	nucleotide(s)
ºC	degrees centigrade
OD	optical density
O/N	over night
oligo	oligonucleotide
PAGE	polyacrylamide gel electrophorosis
PAP	production of anthocyanin pigment
PCR	polymerase chain reaction
PDA	photo diode detector
PDB	protein data base
PEG	poly ethylene glycol
Pfu	*Pyrococcus furiosus*
PVP	polyvinylpyrrolidone
PHZ	purple haze
3RT	anthocyanidin-3-glucoside rhamnosyl transferase
RNA	ribonucleic acid
ROESY	rotational nuclear overhauser effect spectroscopy
rpm	rotations per minute
RT-PCR	reverse transcription-polymerase chain reaction
SAM	S-adenosyl L-methionine
SCPL	serine carboxy peptidase like
SDS	sodium dodecylsulphate
SDT	spermidine hydroxyl cinnamoyl transferase
s	second(s)
Taq	*Thermophilus acquarius*
TBE	tris-borate / EDTA

TE	tris / EDTA
TEV	tobacco etch virus
TOCSY	total correlation spectroscopy
Tris	2 amino-2-(hydroxymethyl)-l, 3-propanediol
U	enzyme unit
UDP	uridine diphosphate
UV	ultra violet light
V	volt(s)
vol	volume
VT	vesicular transport
v/v	volume per volume
WDR	tryptophan aspartic acid repeat
w/v	weight per volume
X-gal	5-bromo-4-chloro-3-indolyl-β-D-galactosidase
µ	micro, 10^{-6} meter
µg	microgram(s)
µl	micro litre(s)
µM	micro molar

“Live as if you were to die tomorrow
Learn asif you were to live forever”

Mahatma Gandhi

CHAPTER I

General Introduction

1.1 Introduction

Plants produce a large and diverse number of secondary metabolites which play unique roles in their interaction with the environment. Amongst secondary metabolites, flavonoids form a major group derived from the phenylpropanoid pathway, with at least 5000 naturally occurring compounds. Anthocyanins represent the most conspicuous and largest class of flavonoids mostly responsible for the orange to blue colours of flowers and other organs of plants (Strack and Wray, 1994). In flowers they are important in attracting pollinators as well as protecting plants from various biotic and abiotic stresses (Harborne and Williams, 2000). In addition to these attributes to plants, dietary consumption of anthocyanins has health promoting effects through the antioxidant activity, anti-inflammatory activity, anti-mutagenic activity and visual function-improving effects (Forkmann and Martens, 2001, Butelli et al., 2008).

The various properties of anthocyanins are attributed to several of their chemical modifications. This project's main focus was to understand some of the properties influencing their functionality. A brief account of the literature leading to an understanding of the anthocyanins in general is presented below with much detailed emphasis given in explaining acyltransferases and anthocyanic vacuolar inclusions.

1.2 Plant secondary metabolites

Plants produce numerous compounds in addition to those involved in their basic metabolism which are referred to as; secondary metabolites. These metabolites include compounds of four major groups; alkaloids, phenylpropanoids, terpenoids, and polyketides. Secondary metabolites are metabolites that are not directly involved in the normal growth, development, or reproduction of an organism. These metabolites play unique roles in interaction between plant and the environment. As a distinct class of molecules they have many properties: functioning as antifeedants, phytoanticipins, phytoalexins, signalling molecules, UV protectants (Li et al., 1993, Wajant et al., 1994, Kuc, 1995, Kliebenstein et al., 2005, Taylor and Grotewold, 2005). These compounds are produced by metabolic pathways often derived from primary metabolic routes [Fig 1.1] and much diversity is achieved by elaboration of the basic skeleton by modifying enzymes (Pichersky et al., 2006).

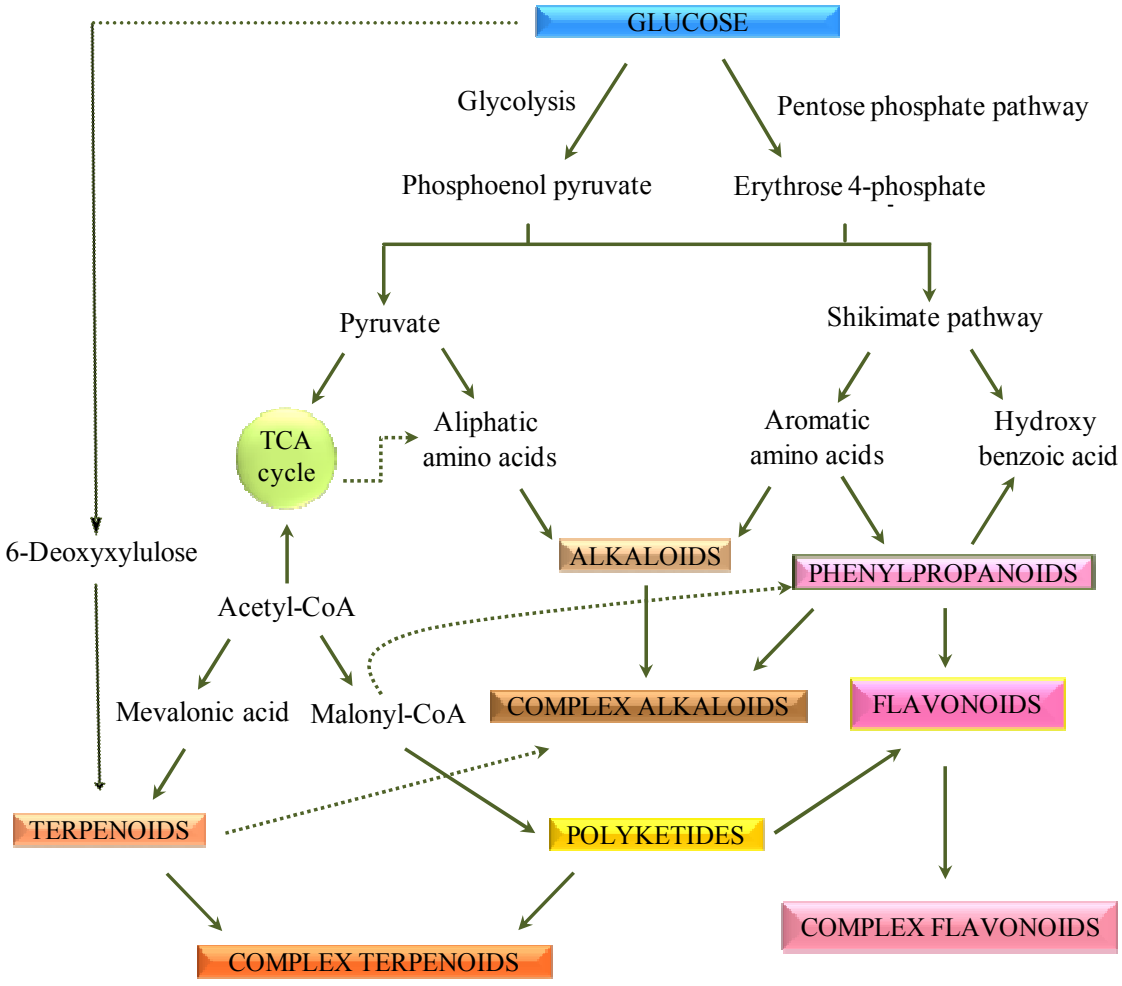

Figure 1.1 | Inter-relations between the four classes of plant secondary metabolites (alkaloids, terpenoids, polyketides and phenylpropanoids) derived from primary metabolic pathways (redrawn from Edwards and Gatehouse, 1999).

1.3 Phenylpropanoid pathway

Phenylpropanoid metabolism is based on phenylalanine, which is produced by the shikimate pathway (Herrmann, 1995). It generates an enormous array of secondary metabolites, the products of which are; flavonoids, coumarins, isoflavonoids, stilbenes, aurones, cutin, proanthocyanidins, lignins, phenylpropene, acylated polyamines and phenylpropanoid esters (Vogt, 2010). Phenylpropanoids are derived from an initial deamination of phenylalanine to provide a C6 + C3 scaffold. In most species the carbon flow from primary metabolism is redirected into entering two major downstream

pathways ie., monolignol and flavonoid biosynthesis by three steps catalysed by; phenylalanine ammonia-lyase (PAL), cinnamic acid 4-hydrozylase (C4H) and *p*-coumaroyl-CoA ligase (4CL) (Ferrer et al., 2008) [Fig 1.2]. A wide array of products is produced from these two major pathways by the action of enzymes, such as oxygenases, ligases, various transferases, and oxidoreductases. When plants are stressed and photosynthesis is limited, the products of the shikimate pathway may be redirected to the production of phenolic phytoalexins, flavonoids, (including anthocyanins), volatiles and de-novo synthesis of defence related polyphenols (Schoch et al., 2006, Abdulrazzak et al., 2006).

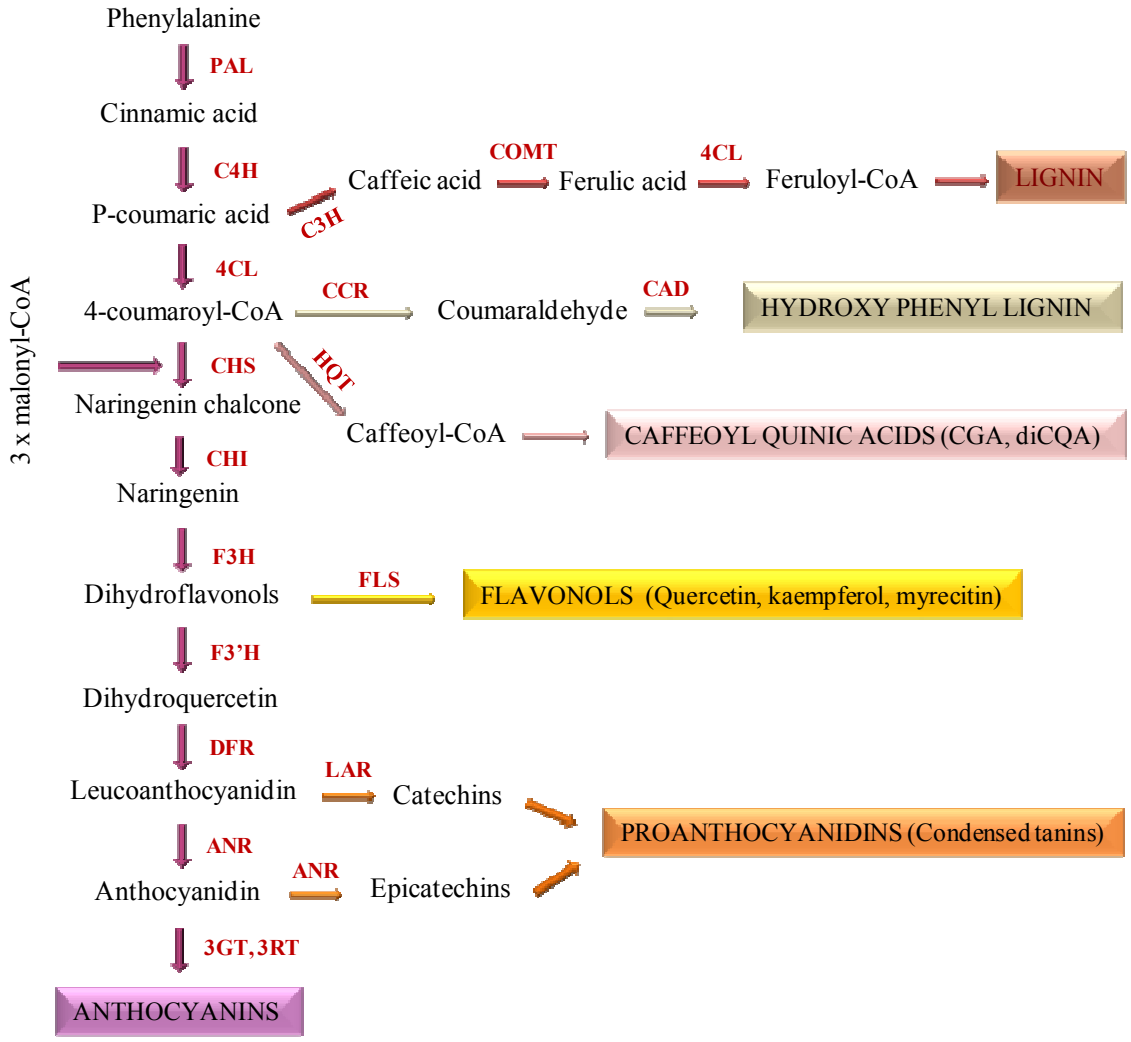

Figure 1.2 | General phenylpropanoid biosynthetic pathway in plants. The pathway was redrawn for depicting different metabolites; along with enzymes that catalyse the formation of metabolites (Deluc et al., 2006, Luo et al., 2008).

1.4 Anthocyanins

Anthocyanins form a major class of flavonoids and their name is derived from the Greek words *anthos* (flower) and *kyanos* (blue) since anthocyanin was first isolated from blue corn flower (Willstätter and Everest, 1913). These compounds exhibit a range of colours; orange, red, blue and purple as pigments in flowers and fruits (Strack and Wray, 1994, Harborne and Grayer, 1988). Production of these bright compounds is important in attracting pollinators and in protecting from various biotic and abiotic stresses (Harborne and Williams, 2000). They have the $C_6C_3C_6$ carbon skeleton typical of flavonoids [Fig 1.3] and the resonating structure of the flavylium ion allows them to absorb visible light strongly (Pauling, 1939). Anthocyanins are extremely diverse comprising more than 539 molecular species that have been identified within the plant kingdom (Andersen and Jordheim, 2006), synthesized from a pathway conserved among higher plants. Despite their diversity in nature, anthocyanidin aglycones are comprised of only six basic structures, namely pelargonidin, cyanidin, delphinidin, peonidin, petunidin, and malvidin (Strack et al., 1992) which differ by the hydroxylation and methoxylation pattern on B-rings. Chemical modifications to these basic structures are brought about by enzymes catalysing glycosylation, methylation and acylation reactions. Such modifications to anthocyanins, which differ in different species, alter significantly many of their properties such as light absorption, stability in solution, ability to interact with other molecules (co-pigmentation) and bioavailability in the diet (Tanaka and Brugliera, 2007).

1.4.1 Biosynthesis

The anthocyanin biosynthetic pathway has been studied extensively. Most of the enzymes (and their encoding genes) involved in the pathway have been characterised (Springob et al., 2003). Anthocyanin and flavonoid biosynthesis has been proposed to occur in the cytoplasm by the action of multi enzyme complex loosely associated with the rough endoplasmic reticulum (Hrazdina and Wagner, 1985), although robust evidence of the necessity of such a 'metabolon' is missing. The first step committed to the production of flavonoids involves synthesis of naringenin chalcone catalysed by chalcone synthase (CHS) which performs a sequential condensation and intramolecular cyclization of *p*-coumaroyl-CoA (from the general phenylpropanoid pathway) and three acetate units from malonyl-CoA. Naringenin chalcone is further cyclised by chalcone isomerase (CHI) to form naringenin; a flavanone. Naringenin, through the addition of a 3-hydroxyl group by flavonoid 3-*β*-hydroxylase (F3H), is converted to

dihydrokeampferol (DHK). Dihydrokeampferol is converted to dihydroquercetin (DHQ) by the addition of a hydroxyl group at 3'-position through the action of flavonoid 3'-hydroxylase (F3'H). Flavonoid 3' 5'-hydroxylase (F3'5'H) acts on DHK to form dihydromyricetin (DHM). The three colourless dihydroflavonols; DHK, DHQ and DHM are reduced to leucoanthocyanidins (leucopelargonidin, leucocyanidin and leucodelphinidin respectively) by dihydro flavonol 4-reductase (DFR) [Fig 1.3]. The type of anthocyanins formed in different plant species depends on the enzyme activities of p450 monooxygenases (F3'H and F3'5'H).

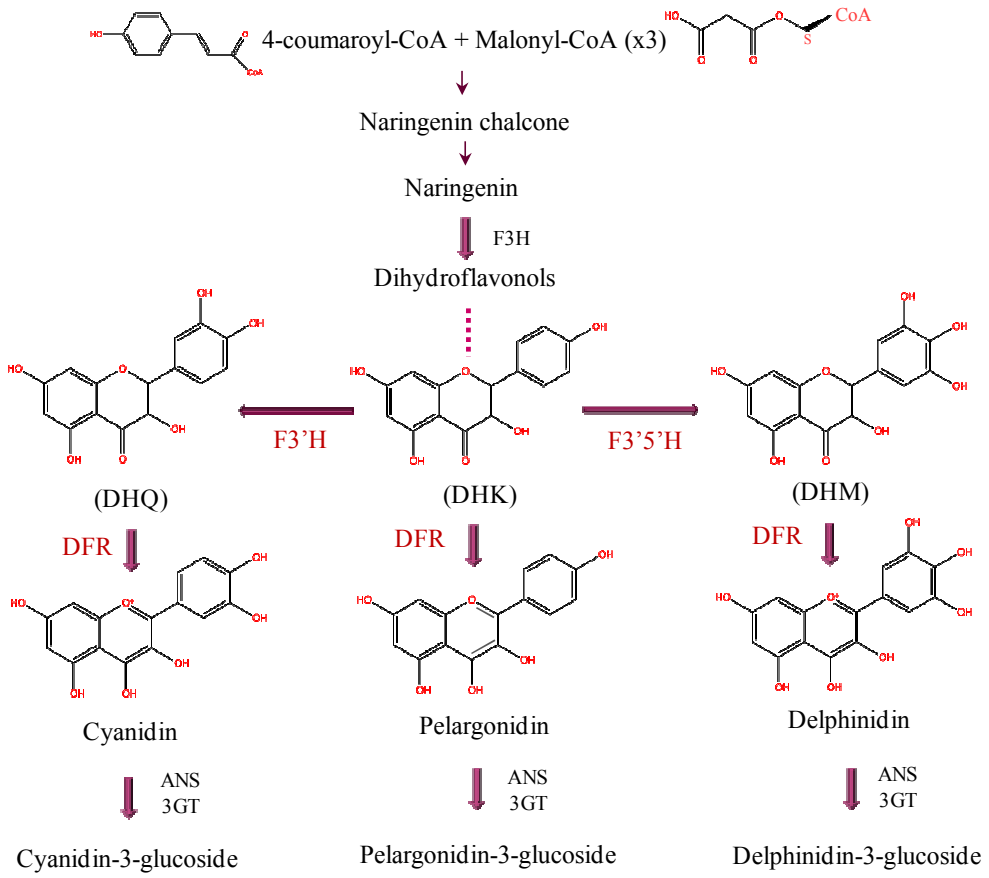

Figure 1.3 | Schematic diagram showing the chemical reaction catalyzed by p450 monooxygenases and DFR leading to formation of different anthocyanidins.

DFR competes for the dihydroflavonols with flavonol synthases (FLS; which synthesise flavonols) for formation of leucoanthocyanidins (Winkel-Shirley, 1999) [Fig 1.2]. cDNAs of DFR have been isolated and characterised from *Antirrhinum majus*, *Arabidopsis thaliana*, *Zea mays* and *Petunia hybrida* (Forkmann et al., 1999). DFRs often have broad substrate specificity but the DFRs from Solanaceous species do not

have the ability to use DHK as a substrate and hence pelargonidin-type anthocyanins cannot be produced in these species. The substrate specificity of DFR was shown to be determined by a single amino acid in petunia and gerbera (Johnson et al., 2001). Leucoanthocyanidins, which are formed by the activity of DFR, are colourless and are oxidised to coloured anthocyanidins by anthocyanidin synthase (ANS) (Schijlen et al., 2004). Based on the number and position of hydroxyl groups on the B-ring, anthocyanidins are; pelargonidin, cyanidin or delphinidin as determined by the activities of F3'H and F3'5'H (detailed explanation is given in section 1.4.4). Anthocyanidins are subsequently glycosylated on the 3-position of the C-ring to form anthocyanins, most often by UDP-glucose-flavonoid 3-*O*-glucosyltransferase. Glycosylation makes the anthocyanidins (aglycons) stable and targets anthocyanins for transport to the vacuole for storage. In the vacuole the C-3-glucosylated pseudobase is converted into coloured flavylium ion due to the acidic vacuolar environment.

1.4.2 Regulation of anthocyanin biosynthesis

The complex regulation of secondary metabolism in plants is dictated by a coordinate transcriptional control through specific transcription factors. Regulation of the phenylpropanoid pathway has been studied extensively both in monocots and dicots (Gray et al., 2012, Weisshaar and Jenkins, 1998). Transcription factors (TFs) are proteins that bind to a specific sequence of the promoter region of a target gene and interact to control transcriptional initiation of mRNA synthesis. TFs regulate the transcription either alone or in complexes with other proteins by activating or repressing the recruitment of RNA polymerase II to the core promoter region in the process of transcription. Regulation by TFs is both temporal and spatial, and is influenced by various internal and external stimuli. In many plant species regulation of anthocyanins is tissue specific, and anthocyanins are accumulated in fruits and flowers. Various studies have shown a co-ordinate regulation of anthocyanin biosynthetic genes in relation to developmental and environmental stimuli (Martin et al., 1991, Jackson et al., 1992).

Two distinct classes of TFs control the regulation of anthocyanin biosynthesis, MYB and basic-Helix-Loop-Helix (bHLH) proteins (also known as MYC proteins) (Mol et al., 1998). Later studies showed an involvement of a third protein, a tryptophan-aspartic acid repeat (WDR or WD 40) protein in regulating the flavonoid pathway along with the MYB/bHLH TFs (Baudry et al., 2004) by forming a Myb-bHLH-WDR (MBW) complex. MYB TFs contain single or multiple repeats of helix-turn-helix motifs which bind to DNA (the MYB domain). In plants, the largest family of MYB TFs contain two

repeats, similar to the R2 and R3 repeats of the prototypic protein from animals, c-Myb, which are responsible for binding to DNA (Martin and Paz-Ares, 1997). Specific R2R3 MYBs are involved in regulation of flavonoid pathway and in complex with bHLH proteins regulate the phenylpropanoid pathway (Vom Endt et al., 2002). Much of the earlier understanding on MYB/bHLH proteins as regulators of anthocyanin biosynthesis comes from studies in *Petunia hybrida*, *Antirrhinum majus* and *Zea mays* and more recently the role of these regulatory proteins has been studied in other plants including *Arabidopsis thaliana*, *Gentiana triflora* etc., (Dooner et al., 1991, Quattrocchio et al., 1998, Zimmermann et al., 2004, Nakatsuka et al., 2008, Jackson et al., 1991). Anthocyanin biosynthesis regulation in maize by COLORLESS1 (C1) (an R2R3 MYB protein) and RED (R) (a bHLH protein) is one of the best studied systems (Ludwig and Wessler, 1990, Mol et al., 1998). Subsequently, TFs having sequence homology to maize C1 and R transcription factors were studied in dicots. Two genes encoding bHLH proteins in *Antirrhinum majus* have been shown to be involved in flower pigmentation. These genes are known as *Delila* and *Mutabilis*, and are responsible for determining pigmentation in the tubes and lobes of the flowers, respectively (Goodrich et al., 1992, Almeida et al., 1989, Schwinn et al., 2006, C.Martin unpublished results). Three genes encoding R2R3 MYB proteins (Rosea1, Rosea2 and Venosa) are involved in controlling flower pigmentation in *A.majus* (Schwinn et al., 2006). A cDNA encoding a WD40 repeat (WDR) protein has also been identified from *A.majus* flowers (K. Schwinn unpublished results) and shown to function in the MBW complex (C. Martin, unpublished results). However, experiments in transgenic tobacco and tomato have shown that expression of only Rosea1 and Delila is required for ectopic anthocyanin production in unpigmented tissues (Butelli et al., 2008). The gene encoding the WDR protein has been reported to be expressed constitutively in plant tissues (Walker et al., 1999). Studies on Antirrhinum provided some evidence that the MBW complex preferentially activates the late biosynthetic genes (LBGs) of the anthocyanin biosynthetic pathway, with the division usually being from DFR (Petunia) or F3H (Antirrhinum) (Martin et al., 1991).

Pattern associated regulation in different floral organs had been studied in *Antirrhinum majus*, where Delila specifically pigments the corolla tube (Almeida et al., 1989) and Venosa (R2R3MYB) controls pigmentation specifically in the epidermal tissues of the flower overlying the veins to create visual nector guides (Schwinn et al., 2006, Shang et al., 2011). In Petunia, R2R3-MYB factors like AN2, AN4 (Quattrocchio

et al., 1998) control pigmentation in the petal limb and petal tube and anthers respectively. These MYB factors work together with AN1, a bHLH factor (Spelt et al., 2000) and AN11, a WDR protein (Vetten et al., 1997). R2R3 MYB TFs encoded by *DEEPPURPLE* (*DPL*) and *PURPLE HAZE* (*PHZ*) control environmentally-regulated anthocyanin production in vegetative tissues in Petunia (Albert et al., 2011). In several plant species ectopic expression of TFs correlates strongly with anthocyanin biosynthesis though, an overlap with other phenylpropanoid pathway were seen. A MYB factor production of anthocyanin pigment1 (PAP1) from Arabidopsis which enhances expression of flavonoid biosynthetic genes (Borevitz et al., 2000) when expressed in tobacco under constitutive regulation showed anthocyanin accumulation (Rowan et al., 2009). Transcription factors regulating anthocyanin and flavonoid biosynthesis have been widely studied in fruits like grapes, apples and strawberries (Matus et al., 2010, Espley et al., 2007).

1.4.2.1 Negative regulation of anthocyanin pathway

Transcription factors can not only activate but also repress anthocyanin biosynthesis and such factors are called repressors. Although not much is known about these factors some studies have shown that members of the R2R3 and R3-MYB families act as transcriptional repressors. *FaMYB1* from strawberry, which encodes a short R2R3 MYB-type protein in ripe fruits showed a considerable decrease in anthocyanin accumulation in floral parts when expressed in tobacco (Aharoni et al., 2001). A significant reduction in expression of late biosynthetic genes was also observed. AtMYBL2 is an R3-MYB factor in Arabidopsis and shows negative regulation of anthocyanin biosynthesis. AtMYBL2 is thought to be able to bind in the MBW complex competing with the R2R3 MYB proteins for interaction with the bHLH proteins. In displacing the R2R3 MYB proteins it reduces the activity of the MBW complex in inducing anthocyanin biosynthesis (Dubos et al., 2008, Matsui et al., 2008).

1.4.3 What controls the regulators?

It is widely known that the genes encoding TFs themselves are subject to temporal and spatial regulation. Various external (environment, light, abiotic and biotic stress etc.,) and internal stimuli (abundance of mRNA, post-translational modifications, hormones, metabolites themselves) are believed to control the expression of the regulatory genes (Vom Endt et al., 2002, Weisshaar and Jenkins, 1998). In maize, light was shown to control the expression of genes encoding Sn, C1 and P1 TFs, and so to control

anthocyanin biosynthesis in pericarp and aleurone of developing maize seeds (Procissi et al., 1997). In fruits like apple, grapes, peach, pear, strawberry, egg plant etc., sunlight influences anthocyanin production. In apple, light induces MdMYB1 which, in turn, regulates anthocyanin biosynthesis (Takos et al., 2006). High temperature reduces anthocyanin accumulation in apple fruit by repressing the regulation of MYB10 and low temperature treatment of such fruits induces the TF and hence anthocyanin accumulation (Lin-Wang et al., 2011). Sugars, particularly sucrose and maltose, have been shown to induce anthocyanin biosynthesis (Rolland et al., 2006, Teng et al., 2005, Solfanelli et al., 2006). Sucrose treatment reduces flavonol accumulation (Solfanelli et al., 2006) suggesting that external stimuli largely control the flux of metabolites. ICX1 (increased chalcone synthase expression 1) of Arabidopsis acts as a negative regulator of induction of CHS expression and anthocyanin accumulation in response to cryptochrome1, phytochrome A, ultraviolet (UV)-B, low temperature, sucrose, and cytokinin (Wade et al., 2003).

1.4.4 Chemical structure of anthocyanins

Anthocyanidins (2-(4'–hydroxyphenyl) - 3, 5, 7-trihydroxybenzopyrylium) consist of an aromatic ring (A), bonded to a heterocyclic ring (C) that contains oxygen which is bonded to an aromatic ring (B) by a carbon-carbon bond [Fig 1.4] (Konczak and Zhang, 2004). Anthocyanidins with a glucose attached at the 3-position of the C-ring are called anthocyanins. Based on the number and position of the OH-groups on the B-ring, anthocyanin type and colour varies. Anthocyanidins with a single hydroxyl group at the 4'-postion of B-ring are called pelargonidins, with two hydroxyl groups at the 3' and 4' positions on the B ring are called cyanidins and with three hydroxyls on the 3', 4', and 5' positions on the B-ring are called delphinidins [Fig 1.5]. Methylated forms of anthocyanidins such as peonidin, petunidin and malvidin also exist [Fig 1.4] (Strack et al., 1992). The non-methylated anthocyanidins: pelargonidin, cyanidin and delphinidin are the most common anthocyanidins and are found in 80% of pigmented leaves, 69% of fruits and 50% flowers. Cyanidin (50%) is the most widely present anthocyanidin among fruits and vegetables followed by pelargonidin, delphinidin and petunidin (12%) where as petunidin and malvidin contribute 7% (Dey and Harborne, 1993).

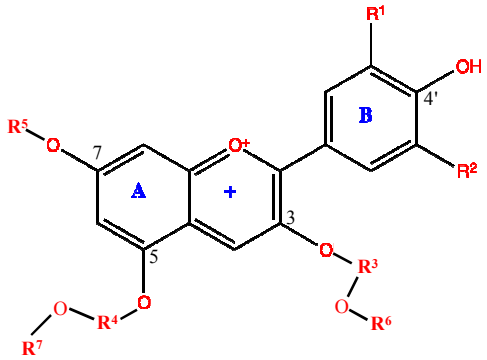

Anthocyanidin	R1	R2
Cyanidin	H	OH
Pelargonidin	H	H
Delphinidin	OH	OH
Malvidin	OCH3	OCH3
Peonidin	OCH3	H
Petunidin	OH	OCH3
Anthocyanin: R3, R4, R5- glucose/arabinose/galactose/ xylose/rhamnose		
R6, R7- coumaroyl/acetyl/malonyl/ caffeoyl etc		

Figure 1.4 | Chemical structure of anthocyanin molecule. Anthocyanins are mostly decorated with glucose at 3-position which offers stability to aglycone (anthocyanidin) in solution. Here the positions at which various decorations are present in nature are shown.

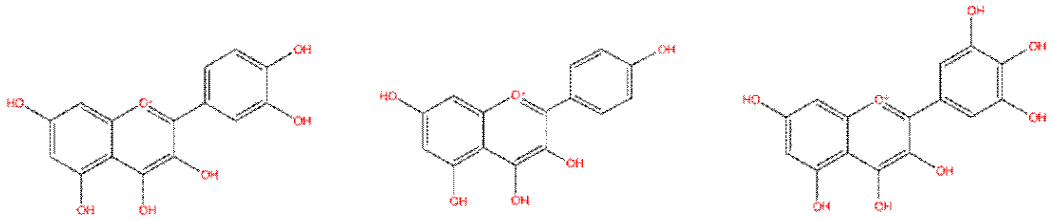

Cyanidin **Pelargonidin** **Delphinidin**

Figure 1.5 | Structures of the three major anthocyanidins. These are differentiated based on number of –OH groups on B-ring. Here cyanidin (pink), pelargonidin (red) and delphinidin (blue) coloured aglycones are shown.

1.4.5 Decoration of anthocyanins

In plants, the properties of anthocyanins, particularly their colour and stability are influenced heavily by chemical modifications of the basic anthocyanidin skeleton, which are brought about by enzymes catalysing glycosylation and methylation. Acylation is another important enzyme catalysing decoration which contributes to many properties of anthocyanin such as stability in solution and ability to interact with other molecules (co-pigmentation) (Tanaka and Brugliera, 2007).

1.4.5.1 Glycosylation

Among the modifications to the core anthocyanidin structure, glycosylation at the 3-OH position with one or multiple sugar residues is the most common. Anthocyanins are ubiquitiously glycosylated at the 3-position of the C ring. Additional modifications at 5, 3', 5', 7' and 7-*O*-position with glucose, galactose, xylose, glucuronic acid, rhamnose or arabinose occurs in various plant species [Fig 1.4]. A rare glycosylation at the C-8 position was reported for *Tricyrtis formosana* (Saito et al., 2003).

Addition of sugar residues to anthocyanins results in a modest hypsochromic shift (to blue) in the corresponding spectral maxima (Harborne, 1988). Glycosylation is also important for further decoration of anthocyanins with methyl, acyl and prenyl molecules. The chemical roles of glycosylation of secondary metabolites are believed to be: stabilisation, detoxification (reduced reactivity) and solubilisation (increased polarity) (Jones and Vogt, 2001). Lack of anthocyanin accumulation was observed in mutants lacking 3GT activity, even though the entire anthocyanin biosynthetic pathway is active (Boss et al., 1996, Tohge et al., 2005). This suggests the importance of glycosylation in anthocyanin accumulation. Glycosylation is also believed to be important for vacuolar transportation (Ono et al., 2006). Glycosylation at 5-*O*-positon is thought to be important in producing stable complexes for co-pigmentation.

1.4.5.1.1 Anthocyanin glycosyltransferases (GTs)

GTs involved in phenylpropanoid biosynthesis belongs to the UGT family of glucosyltransferases as they utilize UDP-sugars as donors. UGTs have broad anthocyanidin/anthocyanin specificity and the acceptor, to some extent, dictates the type of donor accepted. The GTs also have strict regio-specificity. The first glycosyltransferase gene was isolated from maize by transposon tagging (Hugo and Oliver, 1977). Since then many GTs which catalyse glycosylation have been isolated and characterised in different plant species, eg., *Gentiana triflora*, *Perilla frutescens*, *Vitis vinifera*, *Petunia hybrida* etc., using recombinant proteins (Tanaka et al., 1996, Ford et al., 1998, Yamazaki et al., 2002). cDNA of 5-GT was first characterised from pigmented leaves of *Perilla frutescens* (Yamazaki et al., 1999) and all 5-GTs require 3-glucosylated anthocyanins as substrates. Some GTs like 5-GT in perilla have a strict substrate specificity towards anthocyanidin 3-acylrutinoside (Yamazaki et al., 1999). A novel acyl-glucose dependant anthocyanins 5(7)-*O*-glycosyltransferase was isolated from the petals

of carnation and characterised recently (Matsuba et al., 2010). So far characterised UGTs show low, overall sequence similarity but share a conserved 'plant secondary product glycosyltrasferase' (PSPG) motif which is thought to provide a binding site for the nucleotide-diphosphate-sugar donor (Gachon et al., 2005).

1.4.5.2 Methylation

In nature only three kinds of anthocyanidin, petunidin, peonidin and malvidin are methylated although rarely 5-methylcyanidin and 5-methyldelphinidin are formed (Andersen and Jordheim, 2006). Methylation stabilizes the phenolic B ring, thus reducing the overall reactivity of anthocyanins (Sarni et al., 1995) and increases water solubility (Dangles et al., 1993). These properties causes a slight reddening effect (hyperchromic shift) thus increasing the colour properties. Methylation in plant secondary metabolites is due to S-adenosyl-L-methionine (SAM) dependent- *O*-methyltransferase.

1.4.5.2.1 Anthocyanin methyltransferases (AOMT)

Decoration of anthocyanins by methyltransferases has been studied mostly in petunia and grape. The first Anthocyanin Methyl Transferases (AOMTs) to be discovered were from petunia cDNA and the AOMTs localised in the cytosol (Jonsson et al., 1983). The genes encoding anthocyanin 3'-OMT and anthocyanin 3', 5'-OMT have been identified in petunia. In grape, peonidin and petunidin are mono-methylated and malvidin is di-methylated and recently two genes encoding AOMT and FAOMT have been discovered (Hugueney et al., 2009, Lucker et al., 2010). Methylation of anthocyanins in grape is strongly influenced by environment, cultural conditions and genetic factors (Downey et al., 2006, OllÉ et al., 2011). Like other modifications of anthocyanins methylation of anthocyanins is susceptible to transcriptional regulation and structural variation (Fournier-Level et al., 2011).

1.4.5.3 Acylation

Acylation is an important modification of anthocyanins which largely increases their stability and water solubility. Properties such as intramolecular and/or intermolecular stacking caused by acylation lead to increases in such properties. Acyl molecules are attached to glycosyl units, decorations catalyzed by acyltransferases (Springob et al., 2003) and in anthocyanins are brought about by anthocyanin acyltransferases (AATs).

Acylated forms of anthocyanins (modified anthocyanins) exist in many plant species (Harborne, 1986, Honda and Saito, 2002). There are two types of acyl substitutions of anthocyanins; aromatic and aliphatic, where both types of acyl group are linked to the hydroxyl group of a glycosyl moiety. Acylation with aromatic organic acids contribute to stacking of anthocyanins such as intramolecular stacking of the anthocyanins with polyphenols. This results in intensification of colour (Dangles et al., 1993), stability and blueing effect on anthocyanins (Goto and Kondo, 1991). A hypsochromic shift of anthocyanins is caused by decoration with aromatic acids (Goto et al., 1984). Aliphatic acylation enhances the pigment solubility in water (Heller and Forkmann, 1994), protects glycosides from enzymatic degradation (Suzuki et al., 2002), stabilises the anthocyanin structure (Saito et al., 1988, Suzuki et al., 2002) and uptake into vacuoles (Hopp and Seitz, 1987). Although acylation does not result in colour intensification, it enhances the stability of anthocyanin colouration (Suzuki et al., 2002). Acylation also prevents degradation of stored anthocyanins by glycosidases in the vacuole (Suzuki et al., 2002).

1.4.5.3.1 Anthocyanin acyltransferases (AATs)

The vast majority of AATs belong to a large family of acyltransferases which are acyl CoA-utilizing enzymes called BAHD acyltransferases so named after the first letter of each of the first four biochemically characterised BAHD enzymes, namely; benzylalcohol *O*-acetyltransferase (BEAT) from *Clarkia breweria*, deacetylvindoline 4-*O*-acetyltransferase (DAT) from *Catharanthus roseus*, *N*-hydroxycinnamoyl/benzoyltransferase (HCBT) from *Dianthus caryophyllus*, anthocyanin *O*-hydroxycinnamoyltransferase (AHCT) from *Gentiana triflora* (D'Auria, 2006). With the completion of genome sequencing of Arabidopsis and rice it was revealed that there are at least 64 BAHD genes in Arabidopsis encoding members of the BAHD family and *Oryza sativa* has at least 119 BAHD members (D'Auria, 2006). Studies with some of these BAHD acyltransferases showed their capacity to acylate a wide variety of substrates. All BAHD members share approximately 25-34% sequence identity with two distinct conserved domains and one which is exclusive for AATs.

Anthocyanin aromatic acyltransferase activity was first identified in *Silene dioica*; an enzyme that catalyses the acylation of the 3-*O*-rhamnosyl group of anthocyanindin 3-*O*-rutinoside (Kamsteeg et al., 1980).

Table 1.1 | Anthocyanin acyltransferases identified and characterised so far (Nakayama et al., 2003).

Source	Enzyme	Reference/s
Aliphatic acyltransferases		
***Callistepus chinensis* flowers**	Malonyl-CoA:anthocyanidin 3-*O*-glucoside malonyltransferase	(Teusch and Forkmann, 1987)
***Zinnia elegans* folwers**	Acetyl-CoA: anthocyanidin 3-*O*-glucoside acetyltransferase	(Ino and Yamaguchi, 1993)
***Centaurea cyanus* flowers**	Succinyl-CoA:anthocyanidin 3-*O*-glucoside succinyltransferase	(Yamaguchi et al., 1995)
***Dendranthema morifolium* flower buds**	Malonyl-CoA:anthocyanidin 3-*O*-glucoside malonyltransferase	(Ino et al., 1993)
***Lactuca sativa* leaves**	Malonyl-CoA:anthocyanidin 3-*O*-glucoside malonyltransferase	(Yamaguchi et al., 1996)
***Ajuga reptans* cell cultures**	Malonyl-CoA:anthocyanin malonyltransferase	(Callebaut et al., 1996)
***Salvia splendens* flowers**	Malonyl-CoA:anthocyanin 5-*O*-glucoside 6‴-*O*-malonyltransferase	(Suzuki et al., 2001)
***Salvia splendens* flowers**	Malonyl-CoA:anthocyanin 5-*O*-glucoside 4‴-*O*-malonyltransferase	(Suzuki et al., 2004a)
***Dahlia variabilis* flowers**	Malonyl-CoA:anthocyanidin 3-*O*-glucoside 6‴-*O*- malonyltransferase	(Yamaguchi et al., 1999 , Suzuki et al., 2002)
***Senecio cruentus* flowers**	Malonyl-CoA:anthocyanidin 3-*O*-glucoside 6″-*O*-malonyltransferase	(Suzuki et al., 2003b)
***Perilla frutescens* leaves**	Malonyl-CoA:anthocyanin 5-*O*-glucoside 6‴-*O*-malonyltransferase	GenBank: AF405204.1 (Suzuki et al., 2001)
***Arabidopsis thaliana* leaves**	Malonyl-CoA:anthocyanin 5-*O*-glucoside malonyltransferase	(Luo et al., 2007)
Aromatic acyltransferases		
***Silene dioica* flowers**	Hydroxycinnamoyl-CoA:anthocyanidin 3-*O*-rhamnosyl(1-6) glucoside hydroxycinnamoyltransferase	(Kamsteeg et al., 1980)
***Matthiola incana* flowers**	Hydroxycinnamoyl-CoA:anthocyanidin 3-*O*-glucoside hydroxycinnamoyltransferase	(Teusch et al., 1987)
***Ajuga reptans* cell cultures**	Hydroxycinnamoyl-CoA:anthocyanin hydroxycinnamoyltransferase	(Callebaut et al., 1996)
***Gentiana triflora* flowers**	Hydroxycinnamoyl-CoA:anthocyanidin 3,5-*O*-diglucoside 6‴-*O*-hydroxycinnamoyltransferase	(Fujiwara et al., 1997)
***Perilla frutescens* leaves**	Hydroxycinnamoyl-CoA:anthocyanin 3-*O*-glucoside 6‴-*O*-hydroxycinnamoyltransferase	(Yonekura-Sakakibara et al., 2000)
***Arabidopsis thaliana* leaves**	Hydroxycinnamoyl-CoA:anthocyanin 3-*O*-glucoside 6‴-*O*-coumaroyl transferase	(Luo et al., 2007)
***Solanum lycopersicum* fruit**	Anthocyanidin 3-*O*-rahmnosyl 6″-*O*-coumaroyl transferase	GenBank: EU979541.1 (Butelli et al., 2008)

Subsequently, many anthocyanin acyltransferases with different acyl-donor specificities, acyl acceptor specificities and regio-specificities for acyl transfer have been identified [Table 1.1]. To date only four aromatic acyltransferases, Gt5AT from *Gentiana triflora* (Fujiwara et al., 1998), Pf3AT from *Perilla frutesence* (Yonekura-Sakakibara et al., 2000) and two from Arabidopsis At3ATs (Luo et al., 2007) and seven aliphatic acyltransferases have been cloned, sequenced and characterised biochemically [Table 1.2].

Table 1.2 | Anthocyanin acyltransferases biochemically characterised so far.

Species of origin	Enzyme	Short name	References/s
Aromatic anthocyanin acyltransferases			
***Gentiana triflora* flowers**	Hydroxycinnamoyl-CoA:anthocyanidin 3,5-*O*-diglucoside 6‴-*O*-hydroxycinnamoyltransferase	Gt5AT	(Fujiwara et al., 1998)
***Perilla frutescens* leaves**	Hydroxycinnamoyl-CoA:anthocyanin 3-*O*-glucoside 6‴-*O*-hydroxycinnamoyltransferase	Pf3AT	(Yonekura-Sakakibara et al., 2000)
***Arabidopsis thaliana* leaves**	Hydroxycinnamoyl-CoA:anthocyanin 3-*O*-glucoside 6‴-*O*-coumaroyl transferase	At3AT	(Luo et al., 2007)
Aliphatic anthocyanin acyltransferases			
***Salvia splendens* flowers**	Malonyl-CoA:anthocyanin 5-*O*-glucoside 6‴-*O*- malonyltransferase	Ss5MaT1	(Suzuki et al., 2001)
***Salvia splendens* flowers**	Malonyl-CoA:anthocyanin 5-*O*-glucoside 4‴-*O*- malonyltransferase	Ss5MaT2	(Suzuki et al., 2004b)
***Dahlia variabilis* flowers**	Malonyl-CoA:anthocyanidin 3-*O*-glucoside 6‴-*O*- malonyltransferase	Dv3MaT	(Suzuki et al., 2002)
***Senecio cruentus* flowers**	Malonyl-CoA:anthocyanidin 3-*O*-glucoside 6″-*O*- malonyltransferase	Sc3MaT	(Suzuki et al., 2003b)
Dendranthema* x *morifolium	Malonyl-CoA:anthocyanin 5-*O*-glucoside 6‴-*O*- malonyltransferase	Dm3MaT1	(Suzuki et al., 2004b)
Dendranthema* x *morifolium	Malonyl-CoA:anthocyanin 5-*O*-glucoside 6‴-*O*- malonyltransferase	Dm3MaT2	(Suzuki et al., 2004b)
***Arabidopsis thaliana* leaves**	Malonyl-CoA:anthocyanin 5-*0*-glucoside malonyltransferase	At5MaT	(D'Auria et al., 2007 , Luo et al., 2007)

1.4.5.3.2 Versatility of anthocyanin acyltransferases

Aliphatic and aromatic AATs have clear acyl donor specificities. Generally, aromatic acyltransferases do not act on aliphatic acyl CoAs such as malonyl CoA and aliphatic acyltransferases cannot act on aromatic CoAs such as coumaroyl-CoA and caffeoyl CoA as donors (Nakayama et al., 2003). AATs also have strict regiospecificity for the position of acylation of anthocyanins. For example, in the biosynthesis of Salvionin, three AATs are involved; two distinct malonyl transferases, called Ss5MaT1 and Ss5MaT2, transfer two malonyl groups to the 4‴ and 6‴ positions respectively and one 3-aromatic acyl transferase catalyses 6‴-*O*-caffeoylation (Suzuki et al., 2003a).

AATs generally have broad acyl acceptor specificities. The number of B-ring hydroxyls present on the anthocyanin substrate does not affect their reactivity to anthocyanin acyltransferases. They can act equally on pelargonidin, cyanidin and delphinidin. An AAT from a particular plant species can sometimes have the capability of catalyzing acylation of different anthocyanins. In a few AATs like Ss5MaT1 from *Salvia splendens,* acylation is specific for a particular position on the glucose molecule. Ss5MaT1 can act on anthocyanidin 3-*O*-(6-*O*-hydroxycinnamylglucoside) -5-*O*-glucosides but not on anthocyanidin 3, 5-*O*-diglucosides or anthocyanidin 3-*O*-(6-*O*-malonylglucoside)-5-*O*glucosides (Suzuki et al., 2001). In contrast to this, AAT activity from *Ajuja reptans* cell cultures shows relatively broad acyl acceptor specificities with respect to glycosylation and acylation of substrates (Callebaut et al., 1996). In these cell cultures, hydroxycinnamoyl CoA transferase transfers a *p*-coumaroyl group to anthocyanidin 3-*O*-sophorosides, anthocyanidin 3, 5-*O*-diglucosides and 3-*O*-sophoroside-5-*O*-sophoroside. It has been suggested that the broad acyl acceptor specificity of AAT might have led to the existence of polyacylated anthocyanins which are present in 'heavenly blue' anthocyanins in morning glory (Honda and Saito, 2002). Alternatively, multiple acylation may be due to a series of distinct AAT activities. With the existence of a variety of acylated anthocyanins in nature, it is likely that there must be many different AATs with different specificities, but most of these enzymes are yet to be isolated and characterised.

In biosynthesis of plant metabolism an alternate pathway of ester formation was evolved using 1-*O*-β-glucose esters as acyl-donors instead of coenzymeA thioesteres by serine carboxypeptidase-like (SCPL) acyltransferases. These SCPL acyltransferases belong to a divergent α/β class of hydrolases which, during the course of evolution lost their hydrolysis function and gained acylation (Milkowski and Strack, 2004). In

Arabidopsis a sinapoyl group is added on to anthocyanin sinapoyl-Glu:anthocyanin acyltranferase (SAT) which is a serine carboxypeptidase like enzyme (SCPL) (Fraser et al., 2007).

With respect to secondary metabolites, the gain or loss of genes specifying the production of specific compounds is a continuing process as such compounds play unique roles in the plant's interaction with their environment. Phylogenetic analysis of the AATs reveals evolution of substrate specificity within the BAHD family. AATs share their evolutionary relation with other acyltransferases involved in modification of phenolic glucosides, alkoloids etc. Anthocyanin hydroxyl-cinnamoyl transferase from Gentiana, Gt5AT; Pf3AT from Perilla and other malonyl transferases from chrysanthemum and dahlia are closely related to NtMAT1 from tobacco which is involved in decorating malonylated napthol and flavonoid glucosides (D'Auria, 2006). Similarly, in a recent study it was shown that spermidine hydroxycinnamoyl transferases SDT and SCT from Arabidopsis are closely related to the acyltransferases from yew (Taxus spp) involved in taxol synthesis (Luo et al., 2009). The versatility observed with the AATs and other BAHD members may represent an important mechanism whereby diversity in plant secondary metabolism is achieved relatively rapidly during the evolution of species. This versatility makes it difficult to predict function based on primary sequence alone. Enzymes accumulate neutral changes in their sequences over time in addition to incorporating amino acid substitutions that alter their substrate specificities and mode of action and which may lead to changes in their function. Hence sequence comparisons of related extant enzymes involved in secondary metabolite production alone cannot address these questions directly. Therefore, an integrated approach, including metabolite profiling, expression data and structural studies can help predict substrate specificities of BAHD acyltransferases.

1.4.5.3.3 Proposed catalysis of anthocyanin acyltransferases

In most enzymes changes to the active site and binding sites and other functionally important domains that result in altered specificities are not well defined (Wang and Pichersky, 1999). Although BAHD enzymes share only 20-40% sequence similarity between members of the family, they have three important conserved motifs. The first motif His-Xaa3-Asp (H*XXX*D) is located near the central portion of each enzyme. Motif 3, Asp-Phe-Gly-Try-Gly (DFGWG), is located near the carboxy terminus. Motif 1 is conserved in all functionally characterised enzymes of this family. Motif 3 is not so highly conserved in BAHD acyltransferases from monocots (Burhenne et al., 2003).

Motif 2, Tyr-Phe-Gly-Asn-Cys (YFGNC), is conserved in only a few acyltransferases (Nakayama et al., 2003). Site-directed mutagenesis experiments performed on vinorine synthase, an acetyltransferase from the plant *Rauvolfia serpentina* and an anthocyanin malonyl transferase from chrysanthemum have shown that deletions or modifications of amino acids of one or both motifs 1 and 2 result in highly reduced enzyme activities (Suzuki et al., 2003a, Bayer et al., 2004). The histidine residue of motif 1 like sequence (which resembles a motif found in chloramphenicol acetyltransferase [CAT]) is thought to be involved in general acid/base catalysis of acyl transfer (Shaw and Leslie, 1991). When the structure of a BAHD acyl transferaser, vinorine synthase, was first reported, a breakthrough was made in understanding the catalytic mechanism and the importance of these shared motifs to functionality (Ma et al., 2005). The crystal structure of vinorine synthase showed that the active site is located in the solvent channel that runs between the two domains of the globular protein and that the catalytic histidine residue is available from both sides of the channel. With the recently solved crystal structure of anthocyanin malonyl transferase it was shown that the histidine residue of motif 1 is involved in general acid base catalysis and that the channel forms the active site of the enzyme (Unno et al., 2007) [Fig 1.6]. However, alanine scanning mutation studies in malonlytransferease showed histidine role of H*XXX*D motif is not indispensable in catalysis as it can be complemented (Suzuki et al., 2004a). From studies on vinorine synthase and the anthocyanin malonyl transferase it was also shown that the Asp residue of motif 3 is too far from the active site to be involved directly in catalysis. This suggested that this conserved motif is of structural importance rather than of importance in catalysis, contradicting earlier claims.

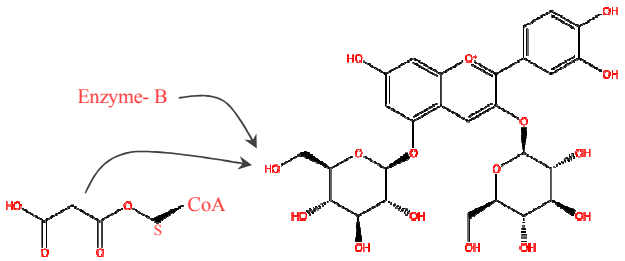

Figure 1.6 | Proposed catalytic mechanism of anthocyanin acyltransferases. Activity of malonyl –CoA anthocyanin acyltransferase from *Salvia splendens* (Ss5MaT1) represented as enzyme-B is shown [redrawn from (Suzuki et al., 2003a)].

1.4.6 Anthocyanin transport

Anthocyanins are thought to be synthesised on the cytosolic side of the rough endoplasmic reticulum where the enzymes may be organised into a multi-enzyme complex called a metabolon. All the enzymes in the multi-enzyme complex thought to be associated with the ER-associated cytochrome P450 enzymes: cinnamate-4-hydrozylase, F3'H and F3'5'H (Winkel, 2004, Jorgensen et al., 2005). However, an exception to the co-localization of anthocyanin biosynthetic enzymes involves serine carboxylpeptidase-like anthocyanin acyltransferases, which are localized in the vacuole (Hause et al., 2002). Anthocyanins are stored in vacuoles and this is obvious under microscope for visibly bright coloured anthocyanins (Winkel-Shirley, 2001) [Fig 1.7] Storage of anthocyanins is necessary to prevent oxidation (Marrs et al., 1995) and to function as coloured plant pigments. Though anthocyanins and in general flavonoid biosynthesis and regulation are well studied, little is understood about the transport mechanisms of these compounds.

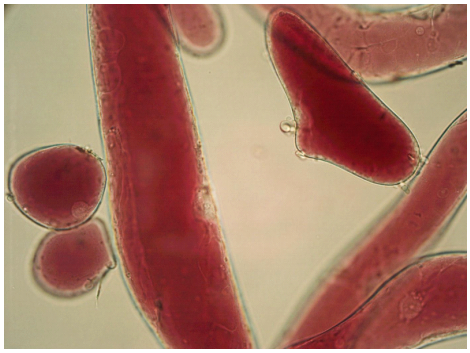

Figure 1.7 | Anthocyanin accumulation in vacuole of a cell. Tobacco callus over-expressing Delila and Rosea1 and accumulating anthocyanins in the vacuole which occupies most of the cell is shown.

1.4.6.1 Trafficking of anthocyanins

Several models have been proposed for the transport of anthocyanins although molecular proof is needed for a robust understanding of the process. Two hypotheses have been proposed for anthocyanin (in general flavonoid) transport; membrane vesicle-mediated, vesicular transport (VT) and membrane transporter-mediated transport, also called ligandin transport (LT) (Kitamura, 2006, Grotewold and Davies, 2008, Zhao and Dixon, 2009).

The concept of vesicle mediated transportation was initially drawn from the observations of anthocyanoplasts, which are thought to be sites of anthocyanin biosynthesis (Pecket and Small, 1980). Storage involves fusion of small vesicles filled with anthocyanins to form large membrane bounded bodies. Zhang et al., (2006) suggested that anthocyanin-containing prevacuolar compartments (PVCs) derived from endoplasmic reticulum, form intracellular vesicles during the sequestration of anthocyanins to the central vacuole. Poustka et al., (2007) proposed that anthocyanin-containing vesicle-like structures can co-localize with protein storage vacuoles (PSVs) and anthocyanins are transported by the trans-Golgi network (TGN)-independent ER-PVC vesicle mediated pathway. However, it is unclear how the anthocyanin containing vesicles are imported into vacuoles. Prevacuole-like vesicle structures were initially studied in the proanthocyanidin (PA) transport pathway where vesicles filled with PAs fuse with the central vacuole (Abrahams et al., 2002). In a similar way, involvement of autophagy was proposed, where the anthocyanin containing ER-derived vesicles might be taken up by vacuoles (Pourcel et al., 2010). Evidence for the role of autophagy mechanisms comes from the studies of Arabidopsis proteins required for autophagy in cellular processes (Bassham, 2007).

The idea of membrane transporter mediated transport of anthocyanins was based on observations in some species with mutations in glutathione *S*-transferase (GST) genes associated with anthocyanin transport, such as *bz2* in maize (Marrs et al., 1995), *tt19* in Arabidopsis (Kitamura et al., 2004) and *an9* in petunia (Mueller et al., 2000). These mutations block vacuolar localization of anthocyanins. A multidrug resistance-associated protein (MRP)-type ABC transporter was able to transport glutathione conjugates into vacuoles (Marrs et al., 1995) and based on such studies GS-X pump type ABC transporter-mediated vacuolar sequestration was proposed. Biochemical studies showed a requirement for the GST protein alone rather than its enzymatic activity for anthocyanin transportation (Alfenito et al., 1998). Mueller et al., (2000) suggested that GSTs serve as ligandins for escorting anthocyanins such as cyanidin 3-*O*-glucoside from the ER to the tonoplast. Transporters located on the tonoplast then recognise the GST-anthocyanin complex and pump anthocyanins into the vacuole. An ATP binding cassette (ABC) transporter involved in anthocyanin transport was first studied in maize where suppression of ZmMRP3 resulted in reduced anthocyanin accumulation (Goodman et al., 2004). A MATE transporter from Arabidopsis, TT12 located on the tonoplast was shown to transport cyanidin 3-*O*-glucoside to the vacuole (Marinova et al., 2007). Gomez et al.,

(2009) characterised two MATE-type transporters; AM1 and AM3 in grape and studied their involvement in transporting acylated anthocyanins. They showed localization of AM1 and AM3 on the tonoplast and membrane vesicles attached to the nucleus. However, in vitro studies were able to demonstrate the transport of acylated anthocyanins only, by AM1 (Gomez et al., 2009). A recent study showed the involvement of a GST, TT19, in Arabidopsis in transporting anthocyanins from the cytosol to the tonoplast (Sun et al., 2011). Complementation studies of a GST-like gene upregulated in red seeds in maize mutant *bz2* suggested the role of GST-associated transporters in anthocyanin transport in maize (Conn et al., 2010). Further evidence of the role of transporters comes from ectopic expression of *MYBA1* along with overexpression of *GST* and *AM3* genes in grapevine hairy roots where vacuolar storage of anthocyanins was observed (Cutanda-Perez et al., 2009).

A recent study in grapevine established the involvement of vesicle mediated trafficking and the contribution of GST, with AM1/AM3 (anthoMATE) transporters in anthocyanin transport in grape (Gomez et al., 2009). In these studies, subcellular localization assays revealed association of anthoMATE tranporters with small vesicles and GST localization in cytoplasm around the nucleus suggesting an association with the ER. Abolishing anthoMATE activity in hairy roots correlated with absence of small vesicles whereas by abolishing the specific activity of the GST, anthocyanins accumulated in vesicles but not in the vacuole (Gomez et al., 2011). Such studies demonstrate the complexity of anthocyanin transport.

1.4.6.2 Anthocyanic vacuolar inclusions (AVIs)

Anthocyanins transported to the vacuole are usually soluble, but in a significant number of plants they are accumulated as discrete sub-vacuolar structures which have been referred to by several different names (Grotewold and Davies, 2008). Plants accumulating red, blue and purple anthocyanins as amorphous structures, in contrast to their normal soluble form, in vacuoles were observed as early as 1905 (Molish, 1905). In some plant species, anthocyanins associate in the cells into globular bodies known as anthocyanic vacuolar inclusions (AVIs). AVIs have been observed in petal cells of carnation (*Dianthus caryophyllus*) and lisianthus (*Eustoma grandiflorum*), grape vine, sweet potato (*Ipomea batatas*) and maize. Under the microscope these appear as localised concentrations of anthocyanins within vacuoles.

Diverse forms of anthocyanin accumulation have been observed in plant cells, including: evenly coloured solutions, vesicle-like, membrane-bound bodies and dense, compact bodies of either regular or irregular shape. Some of the membrane bound bodies enriched in anthocyanins were originally suggested as sites of anthocyanin synthesis, and called anthocyanoplasts (Pecket and Small, 1980). Anthocyanoplasts were later reported in red radish and prunus callus as cytoplasmic membranous vesicles packed with anthocyanin pigments, which fuse to form large anthocyanin-containing bodies (Nozzolillo and Ishikura, 1988). Anthocyanoplasts were reported in over 70 species in 33 families of angiosperms (Pecket and Small, 1980). However, despite being studied for more than a century, little understanding of these structures has been achieved. This has been due partly to the complexity of anthocyanin transport which may give rise to localised concentrations of anthocyanins (usually membrane-bound) which can be confused with AVIs. Recent studies have distinguished the classic, intensely coloured, intravacuolar bodies observed in the cells of highly coloured tissues 'Anthocyanic Vacuolar Inclusions; AVIs', from more globular, membrane-bound 'anthocyanoplasts' which probably represent intermediate stages of transport of anthocyanins to the vacuole (Markham et al., 2000).

Chemically AVIs are composed of selected anthocyanins (but not flavonols or other polyphenols) possibly in association with specific proteins or lipids. AVIs were reported to be associated with a 24 kDa protein (VP24; vacuolar protein 24) in sweet potato cultured cells where this protein was localized to vacuoles and anthocyanoplasts (Nozue et al., 1997). AVIs may result from an extreme form of intermolecular stacking, either through self association or through interaction with other molecules. So far, about 50 plant species have been reported to produce AVIs and they represent the most stable form of anthocyanins (Conn et al., 2010). Formation of AVIs may be dependent on acylation of anthocyanins, particularly coumaroylation (Conn et al., 2003, Mizuno et al., 2006). In some species the recruitment of anthocyanins into AVIs has been reported to be influenced heavily by the degree of glycosylation of the anthocyanins (Markham et al., 2000). In most species the level of production of anthocyanins appears to be a parameter closely associated with the formation of AVIs (Gonnet, 2003).

1.4.7 *In-vivo* properties of anthocyanins

Anthocyanins, unlike most secondary metabolites, exhibit variable responses to the environment in which they are present, pH of the medium, presence and interaction with

other metabolites etc. These interactions impact pigmentation conferred by anthocyanins. Hence, a vast range of colours are derived from relatively few anthocyanidins.

1.4.7.1 Associated with structure

The substitution patterns of anthocyanidins themselves contribute to the colours of the compounds (explained in section 1.4.4.1). Anthocyanidins are seldom seen in nature due to their unstability, proving that addition of sugars to anthocyanins particularly a glucose at 3-OH position increases their stability. Glycosylation also increases the solubility of anthocyanins (Timberlake and Bridle, 1966). Acylation of anthocyanins increases their stability and solubility. Acylation was also shown to be important in the uptake of anthocyanins into vacuoles (Hopp and Seitz, 1987). Aromatic acylation particularly confers stability to pigmentation due to intramolecular staking facilitated by the acyl moieties. Aromatic moieties fold over and interact with the planar pyrylium core of the anthocyanidin and protect the 2 and 4 positions of the chromophore from nucleophilic water attack (Kurtin and Song, 1968). The stability of the flavylium ion is supported by various decorations of the anthocyanins. The concentration of the pigment present can also alter the colouration (Timberlake and Bridle, 1975).

1.4.7.2 pH regulation of anthocyanins

As early as in 1913, Willstatter made a striking observation that the same pigment can give rise to different colours and attributed this to variation of pH in the flower (Willstätter and Everest, 1913). Both genetical and environmental factors are involved in the control of vacuolar pH. Vacuolar pH is generally regulated by vacuolar ATPases and pyrophosphatases. A few regulators of pH have been identified and PH4, a R2R3 MYB factor from Petunia has been shown to regulate acidification of vacuolar pH along with bHLH TFs (Quattrocchio et al., 2006). The *PH5* gene of Petunia encodes an H^+ P-ATPase proton pump which has been shown to regulate vacuolar pH and thus colour (Verweij et al., 2008). Anthocyanin changes its colour in a manner similar to litmus. The colour of anthocyanin is red at pH <3 which is due to various transformations of the flavylium cationic form in aqueous media. On raising the pH, the flavylium cation (AH^+) either deprotonates to give blue or purple quinonoid base (A), or deprotonates and hydrates to give colourless hemiacetals (Brouillard and Dubois, 1977, Dangles et al., 1993). Thus the AH^+ acts as a centre for the change of anthocyanin colour. The polyacylated AH^+ with aromatic acids do not show immediate colour loss at pH>5 (Kondo et al., 1990) and exhibits more stability than non-acylated anthocyanins.

1.4.7.3 Co-pigmentation

In weakly acidic conditions such as those in the plant vacuole, anthocyanins theoretically should exhibit weak colours but often bright colours are seen due to the interaction of anthocyanins with co-pigments (Brouillard, 1982). Co-pigments are colourless compounds such as flavonoids, alkaloids, amino acids, organic acids, polysaccharides, metals and anthocyanins themselves (Robinson and Robinson, 1931). Co-pigmentation was observed as early as in 1916 by Willstatter and Zollinger in grape when the colour changed to bluish from red as a result of addition of tannins (Willstätter and Zollinger, 1916). Co-pigmentation associated to flower colours was studied by Robinson and Robinson (1931). Many factors influence co-pigmentation properties *in-vivo* and co-pigmentation is more complex *in-vivo* compared to that seen *in-vitro*. A shift in flower colour was shown in Petunia to be due to competition between FLS and DFR for common dihydroflavonol substrates leading to a shift in flavonol:anthocyanin ratio (Holton et al., 1993a, Holton et al., 1993b).

Co-pigmentation was proposed to result from three mechanisms: self-association, intra-molecular co-pigmentation and inter-molecular co-pigmentation. Self-association is an inter-molecular association between anthocyanidin nuclei (Tsutomu, 1992) and intra-molecular co-pigmentation (Yoshida et al., 1992) is an interaction between anthocyanidin nuclei and aromatic parts of the same molecule (Nerdal and Andersen, 1992). Whereas, inter-molecular co-pigmentation is an association between anthocyanidin nuclei and co-pigments or acylated molecules and co-pigments (Mazza and Brouillard, 1990). In all the mechanisms it was presumed that the C-2 of the anthocyanidin moiety was protected from acid attack by hydrophobic vertical π stacking on both faces of the chromophore (Goto and Kondo, 1991). The effect of co-pigmentation is seen as a bathochromic shift ($\Delta\lambda_{max}$) which is a shift of the maximum absorption wavelength (λ_{max}) and the colour of anthocyanin changes from red to more blue (Asen et al., 1972) and/or a hyperchromic effect (ΔA) where anthocyanin colour intensity is increased. Occurrence of pure blue flower colour in nature was suggested due to intermolecular hydrophobic association of metalloanthocyanins, stoichiometric self-association of metal-pigment complexes, and metal complexation of flavonoid glycosides (Yoshida et al., 2009, Goto and Kondo, 1991). Several in-vitro studies showed that co-pigmentation is also influenced by pH, pigment-copigment concentrations, chemical structure of anthocyanins and temperature (Mazza and Brouillard, 1990, Sun et al., 2010, Gauche et al., 2010). In case of Himalayan poppy (*Meconopsis grandis*) sky blue flower formation was attained by a

metal complex pigment component consisting of ferric ions, anthocyanin and diglucosyl flavonol (Yoshida et al., 2006).

1.4.8 Functions of anthocyanins

1.4.8.1 In-planta

Anthocyanins mainly serve the purpose of attraction as colourful plant pigments, for example in attracting pollinators like insects and other animals for pollination and for seed dispersal (Strack and Wray, 1994). Anthocyanin pigments may have evolved so that different groups of animals can see the different colours they confer. For example, bumble bees can see pink and violet colours but partial red whereas humming birds can visualize bright red colours (Bradshaw and Schemske, 2003). Anthocyanins also protect plants from various biotic stresses like bacterial, fungal and herbivore attack. Anthocyanins are induced by abiotic stresses such as nutrient deficiency, temperature fluctuations (Christie et al., 1994), UV damage (Sarma and Sharma, 1999, Harborne and Williams, 2000) and may offer protection to photosynthetic tissues by absorbing light under stressful conditions where the dark reactions of photosynthesis are limited and there is a tendency to accumulate damaging reactive oxygen species (ROS).

1.4.8.2 Genetical studies

Anthocyanins played a key role in the discovery of fundamental biological phenomena (Winkel-Shirley, 2001). Fascinating breakthroughs in science like the development of the laws of heredity by Mendel, (1895) the discovery of transposable elements (McClintock, 1950, Fedoroff, 2001), epigenetic phenomena such as paramutation and silencing of duplicated genes in maize (Ronchi et al., 1995, Brink, 1973), co-suppression or RNAi (Napoli et al., 1990) were all detected due to effects on the olour of anthocyanins. The first plant transcription factor was identified in maize by its effects on regulation of anthocyanin biosynthesis (Paz-Ares et al., 1987). Several recent studies of floral patterning have been based on the control of biosynthesis of anthocyanins (Shang et al., 2011). Flavonoids, in general, provide an excellent model for studying subcellular organization of metabolism. Studies addressing anthocyanin transportation have shown the evolution of diversity in metabolite storage

1.4.8.3 Engineering fruits and flowers

The knowledge available from understanding the regulation of anthocyanin biosynthesis has been used to engineer flower colour and fruits for aesthetic properties and health beneficial properties respectively. Flower colours in chrysanthemum (Gutterson et al., 1994), engineering a blue rose (Katsumoto et al., 2007), blue hue commercial carnations (Tanaka and Brugliera, 2007, Florigene Pty, 2006) have been successfully engineered. Anthocyanins were enhanced in cauliflower (Chiu et al., 2010), apple (Espley et al., 2007) and tomato (Butelli et al., 2008) by overexpression of TFs regulating anthocyanin biosynthesis. The benefits of anthocyanins were established for purple tomato where cancer-prone mice showed an extended life span on a diet supplemented with high anthocyanin tomato powder (Butelli et al., 2008).

1.4.8.4 Food colours

Anthocyanins are of great interest for their health benefits and in replacing artificial food colourants (Galvano et al., 2004) due to increased awareness of their beneficial properties. They have also been shown to have potential health benefits in acting as antioxidants, reducing cardio vascular diseases, possible effects in reducing cancer, and improvement of visual acuity (Stintzing et al., 2002, Moyer et al., 2002, Rechner and Kroner, 2005, Jang et al., 2005, Nakaishi et al., 2000).

1.5 Aims of the project

This project was started with an initial aim of understanding the structural properties of anthocyanin acyltransferases that dictate their substrate preferences. For achieving this goal the structural determinants of three aromatic acyltransferases in comparison to one aliphatic acyltransferase were studied. Mutational studies were performed to understand the acyl donor specific evolution of these enzymes.

I also aimed to understand how the different decorations of anthocyanins attained by the acyltransferases changes their functionality both *in-vivo* and *in-vitro*. I studied the effects of side chain modifications of anthocyanins on AVI formation in tobacco.

Finally I aimed to study how each decoration of anthocyanin attributes to its varied *in-vitro* functionality. The results obtained in addressing and achieving the goals are presented in the later chapters of this thesis.

CHAPTER II

General Materials and Methods

2.1 MATERIALS

2.1.1 Chemicals

All chemicals, media, antibiotics, and kits used in this research work were of molecular biology grade obtained from Amersham (GE Healthcare), BioRad, Fluka, Invitrogen, Merck Millipore, New England Biolabs, Promega, Roche, Qiagen, Sigma and Thermo Scientific. HPLC material was obtained from Waters and HPLC grade chemicals were obtained from Fischer Scientific Ltd.

2.1.2 Substrates

Cyanidin 3-*O*-glucoside, cyanidin 3-*O*-rutinoside and kaempferol 3-*O*-rutinodise were obtained from Extrasynthese (France). Cyanidin 3,5-diglucoside and delphinidin 3-*O*-rutinoside were obtained from AP chemicals Ltd (Belgium). Coumaroyl-CoA was obtained from Plant Meta Chem (Germany). Caffeic acid, chlorogenic acid, coumaric acid, malonyl-CoA, rutin and UDP-glucose were obtained from Sigma (USA).

2.1.3 Equipment

The following major pieces of equipment were used in different experiments: High speed centrifuge (Sorvall, USA), Cell disruptor, FPLC system (GE Healthcare, USA), French press, HPLC system (Waters), Nanodrop, Picodrop, prep-HPLC (Gilson), rotary evaporator, spectrophotometer and thermal cycler (BioRad, USA).

2.1.4 Vectors and Strains

The expression vectors used for developing several constructs are summarized in the table 2.1. The bacterial strains used for maintaining of plasmids or expression of genes were DH5α, BL21(DE3), BL21(DE3)pLys, CodonPlus, DB3.1, Rosetta II. *Agrobacterium* strain LBA4404 was used for plant transformation.

2.1.5 Antibiotics

Ampicillin, carbenicillin, cefotaxime, chloramphenicol, gentamicin, kanamycin, rifampicin and streptomycin were used for selecting bacteria and transgenic plant material as necessary. The concentrations of each of the antibiotics used are shown in table 2.2.

Table 2.1 Salient features of the vectors used

Plasmid	Size (bp)	Feature	Selection marker	Supplier
pGEM-T	3003	T/A cloning site	Ampicillin	Promega
pDON-207	5585	Gateway entry vector	Gentamicin and chloramphenicol	Invitrogen
pET-24a	5310	His^6-tag	Kanamycin	Novagen
pET-28b	5369	His^6-tag	Kanamycin	Novagen
pET-29a	5371	S-tag	Kanamycin	Novagen
pMGWA	8209	MBP-tag	Ampicillin	(Busso et al., 2005)
pHGWA	7132	His^6-tag	Ampicillin	(Busso et al., 2005)
pHMGWA	8236	His^6-MBP-tag	Ampicillin	(Busso et al., 2005)
pJAM1502	14992	Double 35S promoter	Kanamycin	(Guerineau and Mullineaux, 1993)

Table 2.2 Stock concentrations of antibiotics used

Antibiotic	Purpose	Working stock concentration	Original stock concentration
Ampicillin	For selection of *E. coli*	100 µg/mL	100 mg/mL
Carbenicillin	Used in place of ampicillin for liquid cultures	50 µg/mL	50 mg/mL
Cefotaxime	For killing *Agrobacterium* after co-cultivation of tobacco leaf discs	250 µg/mL	250 mg/mL
Chloramphenicol	For selecting expression *E.coli*	34 µg/mL	34 mg/mL
Gentamicin	For selecting DB3.1 cells	50 µg/mL	50 mg/mL
Kanamycin	For selecting *E.coli*, *Agrobacterium* and transgenic material	50 µg/mL and 100 µg/mL	50 mg/mL and 100 mg/mL
Rifampicin	For selecting *Agrobacterium*	25 µg/mL	25 mg/mL
Streptomycin	For *Agrobacterium*	30 µg/mL	30 mg/mL

2.1.6 Plant growth hormones

The following plant growth regulators were used in plant transformation experiments: 6-Benzylaminopurine (BAP), kinetin, 1-Naphthaleneacetic acid (NAA) and 2, 4-Dichlorophenoxyacetic acid (2, 4-D). All the hormones were purchased from Duchefa.

2.1.7 Plant material

Tobacco (*Nicotiana tabacum* var Samsun) was used for generating transgenic plant material. Arabidopsis (*Arabidopsis thaliana* Columbia), chrysanthemum (*Chrysanthemum morifolium*) and gentiana (*Gentiana triflora*) were used for isolation of genes.

2.2 METHODS

Standard procedures are described in Sambrook and Russell (Sambrook and Russell, 2001). Additional protocols were followed according to the product specific instructions/protocols with modifications as and when considered necessary.

2.2.1 Primer design

For cloning genes of interest in various vectors and for PCR confirmation of clones and gene expression studies, specific primers were designed. Primers were designed by following standard guidelines. For restriction cloning, care was taken while designing primers to add only those enzyme sites, which were present in the multiple cloning site and beared not elsewhere in the vector/gene. For Gateway cloning™, attB1 and attB2 sites were added to the 5' end of forward and reverse primers respectively. The reading frame was maintained in all clones created by both Gateway and restriction enzyme cloning. The final designed primers were checked for their translation ability using the translator tool present in Expasy proteomic server (http://expasy.org/tools). The Tm values of the primers were calculated using the formula: Tm=2(A/T) + 4(G/C). The primers were synthesized and supplied by Sigma; UK. Primers for quantitative PCR were designed using Primer3®.

2.2.2 PCR amplification

Polymerase chain reactions consisted of 6-10 ng of DNA, 0.2 µM each of the forward and reverse primer, 100 µM of each dNTP, 1x concentration of *Pfu* DNA polymerase or *Taq* DNA polymerase, 1x concentration of *Pfu* or *Taq* buffer, 1.5 mM $MgCl_2$, and milliQ water to a total volume of 20 µL. The cycling parameters adopted for PCR were standard

although the Tm values of the primers used and the length of the amplicon were considered in determining the annealing temperatures and extension times respectively. Standard PCR conditions were as follows: initial denaturation; 4 min at 94°C, 25-35 cycles of denaturation; 2 min at 94°C, annealing; 30 sec at 50°C, extension; 30 sec to 1.5 min at 72°C, and final extension; 5 min at72°C.

Colony PCR was performed in the similar manner except a tiny amount of each colony was taken using a toothpick to replace the template DNA and 0.1 units of *Taq* DNA polymerase were used.

2.2.3 General methods followed during the constructs development

2.2.3.1 Plasmid DNA isolation from *E. coli*

Plasmid DNA was isolated from 3-5 mL of *E.coli* cultures grown overnight with appropriate antibiotic selection. Bacterial cultures were collected by centrifugation at 12,000 rpm for 2 min and the pellet was resuspended in buffer. Plasmid isolation was carried using QIAprep® Spin Miniprep kit (Qiagen) following manufacturer's instructions. Plasmid DNA was eluted in 50 µL of elution buffer or 10 mM Tris; pH 8.

2.2.3.2 Restriction endonuclease digestion

Restriction digestions of PCR products and vectors were performed with suitable enzymes for use in ligation reactions and for confirmation of cloning. The reaction mixture consisted of 0.5-1.0 µg of plasmid DNA, 10-20 units of restriction enzymes, 1x final concentration of buffer and milliQ water as required to make up the final volume. Reactions were incubated at 37°C for 1 h, stopped with loading dye (10 mM Tris; pH 8, 30% glycerol, 0.25% bromophenol blue) and analysed on 0.8% agarose gels.

2.2.3.3 Purification of DNA from agarose gels

The PCR products and restriction digestion products were run on 0.8 % agarose gels in Tris Borate EDTA (TBE 10X: 0.89 mM Tris, 0.89 mM Boric Acis and 20 mM EDTA; pH 8) buffer. The desired fragments were identified on the gels based on standard markers (100 bp or 1 kb ladder) after ethidium bromide staining (0.15 mg/mL) and visualised with a large wavelength UV transilluminator. The agarose gel slab containing the required fragment was excised from the gel using a sharp sterile scalpel blade. DNA was eluted from the excised gel using a QIAGEN gel elution kit following the

manufacturer's instructions. The DNA from the column was collected by adding 25-30 µL of elution buffer or 10 mM Tris; pH 8.

2.2.3.4 Quantification of purified DNA

The purified DNA was quantified by loading 2 µL on an agarose gel. The approximate concentration and quality was checked by visual comparison of the sample with a known amount of DNA in the standard molecular weight markers. Alternatively DNA was quantified using a picodrop (Thermo Scientific).

2.2.3.5 A-tailing

PCR products amplified using *Pfu* DNA polymerase and therefore having blunt ends were A-tailed to be cloned into pGEM-T-easy vector. pGEM-T/A vector was purchased as linearised vectors containing 3' terminal thymidine at both ends. A-tailing was performed following the manufacturer's instructions. The reaction mixture: 1-2 µL PCR product, 1X µL *Taq* 10X buffer, 2.5 mM of $MgCl_2$, 0.2 mM dATP, 5 units of *Taq* DNA polymerase and milliQ water made upto 10 µL reaction volume was incubated at 70°C for 15-30 min. 1-2 µL were used in ligation reactions using T4 DNA polymerase.

2.2.3.6 Ligation

Ligation reactions were set up with a molar concentration ratio of 3:1 for insert to vector DNA. The amount or quantity of insert to be taken for a known concentration of vector was calculated using the formula: Quantity of insert (ng) = 3 x [(base pair of insert x quantity of vector)/ number of base pairs of vector]. The ligation reaction consisted of 55 ng of vector DNA, 50-150 ng of insert, 1x final concentration of ligation buffer, 5-10 units of T4 DNA ligase and milliQ water to make up the final volume. The reaction mixture was incubated at 22˚C in a water bath for 4-5 h or at 4˚C O/N.

2.2.3.7 Gateway cloning

2.2.3.7.1 Generation of entry clones

PCR products amplified using *Pfu* DNA polymerase with Gateway gene specific primers were cloned into pDONOR-207 vector using BP clonase™ (Invitrogen). The BP reaction mixture consisted of 1 µL of pDONOR-207, ~200 ng of PCR product, 1 µL of BP clonase II and 1 µL 10 mM T, 1 mM EDTA; pH 8.0 ($T_{10}E_1$) buffer. Recombination reactions were incubated at 25˚C for 1 h or overnight. The incubated reaction was

stopped by adding 1 µL of proteinase K followed by incubation on ice for 10 min. 2.5 µL of the reaction mix was used for DH5α transformation in order to produce pEntry clones.

2.2.3.7.2 Generation of destination clones

Plasmid DNA of the entry clone can be used to transfer the gene of interest to any number of Gateway destination vectors. The LR reaction mixture: 1 µL of entry clone, 0.7 µL of destination vector, 1 µL LR clonase™ (Invitrogen) and 3.3 µL $T_{10}E_1$ buffer was incubated at 25˚C for 1 h. The reaction was stopped by addition of 0.66 µL of proteinase K and incubated at 37˚C for 10 min. Reaction mixture; 3 µL was transformed into DH5α cells to obtain the final expression clones.

2.2.4 Preparation of heat shock competent *E. coli* cells

Competent cells were prepared following the $RbCl_2$ method of preparation. *E.coli* cells taken from a single colony or glycerol stock were inoculated in 50 mL sterile LB medium (1% tryptone, 0.5% yeast extract, 0.5% NaCl and 0.1% glucose). Expression strains (carrying plasmid for synthesis of specific amino acids) were grown with chloramphenicol and DH5α cells were grown without antibiotics at 37˚C O/N. Overnight grown culture; 500 µL was subcultured in 50 mL LB until the OD_{600} reached to 0.5. The culture was transferred to a prechilled tube and incubated on ice for 5-10 min. A pellet of bacterial obtained by centrifugation at 4,500 rpm for 5 min at 4˚C was gently resuspended in 10 mL sterile buffer (100 mM; $RbCl_2$, 50 mM; $MnCl_2$, 30 mM; potassium acetate, 10 mM; $CaCl_2$-$2H_2O$ and 15% glycerol) and incubated on ice for 15-30 min. Suspended cells were spun at 4500 rpm for 5 min at 4˚C and the pellet finally resuspended gently in 6 mL sterile buffer (10 mM; MOPS, 10 mM; $RbCl_2$, 4.4.g; $CaCl_2$ and 15% glycerol). Aliquots of 100 µL of competent cells were flash-frozen in liquid N_2 and stored in -80˚C.

2.2.5 Preparation of electrocompetent *Agrobacterium tumefaciens* cells

Agrobacterium tumefaciens cells (LBA 4404) taken from a single colony that was grown freshly on TB medium with rifampicin and streptomycin, were used to inoculate 10 mL liquid sterile TB medium (1.3% tryptone, 2.6% yeast extract and 0.5% glycerol) with antibiotics and grown at 28˚C overnight. An overnight culture; 500 µL was subcultured into 50 mL LB and grown until the OD_{600} reached to 0.5-0.6. The cells were centrifuged at 4,500 rpm for 10 min at 4˚C and the pellet was resuspended in ice cold sterile water. The cells were washed five more times in a similar way except 15% glycerol was used in

the last two washes. Finally the cells were resuspended in 5 mL of 10% sterile glycerol and aliquots were flash-frozen in liquid N_2 before storing in -80˚C.

2.2.6 Transformation

2.2.6.1 Heat shock method of *E.coli* transformation

The heat shock method of transformation of competent cells was used for transforming DH5α and expression strains with desired plasmids. Competent cells from -80˚C were thawed on ice and 20 ng of plasmid DNA or ligation mix (which was warmed at 65˚C for 10 min to deactivate ligase and improve the efficiency of transformation) was added to competent cells. Cells were mixed gently and incubated on ice for 15 min. Heat shock was given at 42˚C for 2 min and 1 mL of LB medium was added to the cells and incubated at 37˚C for 1 h with constant shaking. The cells were pelleted by centrifugation at 12,000 rpm for 1 min and resuspended in 200 uL of LB. These cells were divided into $1/3^{rd}$ and $2/3^{rd}$ portions and plated on LB agar with desired antibiotics. The plates were incubated at 37˚C overnight and screened the following day.

2.2.6.2 Electroporation of *Agrobacterium*

Competent cells were thawed on ice and 200 μg of plasmid DNA was added and the cells transferred to chilled electroporation cuvettes. The cells were electrocuted using a BioRad Pulser (BioRad Laboratories) with the following settings: 200Ω, 25 μFD and 1.8 kV. 1 mL liquid LB medium was added to the cells and incubated for 2 hours at 28°C with constant shaking (250 rpm). Pelleted cells were plated on LB agar plates supplemented with 25 μg/mL rifampicin, 30 μg/mL streptomycin and 50 μg/mL kanamycin and incubated for two days at 28°C.

2.2.7 Sequencing of clones

Vectors in potentially positive clones were sequenced using standard Big Dye sequencing reaction which comprises of 0.2 μM desired primer, 5x sequencing buffer, Big Dye 4.0V (Applied Biosystems), and 100-150 ng good quality plasmid DNA. PCR was performed using the following conditions; initial denaturation; 1 min at 96°C, 25 cycles of denaturation; 10 sec at 96°C, annealing; 5 sec at 50°C, and extension; 4 min at 60°C. The reactions were sequenced commercially by Genome Enterprise Ltd (Norwich, UK). Sequencing data was obtained as ABI trace files and were analysed using Invitrogen Vector NTI software.

2.2.8 Preparation of glycerol stocks

Confirmed plasmids for the desired gene sequences in *E.coli* and LBA 4404 were maintained as glycerol stocks in -80°C for long-term storage. Overnight grown culture; 500 µL was suspended in 500 µL of sterile 50% glycerol and flash frozen in liquid N_2 before storing in -80°C.

2.2.9 Plant genomic DNA extraction

Plant genomic DNA was extracted following a modified CTAB method of extraction. Frozen leaf tissue; 200mg was ground to a fine powder and 500 µL of CTAB buffer; pH 5 (2% CTAB, 100 mM Tris; pH8.0, 20 mM EDTA; pH 8.0, 1.4 M NaCl, 1% PVP, 0.2% 2-mercapto ethanol and water) was added. The samples were incubated at 55-60°C for 15 min with intermittent mixing. Chloroform:isoamyl alcohol (24:1) 0.6 volume was added to the cooled samples and the tubes were mixed by inversion for 5 min. Samples were centrifuged at 13000 rpm for 5 min and the aqueous phase was collected, to which double the volume of absolute alcohol was added and incubated for 10 min. The samples were centrifuged at 12000 rpm for 7-8 min and the DNA pellet was washed with 70% absolute alcohol. Air drying gave a gDNA pellet which was dissolved in $Tris_{10}$ buffer; pH 8.0 containing 50 g/mL RNAase and incubated at 37°C. The concentration of DNA was measured using a Nanodrop or Picodrop and diluted with milliQ water for PCR assays.

2.2.10 Plant RNA extraction

RNA was extracted from frozen leaf or flower material using Tri reagent® (Sigma) and following the protocol by Applied Biosystems with modifications. 100 mg of powdered plant material was homogenised in 1 mL of Tri reagent and incubated at room temperature for 5 min. Chloroform; 200 µL was added to the homogenised sample, mixed thoroughly and incubated for 10 min. The samples were centrifuged at 12000 rpm for 10 min at 4°C and the aqueous phase was collected. To this, 500 µL of isopropanol was added. After 10 min of incubation the samples were centrifuged at 1200 rpm for 8 min. Collected RNA pellet was washed with 75% ethanol and the pellet was air dried for 5 min. RNA was dissolved in RNase-DNase free water containing 5 units of DNase. The RNA samples were incubated for 30 min at 37°C and quantified using Picodrop.

2.2.11 First strand cDNA synthesis

First strand cDNA was synthesised from total plant RNA using SuperScript™ III (Invitrogen) or M-MuL V reverse transcriptase (New England Biolabs). 1 µg total RNA, 50 µM oligo$(dT)_{20}$, 100 µM each dNTP mix and RNase free water were mixed and the reaction incubated at 65°C for 5 min. The reaction mix was incubated on ice for 2 min. 5X First-strand reaction buffer/10X RT buffer, 0.5 µL of RT enzyme and 1 µL of RNase OUT were added to the mixture and incubated for 50-60 min at 50°C. The reaction was terminated at 70-80°C for 5 min. 2 µL of this first strand cDNA was used for PCR amplification and PCR reactions of RNA were used as control.

CHAPTER III

Understanding the Substrate Specificities of Anthocyanin Acyltransferases (AATs)

3.1 Introduction

Acylation is one of the biochemical modifications leading to the decoration of anthocyanins. Transfer of acyl- moieties from acyl-CoAs to anthocyanins (acylation) catalysed by anthocyanin acyltransferases (AATs) affects the properties of anthocyanins in solution. Aliphatic and aromatic AATs catalyse the transfer of aliphatic and aromatic acyl moieties respectively to hydroxyl groups of glycosyl moieties of anthocyanins, through ester bond formation. Aromatic acylation leads to more stable and bluer anthocyanins with intra molecular stacking (Goto and Kondo, 1991). Aliphatic acylation increases anthocyanin solubility in water (Heller and Forkmann, 1994), protects glycosides from enzymatic degradation (Suzuki et al., 2002), and stabilizes anthocyanin structure (Saito et al., 1988) and uptake into vacuoles (Hopp and Seitz, 1987).

Primary sequence analysis of AATs has established two highly conserved sequences; motif-1 (H*XXX*DG) and motif-3 (DFGWG) [Fig 3.8] which are shared by all AATs although, overall, they have low sequence similarity (15-30% identity; (Nakayama et al., 2003)). Thus by the presence of these conserved motifs, most AATs belong to the benzylalcohol acetyl-, anthocyanin-*O*-hydroxy cinnamoyl-, anthroanilate-*N*-hydroxy cinnamoyl/benzoyl-, deacetylvindoline acetyltransferase (BAHD) super family of enzymes. Many anthocyanin acyltransferases (AATs) with different acyl-donor, acyl-acceptor and regio-specificities for acyl transfer have been identified. However, individual AATs have strict regio-specific transfer and substrate specificity properties. The reasons for their strict substrate and regio-specificity are unknown and little is known about the three dimensional structure of these enzymes, particularly the structural features determining specificity in these complex modifications of anthocyanins. The first representative of the BAHD family to be studied structurally was vinorine synthase in which His^{160} of the H*XXX*DG motif was found to be involved in general acid base catalysis (Ma et al., 2005). The first crystal structure of an AAT studied, a malonyl transferase, lead to an understanding of the catalytic mechanism and function of conserved domains of AATs (Unno et al., 2007). Deletion or modification of one or both conserved motifs (1 and 3) gave rise to reduced enzyme activities suggesting roles in the active site and protein stabilisation, respectively (Bayer et al., 2004, Suzuki et al., 2003a).

To date, no attempts to understand the structural features that determine the substrate specificities of aromatic acyltransferases have been reported. As it was known

that AATs have strict acyl donor specificities, an *in-vivo* study of the preferences of these enzymes was also required to understand fully their properties. Such understanding could be used to create novel enzymes with different anthocyanin modification/decoration properties. Hence, structural and functional studies of aromatic AATs could provide an insight into the unique properties, particularly the substrate specificities, of these enzymes.

In an attempt to understand the evolution of substrate preferences of aromatic AATs, crystallization attempts were made with the purified proteins of Gt5AT, At3AT and Sl3AT. To further probe into the structural evolution of AATs for specificity to donor substrates; a comparative mutational study of two aromatic (coumaroyl) acyltransferases (Sl3AT and At3AT) and one aliphatic (malonyl) transferase (Ch3MAT) was undertaken. The results obtained are presented in this chapter.

3.2 Experimental procedures

3.2.1 Construction of plasmids

Several vectors having different tag sequences were used for generating expression clones of Sl3AT, Gt5AT and At3AT enzymes. Different tags were tested to obtain high-level protein expression in *E.coli*. In all the vectors, the reading frame of the AAT was maintained with the fusion tags.

3.2.1.1 Generation of Sl3AT clones for recombinant protein expression

The anthocyanidin 3-rutinoside coumaroyl-CoA acyltransferase from tomato (*Sl3AT*; description for this gene is given in section 3.3.1 of this chapter) is encoded by a cDNA of 1365 bp. *Sl3AT* was available in the T/A cloning vector (pGEM-T) and was re-amplified with primers suitable for cloning into different vectors [Table 3.1, 3a; appendix]. For obtaining a C-terminal His_6-tag construct, *Sl3AT* was cloned into pET24a [Fig 3a.ii; appendix]. The gene was amplified with primers having an *Nde*I restriction site in the forward primer and *Xho*I site in the reverse primer (with no stop codon) [Table 3.1]. *Pfu* polymerase was used for amplification. Purified, amplified PCR product was digested with *Nde*I and *Xho*I and cloned into pE24a digested with the same enzymes. Similarly, *Sl3AT* was cloned into pET28b to provide an N-terminal His_6-tag with same forward primer (Sl24aF) with an *Nde*I site and the Sl21aR reverse primer which had *Xho*I site and a stop codon [Fig 3.1b].

For cloning into pMGWA, which adds an N-terminal Maltose Binding Protein (MBP) tag, pHGWA (N and C-terminal His_6-tag) and pHMGWA (N-terminal His_6-MBP tag); the *Sl3AT* cDNA was amplified with primers shown in table 3.1, containing Gateway recombination sequences (attB1 and attB2). *Pfu* polymerase-amplified PCR product was recombined into the pDONR 207 entry vector using BP clonase™. The resulting entry vector, pEnt207Sl3AT, was sequenced and a positive clone containing the full length *Sl3AT* sequence (confirmed by sequencing) was recombined into pMGWA, pHGWA and pHMGWA vectors [Fig 3a.i; appendix] by LR™ recombination to create the respective AAT expression clones [Fig 3.1a].

3.2.1.2 Generation of Gt5AT clones for recombinant protein expression

A codon-optimised coumaroyl transferase cDNA, identical in aminoacid sequence to one from Gentiana (*Gt5AT*; description of this is given in section 3.3.1 of this chapter) was synthesised (GenArt AG, Regensburg) and cloned into the pE21a vector. *Gt5AT,* of size 1410 bp, was reamplified with primers suitable for cloning into different vectors [Table 3.1, 3a; appendix]. For obtaining a C-terminal His_6-tag construct, *Gt5AT* was cloned in to pET24a. The gene was amplified with primers having an *Nde*I restriction site in the forward primer and a *Xho*I site in the reverse primer (with no stop codon) [Table 3.1] using *Pfu* polymerase. Purified, amplified PCR product was digested with *Nde*I and *Xho*I and cloned into pE24a vector digested with the same enzymes. Similarly *GT5AT* was cloned into pET28b (N-terminal His_6-tag) with the same forward and reverse primers (with a stop codon) [Fig 3.1b, 3b; appendix].

For cloning into pMGWA (N-terminal MBP-tag) and pHGWA (N and C-terminal His_6-tag) vectors; *Gt5AT* was amplified with the primers shown in table 3.1 with Gateway recombination sequences (attB1 and attB2). *Pfu* polymerase amplified PCR product was recombined into the pDONR 207 entry vector using BP clonase™. The resulting entry vector pEnt207Gt5AT was sequenced and a positive clone containing the full length *Gt5AT* sequence was recombined into pMGWA and pHGWA vectors by an LR™ recombination reaction to create the respective AAT expression clones [Fig 3.1a].

3.2.1.3 Generation of At3AT clones for recombinant protein expression

The cDNA encoding the anthocyanidin 3-glucoside coumaroylCoA acyltransferase from Arabidopsis (*At3AT*; description of this is given in section 3.3.1 of this chapter) of size 1410 bp, available in the pJAM 1784 vector, was re-amplified with primers suitable for cloning into different vectors [Table 3.1, 3a; Appendix]. For obtaining a C-terminal His_6-

tag construct, *At3AT* was cloned into pET24a. The gene was amplified with primers having an *Nde*I restriction site in the forward primer and a *Xho*I site in the reverse primer (with no stop codon) [Table 3.1] using *Pfu* polymerase. Purified, amplified PCR product was digested with *Nde*I and *Xho*I and cloned into pE24a vector digested with the same enzymes. Similarly *At3AT* was cloned into pET28b (N and C-terminal His_6-tags) with the same forward primer (Sl24aF) with an *Nde*I site and the Sl21aR reverse primer with a *Xho*I site without a stop codon [Fig 3.1b].

For cloning into pHGWA (N and C-terminal His_6-tags) and pHMGWA (N-terminal His_6-MBP tag) vectors; the *At3AT* cDNA was amplified with the primers shown in table 3.1 which had Gateway recombination sequences (attB1 and attB2). *Pfu* polymerase amplified PCR product was recombined into the pDONR 207 entry vector using BP clonase™. The resulting entry vector pEnt207At3AT was sequenced and a positive clone containing the full length *At3AT* sequence was recombined into the pHGWA and pHMGWA vectors by LR™ recombination reactions to create the respective AAT expression clones [Fig 3.1a].

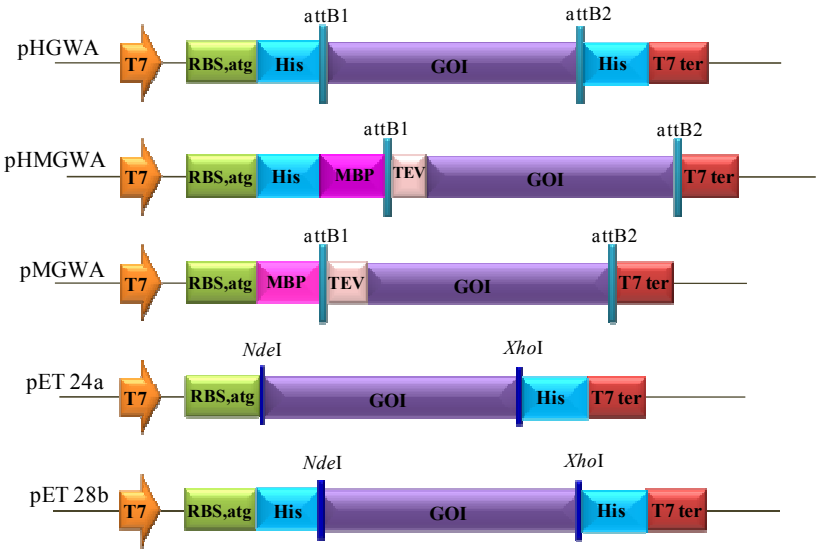

Figure 3.1a | Diagramatic representation of different gene constructs used for recombinant protein expression. T7; T7 promoter, RBS; ribosome binding site, atg; translational start site, His; 6x histidine tag, MBP; maltose binding protein, attB1 and attB2; Gateway recombinant sites, TEV; tev-protease cleavage site, GOI; gene of interest, T7 ter; T7 terminator, *Nde*I and *Xho*I; restriction enzyme sites. GOI is denoted for the different genes; *Sl3AT*, *At3AT* and *Gt5AT* studied. (Picture is not according to scale)

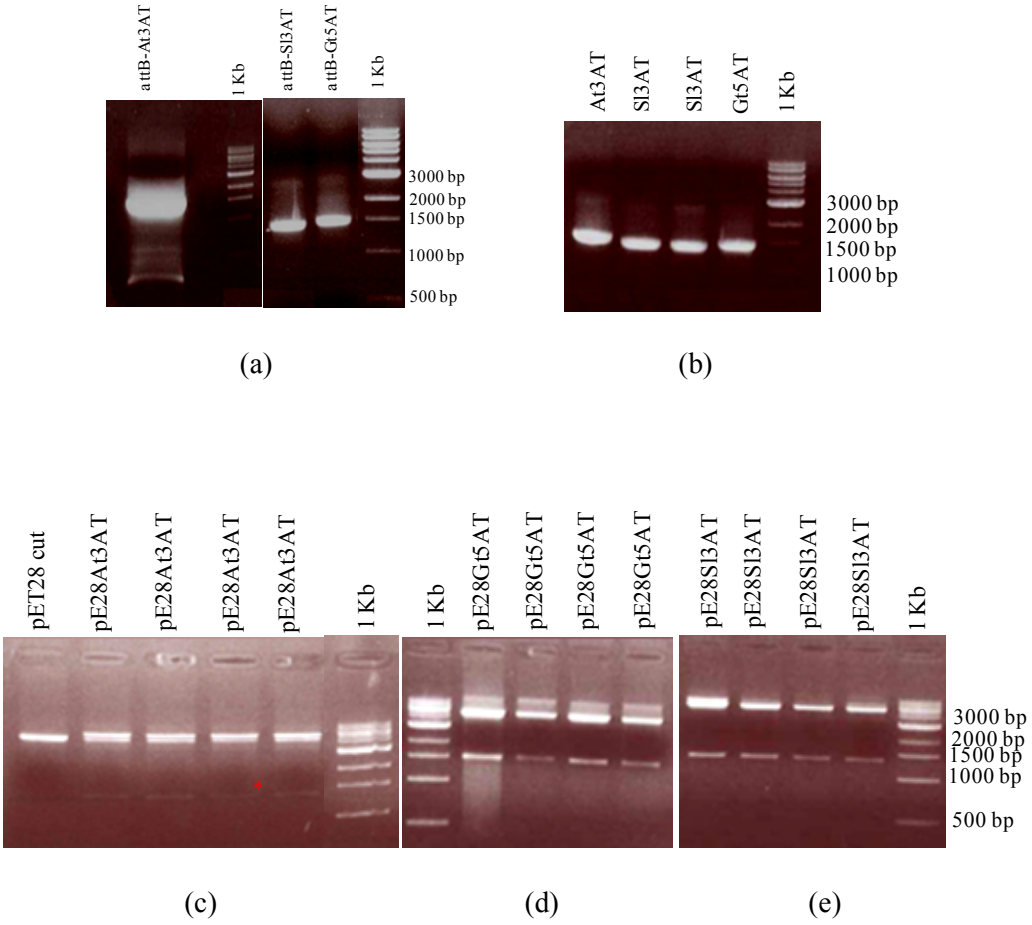

Figure 3.1b | Cloning of *Sl3AT*, *At3AT* and *Gt5AT* into *E.coli* expression vectors (a) *Sl3AT*, *At3AT* and *Gt5AT* genes amplified using gateway gene specific primers and *Pfu* to give each fragment of sizes ~1460 bp, ~1410 bp and ~1460 bp respectively (b) *Sl3AT*, *At3AT* and *Gt5AT* genes of sizes ~1410 bp, ~1365 bp and ~1410 bp amplified with primers having *Nde*I and *Xho*I restriction sites for cloning into pET24a and pET28b (c) Restriction enzyme digestion of the plasmids; pET28b carrying *At3AT* (~200 ng each) with *Nde*I and *Xho*I. Release of *At3AT* was shown with asterisk. (d) Restriction enzyme digestion of the plasmids; pET28b carrying *Gt5AT* (~200 ng each) with *Nde*I and *Xho*I.clones. (e) Restriction enzyme digestion of the plasmids; pET28b carrying *Sl3AT* (~200 ng each) with *Nde*I and *Xho*I. In c,d and e cloning was confirmed in all plasmids by the release of gene of interest of desired size after restriction digestion. The vector band was seen as two bands with upper band; the uncut vector carrying GOI and lower band; linearized plasmid.

3.2.2 Construction of mutant plasmids for expression in *E.coli*

Mutant proteins of Sl3AT, At3AT and Ch3MAT (description of the genes encoding enzymatic activity of these proteins is given in section 3.3.1 of this chapter) were expressed with an S-tag for ease of quantification of recombinant protein within the total soluble protein extract. Isolation of *Ch3MAT* from chrysanthemum inflorescence is given in section 4.2.4.2 of chapter 4.

The pET24a vector was used for cloning the mutant H174N-*Sl3AT*. A sequenced clone pET24SlAT was used as a template to amplify regions using two primer pairs; the Sl24aF forward primer which had an *Nde*I restriction site and the 174HsatN reverse primer; the 174HsatN F forward and the Sl21aR reverse primer which had *Xho*I site [Table 3.1]. *Pfu* amplified PCR products thus obtained were gel extracted and used in the final round of PCR to amplify the full length gene bearing the H174N mutation. The purified final PCR product was digested with *Nde*I and *Xho*I and cloned into pET24a vector digested with the same enzymes. A positive clone, checked by sequencing, was used for subsequent expression studies.

F181R-*Sl3AT*, F181R-*At3AT* and R183F-Ch3MAT mutations were created in *Sl3AT*, *At3AT* and *Ch3MAT* respectively, following similar procedures. Primers shown in table 3.1 were used to obtain the mutant clones and wild type S-tagged clones (pET29a vector, Fig 3b; appendix). Constructs positive for the presence of gene with the desired mutations [Fig 3.2] were used for expression studies in *E.coli*.

3.2.3 Generating mutant constructs for expression in plants

The vectors with mutated genes; p29F181R-At3AT(1) and p29R183F-Ch3MAT(8) were used as templates to obtain *Pfu* amplified PCR products using primers having Gateway recombination sequences [Table 3.1, 3a; Appendix]. Amplified products [Fig 3.3] were purified and cloned into pDONR 207 to obtain entry clones pEnt207 F181R-At3AT and pEnt207 R183F-Ch3MAT. Positive entry clones pEnt207 F181R-At3AT(2) and pEnt207 R183F-Ch3MAT(10) which carried the desired mutations were used to create a destination vector using LR recombination into pJAM1502. Expression clones pJAM1502-F181R-At3AT and pJAM1502-R183F-Ch3MAT were used for *Agrobacterium* mediated transformation of tobacco.

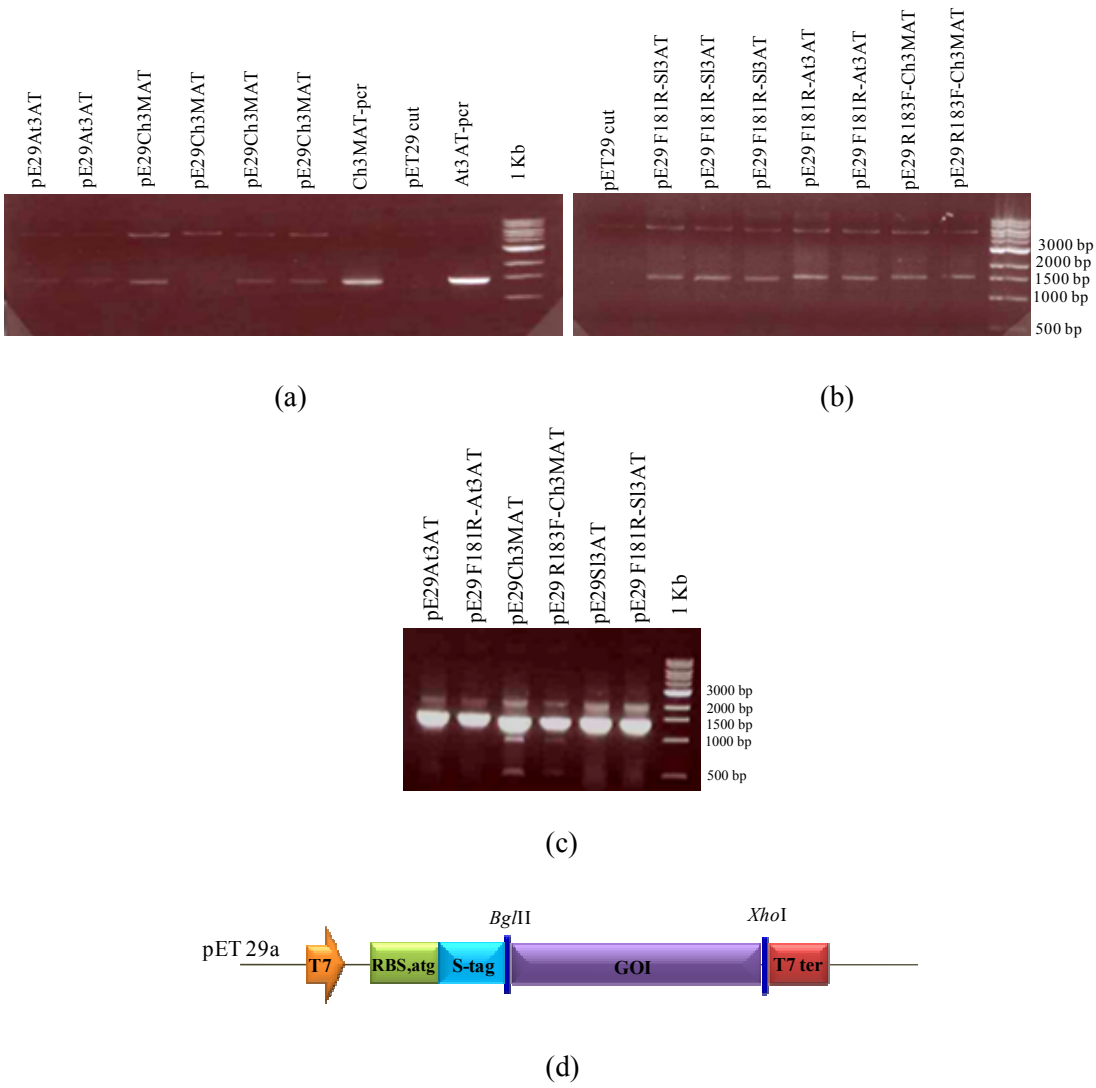

Figure 3.2 | Cloning of *Sl3AT*, *At3AT* and *Ch3MAT* (wild type and mutant) into S-tag expression vector: pET29a (a) Restriction enzyme digestion of pE29At3AT and pE29Ch3MAT plasmids (200 ng each) with *Bgl*II and *Nde*I enzymes. Cloning was confirmed by the release of a fragment of DNA of predicted size after restriction digestion (b) Restriction enzyme digestion of pE29-F181R-Sl3AT, pE29-F181R-At3AT and pE29-R183F-Ch3MAT plasmids (200 ng each) with *Bgl*II and *Nde*I enzymes. (c) PCR confirmation that all the clones pE29Sl3AT, pE29-F181R-Sl3AT, pE29At3AT, pE29-F181R-At3AT, pE29Ch3MAT and pE29-R183F-Ch3MAT contained inserts of the predicted size d) Pictorial representation (not according to scale) of expression clones developed with the S-tag; *Sl3AT*, *At3AT* and *Ch3MAT* (wild type and mutant) genes are represented as GOI; gene of interest. T7; T7 promoter, RBS; ribosome binding site, atg; translational start site, S-tag; S-peptide, GOI; gene of interest, T7 ter; T7 terminator, *Bgl*II and *Xho*I; restriction enzyme sites.

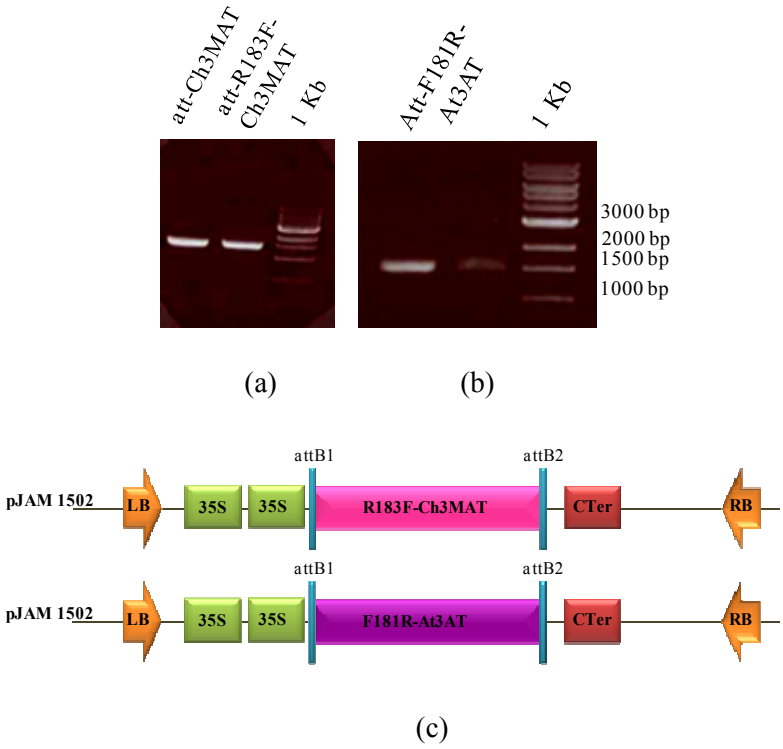

Figure 3.3 | Cloning of R183F-*Ch3MAT* and F181R-*At3AT* (a) The R183F-*Ch3MAT* gene was amplified (~1443 bp) using Gateway-specific primers and *Pfu* enzyme, using pE29R183F-Ch3MAT plasmid as a template in which the desired mutations were created (b) F181R-*At3AT* gene was amplified (~1460 bp) using Gateway-specific primers, *Pfu* enzyme and pE29 F181R-At3AT plasmid as template where the desired mutations were created. (c) Pictorial representation (not according to scale) of T-DNA region of plant expression vector of R183F-*Ch3MAT* and F181R-*At3AT*; pJ15F181R-Ch3MAT and pJ15F181R-At3AT respectively. LB; left border, 35S; CaMV35S promoter, attB1 and attB2; Gateway recombinant sites, Cter; CaMV terminator, RB; right border.

3.2.4 Protein expression in *E.coli*

Vectors for expression in *E.coli* were transferred to expression hosts; BL21 (DE3) for MBP-tagged proteins and BL21 (DE3) pLysS or Rosetta II or CodonPlus for His_6-tagged proteins using heat shock method of transformation as described in chapter II. Bacterial cultures were grown overnight at 37˚C in LB medium containing the required antibiotics and were sub-cultured until an OD_{600} of 0.5-0.7 was reached. Uninduced culture (1 mL) was collected, centrifuged at 12,000 rpm and suspended in 10% SDS for use in SDS-PAGE separation. Protein expression was induced by addition of 0.4 to 1 mM IPTG and the culture was grown for 4 hr at 37˚C (fast induction). His_6-tagged clones for enhanced

protein solubility were induced using 1 mM IPTG and grown with 0.4M sorbitol and 2.5 mM betaine overnight at 12-16˚C after induction (slow induction). After the required period of growth, 1 mL of culture was centrifuged at 12,000 rpm, suspended in 10 % SDS and kept in -20˚C for use in SDS-PAGE analysis. The remaining cells were pelleted at 8000rpm for 15 min and the pellet was stored at -20˚C for use within a short period of time or at -80˚C for long-term storage.

Table 3.1 | Primers used for constructing the different vectors described in this chapter

Gene	Size (bp)	Forward primer	Reverse primer	Final vector
Sl3AT	1365	Sl24aF	Sl24aR	pE24Sl3AT
		Sl24aF	Sl21aR	pE28Sl3AT
		B1tevSAT	B2 R	p525tevSl3AT
		B1 F	B2SAT	p528Sl3AT
		B1tevSAT	B2 R	p530tevSl3AT
		Sl24aF	Sl21aR	pE24H174N-Sl3AT
		SAT29aFnew	Sl21aR	p29Sl3AT
		SAT29aFnew	Sl21aR	p29F181R-Sl3AT
Gt5AT	1410	28GatF	28GatNS R	pE28Gt5AT
		28GatF	28GatNS R	pE24Gt5AT
		B1GAT	B2GAT’	p528Gt5AT
		B1tevGAT	B2GAT	p525tevGt5AT
At3AT	1410	At24aF	At24aR	pE24At3AT
		At24aF	AtATsR	pE28At3AT
		B1AAT	B2AAT	p528At3AT
		B1tevAAT	B2AATs	p530tevAt3AT
		AAt29Fnew	AtATsR	p29At3AT
		AAt29Fnew	AtATsR	p29F181R-At3AT
		B1AAT	B2AATs	pJAM1502- F181R-At3AT
Ch3MAT	1380	CMat29Fnew	C3MaR	p29Ch3MAT
		CMat29Fnew	C3MaR	p29R183F-Ch3MAT
		Ch3MATB1F	Ch3MATB2R	pJAM1502- R183F-Ch3MAT

3.2.5 Preparation of protein from *E.coli*

Frozen culture was thawed on ice in cold 50 mM KH $_2PO_4$ /K_2HPO_4 (potassium phosphate) buffer; pH 7.6 containing 0.9 M NaCl, 50 mM glycine and 5% (v/v) glycerol, mixed with protease inhibitors. The cells were broken with a French press (at 100 mPa) or cell disruptor and cell debris was sedimented by centrifugation at 12,000 rpm for 15 min. The clear supernatant (soluble fraction) was collected and stored at -20˚C until further experiments were carried out. The debris obtained after cell disruption by using the French press, was dissolved/resuspended in phosphate lysis buffer and stored at -20˚C as the insoluble fraction. Pellets from small volume cultures were disrupted using a sonicator.

3.2.6 Small scale protein purification of recombinant proteins

3.2.6.1 Small scale purification of MBP fusion proteins

To optimize the conditions for large scale purification and to check the protein concentration following purification, small scale purification was performed according to the NEB protocol as described below with slight changes as considered necessary. All the steps were carried out at 4˚C unless specified otherwise. The soluble protein fraction was mixed with equilibrated amylose resin (NEB product) for 60 min. Resin equilibration was done by washing he amylose resin suspension twice with water and twice with column buffer (20 mM Tris-HCl; pH7.4, 200 mM NaCl, 1mM EDTA). Resin mixed with the soluble fraction was centrifuged for 3 min at 3,500 rpm and the supernatant was taken separately as unbound protein. The resin beads were washed four to five times with column buffer (washing included mixing and centrifugation for 3 min at 3,500 rpm). Recombinant protein was eluted with elution buffer (column buffer + 20 mM maltose) by performing three to four washes. Elution included incubation of resin with elution buffer for 5 min at RT and centrifugation for 3 min at 3,500 rpm. The eluted products from all the steps were pooled and stored at -20 °C.

3.2.6.2 Small scale purification of His6-tagged proteins

To optimize conditions for large scale purification of His-tagged proteins, small scale purification was initially performed according to the following protocol (http://wolfson.huji.ac.il/purification/TagProteinPurif/HisTag_denature.html). All steps

were carried at 4˚C unless specified otherwise. The soluble protein fraction was mixed with equilibrated Ni-NTA (nickel-nitrilotriacetic acid) resin (QIAGEN) for 60 min. Resin equilibration was achieved by washing the Ni-NTA agarose bead suspension twice with water and twice with lysis buffer. The agarose bead suspension was mixed with the soluble fraction and centrifuged for 3 min at 3,500 rpm. The supernatant was removed as 'unbound protein'. The beads were washed four to five times with column buffer, (washing included mixing and centrifugation for 3 min at 3,500 rpm). Recombinant protein was eluted by washing the beads three to four times with elution buffer (lysis buffer + 250 mM imidazol). Elution involved incubation of agarose beads with elution buffer for 5 min at RT and centrifugation for 3 min at 3,500 rpm. The eluted products from all the steps were pooled as eluted recombinant protein which consisted of His_6-tagged fusion protein.

3.2.7 Large scale purification of His_6- and MBP-tagged proteins

The total soluble protein fraction was filtered through a 0.45 µM filter and loaded on to a 1 mL His-trap column or 1 mL MBP column (Amersham Biosciences). Columns were pre-equilibrated with 50 mM KH_2PO_4 /K_2HPO_4 (potassium phosphate) buffer [pH 7.6 containing 0.9 M NaCl, 50 mM glycine and 5% (v/v) glycerol for His-trap and column buffer for MBP columns connected to an AKTA FPLC (Amersham Biosciences) at a flow rate of 1 mL/min. Unbound proteins were eluted by extensive washing of the columns with equilibration buffer. Bound proteins were eluted with a linear gradient from 20 mM to 0.4 M imidazole (for His-trap) or 0.5 to 1.0 M maltose (for MBP-trap). Pooled fractions were desalted with a PD-10 desalting column or passed over a Sephadex G25 column (Amersham Biosciences). Eluted protein was further purified using HiTrap MonoQ HP column (5 mL, Amersham Bioscience) following manufacturer's instructions. The eluted protein thus obtained was analysed on a SDS-PAGE gel.

3.2.8 Concentration of purified proteins

Eluted proteins were concentrated using centricon 50YM filters (Millipore) which have a cut-off level of 50,000 Da. The pooled eluted protein was added to the sample reservoir fixed with the filtrate vial and spun at 8000 rpm for 15 min. The filterate was discarded and the remaining sample in the reservoir as retentate (concentrated protein) was stored at -20˚C until further use.

3.2.9 SDS-PAGE analysis of proteins

SDS-PAGE separation of protein samples (un-induced extract, induced crude extract, soluble fraction, unbound protein, washed protein, eluted protein) was performed using 4-12% NuPAGE Novex Bis-Tris Gels (Invitrogen) or home-made PAGE gels at 200 V. Protein samples mixed with 2x LDS loading dye (Invitrogen) were boiled for 3-4 min and loaded on the gel along with prestained marker proteins (Broad range marker, New England Biolabs). Gels were washed with distilled water and boiled three times with 100 mL distilled water for 5 min. Protein bands were visualized by staining with SimplyBlue SafeStain (Invitrogen). The gels were washed with distilled water until clear bands were visualised.

3.2.10 Bradford assay

The Bradford assay was performed to measure the concentration of protein in extracts. A standard curve of BSA at 0, 0.05, 0.1, 0.2, 0.3, 0.4, 0.5, 0.6, 0.8, 1.0 mg/mL concentrations was prepared with protein dilution buffer. 20 µL of each BSA standard was added to 1 mL of 1:5 Bradford reagent (Invitrogen) in water and incubated at RT for 5 min. Absorbance readings were recorded at OD_{595}. Protein samples 20 µL each of diluted and undiluted were added to 1 mL of 1:5 Bradford reagent in water and measured for their OD at 595 nm and were compared with the standard curve for BSA to obtain their concentrations.

3.2.11 Removal of fusion tags and protein purification

The eluted MBP fusion proteins were digested with TEV protease to remove the tag. Digested proteins were purified to remove the protease and undigested whole proteins with tag as described below.

3.2.11.1 TEV protease digestion

TEV protease (1-3 µg) was used to cleave 100 µg of fusion protein. The reaction mix consisted of 100 µg AAT enzyme, 1.5 µg of protease, 1x TEV protease buffer (50 mM Tris HCl; pH 7.5, 1 mM EDTA, 5 mM DTT, 50% glycerol, 0.1% Triton X 100) and incubated overnight at 22°C. The enzyme reaction was stopped using 1 mM PMSF.

3.2.11.2 Purification of TEV-protease digested protein

The digested protein mix of His_6-MBP fusion proteins consisted of uncleaved protein, cleaved protein and other components which can hinder the activity of the cleaved

protein and hence needed to be removed. Reactions were mixed with equilibrated His-resin (QIAGEN) for 30 min at 4°C, centrifuged and the supernatant, consisting of cleaved protein, was collected. Cleaved tag and uncleaved fusion protein were left bound to the His-resin. This bound material was eluted with a stringent Imidazole wash, for reuse of the resin.

3.2.12 Western blotting

Proteins were separated by SDS-PAGE gel and transferred onto nitrocellulose membranes (Schleicher and Schuell BioScience GmBH) in transfer buffer (25 mM Bis-Tris, 192 mM Bicine, 10% (v/v) methanol) at 100V for 1 hr. After ensuring complete transfer of proteins using Ponceau stain the blot was blocked with blocking buffer (1x PBS; 50 mM phosphate, 0.9% NaCl pH 7.2, + 3% w/v BSA + 2% w/v dried milk powder) for 1 h at RT. The blot was incubated with primary antibody [dilutions in table 3.2] in blocking solution for 1 h, washed with PBST, twice, and incubated with secondary antibody [Table 3.2] in blocking solution for 1 h. After washing with PBST, twice for 15 min, the blot was developed with 1x alkaline phosphate buffer (100 mM Tris-Cl pH9.5, 100 mM NaCl, 5 mM $MgCl_2$) + 60 µL NBT + 60 µL BCIP and air dried. Target proteins were visualised directly as purple coloured bands.

Table 3.2 | Antibodies used in detecting MBP and His-tag fusion proteins

Fusion protein	Antibody	Type	Dilution
MBP	Primary	Anti MBP raised in rabbit	1:10,000
MBP	Secondary	Goat anti-rabbit IgG AP conjugate	1: 1000
Histidine	Primary	Anti His raised in mouse	1: 1000
Histidine	Secondary	Goat anti-mouse IgG AP conjugate	1: 5000

3.2.13 Enzyme assays

3.2.13.1 Standard assay conditions for the enzymes

The standard reaction mixture consisted of 5-20 µg of enzyme, 20 mM Phosphate buffer pH 7.4, 1 mM EDTA, 60 µM acyl donor and 120 µM acyl acceptor. The reaction mix without enzyme was incubated for 5 min at 30°C and the reaction was initiated by addition of enzyme, and run for 20 min at 30°C. The reaction was terminated by addition of an equal volume of 0.5% ice cold TCA/TFA.

3.2.13.2 Identification of reaction products with LC/MS

Reaction products were separated and identified by LC/MS (Luo et al., 2007). Samples (5 µL) were centrifuged and the supernatants were separated on a Surveyor HPLC system using a 100×2mm 3µm Luna C18 (2) reverse phase column (Phenomenex) by running a gradient of 0.1% formic acid in water versus methanol (2-70%) with a flow rate of 230 µL/min. Detection was by UV at 200-600 nm and positive electrospray MS using a DecaXP^{plus} ion trap (Thermo Fisher). The products were analysed using a QUAL browser.

3.2.13.3 HPLC separation of the reaction products

HPLC separation was the same as described in chapter IV. The eluant was monitored using a diode array detector at 520 nm and the anthocyanins were compared to external standards.

3.2.14 Primary sequence alignment

The protein sequences of some of the biochemically characterised enzymes were taken from the NCBI (http://www.ncbi.nlm.nih.gov/) protein database and were submitted to EMBL ClustalW for analysis.

3.2.15 Tobacco transformation

The leaf disc method of *Agrobacterium*-mediated transformation was performed using the binary vectors described in this chapter. Detailed protocols are presented in chapter IV.

3.2.16 Sequencing of clones

Clones constructed were sequenced before using them for protein and over-expression studies. Big Dye (3.1) sequencing reactions were performed using several primers [Table 3a] per gene (spanning the full length of each gene) and the reactions sequenced at Genome Enterprise Limited™. The raw sequencing data obtained was analysed using VectorNTI software™ (Invitrogen).

3.3 Results

3.3.1 Purification of AAT enzymes for structural studies

Structural studies of enzymes are required for a complete understanding of their biochemical and substrate specificities. Here, attempts were made to study the structures of Sl3AT, At3AT and Gt5AT enzymes. l3AT, At3AT and Gt5AT were expressed as recombinant proteins in *E. coli*. Sl3AT (*Solanum lycopersicum* 3-*O*-acyltransferase), At3AT (*Arabidopsis thaliana* 3-*O*-acyltransferase), Gt5AT (*Gentiana triflora* 5-*O*-acyltransferase) and Ch3MAT (*Chrysanthemum morifolium* 3-*O*-acyltransferase) which have different acceptor and donor specificities were studied.

3.3.1.1 Purification of Sl3AT for structural studies

Sl3AT is an AAT isolated from tomato fruit over expressing the regulatory genes, Delila (Del) and Rosea1 (Ros1) (Butelli et al., 2008) and transfers a *p*-coumaroyl group onto 6‴-position of rhamnose of cyanidin 3-*O*-rutinoside (Kallam K, M.Sc thesis 2007) [Fig 3.4a]. Sl3AT was cloned in different expression vectors with different tags [Table 3.3] regulated by a T7 promoter, to obtain soluble fusion proteins. As initial studies showed a highly insoluble protein, several expression strategies using various constructs were performed. N-terminal His_6-tag Sl3AT protein was purified from the soluble fraction of *E. coli* homogenates using three steps of column chromatography (His-trap HP, Sephadex G-25 and Mono Q). After three steps of chromatography the protein was purified to near homogeneity as shown by SDS-PAGE [Fig 3.4b] although a second protein of smaller size compared to Sl3AT protein (~55 kDa) was observed as a second band on SDS-PAGE gel. The smaller protein could not be separated even after several purification steps. As AATs have been shown to be monomeric enzymes (D'Auria, 2006) the smaller sized protein was interpreted to be a degraded product of the Sl3AT protein. The activity of the His_6-Sl3AT protein was totally lost after long purification procedures. Hence, further attempts to crystallize this protein were abandoned.

3.3.1.2 Purification of At3AT for structural studies

At3AT catalyzes a similar reaction to Sl3AT, but transfers the *p*-coumaroyl moiety onto the 6″ position of 3-glucose of cyanidin 3-*O*-glucoside (Luo et al., 2007) [Fig 3.5a]. A structural comparison of the At3AT was undertaken to identify the evolutionary differences between it and Sl3AT and Gt5AT. At3AT was cloned in different expression vectors [Table 3.3] for parallel expression of soluble protein in large amounts.

Purification of the N-terminal His_6-tag protein was performed using a His-trap column and ion-exchange chromatography [Fig 3.5b]. Soluble protein showed the desired activity; acylation of cyanidin3-*O*-glucoside with a coumaroyl group from coumaroyl-CoA [Fig 3.5c], but the purified protein lost its enzymatic activity [Fig 3.5d]. Crystallization attempts were not made due to loss of protein activity and lack of sufficient time for repetition.

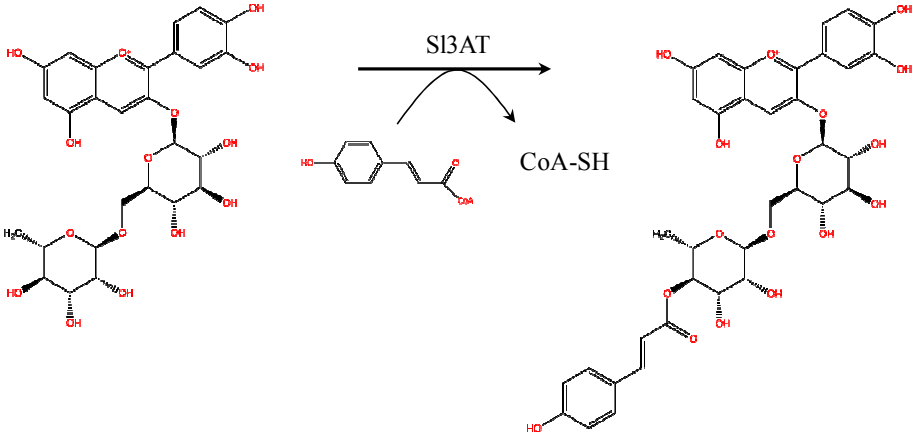

(a)

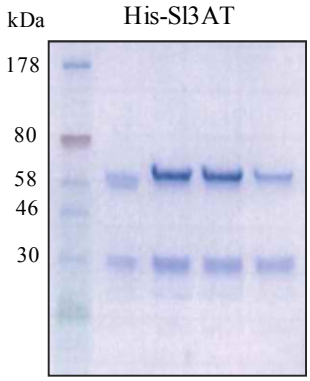

(b)

Figure 3.4 | (a) Reaction catalyzed by Sl3AT depicting the position of coumaroylation; cyanidin 3-*O*-rutinoside was converted to cyanidin 3-(6″ coumaroyl) rutinoside (b) SDS-PAGE analysis of His-Sl3AT protein after three steps of chromatographic purification. Sl3AT protein was observed as a band of size ~55 kDa. The degradation product of the Sl3AT protein was around size <30 kDa.

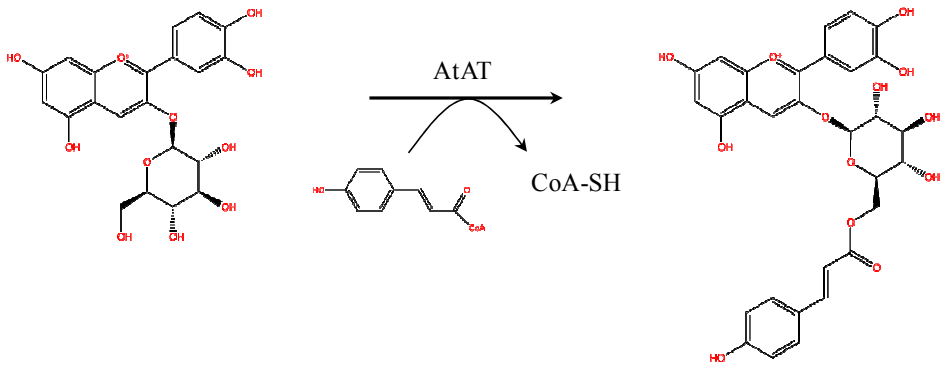

(a)

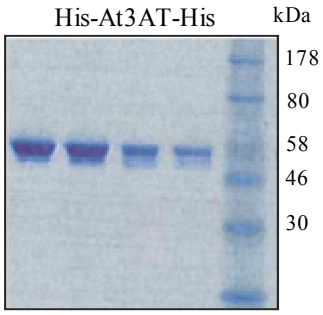

(b)

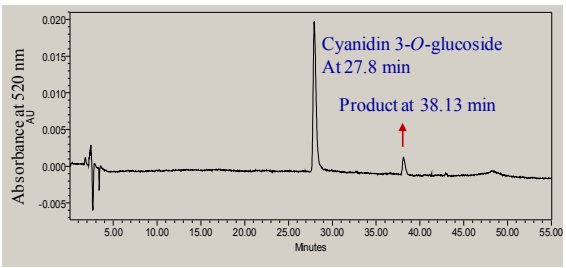

(c)

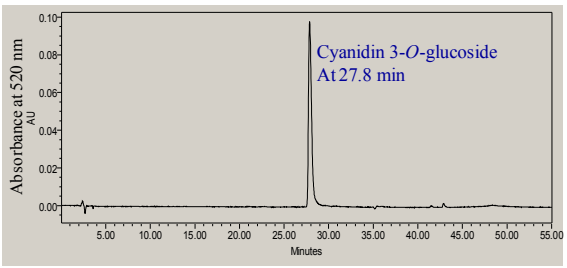

(d)

Figure 3.5 | (a) Reaction catalyzed by At3AT depicting the position of coumaroylation; cyanidin 3-*O*-glucoside was converted to cyanidin 3-(6″ coumaroyl) glucoside (b) SDS-PAGE analysis of His-At3AT-His protein, size ~55 kDa after two step chromatographic purification (c) HPLC chromatogram of soluble His-At3AT-His enzymatic reaction showing cyanidin 3-(6″ coumaroyl) glucoside formation as product at 38.13 min. (d) HPLC chromatogram of purified His-At3AT-His enzymatic reaction showing cyanidin 3-*O*-glucoside alone at 27.8 min.

3.3.1.3 Purification of Gt5AT for structural studies

Gt5AT is an aromatic acyltransferase which was cloned and characterized by (Fujiwara et al., 1997) and transfers a caffeoyl group onto the 5-glucose moiety of delphinidin 3-*O*-glucoside 5-*O*-glucoside. Codon optimised Gt5AT was cloned in different vectors with different tags as shown in table 3.3. Protein expressed in *E. coli* Rosetta II cells accumulated in the soluble fraction in moderate amounts as observed by SDS-PAGE. Extracts of N-terminally His_6-tagged Gt5AT showed many proteins which interacted with a His-trap HP ml column and several optimization protocols did yield a partially homogenous protein [Fig 3.6b]. His_6-Gt5AT purified protein, though not pure, showed activity as analysed by HPLC [Fig 3.6d]. Incubation of the recombinant protein with cyanidin 3, 5-*O* di-glucoside and coumaroyl-CoA showed a new peak compared to a control reaction with no enzyme [Fig 3.6c]. Preliminary crystallization trails with the His_6-Gt5AT purified protein were performed using the sitting drop-vapour diffusion method with an "in-house" classic screen (performed by Dr. Clare Stevenson) at 4°C. After nearly fifteen days of incubation protein in few conditions precipitated and tiny crystals were formed in screens with PEG. But as the crystals never grew bigger for further diffraction studies the crystallisation attempts were abandoned.

Table 3.3 | Expression clones constructed for Sl3AT, Gt5AT and At3AT

Gene	Expression vector	Position of tag	Clone obtained	Fusion protein size in kDa
Sl3AT	pET24a	C-terminal His_6-tag	pE24Sl3AT	53.14
	pET28b	N-terminal His_6-tag	pE28Sl3AT	53.14
	pMGWA	N-terminal MBP-tag	p525tevSl3AT	95.78
	pHGWA	N and C-terminal His_6-tag	p528Sl3AT	54.87
	pHMGWA	N-terminal His_6-MBP tag	p530tevSl3AT	90.06
Gt5AT	pET24a	C-terminal His_6-tag	pE24Gt5AT	56.7
	pET28b	N-terminal His_6-tag	pE28Gt5AT	56.7
	pHGWA	N and C-terminal His_6-tag	p528Gt5AT	57.7
	pMGWA	N-terminal MBP-tag	p525tevGt5AT	96.72
At3AT	pET24a	C-terminal His_6-tag	pE24At3AT	54.08
	pET28b	N and C-terminal His_6-tag	pE28At3AT	55.15
	pHGWA	N and C-terminal His_6-tag	p528At3AT	55.35
	pHMGWA	N-terminal His_6-MBP-tag	p530tevAt3AT	95.5

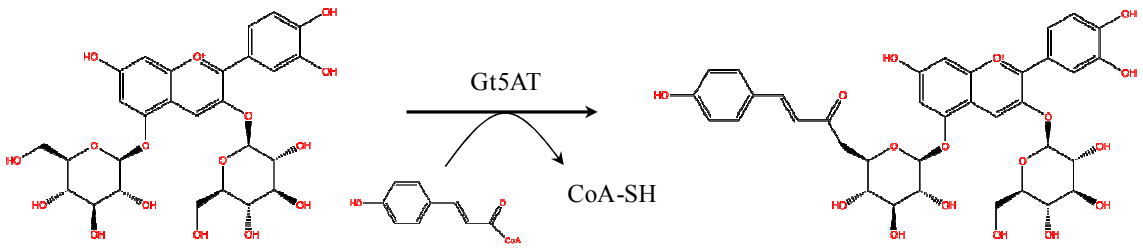

(a)

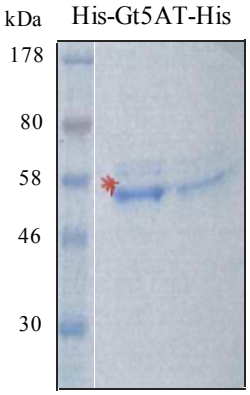

(b)

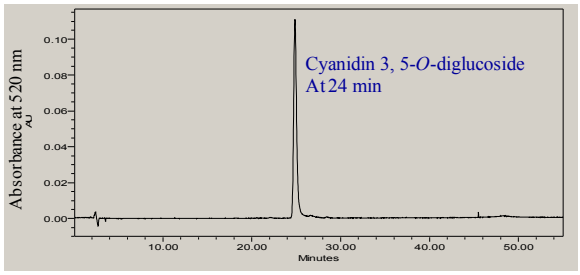

(c)

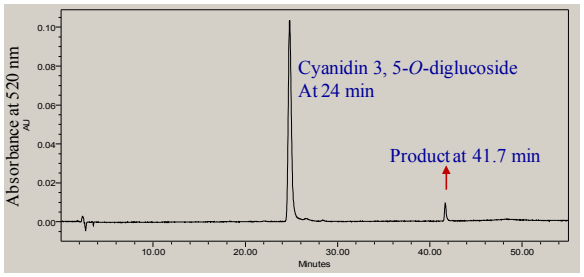

(d)

Figure 3.6 | (a) Reaction catalyzed by Gt5AT depicting the position of coumaroylation; cyanidin 3,5-*O*-diglucoside was converted to cyanidin 3,5-(6″ coumaroyl) diglucoside (b) SDS-PAGE analysis of His-Gt5AT-His protein after two steps of chromatographic purification, size ~55 kDa (c) HPLC chromatogram of control reaction without His-Gt5AT-His protein showing cyanidin 3,5-*O*-diglucoside at 24 min. (d) Chromatogram of enzyme catalysed reaction with reaction product cyanidin 3-(6″ coumaroyl) 5-diglucoside eluting at 41.7 min is shown.

3.3.2 Identification of residues that determine the donor specificity of AATs

Anthocyanin acyltransferases (AATs) have broad acyl acceptor specificities but strict acyl donor specificities and strict regio-specificities for the position of acylation on the acyl acceptor. Aliphatic acyltransferases generally do not use aromatic acyl-CoAs, such as p-coumaroyl-CoA and caffeoyl-CoA as substrates, and aromatic acyltransferases generally do not use aliphatic acyl-CoAs, such as malonyl-CoA and acetyl-CoA as substrates (Nakayama et al., 2003).

I compared Sl3AT, At3AT, Gt5AT and Ch3MAT anthocyanin acyltransferases in this study. Ch3MAT is an aliphatic acyltransferase which transfers a malonyl moiety onto the 6″ position of the 3-glucose of cyanidin 3-*O*-glucoside (Suzuki et al., 2004a) [Fig 3.7] and was used for comparative studies with aromatic AATs.

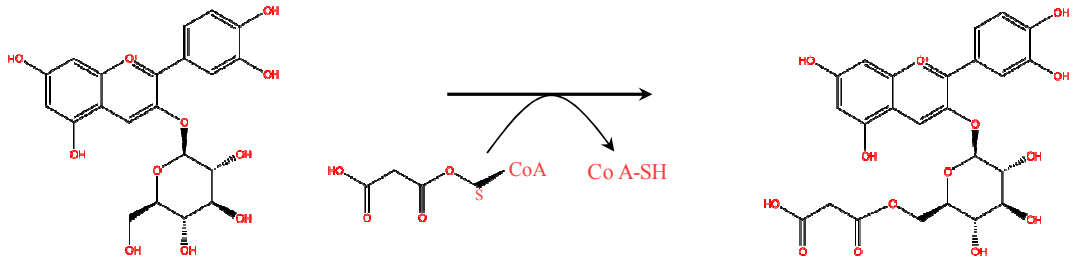

Figure 3.7 | (a) Reaction catalyzed by Ch3MAT depicting the position of malonylation; cyanidin 3-*O*-glucoside was converted to cyanidin 3-(6″ malonyl) glucoside.

3.3.2.1 Primary sequence guided donor specificity determination

Although BAHD acyltransferases have sequence identities between 15-30% only, they share two important conserved motifs, motif-1; His-Xaa3-Asp (H*XXX*D) located near the central portion of each enzyme and motif-3; Asp-Phe-Gly-Trp-Gly (DFGWG) which is located near the carboxy terminus (D'Auria, 2006). Motif-2; Tyr-Phe-Gly-Asn-Cys (YFGNC) is conserved mainly in AATs which share 20-40% sequence similarity (Nakayama et al., 2003). The histidine in motif-1 was shown to be involved in acid base catalysis, whereas motif-3 is thought to have a structural role in BAHD acyltransferases (Ma et al., 2005). Alignment studies of several AAT sequences led to identification of several conserved amino acids within AATs exhibiting similar acyl-donor specificities (Suzuki et al., 2002, Nakayama et al., 2003). Multiple alignment of amino acid sequences of Sl3AT, At3AT, Gt5AT, Ch3MAT along with some of the other characterised AATs showed the conserved motifs –H*XXX*D- (motif-1), – YFGNC- (motif-2) and –DFGWG-

Figure 3.8 | Multiple sequence alignment of some of the characterised AATs.

Alignment of the amino acid sequences of AATs: At3AT1 and At3AT2, Pf3AT, SsMAT1, Gt5AT, Dm3MAT1 and Dm3MAT2, Sc3MAT, Dv3MAT, At5MAT, Ss5MAT2, ToAT (Sl3AT) (details of these AATs are presented in Table 1.2; chapter 1) and VS; vinorine synthase a BAHD enzyme was performed using ClustalW. Conserved motifs among AATs were showed. Motif-1 is the conserved H*XXX*D sequence, motif-2 is the YFGNC and motif-3 is the DFGWG sequence. Amino acid sequences of enzymes used in this study were indicated in the figure. Different colours in the alignment represent similar amino acids.

(motif-3) [Fig 3.8]. Comparison of these sequences showed a phenylalanine (aromatic amino acid) present near motif 1 (Phe^{181} of At3AT, Gt5AT and Phe^{180} of Sl3AT) to be conserved in aromatic AATs and replaced by an aliphatic amino acid (Arg^{183} of Ch3MAT) in the aliphatic AATs. These observations were in accordance with earlier observations (Nakayama et al., 2003, Suzuki et al., 2002) [Fig 3.9] although no attempts to understand the importance of these residues had been performed. Hence, based on this observation, site directed mutagenesis of amino acids might give a clue in understanding the role of these residues in determining specificity for acyl donor substrates.

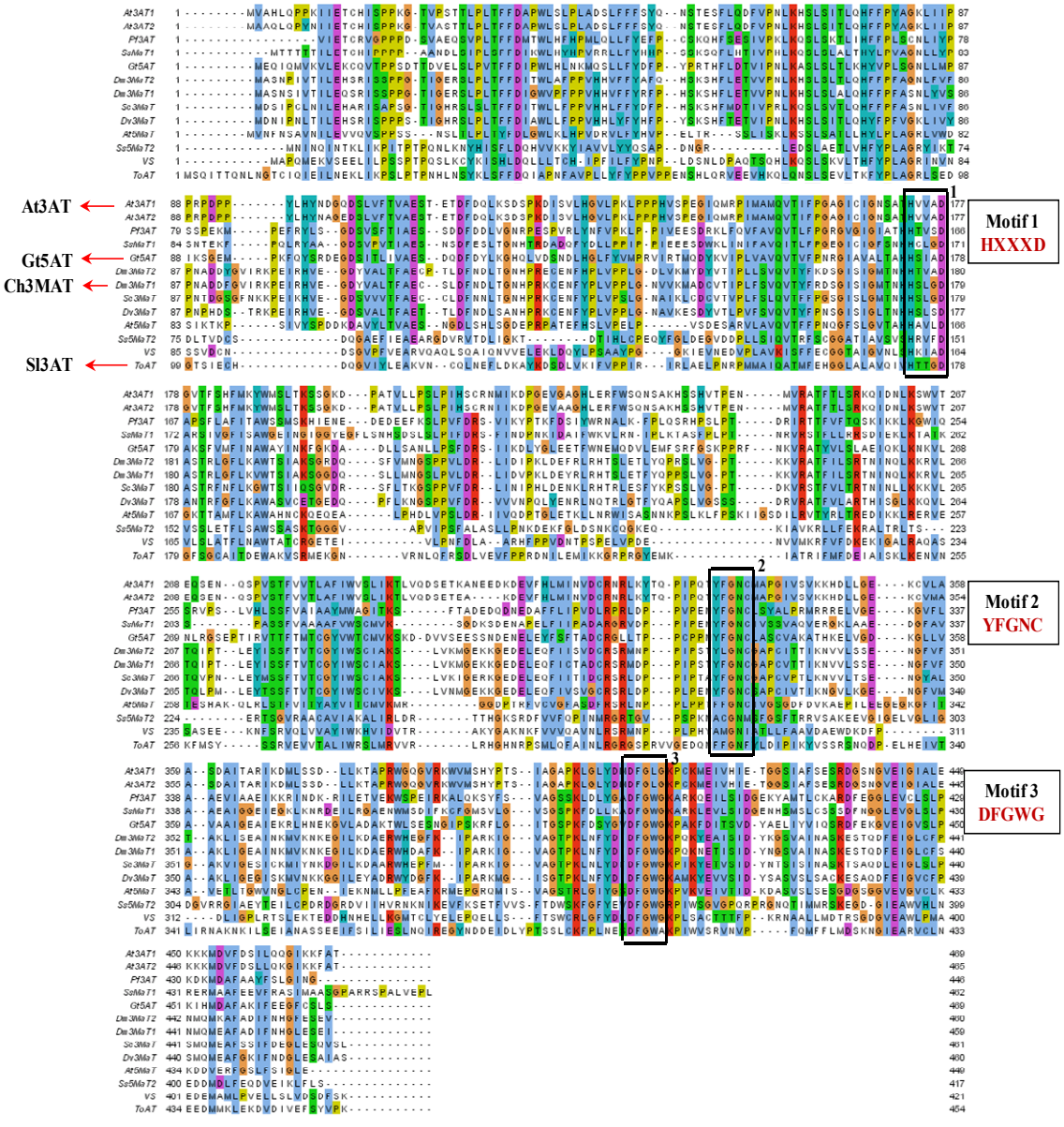

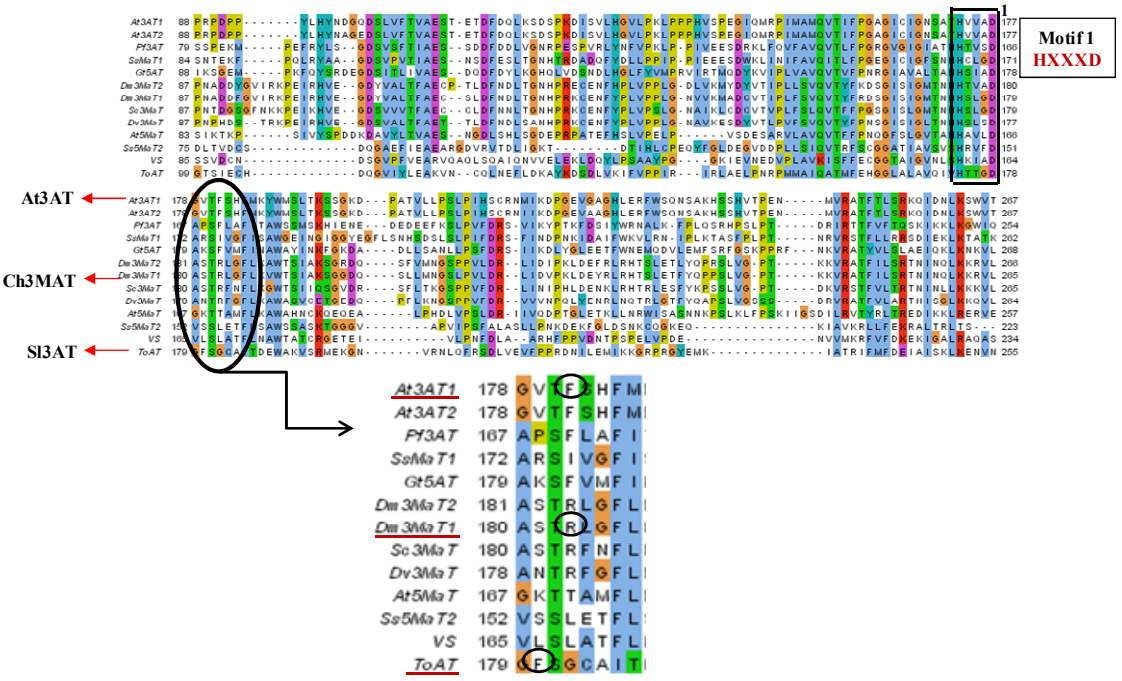

Figure 3.9 | Conserved aromatic amino acids adjacent to motif-1 in AATs predicted to be responsible for acyl donor specificity of the enzymes. Phenyl alanine (F) of aromatic AATs which is replaced by Arginine (R) in aliphatic AATs was predicted to influence the specificity of the enzymes for acyl donors. Motif-1 is shown in box and the amino acids mutated in At3AT, Dm3MAT1 (Ch3MAT) and ToAT (Sl3AT) enzymes in this study are shown enlarged below. In this alignment aromatic AATs are: At3AT1, At3AT2, Pf3AT, Gt5AT and ToAT (Sl3AT) and aliphatic AATs are: SsMaT1, Dm3MaT2, Dm3MaT1, Sc3MaT, Dv3MaT, At5MaT and Ss5MaT2.

3.3.2.2 Homology modelling guided determination of donor specificity

Homology modelling predictions of Sl3AT and At3AT structures (based on the co-ordinates of Dm3MAT3 (PDB Id: 2E1T); identified His^{171} in the catalytic centre of the enzymes [Fig 3.10a] (Kallam K, M.Sc, 2007). Independent docking of 3MAT (Dm3MAT3) with substrates cyanidin 3-*O*- glucoside and malonyl-CoA showed proximity of the His^{170} and Arg^{183} residues to the substrates [Fig 3.10b]. Unno et al., (2007) showed that Arg^{178} in MAT near motif1 and Gly^{386} are involved in binding malonyl-CoA. Superimposition of the modelled structure of At3AT and 3MAT structures showed overlap of Phe^{181} of At3AT and Arg^{183} of MAT [Fig 3.10c] (Kallam K, M.Sc, 2007). Based on these modelling predictions, single amino acid substitutions were constructed for understanding the specificity of AATs.

Figure 3.10 | Homology modelled structures of Sl3AT, At3AT and Ch3MAT

(a) Structure of Sl3AT based on modelling to Ch3MAT showing His^{174} residue in blue.

(b) Super imposed Sl3AT model with Ch3MAT structure showing overlap of histidine of motif-1 of both the proteins.

(c) Malonyl-CoA (stick model) is shown entering the channel of the Ch3MAT based on autodocking of malonyl Co-A to the Ch3MAT structure.

(d) Cyanidin 3-*O*-glucoside (purple/red stick model) and malonyl-CoA (green/red stick model) entering through the Ch3MAT enzyme pocket from opposite sides is shown.

(e) Internal view of the interaction of His^{170} (shown as red patch) and Arg^{183} (shown as violet patch) with the acyl donor substrates as obtained through docking results for Ch3MAT.

(f) Super imposition of model of At3AT with Ch3MAT structure showing the overlap of residues (His and Phe) of At3At with those (His and Arg) involved in catalysis of Ch3MAT.

(a)

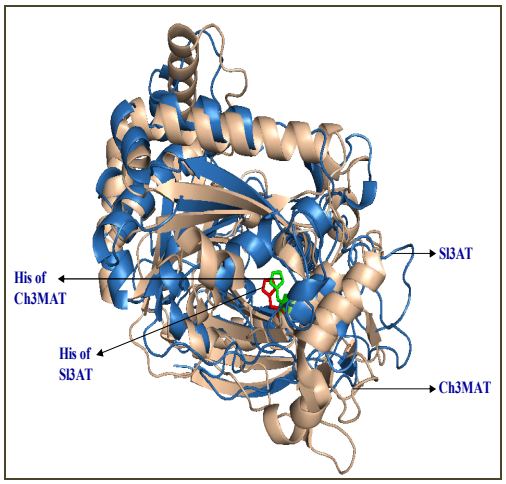
His of
Ch3MAT
His of
Sl3AT
Sl3AT
Ch3MAT

(b)

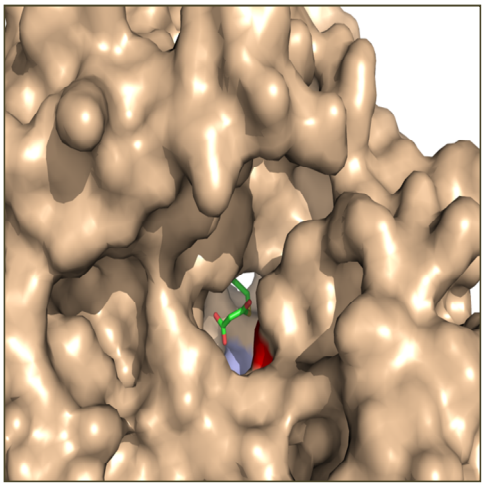

(c)

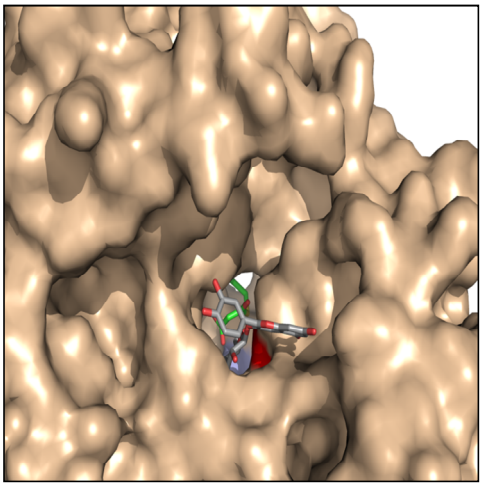

(d)

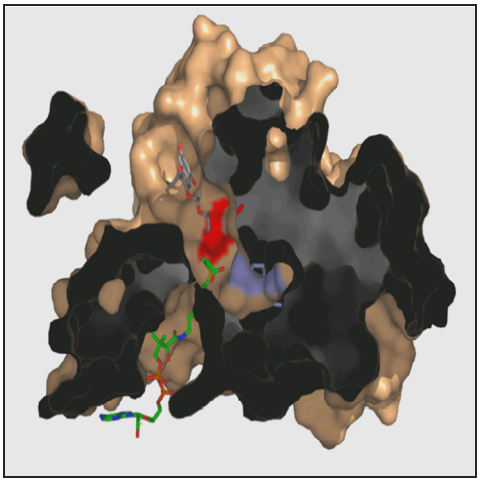

(e)

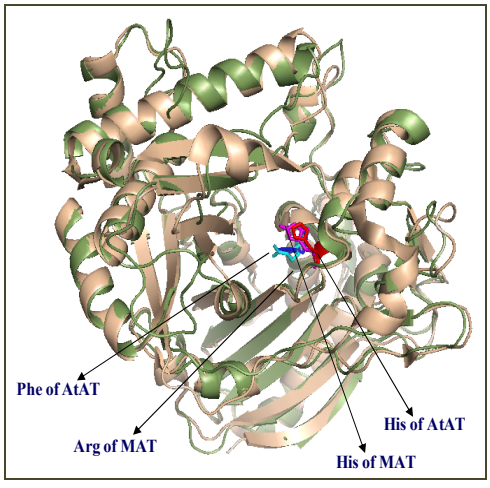
Phe of AtAT
Arg of MAT
His of AtAT
His of MAT

(f)

3.3.3 Understanding the catalytic site of aromatic AATs

The histidine residue of motif-1 H*XXX*DG has been shown to be involved in general acid base catalysis in the BAHD family of enzymes (Ma et al., 2005, Unno et al., 2007). In order to understand the role of this histidine in aromatic AATs, His^{174} (a polar charged amino acid) of Sl3AT was mutated to asparagine (a polar uncharged amino acid) using site directed mutagenesis [Fig 3.11], and the mutated H174N-Sl3AT was expressed as a His_6-tag protein. Enzymatic analysis of the mutated H174N-Sl3AT protein with cyanidin 3-*O*-rutinoside and coumaroyl-CoA showed coumaroylated anthocyanin (~2.5% of total anthocyanin) as a peak at 40.39 minutes [Fig 3.12] similar to wild type protein (whose product is also ~2.5% of total anthocyanin). An earlier study by Suzuki et al., (2003a) showed a reduced enzymatic activity of AAT when the histidine of motif 1 was replaced by alanine. However, I could not determine the activity levels of the H174N-Sl3AT protein in comparison with Sl3AT due to low enzymatic activity of the wild type protein. Additionally, the kinetic properties of the mutated protein could not be studied due to low product formation. This study showed that histidine in the H*XXX*D motif-1 can be complemented to maintain the catalysis of acyltransferases. However, a more thorough kinetic study of the mutated protein is essential to understanding the role of histidine of motif 1 in aromatic AATs. Together with earlier studies it can be concluded that other residues in the enzymes can complement the loss of crucial residues involved in catalysis.

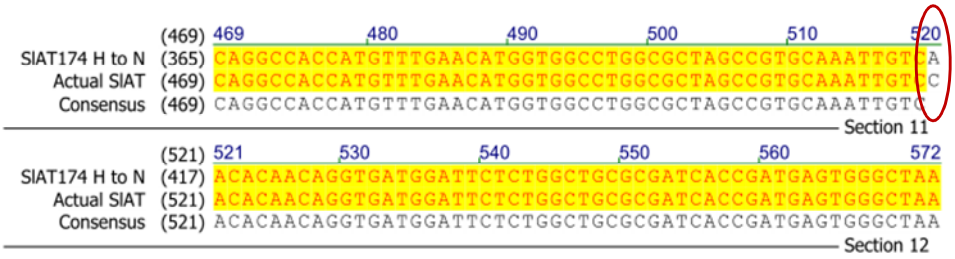

(a)

Sl3AT	RPMMAIQATMFEHGGLALAVQIVHTTGDGFSGCAITDEWAKVSRMEKGNV	50
Sl3AT-H174N	RPMMAIQATMFEHGGLALAVQIVNTTGDGFSGCAITDEWAKVSRMEKGNV	50

(b)

Figure 3.11 | Mutagenesis of histidine of *Sl3AT* (a) Nucleotide sequence showing the nucleotide mutated to attain a mutation in H174N-Sl3AT protein (b) Mutation of His^{174} (H) of Sl3AT protein sequence to aspargine (N) is illustrated with a colour change

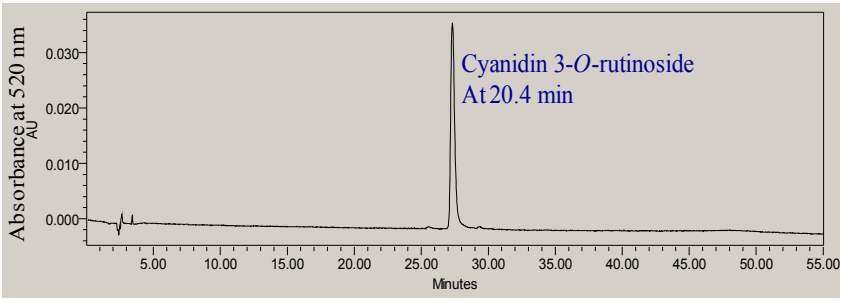

(a)

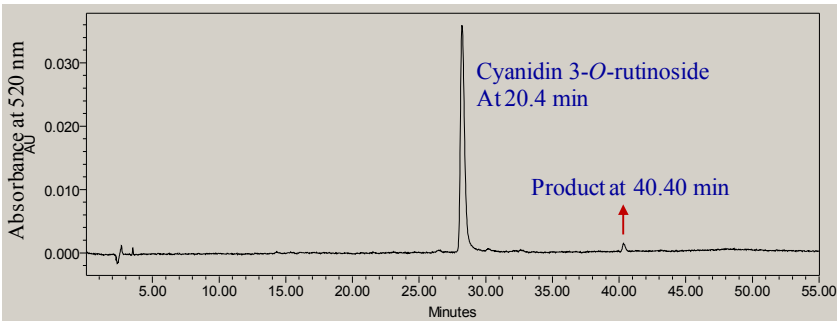

(b)

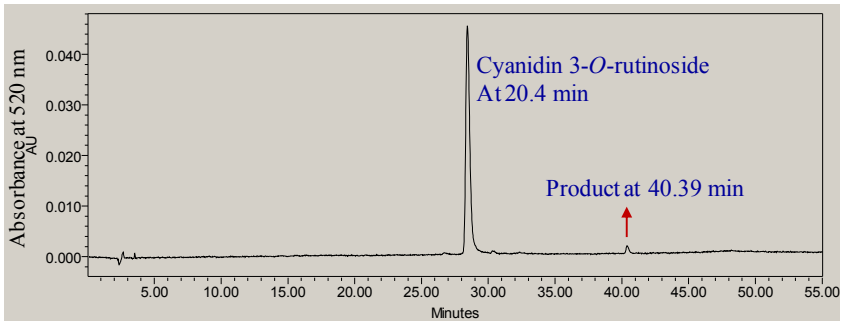

(c)

Figure 3.12 | Enzymatic analysis of wild type and mutant Sl3AT (a) HPLC chromatogram of control reaction showing cyanidin 3-*O*-rutinoside at 20.4 min (b) Enzyme reaction catalysed by His_6-Sl3AT soluble protein using cyanidin 3-*O*-rutinoside and coumaroyl-CoA as substrates for 20 min at 30°C. Reaction product cyanidin 3-(6″ coumaroyl) rutinoside was eluted at 40.4 min. (c) Enzyme reaction catalysed by His^6-H174N-Sl3AT soluble protein using cyanidin 3-*O*-rutinoside and coumaroyl-CoA as substrates. Reaction product was eluted at 40.4 min similar to His_6-Sl3AT reaction.

3.3.4 Understanding acyl-donor specificity of acyltransferases

3.3.4.1 An in-vitro donor specificity study

Based on the comparison of primary sequences and the modelling predictions as described in section 3.3.2.1 and 3.3.2.2 respectively, an amino acid in each AAT (Sl3AT, At3AT and Ch3MAT) was substituted to study their substrate specificity determinants. The Phe^{180} residue of Sl3AT was mutated to Arg^{180} (SlAT-F180R), the Phe^{181} residue of At3AT was mutated to Arg^{181} (AtAT-F181R) and the Arg^{183} of Ch3MAT was mutated to Phe^{183} (Ch3MAT-R183F) through site-directed mutagenesis [Fig 3.13].

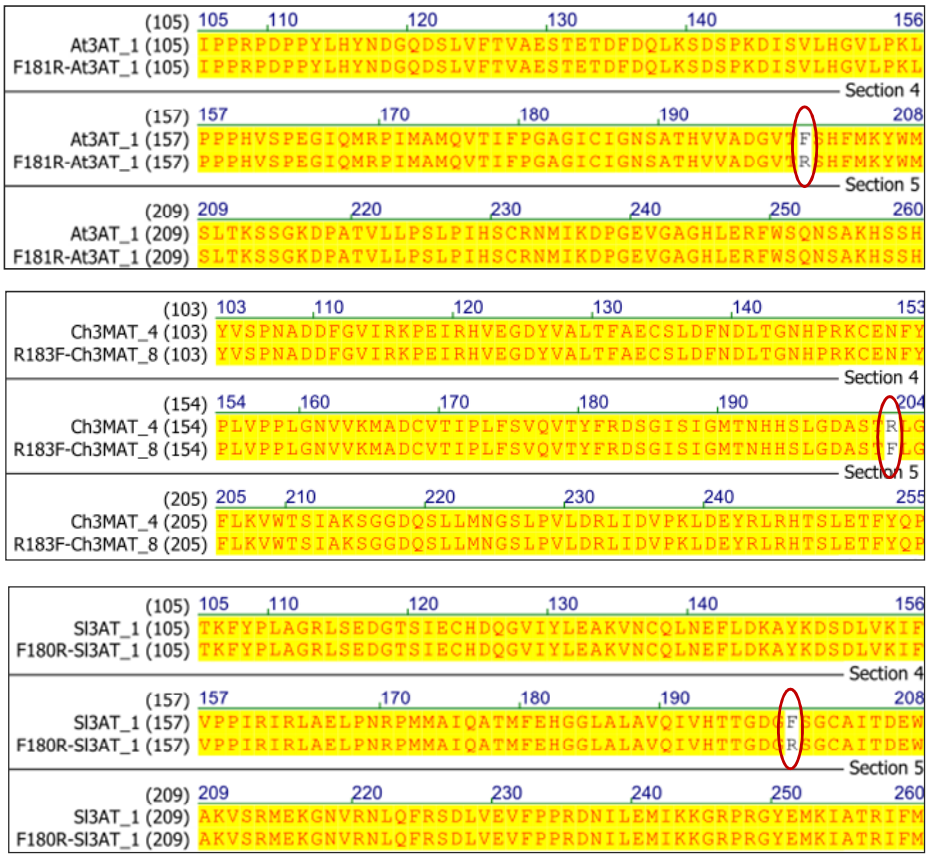

Figure 3.13 | Site directed mutagenesis of At3AT, Ch3MAT and Sl3AT to obtain the mutant proteins; F18R-At3AT, R183F-Ch3MAT and F180R-Sl3AT. Translated protein sequences from positive gene constructs of each gene (wild type and mutated) were aligned and the desired mutation is indicated by red circle.

The mutagenised plasmids were expressed as S-tag fusion proteins in *E.coli* regulated by the T7 promoter. Crude, soluble fusion protein extracts of both wild type and mutant proteins were assayed for enzymatic activity with different substrates. Wild type and mutant Sl3AT proteins could not be studied due to their low activities, although expression of soluble protein was observed [Fig 3.14].

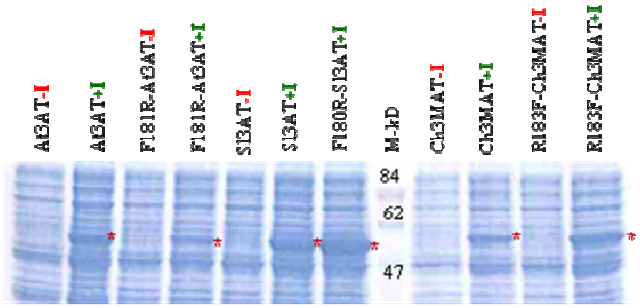

Figure 3.14 | Total protein expression analysis of wild type and mutant proteins of At3AT, Sl3AT and Ch3MAT. SDS-PAGE gel of At3AT, Sl3AT and Ch3MAT and their mutant proteins. Expressed proteins are indicated by asterisk * (size 55 kDa). -I in red; uninduced protein, +I in green; induced proteins.

At3AT is an aromatic acyltransferase which can accept only aromatic-CoAs (Luo et al., 2007). S-tag fusion-At3AT protein showed activity with cyanidin 3-*O*-glucoside (acceptor) and coumaroyl-CoA (as donor) but no activity with malonyl-CoA as donor. The mutant F181R-At3AT protein did not abolish aromatic acylation but gained aliphatic acylation specificity by accepting malonyl-CoA as donor. The gain of new preference by F181R-At3AT was shown by the formation of cyanidin 3-(malonyl) glucoside (m/z 535). The control reactions of empty vector proteins showed no activity. Mass fragmentation data obtained confirmed these results [Table 3.4 & Fig 3c; appendix].

Ch3MAT is an aliphatic acyltransferase that can accept only aliphatic-CoAs to catalyse the malonylation of cyanidin 3-*O*-glucoside (Suzuki et al., 2004a). Wild type Ch3MAT S-tag fusion protein showed activity with cyanidin 3-*O*-glucoside and malonyl-CoA whereas no detectable activity was observed when coumaroyl-CoA was used as the

donor in combination with the same acceptor. The mutation of R183F in Ch3MAT did not abolish the ability of the enzyme to transfer a malonyl group to anthocyanin but it gained an acetylation property. MS data confirmed the same result [Table 3.4 & Fig 3c; appendix]. A very small amount of coumaroylated anthocyanin product was detected (chromatography data are provided in the appendix) which was identified based on its retention time, but which could not be detected by mass fragmentation.

In all the enzymatic reactions two products of masses 549 (m/z) and 491(m/z) were observed at 520 nm. Based on molecular weight, the compound of mass 549 (m/z) was identified as cyanidin 3-*O*-glucoside (m/z; 449) with sodium fluoroacetate (m/z 100) attached to it. And the product at 491 (m/z) was cyanidin 3-(6-acetyl) glucoside. The fragmentation pattern of these two compounds confirmed cyanidin as the parent molecule [Table 3.4 & Fig 3c; appendix]. This showed that the TFA used to stop the enzymatic reaction and sodium from the buffer are competing with acyl-CoAs for the anthocyanins. Since these products are artefacts of the assay, they were ignored in the analysis.

Based on the *in-vitro* data obtained with the mutant proteins, F181R-At3AT and R183F-Ch3MAT, it is likely that the phenylalanine situated close to motif 1 may not be crucial for aromatic acyl-CoA specificity. And other residues present in the enzyme pocket which are specific to aromatic AATs are important in dictating coumaroylation activity. However a partial switch to aliphatic acyl-CoA donor specificity was obtained by presence of Arg^{181} in At3AT supporting the hypothesis that the Arg residue at around position 180 is responsible for influencing acyl donor specificity (Unno et al., 2007). The specificity was not completely changed by the mutations emphasising the importance of other residues in determining donor specificity. The features that determine the position of acylation on the acceptor were not influenced by the mutations.

Table 3.4 | Characteristics of the anthocyanin products obtained in enzyme catalysed reactions of wild type S-tag At3AT, Ch3MAT and mutated S-tag F181R-At3AT, R183FCh3MAT proteins using Cyanidin 3-*O*-glucoside and coumaroyl-CoA/malonyl-CoA as substrates and studied through ESI-LC-MS (Fig 3c; appendix).

Sample	Rt (min)	ESI-MS (m/z)	MS/MS fragments (m/z)	Compound indicated with *
C3Gcou-29vector	15.2	449*	287.2 $[Cy]^+$	Cyanidin 3-*O*-glucoside
At3AT-C3Gcou	15.03 17.22 19.5	449 491 & 549 595*	287.2 $[Cy]^+$ 287.2 $[Cy]^+$ 287.2 $[Cy]^+$	Cyanidin 3-(6″ coumaroyl) glucoside
At3AT-C3GMal	14.97 17.13	449 491 & 549	287.2 $[Cy]^+$ 287.2 $[Cy]^+$ 287.2 $[Cy]^+$	
F181R-At3AT-C3Gcou	15.07 16.97 19.35	449 491 & 549 595*	287.2 $[Cy]^+$ 287.2 $[Cy]^+$ 449 $[Cy+Glc]^+$+ 287.2 $[Cy]^+$	Cyanidin 3-(6″ coumaroyl) glucoside
F181R-At3AT-C3GMal	14.93 16.65 16.88	449 535* 549	287.2 $[Cy]^+$ 449 $[Cy+Glc]^+$+ 287.2 $[Cy]^+$ 287.2 $[Cy]^+$	Cyanidin 3-(6″ malonyl) glucoside
C3Gmal-29vector	14.97	449*	287.2 $[Cy]^+$	Cyanidin 3-*O*-glucoside
Ch3MAT-C3GMal	14.93 16.63 16.88	449 535* 549	287.2 $[Cy]^+$ 449 $[Cy+Glc]^+$+ 287.2 $[Cy]^+$ 287.2 $[Cy]^+$	Cyanidin 3-(6″ malonyl) glucoside
Ch3MAT-C3Gcou	15.0 16.97	449 549	287.2 $[Cy]^+$ 287.2 $[Cy]^+$	
R183FCh3MAT-C3GMal	15.55 17.15 17.45 17.67	449 535* 549 491*	287.2 $[Cy]^+$ 449 $[Cy+Glc]^+$+ 287.2 $[Cy]^+$ 287.2 $[Cy]^+$ 287.2 $[Cy]^+$	Cyanidin 3-(6″ malonyl) glucoside Cyanidin 3-(6″ acetyl) glucoside
R183FCh3MAT-C3Gcou	14.98 16.93 17.17	449 491 549	287.2 $[Cy]^+$ 287.1 $[Cy]^+$ 287.2 $[Cy]^+$	

C3G; Cyanidin 3-*O*-glucoside, 29vector; pET29 empty vector protein, cou; coumaroyl-CoA, Mal; malonyl-CoA, Rt; retention time, Cy; cyanidin, Glc; glucose.

3.3.4.2 Investigation of AAT donor specificity in-vivo

To study the donor specificity of AATs in plants in their native structural folds I studied the activity of the mutant proteins (R183F-Ch3MAT and F181R-At3AT) in tobacco. The presence of tags on the enzymes and their expression in a prokaryotic system can have different effects on activity compared to those expressed in plants. Hence, it is appropriate to study specificity of mutant proteins in plants. I choose tobacco (*Nicotiana tabaccum* var Samsun) as a model system and for ease of transformation. Tobacco accumulates mainly cyanidin 3-*O*-rutinoside in its flowers along with minor amounts of pelargonidin 3-*O*-rutinoside both of which do not have any decoration with acylated molecules (Timberlake and Bridle, 1975). Hence the effect of mutated proteins could be interpreted relatively easily.

3.3.4.2.1 Acyl-donor preference of an aliphatic acyltransferase

To identify the region of substrate specificity of an aliphatic acyltransferase; cDNA of *Ch3MAT* isolated from inflorescence of red chrysanthemum (details of *Ch3MAT* isolation is presented in section 4.2.4.2; chapter 4) was mutated to obtain mutant Ch3MAT at Arg^{183}. Mutated R183F-*Ch3MAT* was cloned under the control of a double 35S promoter for constitutive expression in a plant transformation vector conferring kanamycin resistance for selection. The R183F-*Ch3MAT* construct was transferred to tobacco and nine positive primary transformants [Fig 3.15]; 2x35S::R183F-Ch3MAT, were compared to the wild type 2x35S::Ch3MAT transformants (information on 2x35S::Ch3MAT lines is presented in section 4.3.2.2; chapter 4).

The flowers of nine positive plants carrying 2x35S::R183F-Ch3MAT appeared to have darker hue compared to wild type Samsun flowers [Fig 3.16]. A difference in colour was observed between 2x35S::Ch3MAT and 2x35S::R183F-Ch3MAT flowers.

HPLC analysis of anthocyanins from flowers of nine 2x35S::Ch3MAT and 2x35S::R183F-Ch3MAT showed products at different retention times compared to each other and with wild type. The product of 2x35S::Ch3MAT flowers eluted at 21 minutes in hplc separation is a cyanidin 3-(6″ malonyl) glucoside [Fig 3.17]. The amount of new anthocyanin formed in 2x35S::R183F-Ch3MAT lines was low compared to malonylated cyanidin 3-*O*-glucoside in 2x35S::Ch3MAT producing the native enzyme, suggesting a reduced R183F-Ch3MAT activity in plants. The anthocyanin product formed in 2x35S::R183F-Ch3MAT lines was not cyanidin 3-(6″ coumoroyl) glucoside as was understood based on the retention time in comparison to the anthocyanin product of

2x35S::At3AT line (see section 4.3.2.1.3 in chapter IV for details of this transgenic) [Fig 3.17]. Mass fragmentation analysis identified the product of 2x35S::R183FCh3MAT at 22.37 min to be a cyanidin 3-(6″ acetyl)-glucoside having a mass of 491 (m/z) [Fig 3.18].

The presence of a shoulder at around 330 nm in the absorbance peak of anthocyanin at 22.37 min suggested the presence of an acylated compound. A similar product of m/z 491 was obtained in *in-vivo* enzymatic analysis using the S-tag fusion recombinant R183FCh3MAT protein. In 2x35S::R183FCh3MAT flower extracts, tiny amounts of pelargonidin 3-(6″ acetyl)-glucoside were also identified.

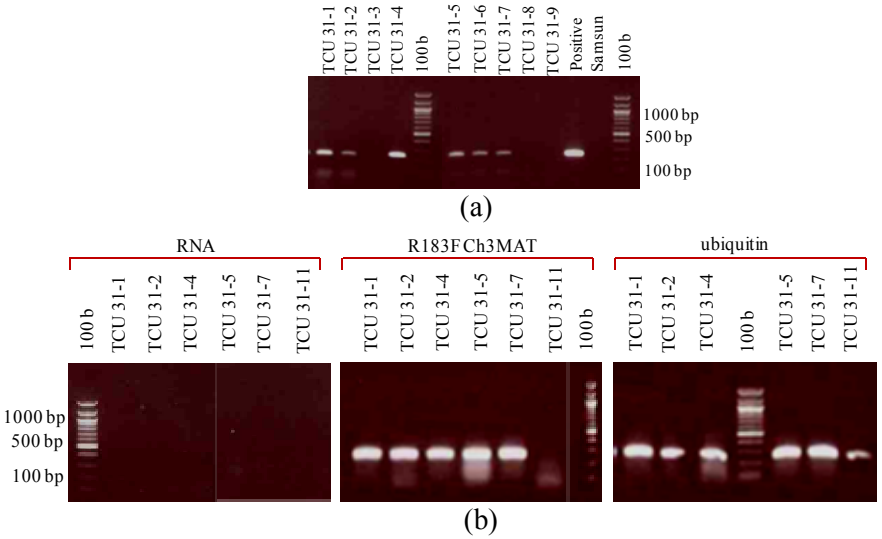

Figure 3.15 | PCR confirmation of R183F-*Ch3MAT* from primary transformants of 2x35S::R183F-Ch3MAT lines (TCU 31-1 to TCU 31-9) compared to Samsun. (a) Genomic DNA analysis of transgene insertion of R183F-*Ch3MAT* in leaves of primary transformants of 2x35S::R183F-*Ch3MAT* were compared to samsun (b) RT-PCR analysis of *ubiquitin* and R183F-*Ch3MAT* transcripts from flowers of 2x35S::R183F-Ch3MAT lines (TCU 31-1, 2, 4, 5, 7 and 11). PCR of RNA was performed as RT control.

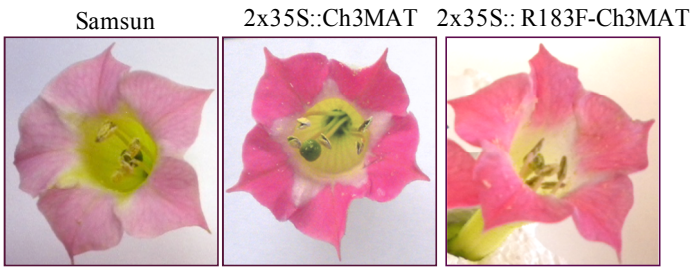

Figure 3.16 | Flowers of Samsun compared to 2x35S::Ch3MAT and 2x35S::R183F-Ch3MAT lines. An increase in the colour of flowers of 2x35S::Ch3MAT and 2x35S::R183F-Ch3MAT lines was observed compared to wild type ie., samsun.

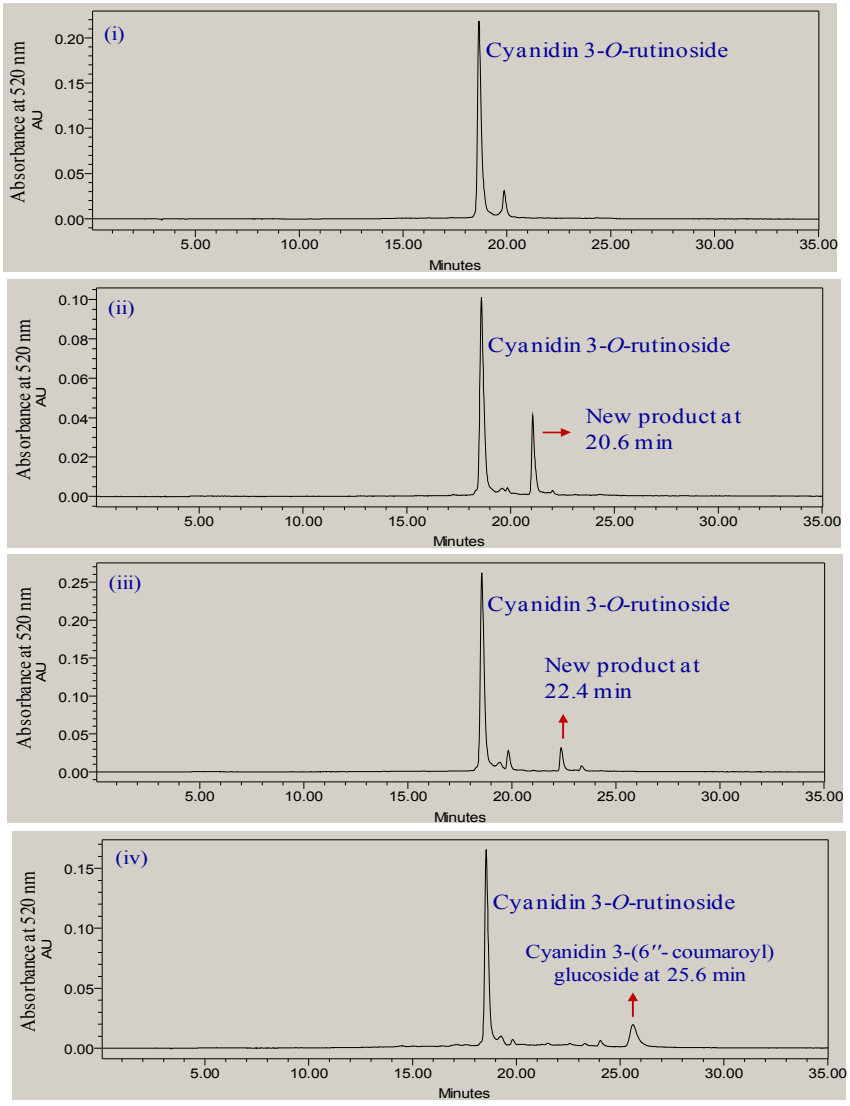

Figure 3.17 | HPLC analysis of anthocyanins from flowers of 2x35S::R183F-Ch3MAT over-expression lines. (i) Chromatogram of flower extracts of Samsun showing cyanidin 3-*O*-rutinoside as the major anthocyanins at 520 nm (ii) flower extracts of 2x35S::Ch3MAT showing new anthocyanin at 20.6 min which is cyanidin 3-(6″ malonyl) glucoside (iii) chromatogram of flower extracts of 2x35S::R183F-Ch3MAT showing elution of new anthocyanins at 22.4 min as observed at 520 nm wavelength (iv) flower extracts of 2x35S::At3AT showing cyanidin 3-(6″ coumaroyl) glucoside at 25.6 min (for information of 2x35S::At3AT lines refer to section 4.3.2.1.3; chapter 4). 2x35S::At3AT line producing cyanidin 3-(6″ coumaroyl) glucoside was showed for comparasion of retention times based on which the metabolites can be studied.

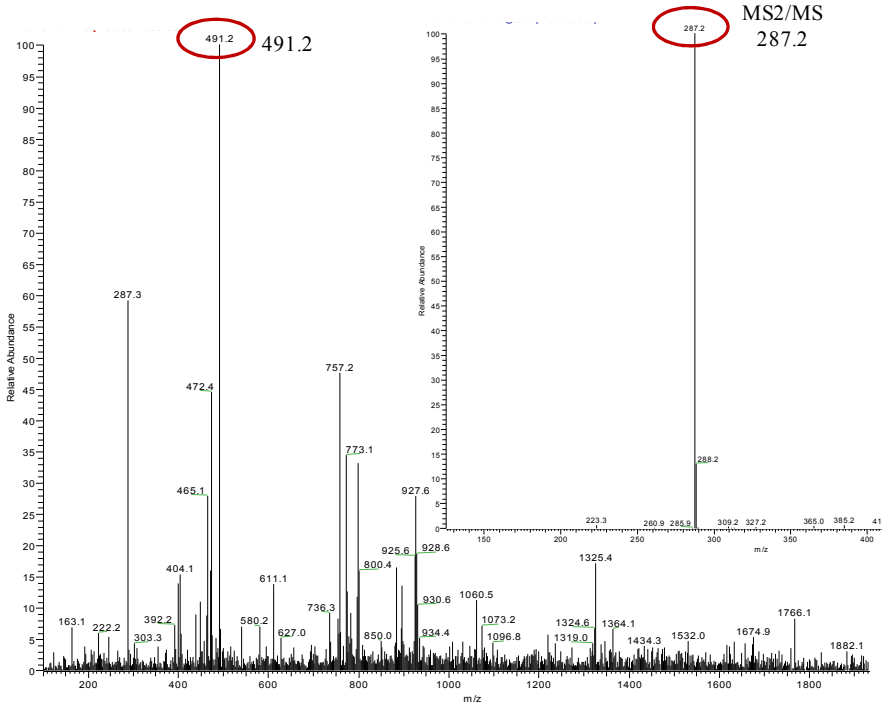

Figure 3.18 | Mass fragmentation analysis of anthocyanins from flowers of 2x35S::R183F-Ch3MAT. Anthocyanin eluted at 22.4 min (Fig 3.17iii) based on its mass of 491.2 was identified as cyanidin 3-(6″ acetyl)-glucoside. In inset MS2 fragmentation of 491.2 was shown.

The mutation R183F of Ch3MAT completely abolished the malonylation activity of the original enzyme *in-vivo* although the aliphatic acylation property (acetic acid being an aliphatic acid) was retained. The accumulation of acetylated anthocyanin suggests the crucial role of Arg[183] in maintaining malonylation of Ch3MAT. The presence of phenylalanine might have changed the structural conformation of the enzyme hindering the specific malonylation activity. However, other amino acid residues of the Ch3MAT enzyme, capable of acting on acyl-CoA, can maintain the specificity for aliphatic donors.

3.3.4.2.2 Substrate specificity of an aromatic acyltransferase

In order to understand if a single amino acid can alter the acyl-donor substrate preference of a coumaroyl transferase; Phe[181] was changed to arginine in At3AT. Mutated F181R-At3AT was cloned into a plant transformation vector under the control of a double 35S promoter and transferred to tobacco. Eight positive primary transformants of 2x35S::F181R-At3AT were compared to wild type Samsun and 2x35S::At3AT flowers.

There was no difference in hue observed in 2x35S::F181R-At3AT flowers compared to wild type [Fig 3.19] whereas 2x35S::At3AT flowers showed a darker hue(visual comparison data not provided).

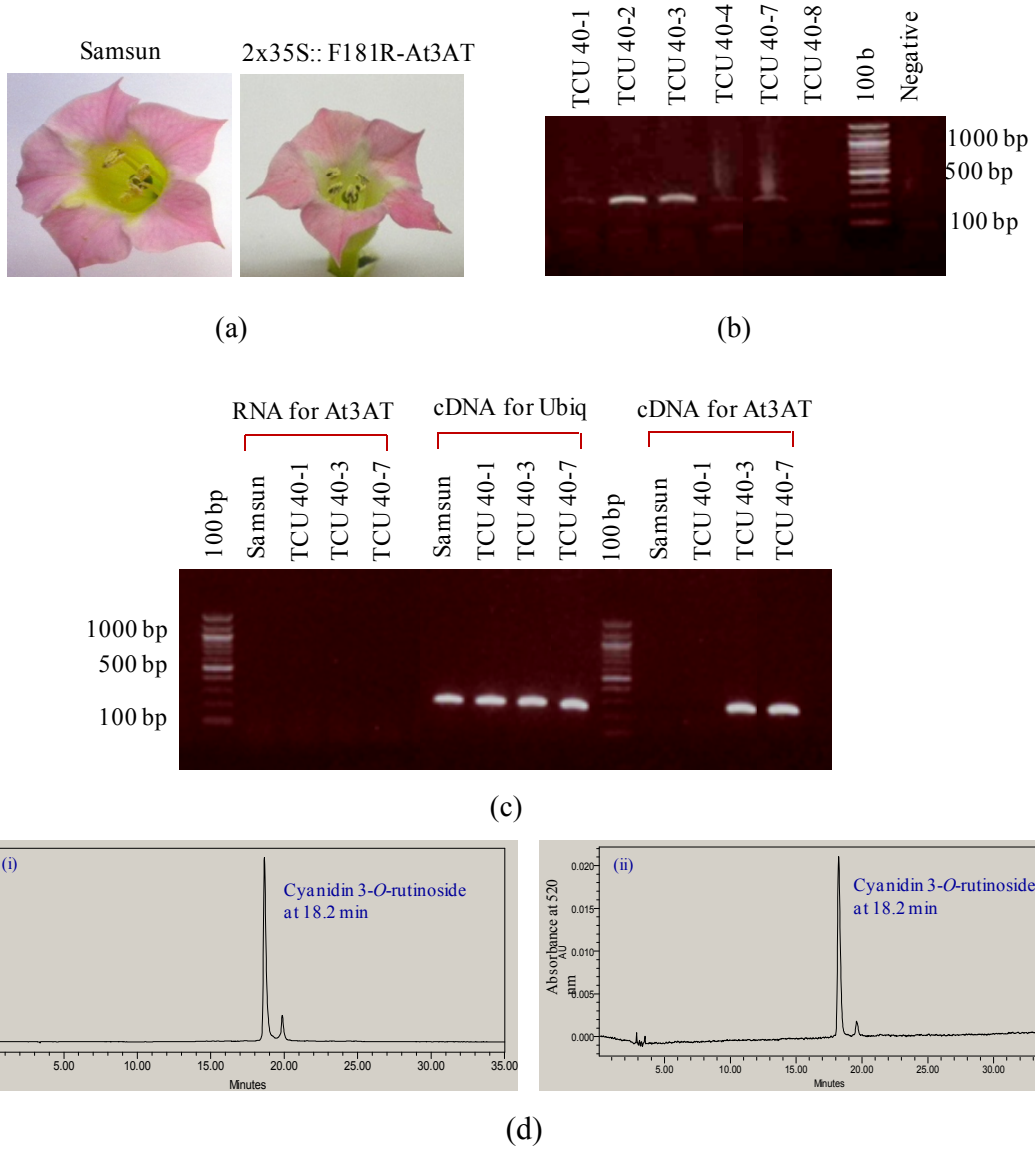

Figure 3.19 | Analysis of 2x35S::F181R-At3AT over-expression lines. (a) Flowers of Samsun compared to 2x35S::F181R-At3AT primary transformant. No colour difference of flowers was observed in 2x35S::F181R-At3AT line compared to Samsun. (b) Genomic confirmation of F181R-*At3AT* insertion from leaves of 2x35S::F181R-At3AT compared to Samsun. (c) RT-PCR analysis of 2x35S::F181R-At3AT lines for expression of *F181R-At3AT* gene; here At3AT was amplified from RNA as RT control and level of *At3AT* expression was compared with *Ubiqutin* expression. (d) HPLC analysis of anthocyanins from flowers. (i) Chromatogram of flower extracts of Samsun showing cyanidin 3-*O*-rutinoside as the major anthocyanin at 520 nm (ii) flower extracts of 2x35S::F181R-At3AT showing no new anthocyanin production.

HPLC analysis of the anthocyanins extracted from flowers of two positive primary transformants expressing the mutated *F181R-At3AT* (Fig 3.19c) did not show any new product formation [Fig 3.19d], whereas, the plants carrying the wild type At3AT protein (2x35S::At3AT) showed a product at 25.6 min with HPLC which was identified to be cyanidin 3-(6″ coumaroyl) glucoside [Fig 3.17iv].

This study showed that the mutation F181R did not result in gain of aliphatic-CoA specificity in vivo, but completely abolished the coumaroylation activity. With this study it can be understood that Phe^{181} near motif 1 is crucial for retaining coumaroylation activity and no other amino acids can directly complement its role. Conversely, for aliphatic acylation to occur, other residues which interact with the –CoA moiety are important as shown with R183FCh3MAT over-expression study in tobacco.

3.4 Discussion

Secondary metabolism in plants is based on the activity of enzyme families which catalyse a number of 'modular reactions' including oxidation, reduction, methyl transfer, acyl transfer, glycosyl transfer, condensation. These reactions use very diverse substrates and provide an enormous variety of metabolites. How individual members of these enzyme families evolve new specificities rapidly has been the subject of investigation for several decades. Understanding the evolution of specificity of acyltransferases can address the chemical diversity in plant anthocyanins. Such modifications are catalysed by AAT enzymes.

The major anthocyanin accumulated in the leaves and stems of *Arabidopsis thaliana* is cyanidin-3-*O*-[2-*O*-(2-*O*-(sinapoyl)-β-xylopyranosyl)-6-*O*-(4-*O*-(β-glucopyranosyl)-*p*-coumaroyl-β-glucopyranoside] 5-*O*-[6-*O*-(malonyl) β-gluco-pyranoside] (Bloor and Abrahams, 2002). These various modifications to anthocyanins are achieved by acyltransferases. Malonylation is achieved by a malonyltransferase belonging to the BAHD family (Luo et al., 2007). A sinapoyl group is added by sinapoyl-Glu:anthocyanin acyltransferase (SAT) which is a serine carboxypeptidase like enzyme (SCPL) (Fraser et al., 2007). This SCPL sinapoyl-Gluc acyltransferases (SGA) represents one of the acyltransferases that does not belong to BAHD family of enzymes. A *p*-coumaroyl group is added to the 6″ position of the glucose residue of cyanidin 3-*O*-glucoside by anthocyanin p-coumaroyl CoA transferase; At3AT (Luo et al., 2007). Addition of a *p*-coumaroyl side chain to the 3-glycoside increases the stability of the pigment in solution. In tomato, a distinct anthocyanin *p*-coumaroyl CoA transferase

(belonging to the same BAHD family) transfers a *p*-coumaroyl group onto the 6 ‴ position of the rhamnose residue of cyanidin 3-*O*-rutinoside. In gentian an aromatic moiety is added to the 5-glucoside of anthocyanin by an aromatic AAT (Fujiwara et al., 1997).

My aim was to understand how the structural differences between these anthocyanin acyltransferases; Sl3AT, At3AT and Gt5AT dictate the differences in their specificity for the hydroxyl residues that receive the acyl moiety (i.e. their regio-specificity). This understanding can provide an insight into how specificity evolves from versatility in plant secondary metabolism. However, my attempts to obtain a crystal structure from the recombinant proteins of these AATs failed due to aberrant activity of purified recombinant proteins and a failure to produce crystals. Consequently, *in-vitro* and *in-vivo* mutagenesis studies were performed to understand the determinants of acyl donor specificity. The structures of these enzymes are so complex that identification of the exact residues that dictate many of their biochemical properties is not easy. As AATs have a broad acyl-acceptor preference it was inevitable that many residues could be involved in interaction and even complement each other for the determinants of specificity. Since AATs have strict acyl-donor specificities it was likely that just a few residues might be involved in determining the specificity for these substrates. In addition, BAHD acyltransferases are very versatile in their substrate specificities. This versatility can be best studied by comparing two malonyl CoA anthocyanin acyltransferases from *Salvia splendens* where the two AATs transfer malonyl groups to the 6‴ and 4‴ positions of the glucose in cyanidin 5-*O*-glucoside (Suzuki et al., 2001, Suzuki et al., 2004b). Despite having similar substrate specificities they belong to different clades of the BAHD family suggesting an independent evolutionary origin (Luo et al., 2007).

The H*XXX*D motif is highly conserved in BAHD members and the histidine in this motif was shown to be indispensable for the activity of acetyltransferases (Ma et al., 2005). However with respect to aliphatic AATs, although the histidine of motif 1 impacts activity, and is therefore likely involved in catalysis (Unno et al., 2007), it is not indispensable as it can be complemented by other residues as shown by Suzuki et al., (2004b). In a similar way, mutation of the histidine at position 174 in Sl3AT to asparagine still showed coumaroylation activity in my study, although the activity levels were not compared.

In studying whether a single amino acid can alter the substrate specificity of AAT, Ch3MAT (using an aliphatic acyl donor) and At3AT (using an aromatic acyl

donor) were chosen. Both these enzymes add acyl molecules onto the 6″ position of 3-glucuose and so a direct comparison of substrate specificity contributed by the amino acid residues can be made. The structure of malonyl transferase identified Arg^{178} of Dm3MAT3 to have an electrostatic interaction with the malonyl group in the catalytic process (Unno et al., 2007). Auto docking of cyanidin 3-*O*-glucoside and malonyl-CoA onto 3MAT structure showed the histidine of motif 1 and Arg^{183} in the active site channel. Mutation of Arg^{183} to phenylalanine (Phe^{183}) in Ch3MAT and expression in tobacco completely abolished the malonylating activity of enzyme, which acquired acetylation activity. The same functional switch of substrate from malonyl-CoA to acetyl-CoA was established in assays using recombinant S-tag fusion protein from *E.coli*. However the recombinant R183F-Ch3MAT protein still retained the malonylating activity. The difference in *in-vivo* and *in-vitro* activity of R183F-Ch3MAT enzyme suggests the effect of structural changes in the fold of the enzyme in altering the availability of certain amino acids in the catalytic site. Ch3MAT is a plant AAT and functional analysis in a eukaryotic system can provide a valid interpretation in understanding the evolution of specificity. A structural study of the Dm3MAT3 in the native complex showed interaction of the CoA moiety with Ala-175, Lys-260, Glu-271, Tyr-272, Val-273, Ser-274, Ser-275, Phe-276, Pro-301, Ile-302, Asp-303, Arg-307, Thr-387, and Lys-389 residues, whereas His-170, Arg-178 and Gly-386 interacted with malonyl group. Dm3MAT3 showed 55% sequence similarity to Dm3MAT1 (Unno et al., 2007). In my study Dm3MAT1 was isolated and re-named as Ch3MAT. Sequence comparison of Ch3MAT and Dm3MAT3 with respect to their CoA-interacting residues showed similarity in all residues except Val-273, Pro-301 and Ile-302 which are replaced by Ile, Thr and Ala respectively in Ch3MAT. This suggests that other CoA interacting residues are sufficient to interact with CoA moiety of aliphatic groups. Some malonyltransferases have been shown to have strict substrate specificity accepting only malonyl-CoA (Luo et al., 2007). The arginine near motif 1 is conserved exclusively in 3MATs. Together with these observations and the mutant study of Ch3MAT in tobacco, it can be concluded that Arg^{183}, which is present close to motif 1, is crucial for exclusive malonylation activity. The CoA-binding residues are important in determining the type of acylated molecule involved, because the pocket of the enzyme depends on spatial arrangement of the amino acids. The presence of Phe^{183} did not change the aliphatic behaviour of the Ch3MAT and suggests the importance of CoA binding residues. Thus,

the CoA binding specificity might have evolved initially and further divergence to specific acylation might have evolved later.

I undertook further investigation to understand the specificity preferences conferred by phenylalanine and arginine near motif 1. The Phenylalanine at position 181 in At3AT protein chain was mutated to arginine and the protein was studied for its donor specificity. F181R-At3AT did not gain new function but instead completely lost its coumaroylation activity. This shows that Phe^{183} is crucial for coumaroylation. Phenylalanine is an aromatic amino acid with a phenyl ring structure and replacing this with arginine might have changed the spatial arrangement of acyl binding site and hence the loss of activity. Comparison of CoA binding residues from Ch3MAT and Dm3MAT3 showed only 35% sequence similarity with At3AT. This observation suggests that both CoA binding residues and Phe^{183} are required for aromatic acylation unlike aliphatic acylation. Since aromatic-CoAs consist of a phenyl ring; a wider pocket is required in order for the acyl donor to enter the enzyme. However, recombinant S-tag fusion F181R-At3AT gained malonylation activity while retaining the coumaroylation activity. This further strengthens the role of Arg^{183} in malonylation suggesting that the 35% similarity in the residues binding CoA can assist in malonylation. In a plant cell, the structural folds of enzymes determined by certain aminoacids can alter their catalytic preferences. Thus the stringent requirement of specific amino acids for aromatic AATs may explain the presence of fewer aromatic anthocyanins in nature compared to aliphatic anthocyanins. Therefore the ability of AATs to bind to specific acyl-CoAs depends on the specific folding of the polypeptide chain along with conservation of amino acid residues.

Understanding the enzymes in their native form is vital in studies to understand the evolution of substrate preferences, compared to studies in *E.coli* although the information obtained from both the systems is valuable. Such studies are widely useful in obtaining plants producing novel acylated anthocyanins. Polyacylated anthocyanins were engineered previously by alteration of acyl-donor specificity of Ss5MAT where aliphatic acyltransferase acquired specificity for hydroxycinnamoyl-CoA while still retaining activity with aliphatic acyl groups. Alteration of this specificity was achieved by three contiguous amino acid substitutions Val^{39}-Arg^{40}-Arg^{41} to corresponding Met-Leu-Gln in Ss5MAT (Suzuki et al., 2007). Such studies are useful for engineering AATs.

Only limited study investigation of the specificities of AATs was undertaken in this project due to time constraints. Further studies looking into the residues interacting with CoA moiety and in motif 3 (DFGW) which was thought to have a structural role in

AATs need to be undertaken. This information obtained in understanding the AATs will be useful in engineering acyltransferases to offer the possibility of obtaining different complex anthocyanins with enhanced properties.

CHAPTER IV

Insight into Anthocyanic vacuolar inclusion (AVI) Formation in Plants

4.1 Introduction

Molish in 1905 observed that, in some plants, red, blue and purple anthocyanin pigments accumulate as amorphous structures in contrast to their more usual, soluble form in the vacuoles of coloured cells. More recent studies suggested that the anthocyanins associate to form globular bodies called anthocyanic vacuolar inclusions (AVIs) which appear as insoluble localized concentrations of anthocyanin. Markham et al., (2000) suggested that anthocyanins are sequestered in AVIs primarily to increase their stability, but also to reduce their inhibition of certain vacuolar enzymes. AVIs are composed of selected anthocyanins, possibly in association with specific proteins. Association of AVIs with a 24 kDa protein called VP24 were studied in sweet potato (Nozue et al., 1997). Some correlative evidence suggests that the formation of AVIs is dependent on acylation of anthocyanins, particularly coumaroylation (Conn et al., 2003). In other species the recruitment of anthocyanins into AVIs is correlated with the degree of glycosylation of the anthocyanins (Markham et al., 2000) or the level of accumulation of anthocyanins (Gonnet, 2003). These theories have arisen from studies on different plant systems, so various factors could be influencing the AVI formation. And whether AVIs are derived from the digestion of membranes of anthocyanoplasts after entering the vacuole or formed due to aggregation of pigments within the vacuole or whether anthocyanoplasts and AVIs have different origins is still unresolved. To date no systematic study has established precisely the environmental conditions or the side chain decorations of anthocyanins that are responsible for AVI formation. Hence studies on the factors responsible for AVI formation can give an understanding of the properties of anthocyanins.

A preliminary study using transgenic tobacco had suggested that aromatic acylation of anthocyanins was necessary for AVI formation in this species (Jie Luo personal communication). Coumaroylation of anthocyanins is an aromatic acylation found in many plant species. Aliphatic acylation is another type of anthocyanin modification widely present across plant kingdom. I studied whether AVI formation is due solely to aromatic acylation or whether other modifications can lead to AVI formation? As AVI formation has been reported only in cells producing relatively large amounts of anthocyanins, I used high anthocyanin producing tobacco lines generated by Cathie Martin, in my studies.

In order to fully understand the drivers for AVI formation I set out to identify the factors triggering AVI formation using systematic alteration of glycosylation and acylation in a simple plant model species, tobacco.

4.2 Experimental procedures

4.2.1 Seed sterilization

Seeds were sterilized in 10% commercial bleach for 20 minutes with vigorous shaking. Seeds were washed three times with sterilized water and sown with sufficient spacing on MS agar (0.8%) plates with kanamycin 100 mg/L. The plates were kept in a growth room at 23 - 25°C under a 16 h light and 8 h dark cycle.

4.2.2 Plant material and growth conditions

Wild type and transgenic tobacco (*Nicotiana tabacum* var Samsun) plants were grown at 23- 25°C under 16 h light and 8 h dark cycle. These conditions were maintained both in growth room when the plants were on MS medium and in the glass house. For sucrose treatment, seeds were sown on MS medium containing no sucrose (0%), 3% sucrose or 6% sucrose with kanamycin (100 mg/L) and 0.8% agar. Transgenic plants were grown for 3-4 months until flowering and crossed with the desired parents. The desired plant material was harvested in liquid nitrogen for subsequent analysis.

Arabidopsis thaliana sterilized seeds were sown on MS medium containing 0.8% agar and incubated at 4°C for 4 days. Later they were grown at 23- 25°C under 16h light and 8h dark cycle. Leaf material was frozen and stored at -80°C for genomic DNA isolation. Red and purple chrysanthemum cut flowers were purchased from local supermarket and opened and unopened flowers were frozen in liquid nitrogen and stored at -80°C for RNA isolation.

4.2.3 Callus induction

Young and healthy leaf material from transgenic plants was sterilized in 10% bleach for 20 minutes with gentle shaking and washed three times with sterile water. Care was taken not to damage the leaf material. Sterilized leaves were cut into small pieces and plated on callus induction medium containing MS agar (0.8%) supplemented with kanamycin 100 mg/L, kinetin 0.5 mg/L, 2,4 D 1.0 mg/L and NAA 0.5 mg/L. The plates were incubated in a growth room at 23-25°C under 16 h light/8 h dark or in complete darkness at 23-25°C. Sub-culturing was performed every 15 days using callus induction medium, for 45 days until sufficient callus was produced to take to liquid culture.

4.2.4 Construction of binary vectors for plant transformation

All the gene constructs developed in this chapter were created in Gateway destination vector™ (Invitrogen) pJAM1502 (Luo et al., 2007) having a double 35S promoter, a Gateway recombination site and the CaMV terminator sequence, for high-level, constitutive expression in plants [Fig 4a; appendix]. Glycerol stocks of all positive clones were maintained at -80˚C.

4.2.4.1 Cloning of At5GT

4.2.4.1.1 Generating the *At5GT* plant expression construct

The full length gene, encoding UDP-glucoronosyl/UDP-glucosyl transferase (Gene bank data base accession number AT4G14090, (Tohge et al., 2005) was amplified from genomic DNA isolated from Arabidopsis leaves. Since this gene has no introns, genomic DNA was used to amplify it using AtGF and AtGR gene specific primers having Gateway recombination sequences; attB1 and attB2 [Table 4.1 and 4a; appendix]. *Pfu* polymerase was used to amplify a PCR product [Fig 4.1] of size 1371 bp. This At5GT fragment of DNA was recombined into the pDONR207 entry vector using BP clonase™. The resulting Entry vector pEnt207At5GT(7) containing the full length sequence of At5GT was recombined into the pJAM1502 vector by an LR™ recombination reaction to create a binary vector for gene expression in plants. One of the positive clones was sequenced and called pJ15At5GT(7.1) [Fig 4.1]; this was used for *Agrobacterium*-mediated transformation of tobacco.

4.2.4.1.2 Generating the *At5GT* construct for expression in *E.coli*

The full length *At5GT* gene was amplified from the clone pEnt207At5GT(7) using the forward primer 5' GGGGACAAGTTTGTACAAAAAAGCAGGCTGGGAAAATC - TGTACTTTCAGGGCATGGCCACTTCCGTCAATGG 3' which contained an attB1 site followed by a TEV protease cleavage site and the reverse primer 5' GGGGACCACTTTGTACAAGAAAGCTGGGTCCTCATCCTCGTCCACAAAAC 3' which contained the attB2 site. Primers were designed in such a way that the reading frame of the gene was not shifted with respect to the N-terminal tag. Cloning into entry vector pDONR207 and destination vector pMGWA (Maltose Binding Protein (MBP)-tagged Gateway vector; [Fig 4b; appendix] (Busso et al., 2005) was performed to create clone p525tevAt5GT [Fig 4.1].

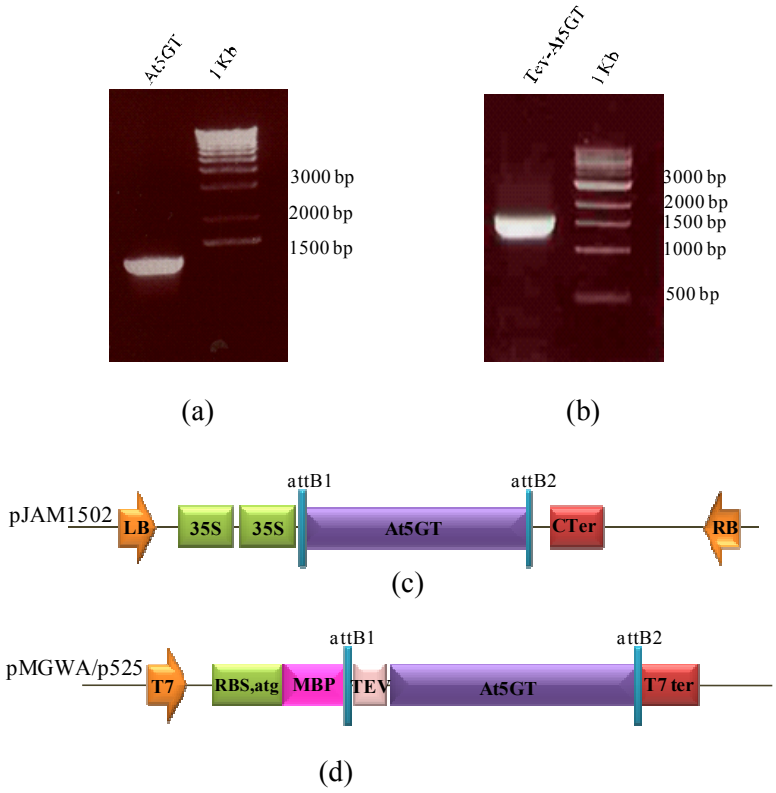

Figure 4.1 | Cloning of *At5GT* (a) The *At5GT* gene amplified using gateway gene specific primers and *Pfu* to give a fragment of size ~1434 bp from Arabidopsis genomic DNA (b) The *Tev-At5GT* fusion amplified from clone pEnt207At5GT(7) with gateway gene specific primers and *Pfu* to give a fragment of size ~1455 bp (c) Pictorial representation of T-DNA region of plant expression vector of *At5GT*; pJ15At5GT used for generating 2x35S::*At5GT* lines. LB; left border, 35S; CaMV 35S promoter, attB1 and attB2; Gateway recombinant sites, Cter; CaMV terminator, RB; right border. (d) Pictorial representation of bacterial expression vector of *At5GT*; p525tevAt5GT. T7; T7 promoter, RBS; ribosome binding site, atg; translational start site, MBP; maltose binding protein, attB1 and attB2; Gateway recombinant sites, TEV; tev-protease cleavage site, T7 ter; T7 terminator.

4.2.4.2 Cloning of Ch3MAT

The *Ch3MAT* gene from *Chrysanthemum x morifolium* encoding anthocyanidin 3-*O*-glucoside-6″-*O*-malonyltransferase (gene bank database accession number AY298809, (Suzuki et al., 2004a) was amplified from cDNA of dark red (maroon) chrysanthemum inflorescence. cDNA was prepared from RNA isolated from partially opened flowers using the Trizol method.

4.2.4.2.1 Site directed mutagenesis to obtain *Ch3MAT* gene with no errors

The cDNA encoding *Ch3MAT*, 1380 bp, was amplified with gene specific primers [Table 4.1 and 4a; appendix] using *Pfu* polymerase [Fig 4.2]. The purified PCR product was A-tailed and cloned into the pGEM- T/Easy vector™ (Promega) and later transferred to pET29. As the gene was isolated from an unknown variety, three nucleotide differences compared to the published sequence were modified through site directed mutagenesis. Only two nucleotides were changed as they were leading to amino acid changes. Primers were designed in such a way to remove the nucleotide errors at positions viz., C at 281 to T, C at 566 to T and for the PCR products to overlap with each other [Fig 4.2]. Thus amplified PCR products were used to reamplify the gene using Gateway specific primers and *Pfu* polymerase [Table 4.1, 4a; appendix].

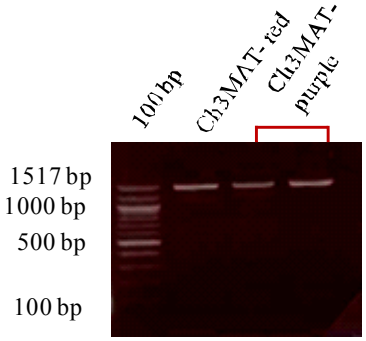

(a)

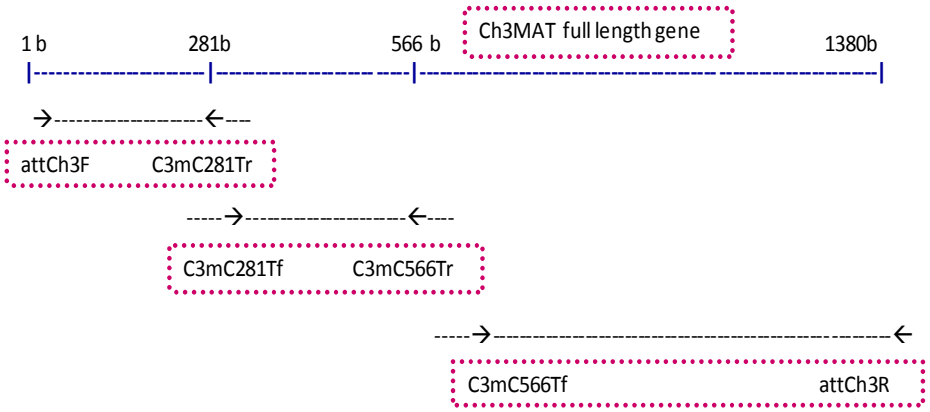

(b)

Figure 4.2 | Site directed mutagenesis of *Ch3MAT* (a) *Ch3MAT* amplified (size ~1443 bp) from cDNA isolated from red and purple chrysanthemum inflorescence. (b) Pictorial depiction of site directed mutagenesis performed to remove errors in *Ch3MAT*.

4.2.4.2.2 Generating the *Ch3MAT* plant expression construct

Purified PCR product (of size ~1443 bp) obtained from site directed mutagenesis PCR was recombined into pDONR207 using BP clonase. A positive entry clone

pEnt207Ch3MAT(6) which was confirmed by sequencing [Fig 4.3] was introduced into pJAM1502 creating pJ15Ch3MAT(1) [Fig 4.3] and was used to transfer to *Agrobacterium*.

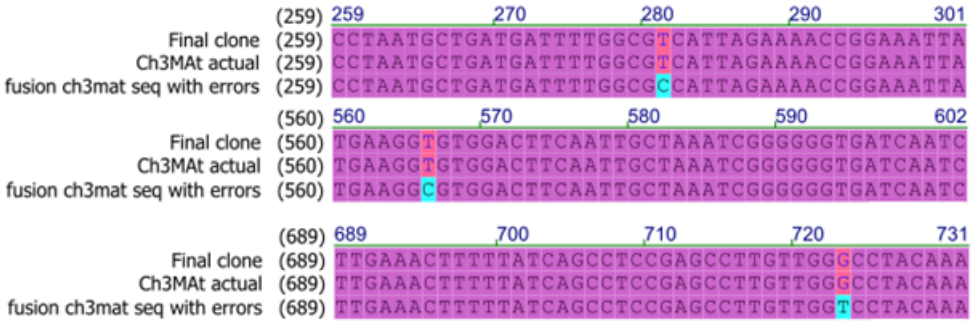

(a)

(b)

Figure 4.3 | Cloning of *Ch3MAT* (a) Alignment of the final positive mutated clone with the characterised *Ch3MAT* sequence showing the nucleotides which were modified. (b) Pictorial representation of T-DNA region of plant expression vector of *Ch3MAT*; pJ15Ch3MAT. LB; left border, 35S; CaMV 35S promoter, attB1 and attB2; Gateway recombinant sites, Cter; CaMV terminator,

Table 4.1 | Primers used for constructing different vectors studied in this chapter

Gene	Size (bp)	Forward primer	Reverse primer	Final vector	Positive clone
At5GT	1371	AtGF	AtGR	pJAM1502	pJ15At5GT (7.1)
At5GT	1371	B1TevAGT	B2AGT	pMGWA	p525 At5GT
Ch3MAT	1380	Ch3MATB1F	Ch3MATB2R	pJAM1502	pJ15Ch3MAT(1)
PhF3'5'H	1521	B1Ptf35hF	B2Ptf35hR	pJAM1502	pJ15PhF3'5'H (15)

4.2.4.3 Cloning *PhF3'5'H* for generating tobacco transgenics

The flavonoid 3' 5' hydroxylase gene from Petunia (size 1521 bp) was available in T/A cloning vector (pGEM-T) and was reamplified with primers suitable for Gateway

recombination™ and *Pfu* [Table 4.1 and 4a; appendix]. Amplified product [Fig 4.4] was purified and cloned into pDONR207 to obtain entry clone pEnt207 PhF3'5'H. Clone 5 which carried the correct sequence was used to create a destination vector using LR recombination into pJAM1502. Expression clone pJ15PhF3'5'H(15) was used for *Agrobacterium* mediated transformation of tobacco.

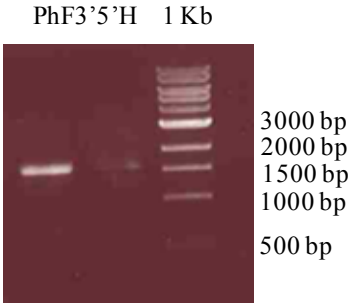

(a)

(b)

Figure 4.4 | Cloning of *PhF3'5'H*. (a) *F3'5'H* gene amplified with gene specific Gateway primers (of size 1584 bp along with GW sites) from clone provided by Cathie Martin (b) Pictorial representation of T-DNA region of plant expression vector of *PhF3'5'H*; pJ15PhF3'5'H. LB; left border, 35S; CaMV 35S promoter, attB1 and attB2; Gateway recombinant sites, Cter; CaMV terminator,

4.2.5 Sequencing of constructs

Clones constructed as described in section 4.2.4 were initially sequenced before using them for transformation and over-expression studies. Big Dye (3.1) sequencing reactions were performed using several primers [Table 4a; appendix] per gene (spanning the full length of each gene) and the reactions sequenced at Genome Enterprise Limited™. The raw sequencing data obtained was analysed using VectorNTI software™ (Invitrogen). Contigs were formed from the sequences obtained with different primers using ContigExpress. Contigs were then aligned using AlignX on the original sequence of each

gene taken from NCBI. Alignments of all the sequences are provided in appendix to this thesis.

4.2.6 Generation of transgenic tobacco

Stable transgenic tobacco plants were obtained through a leaf disc transformation procedure (Horsch et al., 1985). Positive expression clones (pJAM15At5GT(7.1), pJAM15Ch3MAT(1), pJ15PeF3'5'H(15)) with desired genes were transferred to *Agrobacterium tumefaciens* (LBA4404) through electroporation and the transformed culture was maintained at 28˚C on TB medium containing 50 mg/L kanamycin, 30 mg/L streptomycin and 25 mg/L rifampacin. Colonies were screened for the presence of each binary vector using gene-specific PCR and *Taq* polymerase. Positive colonies were grown in TB medium with antibiotics at 28˚C until the OD_{600} of the culture reached 0.6. Collected bacterial culture was resuspended in sterile MS liquid medium with few drops of 1 M $MgCl_2$ to avoid aggregation of bacterial cells when in contact with leaf material. Young tobacco leaves were collected fresh from the green house and treated with 10% bleach and washed three times with sterile water. Leaf material was cut into ~1 cm^2 pieces directly in suspended *Agrobacterium* culture and blotted dry before placing on MS agar plates. The plates were left in the dark at 25˚C for two days before placing the leaf material on sub-culturing medium containing kanamycin 100 mg/L, BAP 1 mg/L, NAA 0.1 mg/L and cefotaxime 350 mg/L in MS agar (0.8%).

The plates with leaf material were incubated in a growth room at 25˚C with 16 h light/8 h dark periods. Sub-culturing of the leaf material onto fresh medium was performed every 14 days until callus regeneration and shooting occurred. After 45-60 days of sub-culturing, shoots which had grown sufficiently big, were cut and transferred to rooting medium containing kanamycin 100 mg/L and NAA 1 mg/L. Rooted shoots (7-14 days) were kept in soil and acclimatised before transferring to the green house. After 4-5 months selfed seeds were collected, labelled and stored in a dry place.

4.2.7 Analysis of transgenic tobacco plants

Kanamycin resistant transgenic tobacco plantlets were screened during the process of acclimatisation for the presence of transgene so that no false positives were transferred to green house. DNA was isolated from frozen leaf material following the modified CTAB method. PCR was performed with 50-80 ng of DNA, 2 µM each of forward and reverse primers, 0.1x *Taq* DNA polymerase, 1.5 mM $MgCl_2$, and 100 µM of each dNTP and milliQ water to make up the volume. Gene specific primers which could amplify either

the full length or part of the gene were used, as shown in table 4.2. CR reactions were performed with 2 min initial denaturation at 94°C followed by 25-30 cycles of denaturation at 92°C for 30 sec, annealing at 55-60°C for 30 sec and extension at 72°C for 30 sec to 1 min 30 sec with final extension of 5 min at 72°C. The annealing temperature was set, based on the Tm values of the primer pairs used in the reaction. Expression analysis of the transgenes in positive plants and untransformed *N. tabaccum* (Samsun) as a control was studied with the total RNA isolated from the flowers or leaf material. RNA was isolated using the Tri-reagent (Sigma) using the Ambion protocol. DNase treated RNA 1-2 µg, oligodT(17) 1 µM, 100 µM of each dNTP, 1x RNase OUT, 0.5x Superscript II (Invitrogen) were used for first strand cDNA synthesis. Diluted first strand cDNA was used to perform semi-quantitative PCR reactions using the same PCR conditions described above. PCR was also performed on DNase treated RNA without reverse transcription to ensure that the amplified products were not from genomic DNA.

Diluted first strand cDNA was also used to perform quantitative PCR on sucrose treated plants with gene specific primers [Table 4.2]. Quantitative PCR reactions consisted of diluted cDNA, 2x SYBR Green master mix (Sigma), 0.2 µM each of forward and reverse primers, milliQ water to make up the reaction mix. PCR reactions were carried out with the BioRad Opticon detection system with 2 min initial denaturation at 94°C followed by 34 cycles of denaturation at 92°C for 20 sec, annealing at 60°C for 20 sec and extension at 72°C for 20 sec with final extension of 5 min at 72°C. Two independent genotypes for each treatment were analysed and three technical replicates were included for each primer pair along with one blank reaction for that particular primer combination. The data obtained was analysed with Opticon Monitor 3 software (BioRad™) and relative quantification for the expression of each gene was performed using comparative C_T method.

4.2.8 Tobacco crosses

Transgenic tobacco plants expressing both 2x35S::*Del* and 2x35S::*Ros1* were used as male parents in generating progeny with high anthocyanin accumulation. A minimum of four independent transgenics expressing 2x35S::*At5GT* (T1 generation), 2x35S::*Ch3MAT* (T0 generation), 2x35S::*PhF3'5'H* (T0 generation) were used as female parents [Table 4.2]. Flowers of female parents were emasculated (removal of stamens) during the stage just before flower opening ie., when the stamens were immature; with forceps wiped with 70% ethanol. After two days when the carpel was fully receptive (stigma was shiny and sticky) pollen from male parents was dusted on the stigma and the flower was

tagged. Mature and dried crossed seeds were collected after 4 weeks and stored in a dry place. For generating lines producing coumaroylated and 5-glucosylated anthocyanins 2x35S:: *At5GT* (T1 generation) plants were crossed with a parent carrying 2x35S::*Del*, 2x35S::*Ros1* and 2x35S::*At3AT* developed by Jie Luo. The seeds of the crosses were sown on MS agar medium with kanamycin and the plants were analysed further.

Table 4.2 | Tobacco crossings performed to generate transgenics producing different anthocyanins

Female parent	Male parent
2x35S::*At5GT*	2x35S::*Del* /2x35S::*Ros1*
2x35S:: *At5GT*	2x35S::*Del* /2x35S::*Ros1*/2x35S::*At3AT*
2x35S::*Ch3MAT*	2x35S::*Del* /2x35S::*Ros1*
2x35S::*PhF3'5'H*	2x35S::*Del* /2x35S::*Ros1*

4.2.9 Anthocyanin extraction

Flowers (mainly petals) and leaf samples (fresh/frozen or dry) from which anthocyanins were to be extracted were ground to fine powder. Extraction solvent, 70% methanol with 0.1 % HCl, at 40 µL/mg was added to the samples, vortexed thoroughly and sonicated in a water bath for 10 min. Flower extracts were processed immediately by centrifugation at 12,000 rpm for 10 min at 4°C. Supernatants were collected and stored at -20°C for further analysis. Leaf extracts were left at 4°C overnight and chloroform treatment was undertaken the following day to remove the chlorophyll. An equal volume of chloroform was added to the leaf extracts and centrifuged at 12,000 rpm for 10 min at 4°C. The supernatant was collected for analysis or stored in -20°C.

4.2.10 HPLC analysis of anthocyanins

Anthocyanin extracts either diluted (from leaf) or concentrated (from petals) were run on a 250 x 4.6 mm internal diameter Spherisorb® 5 µm C18 column using Waters HPLC system (Waters, http://www.waters.com). The column was initially equilibrated with 96% solvent A (0.5% TFA) and 4% solvent B (0.5% TFA in 50% ACN) and eluted with a gradient of increasing solvent B at a flow rate of 1 mL/ min. After injection the column was washed with 96% A followed by a linear gradient of solvent B from 4% to 20% in 5 min, 20% to 40% in 10 min, 40% to 60% in 5 min, 60% to 20% in 10 min and 20% to 4% in 5 min. The elution products were monitored with a photo diode array (PDA) detector over the range 200–600 nm. Anthocyanin contents were analysed based on the

peaks obtained at various retention times compared to controls and quantified (using Excel) based on the peak areas at 520 nm in the chromatograms.

4.2.11 LC-MS analysis of anthocyanins

Anthocyanins and their structural modifications were confirmed by LC/MS using a Thermo Finnigan Surveyor HPLC system (Thermo Scientific, http://www.thermo.com) equipped with a diode array (PDA) detector and a Deca XP plus ion trap mass spectrometer (Thermo Scientific). The runs were performed by Dr. Lionel Hill. Anthocyanin masses and fragmentation patterns were analysed using Quant browser.

4.2.12 Recombinant protein expression and *in-vitro* enzymatic assay

The p525tevAt5GT vector was transferred to BL21 codon plus expression host *E.coli* cells using the heat shock method of transformation. A positive colony was cultured in 5 mL liquid LB medium with carbencillin 50 mg/L and chloramphenicol 50 mg/L at 37°C at 250 rpm. An overnight culture was used as starter culture to inoculate 200 mL of liquid LB with antibiotics and cultured at 37°C for 2 h until the OD_{600} reached 0.6. The culture was induced with 1 mM IPTG and grown for 4 h before harvesting and storing in -80°C. The bacterial pellet was resuspended in column buffer (New England Biolabs), broken with three passes through a French press and centrifuged at 13,000 rpm for 30 min. The collected supernatant was used for enzyme assays. The assay reaction was performed using ~20 µg of soluble protein, 20 mM potassium phosphate buffer (pH 7.0), 1 mM EDTA, 60 µM UDP-glucose and 120 µM cyanidin 3-*O*-rutinoside or cyanidin 3-*O*-glucoside (Luo et al., 2007). After incubation at 30°C for 20 min the reaction was stopped with two volumes of ice cold 0.5% Trichloroacetic Acid (TCA). The reaction mix was analysed by HPLC.

4.2.13 AVI isolation

4.2.13.1 Protoplast isolation

A protocol for protoplast isolation was adapted from several available protocols from the literature. Leaf material or flower material was cut into small pieces in protoplast buffer (0.7 M Mannitol, 0.25 mM MES, 1% cellulose, 0.25% macerozyme and driselase 0.5%; pH 5.5) and incubated at 30°C for 4-6 h in dark with gentle shaking (30 rpm). The solution was strained through two layers of mira cloth and a layer of 50 µm cheese cloth. The filterate was centrifuged at 4°C for 10 min at 100 rpm. The pellet was washed in

protoplast buffer without enzymes and suspended in a small amount of buffer. 0.7 M sucrose (ten times the volume of suspended pellet) was layered on top of the pellet, centrifuged for 15 min at 100 rpm, 4°C. Intact and healthy protoplasts are collected on top of the sucrose solution. Protoplasts were washed twice with the buffer and suspended in a small amount of buffer and stored in -20°C.

4.2.13.2 AVI isolation

Freeze-thawed protoplasts were sonicated to break them and layered on a percoll gradient (obtained with sequential layering of 80%/50%/30%/10% percoll with mannitol buffer without hormones) and centrifuged at 100 rpm for 10-15 min. AVIs were collected from the bottom of the tube and analysed.

4.2.14 SEM and TEM

Both Transmission Electron Microscopy (TEM) and Scanning Electron Microscopy (SEM) were performed by Kim Findlay

4.2.14.1 Scanning Electron Microscopy

Drops of the tobacco suspension cell cultures were mounted on a rivet attached to a sample holder. The sample was then immediately plunged into liquid nitrogen slush at approximately -210^{o}C to cryo-preserve the material. This was transferred, onto the cryostage of an ALTO 2500 cryo-transfer system (Gatan, Oxford, England) attached to a Zeiss Supra 55 VP FEG scanning electron microscope (Zeiss SMT, Germany). The samples were fractured at -100 ^{o}C before sputter coating with platinum for 90 secs at 10mA, at colder than -110^{o}C. After sputter-coating, the sample was moved onto the cryo-stage in the main chamber of the microscope, held at approximately -130^{o}C. The sample was imaged at 3kV and digital TIFF files were stored.

4.2.14.2 Transmission electron microscopy

The samples were pre-embedded in agarose before the final fixation as follows: a volume of 25% glutaraldehyde was added to the cell suspension cultures to make 2.5% final concentration, gently mixed then left for 1 hr to gradually settle. These settled cells were then harvested and mixed with an equal volume of 2% (v/v) low gelling temperature agarose in water at approximately 37^{o}C before plunging briefly on ice. Once the agarose had set, blocks of approximately 1mm^{3} were cut out containing the concentrated cells and these were placed in a solution of 2.5% (v/v) glutaraldehyde in 0.05M sodium

cacodylate, pH 7.3 and left overnight to fix the cells. Samples were then placed in baskets and loaded into the Leica EM TP embedding machine (Leica, Milton Keynes) using the following protocol. The fixative was washed out by three successive 15-minute washes in 0.05M sodium cacodylate and then post-fixed in 1% (w/v) OsO_4 in 0.05M sodium cacodylate for two hours at room temperature. The osmium fixation was followed by three, 15-minute washes in distilled water before beginning the ethanol dehydration series (30%, 50%, 70%, 95% and two changes of 100% ethanol, each for an hour). Once dehydrated, the samples were gradually infiltrated with LR White resin (London Resin Company, Reading, Berkshire) by successive changes of resin:ethanol mixes at room temperature (1:1 for 1hr, 2:1 for 1hr, 3:1 for 1hr, 100% resin for 1 hr then 100% resin for 16 hrs and a fresh change again for a further 8 hrs) then the samples were transferred into gelatin capsules full of fresh LR White and placed at 60^{o}C for 16 hrs to polymerize. The material was sectioned with a glass knife using a Leica UC6 ultramicrotome (Leica, Milton Keynes) and ultrathin sections of approximately 90nm were picked up on 200 mesh copper grids which had been pyroxylin and carbon coated. The sections were stained with 2% (w/v) uranyl acetate for 1hr and 1% (w/v) lead citrate for 1 minute, washed in distilled water and air dried. The grids were viewed in a FEI Tecnai 20 transmission electron microscope (FEI UK Ltd, Cambridge, UK) at 200kV and imaged using an AMT XR60 digital camera (Deben, Bury St Edmunds, UK) to record TIF files.

4.3 Results

4.3.1 Regulation of the anthocyanin pathway in tobacco through over-expression of Delila and Rosea1

Delila (*Del*) and *Rosea1* (*Ros1*) are genes from snapdragon (*Antirrhinum majus)* encoding for a basic helix-loop-helix and a MYB-related transcription factor respectively (Goodrich et al., 1992, Schwinn et al., 2006) that interact to induce anthocyanin production. These two transcription factors were successfully used to generate transgenic tomato lines that produce high levels of anthocyanins (Butelli et al., 2008). In order to produce anthocyanins constitutively in tobacco (*Nicotiana tabaccum* var Samsun); cDNA of *Delila* and *Rosea1* were expressed under the control of the cauliflower mosaic virus 35S promoter. Stable transgenic lines expressing 2x35S::*Delila* (2x35S::*Del*) and 2x35S::*Rosea1* (2x35S::*Ros1*) were dark red in colour [Fig 4.5a] and grew much more slowly than the controls due to constitutive anthocyanin accumulation.

To determine whether together, Delila and Rosea1 affect other branch pathways in phenylpropanoid metabolism, expression of some genes encoding enzymes involved in the branch pathways were compared in control plants (Samsun), plants expressing 2x35S::*Del* and 2x35S::*Ros1* independently and plants expressing 2x35S::*Del* and 2x35S::*Ros1* together.

Expression of 2x35S::*Del* on its own gave plants with more intensely pigmented petals and red staminal filaments (as described by Mooney et al., 1995). Expression of 2x35S::*Ros1* on its own gave rise to plants which had moderate pigmentation of the vegetative tissues, as well as more intensely pigmented petals. Pigmentation was restricted to the epidermal layer and was rather variable between independent transgenic lines. Expression of 2x35S::*Del* and 2x35S::*Ros1* together resulted in strong pigmentation of all tissues of the plant involving accumulation of cyanidin 3-*O*-rutinoside [Fig 4.5b] although pelargonidin 3-*O*-rutinoside was also present in small amounts (similar to earlier observations by Timberlake and Bridle, 1975). From here onwards the plants expressing both 2x35S::*Del* and 2x35S::*Ros1* are referred to as 2x35S::*Del*/2x35S::*Ros1*.

Figure 4.5 | Regulation of anthocyanin pathway and analysis of anthocyanins in tobacco by over-expression of Del/Ros1.

(a) Flowers of wild type tobacco variety Samsun on left and flower of 2x35S::*Del*/2x35S::*Ros1* on right showing high anthocyanin pigmentation.

(b) Genomic confirmation of 2x35S::*Del*/2x35S::*Ros1* lines (TCU 24-1, 4, 5, 7 and 9) for both the genes.

(c) Spectrophotometric profile of anthocyanins extracted from flowers of Samsun and 2x35S::*Del*/2x35S::*Ros1* lines (TCU 170-4 and TCU 24-4).

(d) HPLC chromatogram of anthocyanin from leaves of 2x35S::*Del*/2x35S::*Ros1* line scanned at 520 nm.

(e) Mass spectrum analysis of the anthocyanin peak identified from HPLC correlated to cyanidin 3-*O*-rutinoside; inset is the MS2 of cyanidin 3-*O*-rutinoside is shown with cyanidin 3-*O*-glucoside obtained due to loss of rhamnose.

(a)

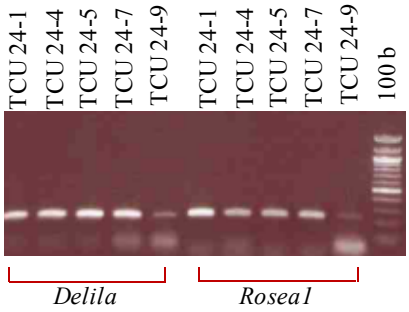
TCU 24-1
TCU 24-4
TCU 24-5
TCU 24-7
TCU 24-9
TCU 24-1
TCU 24-4
TCU 24-5
TCU 24-7
TCU 24-9
100 b
Delila
Rosea1

(b)

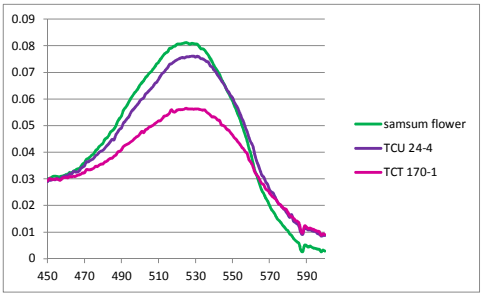
samsum flower
TCU 24-4
TCT 170-1

(c)

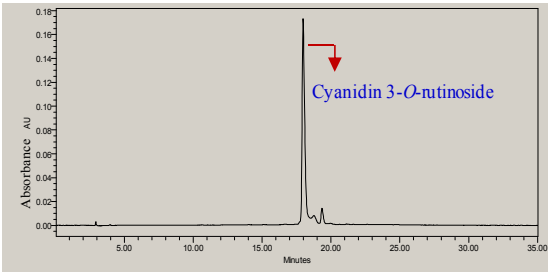
Cyanidin 3-O-rutinoside
Absorbance
AU
Minutes

(d)

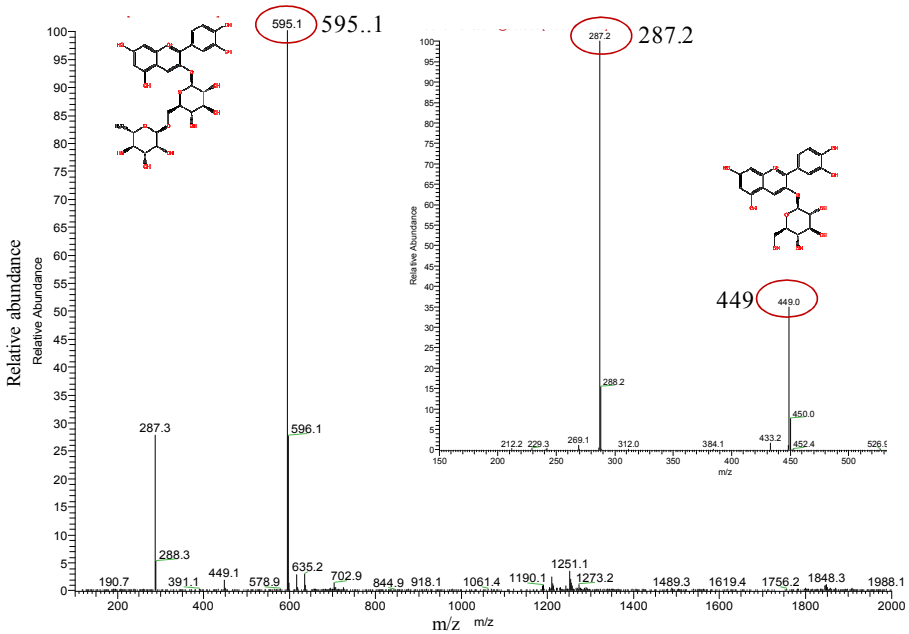
595.1
595..1
287.2
287.2
449
449.0
Relative abundance
Relative Abundance
m/z

(e)

4.3.2 Decoration of anthocyanins in tobacco with modifying enzymes

Tobacco anthocyanins were engineered in order to study the effects of different side chain modifications of anthocyanins on AVI formation. Tobacco accumulates simple anthocyanins mainly cyanidin 3-*O*-rutinoside in its flowers and it is amenable to genetic engineering using genes encoding enzymes from heterologous species capable of decorating the different hydroxyl (OH) groups of anthocyanins. The general structure of anthocyanin is depicted in Figure 4.6. The ease of tobacco transformation and the fact that tobacco normally makes no anthocyanins in its vegetative tissues make it an ideal species with which to study the formation of AVIs.

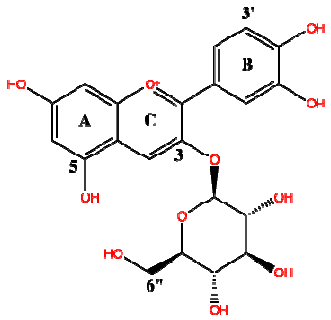

Figure 4.6 | General structure of anthocyanin. Here cyanidin 3-*O*-glucoside is depicted. Anthocyanidin has a three ring (A, B and C) structure and addition of glucose at 3-OH makes it 'anthocyanin'. An –OH at only 4' position converts anthocyanidin to pelargonidin type, at 3' and 4' gives a cyanidin and at 3', 4' and 5'converts it to delphinidin molecule.

4.3.2.1 Engineering 5-glucosylated anthocyanins

4.3.2.1.1 Studying the activity of At5GT on cyanidin 3-O-rutinoside

The *At5GT* gene (*Arabidopsis thaliana* 5- UDP glucosyltransferase; At4g14090) has been reported to encode an anthocyanidin 5-*O*-glucosyltransferase specifically glucosylating the 5-position of the flavonoid A-ring [Fig 4.7] (Tohge et al., 2005). The major anthocyanin accumulated in stressed wild type mature *Arabidopsis thaliana* is cyanidin 3-*O*-[2-*O*(2-*O*-(sinapoyl)-b-d-xylopyranosyl)-6-*O*-(4-*O*-(b-d-glucopyranosyl)-*p*-coumaroyl-b-d-glucopyranoside]5-*O*-[6-*O*-(malonyl)b-d-gluco-pyranoside] (Bloor and Abrahams, 2002). Since enzymes may have strict substrate specificity and as At5GT was

not characterised, confirming the activity of At5GT on cyanidin 3-*O*-rutinoside was crucial before over expressing it in tobacco. Hence, *At5GT* was recombined into a Gateway expression vector, pMGWA, in frame with an N-terminal Maltose Binding Protein (MBP) tag under the regulation of the T7 promoter. The insertion of *At5GT* in frame in pMGWA was confirmed by sequencing. The MBP-At5GT was expressed in *E. coli* and the full length protein with the MBP tag left in place was used for enzymatic assay. The soluble fraction of the recombinant protein was assayed using cyanidin 3-*O*-rutinoside and UDP-glucose as substrates. At5GT was able to glucosylate cyanidin 3-*O*-rutinoside giving a new product peak at 15.68 min as analysed by HPLC [Fig 4.7]. Only weak activity of the recombinant enzyme was detected which could be due either to reduced activity of MBP tagged protein or to a preference of the enzyme for acylated substrate as is found in Arabidopsis.

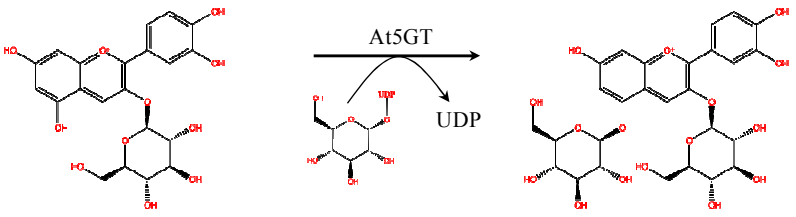

(a)

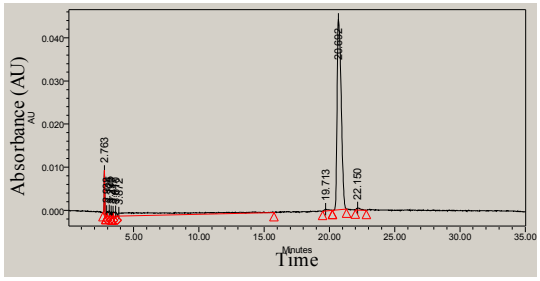

(b)

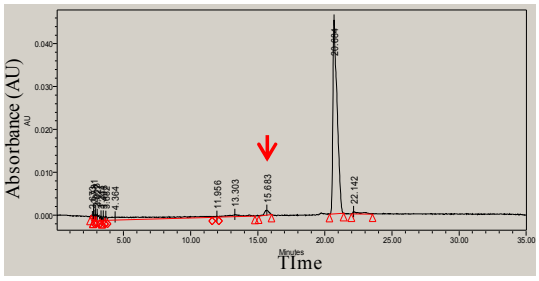

(c)

Figure | 4.7 HPLC analysis of the MBP-At5GT enzyme reaction. (a) Reaction catalysed by At5GT depicting the position of glucosylation; anthocyanidin 3-glucoside was converted to anthocyanidin 3, 5-diglucoside. (b) Cyanidin 3-*O*-rutinoside standard reaction with no enzyme (c) MBP-At5GT enzyme reaction with the product peak seen at 15.68 min.

4.3.2.1.2 Engineering 5-glucosylated anthocyanin in tobacco

In order to study the effect of glucosylation at the 5-position of the A-ring on anthocyanin in AVI formation; At5GT was over expressed in tobacco. The gene encoding At5GT (intron-less) was amplified from Arabidopsis genomic DNA and was recombined into a plant transformation vector pJAM1502 under the control of the double 35S promoter using Gateway recombination technology.

Twenty independent kanamycin-resistant lines were analysed for gene insertion and expression [Fig 4.8d] before analysing their anthocyanins. HPLC analysis of flower extracts of 2x35S::*At5GT* transgenic lines (all the 20 lines) showed a new peak in comparison to that of wild type (Samsun) flowers [Fig 4.8c]. Cyanidin 3-*O*-rutinoside was still the dominant anthocyanin in the At5GT flowers, but a new anthocyanin, cyanidin 3-*O*-rutinoside-5-glucoside, was present in very small amounts. The product of the new peak at 15.1 min was confirmed to be cyanidin 3-*O*-rutinoside-5-*O*-glucoside by LC-MS, the new anthocyanin having a molecular weight (m/z) value of 757.1 with a major fragment at m/z 595, which corresponds to cyanidin 3-*O*-rutinoside. The ion at m/z 595 is due to loss of glucose with m/z 162. Further MS2 of m/z 595 showed fragments of $[M+H]^+$ at m/z 449 and 287 due to loss of rhamnose of m/z 146 [Fig 4.8d]. Spectral measurements are a way of determining attachment of the sugars in the anthocyanin molecule with a shift towards shorter wavelengths called a hypsochromic shift (Harborne, 1957). A spectral shift to 516.9 nm compared to cyanidin 3-*O*-rutinoside at 519.4 nm was also observed in online spectra whereas no shift was observed with the total anthocyanins extracted from the flowers [Fig 4.8b]. This could be due to the low amount of glucosylated anthocyanin.

Five selfed positive 2x35S::*At5GT* lines showed an enhancement in cyanidin 3-*O*-rutinoside-5-*O*-glucoside in flowers with the relative amount of cyanidin 3-*O*-rutinoside-5-*O*-glucoside being 2-6% of total anthocyanin, whereas cyanidin 3-*O*-rutinoside constituted nearly 80%. Flowers of 2x35S::*At5GT* lines did not show any significant colour change compared to the wild type flowers, probably because of the low level of cyanidin 3-*O*-rutinoside-5-*O*-glucoside [Fig 4.8a]. To generate lines producing high amounts of anthocyanin including cyanidin 3-*O*-rutinoside-5-*O*-glucoside; 2x35S::*At5GT* positive lines were crossed with 2x35S::*Del*/2x35S::*Ros1*. However, the positive lines expressing 2x35S::*Del*/2x35S::*Ros1* and 2x35S::*At5GT* [Fig 4.8e, f] looked paler than lines expressing 2x35S::*Del*/2x35S::*Ros1* only.

Figure 4.8 | Over-expression of At5GT in tobacco and LC-MS analysis of anthocyanins from flower extracts.

(a) Flowers of wild type (left) and At5GT over-expression (2x35S::*At5GT*) lines (middle); no visual colour differences were observed between the control and OX lines. Flower of triple transgenic 2x35S::*Del*/2x35S::*Ros*/2x35S::*At5GT* is shown on right.

(b) Spectral shift analysis of the anthocyanins extracted from flower samples of Samsun and 2x35S::*At5GT* primary transformants (T_0) (TCU 143-15, TCU 145-18, TCU 145-11). No shift in absorbance was observed.

(c) HPLC analysis of anthocyanins from flower extracts of pJ1502 (empty vector) expressing tobacco (left) and 2x35S::*At5GT*T_1 generation line (right). New compound formed is separated as a new peak at 15 min.

(d) RT-PCR analysis of *At5GT* transcript in T_0; 2x35S::*At5GT* lines (TCT 142, TCT 143) and Samsun (wild type). *Ubiquitin* was amplified from these lines as control and RNA was used as negative control for RT reaction.

(e) Genomic analysis of 2x35S::*Del*/2x35S::*Ros*/2x35S::*At5GT* F_1 progeny for insertion of *At5GT* with 2x35S::Del/2x35S::Ros (TCU 24) F_2 plant as control.

(f) RT-PCR analysis of transcription of *Del*, *Ros1* and *At5GT* in 2x35S::*Del*/2x35S::*Ros*/2x35S::*At5GT* lines (TCU 10g13, TCU 10g14, TCU 10g15).RT-PCR with *ubiquitin* primers was performed as control amplification and PCR from RNA was performed as RT negative control.

(g) Mass spectrum analysis of the novel peak obtained in the 2x35S::*At5GT* line; in inset MS2 fragmentation of cyanidin 3-*O*-rutinoside-5-glucoside into cyanidin 3-*O*-rutinoside due to loss of 5-glucose is represented.


Samsun
2x35S::At5GT
2x35S::Del/2x35S::Ros1/
2x35S::At5GT

(a)

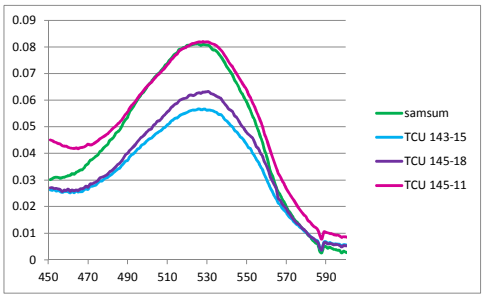
samsum
TCU 143-15
TCU 145-18
TCU 145-11

(b)

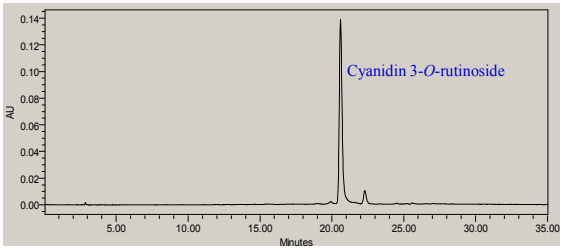
Cyanidin 3-O-rutinoside
AU
Minutes

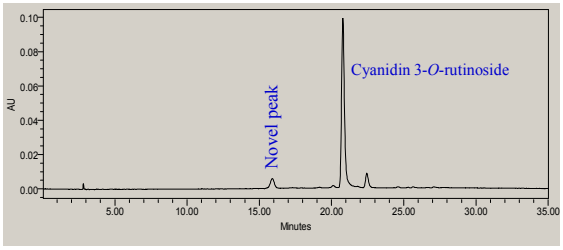
Novel peak
Cyanidin 3-O-rutinoside
AU
Minutes

(c)

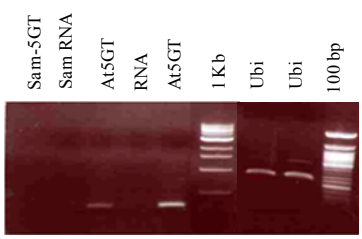
Sam-5GT
Sam RNA
At5GT
RNA
At5GT
1 Kb
Ubi
Ubi
100 bp

(d)

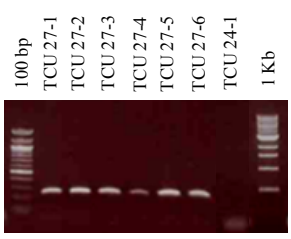
100 bp
TCU 27-1
TCU 27-2
TCU 27-3
TCU 27-4
TCU 27-5
TCU 27-6
TCU 24-1
1 Kb

(e)

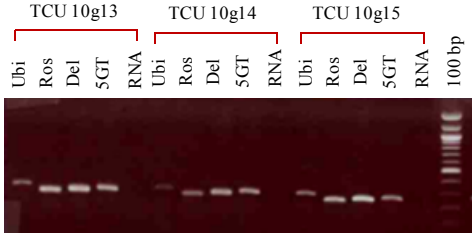
TCU 10g13
TCU 10g14
TCU 10g15
Ubi
Ros
Del
5GT
RNA
100 bp

(f)

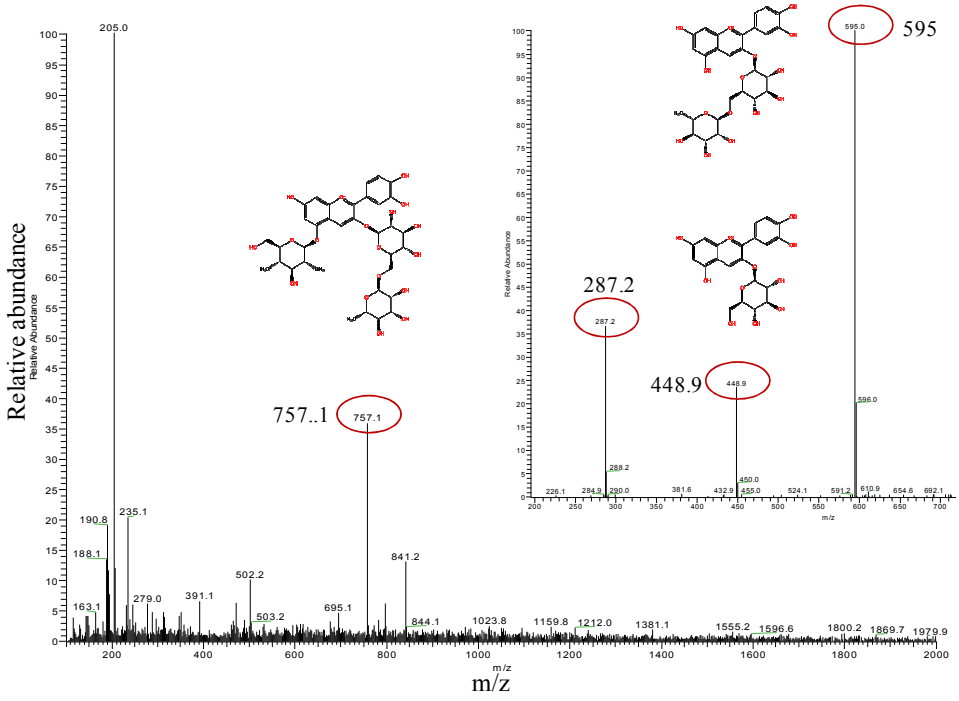
Relative abundance
205.0
757..1
595
287.2
448.9
m/z

(g)

4.3.2.1.3 Engineering coumaroylated anthocyanins in tobacco

Tobacco transgenics accumulating high levels of anthocyanins along with coumaroylated anthocyanins were generated by Jie Luo as described in this section. Anthocyanidin 3-*O*-glucoside acyl CoA transferease (At3AT; gene bank accession number At1g03940) is an aromatic acyl transferase which catalyses the transfer of a coumoryl group on to 6″ *O*-position of 3-glucose in anthocyanin (Luo et al., 2007) [Fig 4.9a]. *At3AT* was over-expressed in tobacco under the control of the double 35S promoter using the pJAM1502 expression vector and the resulting 2x35S::*At3AT* line was crossed with a line expressing 2x35S::*Del*/2x35S::*Ros1* to obtain high anthocyanin producing lines. The At3AT enzyme is specific for acylating cyanidin 3-*O*-glucoside and significant amounts of cyanidin 3-*O*-(6″ coumaroyl) glucoside are made instead of coumaroylated cyanidin 3-*O*-rutinoside (Luo et al., 2007).

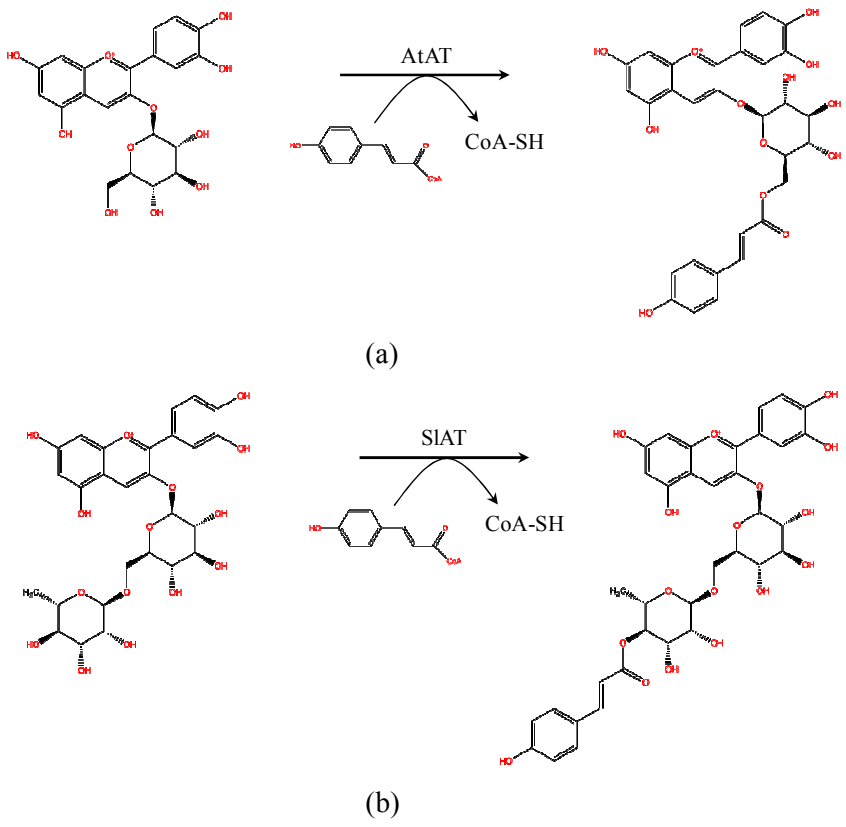

Figure 4.9 | Enzymatic catalysis carried by At3AT and Sl3AT in tobacco. (a) Enzymatic reaction catalysed by At3AT is depicted. At3AT transfers a coumaroyl residue from coumaroyl-CoA on to 6″-positon of the 3-glucose of cyanidin 3-*O*-glucoside (b) Sl3AT transfers a coumaroyl residue on to 4‴-position of 3- rhamnose of cyanidin 3-*O*-rutinoside.

To generate transgenics producing coumaroylated cyanidin 3-*O*-rutinoside; anthocyanidin acyl transferase from tomato (Sl3AT; gene bank accession number EU979541.1) was cloned into the plant expression vector pJAM 1502 (Jie Luo). Sl3AT is a putative anthocyanin acyltransferase isolated from *Del/Ros1* tomato lines through substractive hybridization (Butelli et al., 2008). This putative enzyme was partially characterised using recombinant protein expressed in *E.coli* and studied to be an aromatic acyl transferase capable of catalysing the transfer of a coumaroyl group on to 4‴ *O*-postion of 3-rhamnose in anthocyanin [Fig 4.9b]. Transgenics expressing 2x35S::*Sl3AT* accumulated cyanidin 3-*O*-(4‴ coumaroyl) rutinoside and these line were crossed with a line expressing 2x35S::*Del*/2x35S::*Ros1* for studies in AVI formation.

4.3.2.1.4 Accumulation of coumaroylated and 5-glucosylated anthocyanin in tobacco

Glycosylation at the 5-positon of the anthocyanidin A ring has been suggested to decrease the stability of anthocyanins (Luo et al., 2007). In order to study the combined effects of 5-glycosylation and coumarylation of anthocyanin on AVI formation in tobacco, 2x35S::*At5GT* was crossed with the line 2x35S::*Del*/2x35S::*Ros1*/ 2x35S::*At3AT* (producing cyanidin 3-*O*-(6″ coumaroyl) glucoside).

Out of twelve positive F_2 plants expressing the four genes *Del/Ros1/3AT/5GT* [Fig 4.10a, b] and screened for metabolites, five independent transgenics showed the accumulation of three new anthocyanins along with cyanidin 3-*O*-rutinoside [Fig 4.10c]. ESI-MS identified the products at 14.26 min and 24.75 min as cyanidin 3-*O*- rutinoside-5-glucoside (m/z 757.1) and cyanidin 3-*O*-(6″ coumaroyl) glucoside (m/z 595.1) [Fig 4.10f, g]. The product obtained at 22.31 min could not be identified, but had a mass and fragmentation pattern similar to cyanidin 3-*O*-rutinoside-5-*O*-glucoside (m/z 757.1). The compound at 22.31 min was predicted to be a 5-glucosylated cyanidin 3-*O*-(6″ coumaroyl) glucoside based on the retention time, having a mass of 757.1(m/z). This product was confirmed to be cyanidin 3-*O*-(6″ coumaroyl) 5-diglucoside through NMR spectrometry (Refer section 5.3.2.1; chapter V). The MS2 fragmentation pattern is explained in the table 4.3.

Figure 4.10 | Analysis of 2x35S::*Del*/2x35S::*Ros*/2x35S::*At5GT*/2x35S::*At3AT* lines

(a) RT-PCR analysis of 2x35S::*Del*/2x35S::*Ros*/2x35S::*At5GT*/2x35S::*At3AT* F_1 generation lines for transcripts of *Delila*, *Rosea1* and *At5GT* along with *ubiquitin* as control and RNA of each as RT negative control.

(b) Genomic confirmation of F_2 lines (TCU 33 series) for *At3AT* and *At5GT* insertion; and the lines with both the genes were taken for further analysis.

(c) HPLC profile of the anthocyanins extracted from 2x35S::*Del*/2x35S::*Ros* line with cyanidin 3-O-rutinoside (top); flower anthocyanins extracted from 2x35S::At3AT line showing cyanidin 3-*O*-(6″ coumaroyl) glucoside at 24.75 min (middle) and from 2x35S::*Del*/2x35S::*Ros*/2x35S::*At5GT*/2x35S::*At3AT* line with three new anthocyanins eluted at different time points (bottom).

(d) Spectral shift measurement (at visible wavelength) of anthocyanins extracted from the flowers of 2x35S::*At3AT* (TCU 21-10) compared with Samsun flowers.

(e) Spectral measurements (at visible wavelength) of anthocaynins extracted from leaves of 2x35S::*Del*/2x35S::*Ros*/2x35S::*At5GT*/2x35S::*At3AT* lines (TCU 12b3, TCU 12b5, TCU 33-3, TCU 33-7) compared to 2x35S::*Del*/2x35S::*Ros* (TCU 24-4). A slight bathochromic shift (1 nm) in the absorbance was observed with the addition of the coumaroy moeity.

(f) and (g) on page 104

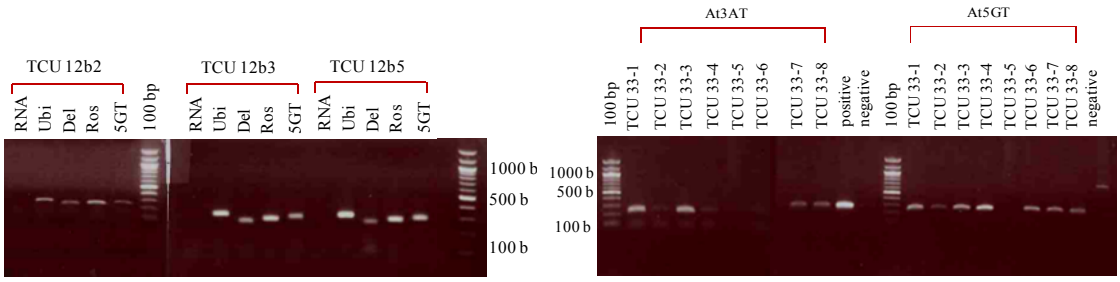
TCU 12b2
TCU 12b3
TCU 12b5
RNA
Ubi
Del
Ros
5GT
100 bp
1000 b
500 b
100 b
At3AT
At5GT
TCU 33-1
TCU 33-2
TCU 33-3
TCU 33-4
TCU 33-5
TCU 33-6
TCU 33-7
TCU 33-8
positive
negative

(a) (b)

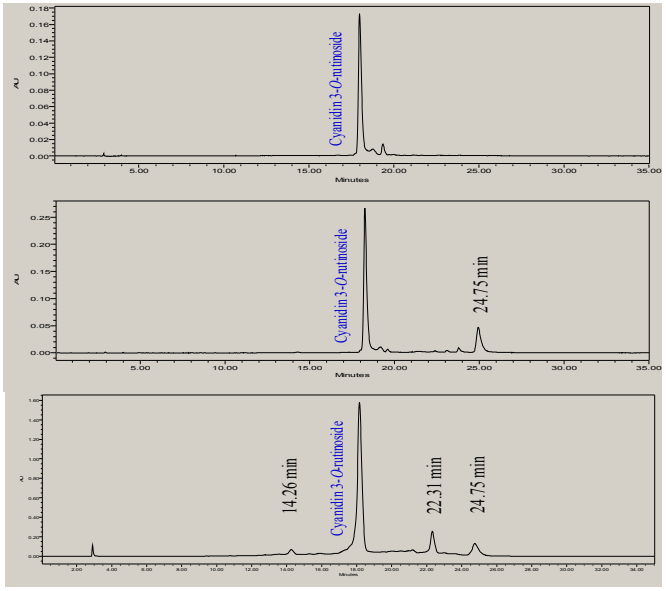
Cyanidin 3-O-rutinoside
24.75 min
14.26 min
22.31 min
Minutes
AU

(c)

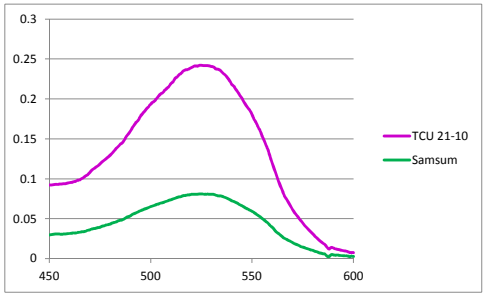
TCU 21-10
Samsum

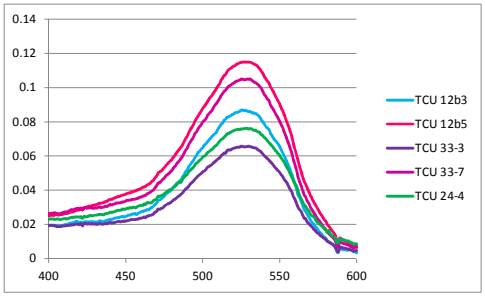
TCU 12b3
TCU 12b5
TCU 33-3
TCU 33-7
TCU 24-4

(d) (e)

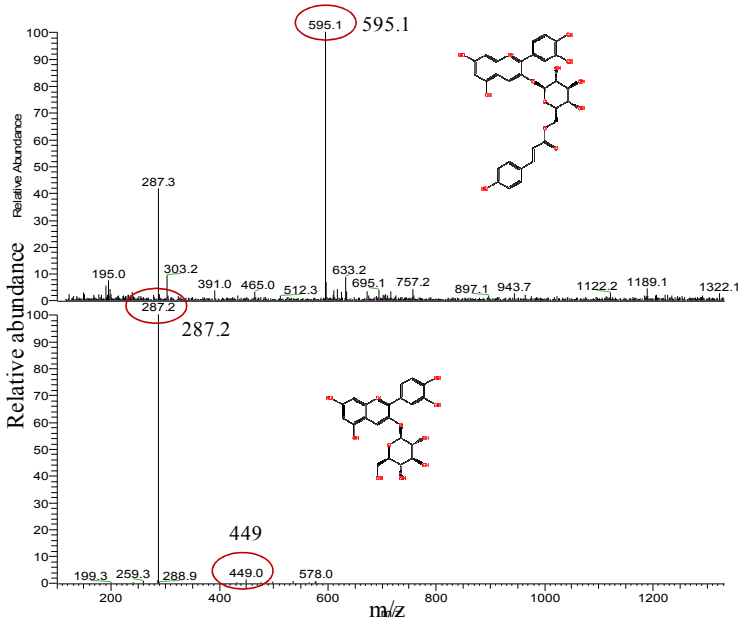

(f)

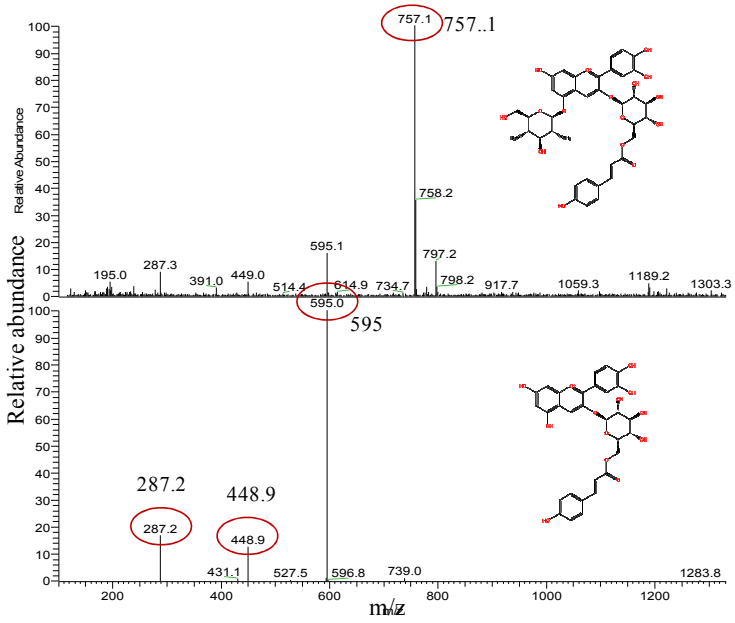

(g)

Figure 4.10 | Analysis of 2x35S::*Del*/2x35S::*Ros*/2x35S::*At5GT*/2x35S::*At3AT* lines

(f) Mass analysis of cyanidin 3-*O*-(6″ coumaroyl) glucoside (m/z 595.1) from 2x35S::*Del*/2x35S::*Ros*/2x35S::*At5GT*/2x35S::*At3AT* line obtained at 24.75 min and MS2 fragmentation pattern showing cyanidin 3-O-glucoside (m/z 449) after loss of coumarate group and cyanidin (m/z 287.2) after loss of glucose.

(g) Mass analysis of cyanidin 3-*O*-(6″ coumaroyl) 5-diglucoside (m/z 757.1) from 2x35S::*Del*/2x35S::*Ros*/2x35S::*At5GT*/2x35S::*At3AT* line obtained at 22.31 min and MS2 fragmentation pattern showing cyanidin 3-*O*-(6″ coumaroyl) glucoside (m/z 595.1) after loss of glucose moeity.

Table 4.3 | Characterisation of anthocyanin peaks identified in 2x35S::*Del*/2x35S::*Ros1*/2x35S::*At3AT*/2x35S::*At5GT* lines as in figure 4.10

Rt (min)	ESI-MS (m/z)	MS/MS fragments	compound
14.26	757.1	595 [Cy+Rha]+449[Cy+Glc]+287 [Cy]+	Cyanidin 3-*O*-rutinoside 5-*O*-glucoside
22.31	757.1	595[Cy+Glc+Cou]+449[Cy+Glc]+287 [Cy]+	cyanidin 3-*O*-(6″ coumaroyl) 5-diglucoside
24.75	595	449[Cy+Glc]+287 [Cy]+	cyanidin 3-*O*-(6″ coumaroyl) glucoside

Rt, retention time; Cy, cyanidin; Rha, rhamnose; Glc, glucose; Cou, coumaroyl; ESI-MS, Electro spray ionization mass spectra; m/z, molecular mass of compound

No phenotypic differences were observed in 2x35S::*Del*/2x35S::*Ros1*/2x35S::*At3AT*/2x35S::*At5GT* plants compared to 2x35S::*Del*/ 2x35S::*Ros1*/2x35S::*At3AT* plants except that the extracted anthocyanins showed a 1 nm spectral shift towards a longer wavelength [Fig4.10d]. The amount of cyanidin 3-*O*-(6″ coumaroyl) 5-diglucoside accumulated in 2x35S::*Del*/2x35S::*Ros1*/2x35S::*At3AT*/ 2x35S::*At5GT* lines was considerably higher than the levels of Cyanidin-3-*O*-rutinoside-5-*O*-glucoside accumulated in 2x35S::*Del*/2x35S::*Ros1*/2x35S::*At5GT* lines; indicating that At5GT has higher preference for acylated anthocyanins for 5-glucosylation than non-acylated anthocyanins. However not every molecule of cyanidin 3-*O*-(6″ coumaroyl) glucoside was 5-glucosylated. This could be due to the lower turnover efficiency of At5GT enzyme for this particular substrate.

4.3.2.2 Engineering malonylated anthocyanin in tobacco

To decorate cyanidin 3-*O*-rutinoside with a malonyl molecule, *Ch3MAT* was isolated from the flowers of dark red chrysanthemum (purchased from local supermarket). *Ch3MAT* (GenBank: AY298809.1) from *Chrysanthemum x morifolium* encodes an anthocyanidin 3-*O*- glucoside- 6″-*O*-malonyltransferase which catalyses the transfer of a malonyl group from malonyl Co-A to the 6″ -OH of the 3-glucose of anthocyanin 3-*O*-glucoside (Suzuki et al., 2004a) [Fig 4.11a]. As the cDNA was prepared from an unknown variety of chrysanthemum, it showed three base pair differences to the published *Ch3MaT* sequence leading to two amino acid changes which could be due to

errors incorporated during the PCR or due to natural variation. Substitution of Ala-94 to Val-94 and Ala-189 to Val189 was achieved by mutagenesis to obtain a clone with identical sequence to that of characterised *Ch3MaT* [Fig4.11b]. The positive sequence cloned under the control of double 35S promoter was transferred to tobacco.

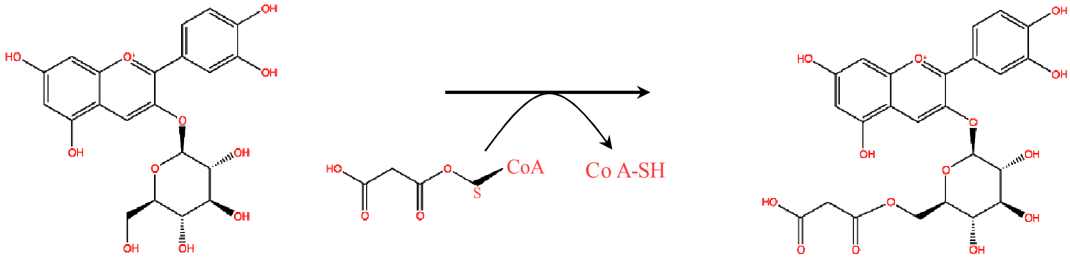

(a)

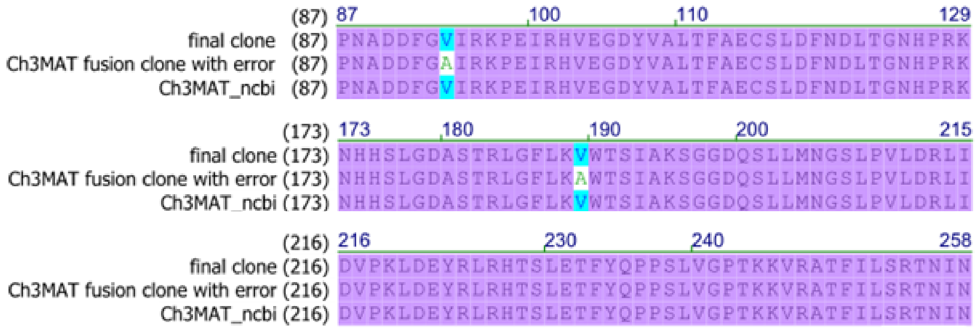

(b)

Figure 4.11 | (a) Enzymatic reaction catalyzed by Ch3MAT; malonyl moiety is transferred from malonyl-CoA to the 6″-positon of 3-glucose of cyanidin 3-*O*-glucoside. (b) Final sequence of *Ch3MAT* obtained through site-directed mutagenesis PCR to remove the bases that are leading to change in amino acid. Here the sequence of amino acids from the final *Ch3MAT* construct (without errors), the fusion construct (with errors; before site-directed mutagenesis PCR) and the original *Ch3MAT* sequence from NCBI are aligned (part of alignment is shown). The full length sequence of the gene in the final construct from the above depiction is presented in the appendix.

Figure 4.12 | Analysis of anthocyanins from flower extracts of Ch3MAT over-expression lines.

(a) Flowers of Samsun (left) compared to 2x35S::*Ch3MAT* lines (middle). An increase in colour of flowers of Ch3MAT lines was observed. Flower of triple transgenic 2x35S::*Del*/2x35S::*Ros*/2x35S::*Ch3MAT* is shown on right.

(b) Genomic confirmation of *Ch3MAT* from leaves of T_0; 2x35S::*Ch3MAT* compared to wild type (Samsun).

(c) RT-PCR analysis of transcription of *ubiquitin* and *Ch3MAT* in the leaves of; 2x35S::*Del*/2x35S::*Ros1*/2x35S::*Ch3MAT* F_1 lines and Samsun (wild type).

(d) HPLC analysis of anthocyanins extracted from flowers of 2x35S::*Ch3MAT* shows a new product at 21.06 minutes compared to the anthocyanins extracted from Samsun flowers.

(e) Spectral measurements of anthocyanins extracted from flowers of a line with 2x35S::*Ch3MAT* (TCU 30-4) compared to Samsun (top) and from 2x35S::*Del*/2x35S::*Ros*/2x35S::*Ch3MAT* line (TCU 75-1, 2, 5, 8) compared to 2x35S::*Del*/2x35S::*Ros1* lines (TCU 24-4 and TCU 170-1). A slight bathochromic shift of 1-2 nm was observed with the addition of malonyl molecule.

(f) Mass analysis of the new product at 21.06 min was identified as cyanidin 3-*O*-(6″ malonyl) glucoside of m/z 535.1.

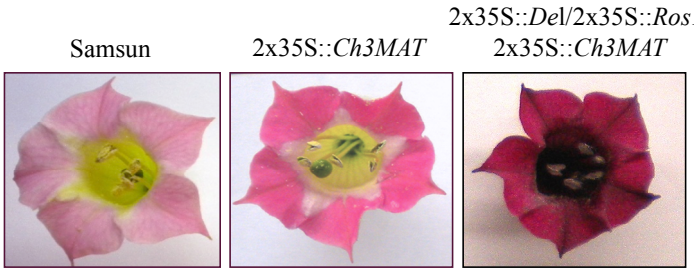
Samsun
2x35S::*Ch3MAT*
2x35S::*Del*/2x35S::*Ros1*/
2x35S::*Ch3MAT*

(a)

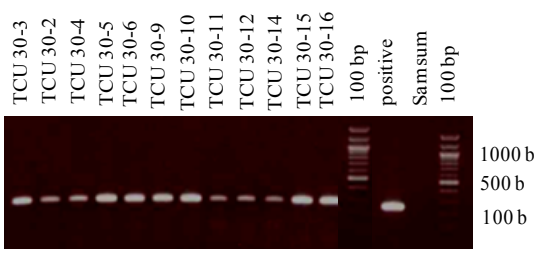
TCU 30-3
TCU 30-2
TCU 30-4
TCU 30-5
TCU 30-6
TCU 30-9
TCU 30-10
TCU 30-11
TCU 30-12
TCU 30-14
TCU 30-15
TCU 30-16
100 bp
positive
Samsum
100 bp
1000 b
500 b
100 b

(b)

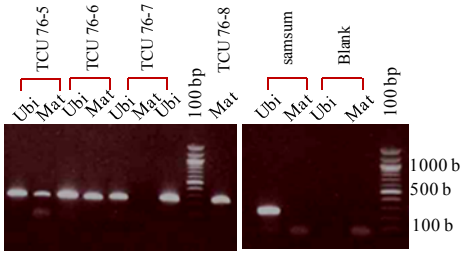
TCU 76-5
TCU 76-6
TCU 76-7
TCU 76-8
samsum
Blank
Ubi
Mat
100 bp
1000 b
500 b
100 b

(c)

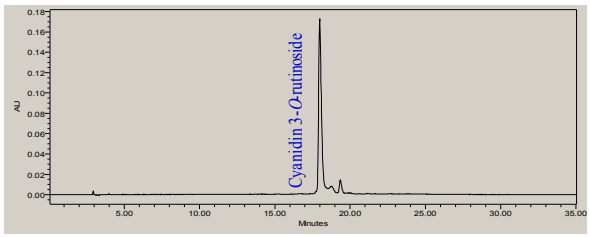
Cyanidin 3-*O*-rutinoside
AU
Minutes

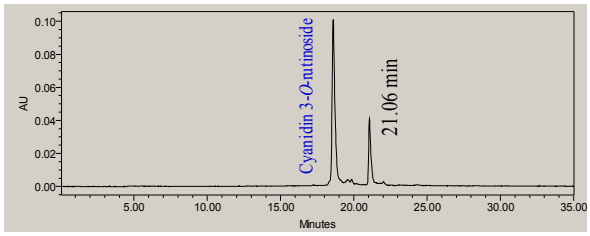
Cyanidin 3-*O*-rutinoside
21.06 min
AU
Minutes

(d)

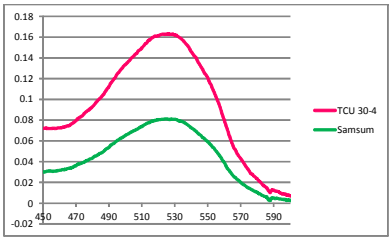
TCU 30-4
Samsum

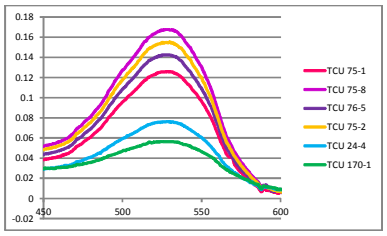
TCU 75-1
TCU 75-8
TCU 76-5
TCU 75-2
TCU 24-4
TCU 170-1

(e)

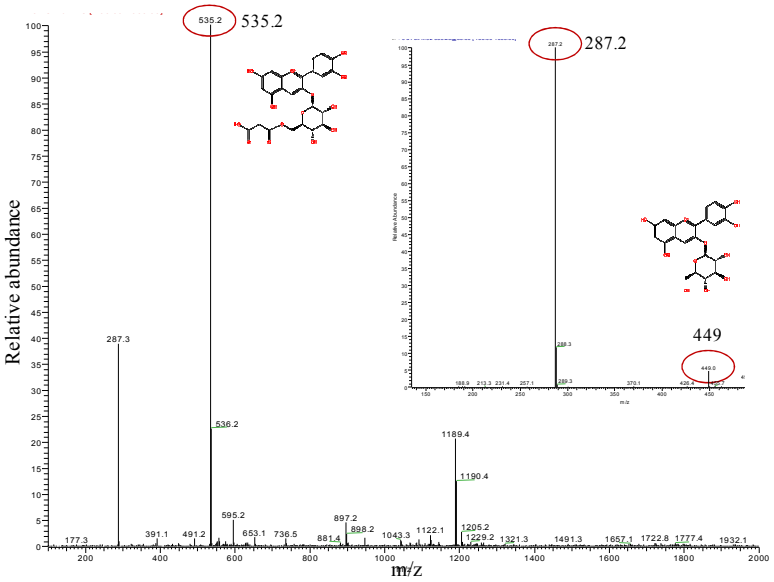
535.2
287.2
449
Relative abundance
m/z

(f)

Fifteen independent kanamycin resistant 2x35S::*Ch3MaT* lines were analysed for the insertion and expression of the gene [Fig 4.12b]. Flowers of 2x35S::*Ch3MaT* lines showed intense pigment colour compared to control [Fig 4.12c] and this could be due to the stability offered by malonylation. Anthocyanins extracted from the flowers of 2x35S::*Ch3MaT* lines showed a shift in absorbance of 1-2 nm towards the bluer wave length due to addition of the malonyl moiety [Fig 4.12e]. HPLC analysis of the extracted anthocyanins from flowers of 2x35S::*Ch3MaT* lines identified a new compound at 20.1 min along with cyanidin 3-*O*-rutinoside [Fig 4.12d]. Seven independent lines showed variable levels of metabolite production. The new anthocyanin produced eluted with kaempferol-3-rutinoside, making mass analysis difficult. Performing a polar RP column separation along with ion trap showed the new product to be cyanidin 3-*O*-(6″ malonyl) glucoside (m/z 535.0) [Fig 4.12f]. Similar to At3AT, this enzyme specifically acylates the 6″ OH group of cyanindin 3-*O*-glucoside. The 2x35S::*Ch3MaT* lines producing the highest levels of malonylated anthocyanin were crossed with a line expressing 2x35S::*Del/*2x35S::*Ros1* for high anthocyanin production [Fig 4.12c].

4.3.2.3 Engineering delphinidin production in tobacco

Tobacco can accumulate only cyanidin-based anthocyanins due to lack of flavonoid 3' 5' hydroxylase (F3'5'H) enzyme [Fig 4.13]. F3'5'H activity is essential for the formation of delphinidin-based anthocyanins, which are blue anthocyanins with a shift in maximum absorption compared to cyanidin based anthocyanins (Fukui et al., 2006). F3'5'H was expressed in tobacco to understand whether the formation of AVIs is affected by the type of anthocyanin available. The cDNA of *F3'5'H* from Petunia was cloned under the control of a double 35S promoter in a plant transformation vector. Kanamycin resistant 2x35S::*PhF3'5'H* lines positive for the presence of gene [Fig 4.14b] showed the accumulation of a mixture of cyanidin 3-*O*-rutinoside and delphinidin 3-*O*-rutinoside (m/z 611.1) in their flowers as analysed in seven independent lines [Fig 4.14e]. Due to the accumulation of delphinidin 3-*O*-rutinoside, the flowers showed a dark pink/mauve colour compared to wild type [Fig 4.14a]. The anthocyanins extracted from the flowers showed a spectral shift of 10-12 nm towards higher wavelength (bluer) compared to samsun [Fig 4.14d] as is expected with delphinidin based anthocyanins. 2x35S::*PhF3'5'H* lines accumulating high levels of delphinidin 3-*O*-rutinoside were crossed with 2x35S::*Del/*2x35S::*Ros1* for AVI studies.

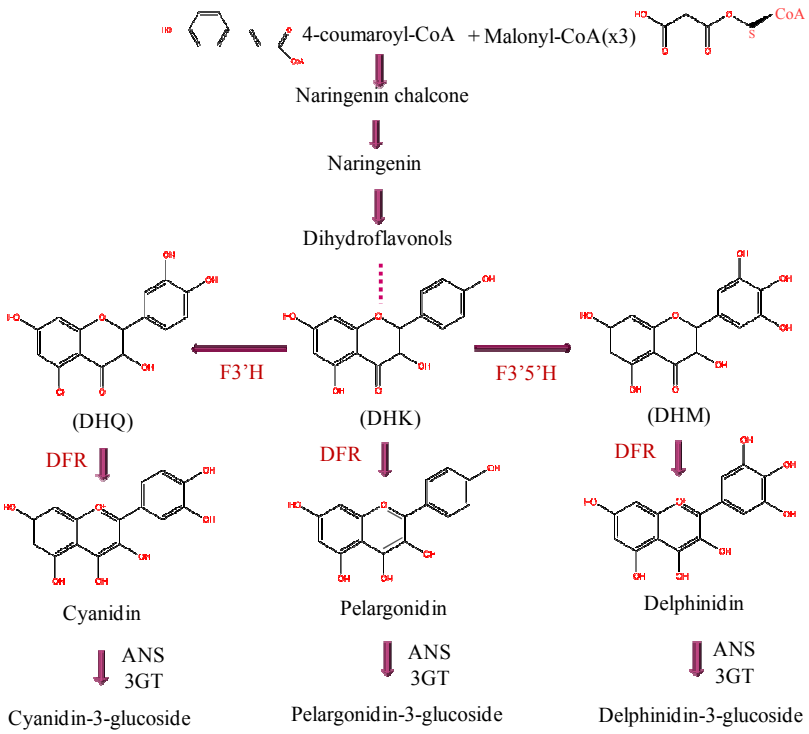

Figure 4.13 | Schematic representation of the biosynthesis of different anthocyanins from dihydrokaempferol (DHK) catalysed by enzymes; flavonoid 3' hydroxylase (F3'H), flavonoid 3'5' hydroxylase (F3'5'H), dihydro flavonol 4-reductase (DFR).

Figure 4.14 | Analysis of tobacco 2x35S::*PhF3'5'H*-OX lines.

(a) Flowers of Samsun on left and 2x35S::*PhF3'5'H* lines on right.

(b) Absorbance spectrum of anthocyanins isolated from flowers of 2x35S::*PhF3'5'H* T_0 lines; a clear shift of 12nm towards bluer wavelength was observed compared to anthocyanins from Samun flowers.

(c) RT-PCR and genomic analysis of T_0; 2x35S::*PhF3'5'H* lines for gene expression and insertion compared to a control

(d) HPLC profile showing the new product in the transgenics at 16.78 min (right) compared to wild type flower where the anthocyanin; cyanidin 3-*O*-rutinoside eluted at 18.2min (left).

(e) Mass analysis of new product at 16.78 min confirmed the new anthocyanin to be delphinidin 3-*O*-rutinoside (m/z 611.11) and MS2 fragmentation shows delphinidin 3-*O*-glucoside (m/z 464.97) due to loss of rhamnose.

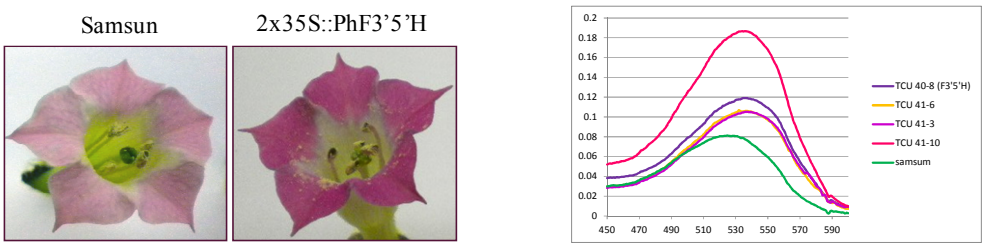
Samsun
2x35S::PhF3'5'H
TCU 40-8 (F3'5'H)
TCU 41-6
TCU 41-3
TCU 41-10
samsum

(a) (b)

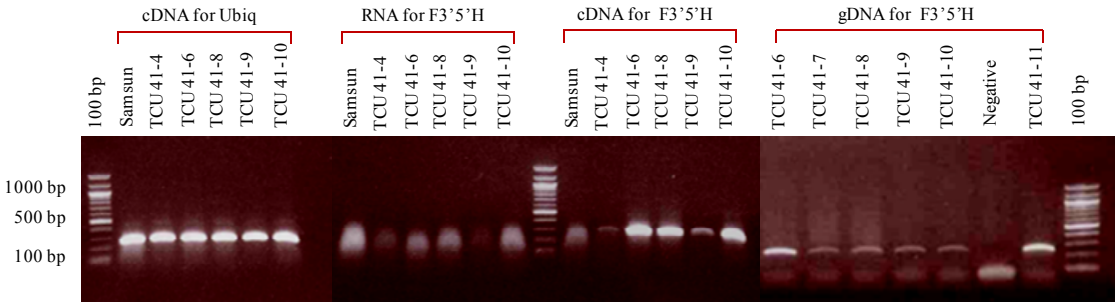
cDNA for Ubiq
RNA for F3'5'H
cDNA for F3'5'H
gDNA for F3'5'H
100 bp
Samsun
TCU 41-4
TCU 41-6
TCU 41-8
TCU 41-9
TCU 41-10
TCU 41-7
TCU 41-11
Negative
1000 bp
500 bp
100 bp

(c)

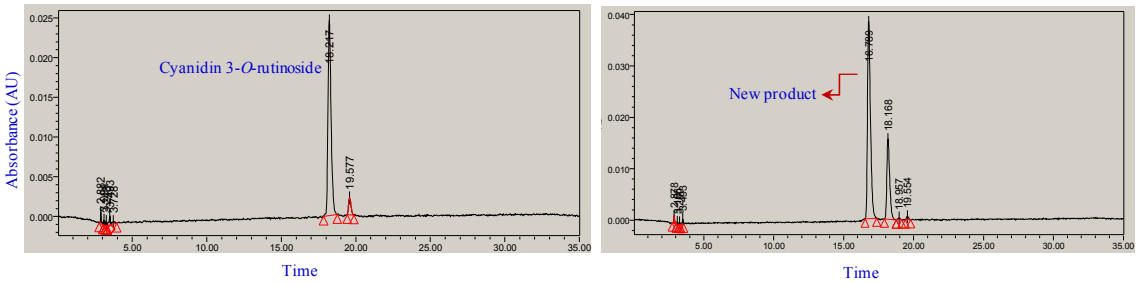
Absorbance (AU)
Cyanidin 3-O-rutinoside
New product
Time
Time

(d)

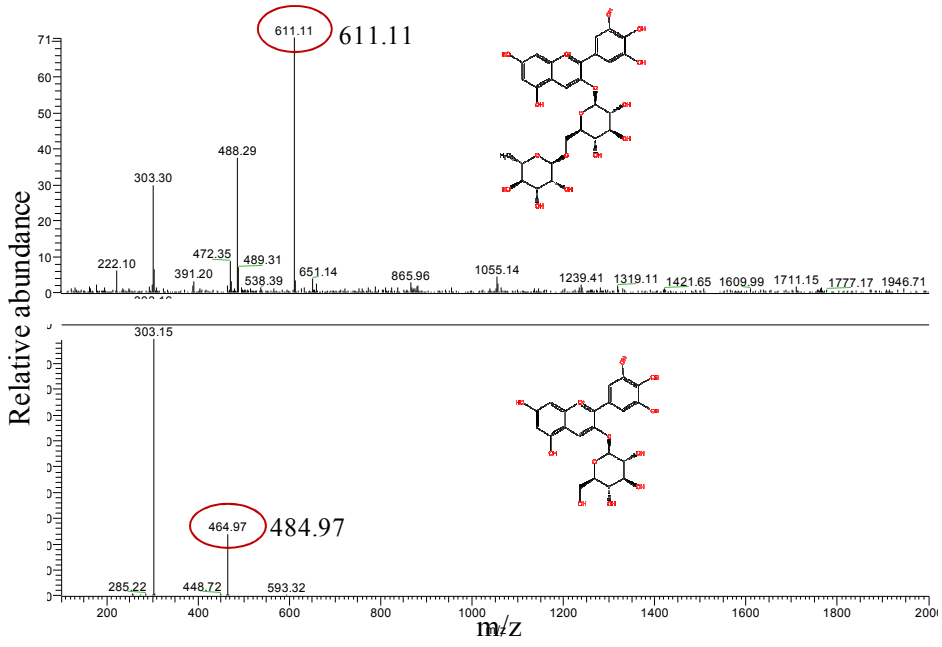
Relative abundance
611.11
611.11
488.29
303.30
222.10
472.35
489.31
391.20
538.39
651.14
865.96
1055.14
1239.41
1319.11
1421.65
1609.99
1711.15
1777.17
1946.71
303.15
464.97
484.97
285.22
448.72
593.32
m/z

(e)

4.3.3 Are AVIs the result of high concentrations of anthocyanins?

Gonnet et al (2003) studied the formation of AVIs in blue rose as the cells reached maturity and they attributed AVI formation to the increasing concentration of the pigment. AVIs are not seen in normal tobacco petals which produce moderate levels of anthocyanins [Cathie Martin personal communication]. To study whether increased anthocyanin concentration can cause AVI formation, anthocyanin pigment accumulation was enhanced in tobacco plants by combined over expression of Delila and Rosea1 transcription factors. Callus obtained from the leaf material from 2x35S::*Del*/2x35S::*Ros1* plants was grown on MS medium with 3% sucrose and hormones, and accumulated high levels of anthocyanins [Fig 4.15 callus]. Microscopic observation of the callus cells from 2x35S::*Del*/2x35S::*Ros1* plants did not show any AVIs; anthocyanins were present exclusively in soluble form. Therefore, increased concentrations of anthocyanins are not sufficient to induce AVI formation.

The anthocyanin pathway is strongly upregulated by sucrose in all plant species (Solfanelli et al., 2006) and sucrose acts as an *in-vivo* trigger for biosynthesis (Lloyd and Zakhleniuk, 2004). To investigate further the concentration effect in AVI formation; anthocyanins were enhanced by sucrose treatment. Anthocyanin regulation by sucrose in 2x35S::*Del*/2x35S::*Ros1* line and Samsun seedlings was studied by growing on medium containing 0%, 3% and 6% sucrose. Gene expression levels of six genes encoding; *phenyl ammonia-lyase* (*PAL*), *4-coumarate-CoA ligase* (*4CL*), *chalcone synthase* (*CHS*), *dihydroflavonol 4-reductase* (*DFR*), *hydroxycinnamoyl CoA quinate transferase* (*HQT*) and *flavonol synthase* (*FLS*) involved in the phenylpropanoid biosynthetic pathway were measured at different sucrose treatment [Fig 4.17]. Sucrose does not have effect on expression of *Delila* and *Rosea1* (0% and 3% observation) however, their expression was reduced at 6% sucrose. Expression levels of *4CL*, *HQT* and *FLS* in 2x35S::*Del*/2x35S::*Ros* plants were less compared to samsun probably due to the precursors being diverted to anthocyanin synthesis. Upregulation of *CHS* and *DFR* involved in anthocyanin biosynthesis was observed in lines treated with 3% and 6% sucrose compared to those grown without sucrose. Therefore it indicates that sucrose enhances the expression of late anthocyanin biosynthetic genes. When the amount of anthocyanin produced was measured in 2x35S::*Del*/2x35S::*Ros1* plants grown with sucrose (3%) and without sucrose; higher amounts were observed in 3% sucrose (3200.95 mg/100g and 3867.56 mg/100 g dry weight) compared to those grown without

Figure 4.16 | Effect of sucrose on anthocyanin production in 2x35S::*Del*/2x35S::*Ros1*.
(a) 2x35S::*Del*/2x35S::*Ros1* (TCS 113-5) seedlings (purple coloured) grown on MS medium with sucrose (3% and 6%) and without sucrose compared to samsun (green coloured) grown in similar conditions. Phenotypic and visual color differences in 2x35S::*Del*/2x35S::*Ros1* seedlings grown on medium with and without sucrose are depicted. TCS 113-5 plants grown of 6% sucrose showed intense anthocyanin accumulation and were stunted in growth when visually compared to those grown in medium without sucrose (b) Two independent anthocyanin extractions from four lines of 2x35S::*Del*/2x35S::*Ros1* (TCS 113-5) grown without sucrose (B4, B5 lines) and 3% sucrose (B6, B7) were compared for anthocyanin accumulation. The amount of anthocyanin has increased significantly with sucrose treatment.

sucrose (290.99 mg/100g and 1576.74 mg/100 g dry weight) [Fig 4.16b]. AVI formation was not observed in callus of

2x35S::*Del*/2x35S::*Ros1* grown in medium containing 3%, 6% sucrose and no sucrose. Hence, increased concentration of anthocyanins does not induce anthocyanic vacuolar inclusion formation.

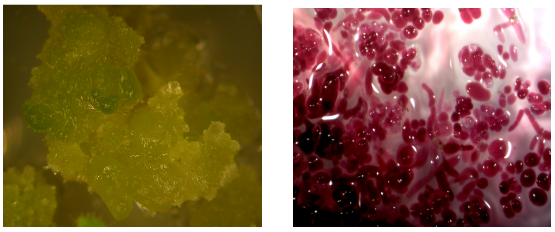

Figure 4.15 | Callus culture of tobacco carrying empty vector compared to those of 2x35S::*Del*/2x35S::*Ros1*. Anthocyanin accumulation is seen in each and every cell of *Del*/*Ros1* line (right panel), while control cells do not show any accumulation (left panel) under same growth condition.

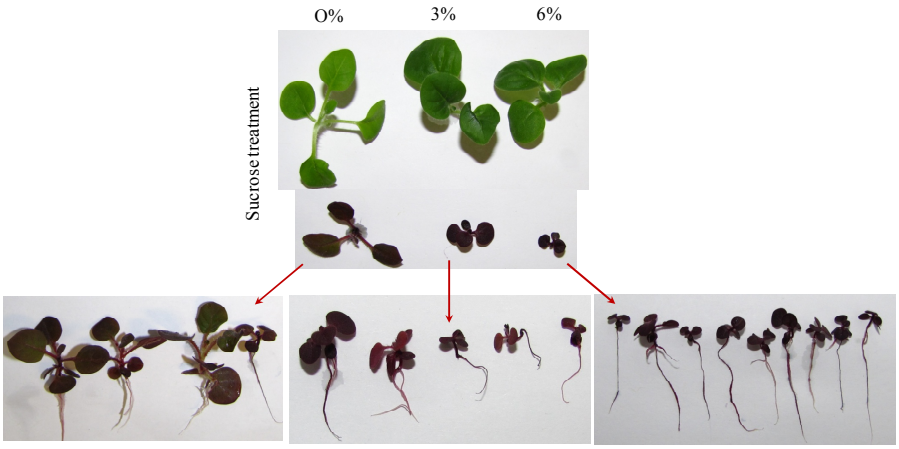

(a)

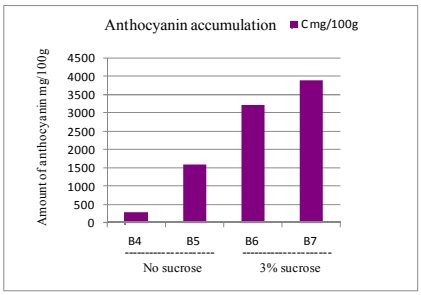

(b)

Figure 4.16 | Effect of sucrose on anthocyanin production in 2x35S::*Del*/2x35S::*Ros1*. Legend is shown beside (on page 116).

Figure 4.17 | Effect of sucrose on the expression of selected genes in anthocyanin biosynthesis pathway in 2X35S::*Del*/2X35S::*Ros1* line.

RNA isolated from the leaves of two Samsun plants and four independent 2X35S::*Del*/2X35S::*Ros1* (F_1 generation) transgenics each grown on MS medium with (3%, 6%) and without sucrose was used to study the expression of several genes in the pathway.

(a) Relative expression of *Del* and *Ros1* in 2X35S::*Del*/2X35S::*Ros1* plants under no sucrose (0%) and with sucrose (3%, 6%). Sucrose does not affect the expression of these TFs.

(b) Relative expression of six genes *PAL*; *phenyl ammonia-lyase*, *4CL; 4-coumarate-CoA ligase*, *CHS; chalcone synthase*, *DFR; dihydroflavonol 4-reductase*, HQT; *hydroxycinnamoyl CoA quinate transferase* and FLS; *flavonol synthase* involved in the phenylpropanoid biosynthetic pathway. mRNA levels are expressed relative to *ubiquitin* levels. Sucrose at higher percent (6%) has an effect on expression of *PAL*, *CHS* and *DFR*. However, increasing sucrose concentrations effected the expression of later gene; DFR where a lower expression with 0% sucrose is evident. However, sucrose as such do not have significant effect on the expression level of *Delila* and *Rosea1* at 0 and 3% sucrose but at 6% there was a decrease in expression. This result shows that sucrose effects anthocyanin biosynthesis irrespective of *Del* and *Ros1*.

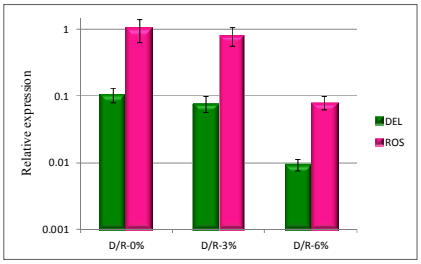
Relative expression
1
0.1
0.01
0.001
DEL
ROS
D/R-0%
D/R-3%
D/R-6%

(a)

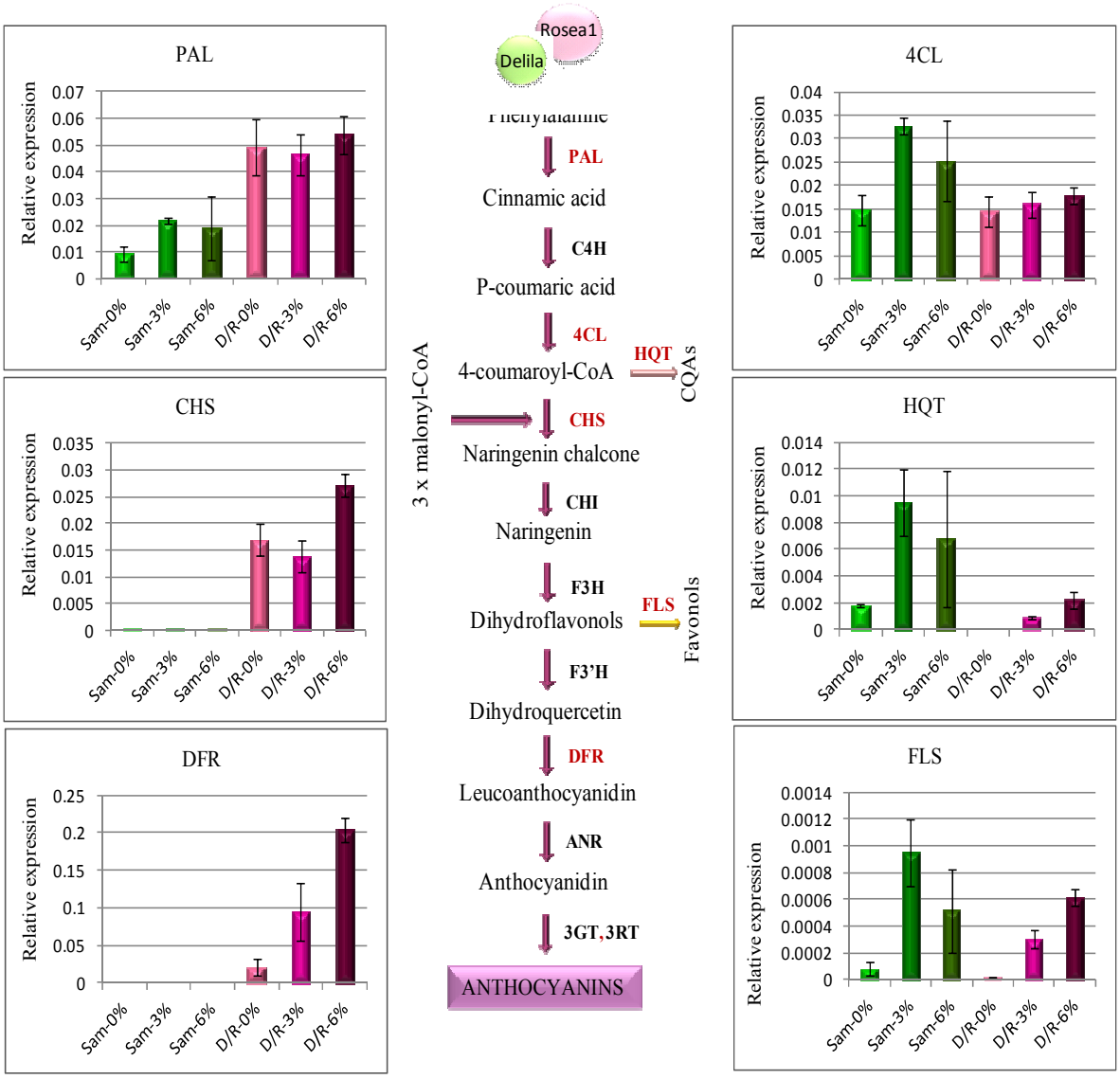
PAL
CHS
DFR
4CL
HQT
FLS
Relative expression
Sam-0%
Sam-3%
Sam-6%
D/R-0%
D/R-3%
D/R-6%
Rosea1
Delila
Phenylalanine
PAL
Cinnamic acid
C4H
P-coumaric acid
4CL
4-coumaroyl-CoA
HQT
CQAs
3 x malonyl-CoA
CHS
Naringenin chalcone
CHI
Naringenin
F3H
Dihydroflavonols
FLS
Favonols
F3'H
Dihydroquercetin
DFR
Leucoanthocyanidin
ANR
Anthocyanidin
3GT,3RT
ANTHOCYANINS

(b)

4.3.4 Aromatic acylation is the trigger for formation of anthocyanic vacuolar inclusions (AVIs)

Conn et al., (2003) correlated AVI formation in grape suspension cells to a significantly higher proportion of acylated anthocyanins (specifically *p*-coumaroylated). Tobacco plants expressing 2x35S::*At3AT* and producing mixture of cyanidin 3-*O*-rutinoside and cyanidin 3-*O*-(6″ coumaroyl) glucoside, showed no AVIs as observed in the palely pigmented petal lobes [Cathie Martin, personal communication]. However, the lines expressing 2x35S::*Del*/2x35S::*Ros1*/2x35S::*At3AT* showed AVI formation as observed in the root hairs [Fig 4.18a]. AVIs purified from the 2x35S::*Del*/2x35S::*Ros1*/2x35S::*At3AT* lines contained only cyanidin 3-*O*-(6″-coumaroyl) glucoside [Fig 4.18b], indicating that aromatic acylation is required for AVI formation.

Accumulation of coumaroylated anthocyanins as AVIs was also observed in tobacco leaf callus accumulating cyanidin 3-*O*-(6″ coumaroyl) glucoside (as well as cyanidin 3-*O*-rutinoside) compared to control callus [Fig 4.19] producing cyanidin 3-*O*-rutinoside. Under high magnification bright field microscopy, AVIs appeared as inter-twined thread-like, irregular crystalline structures. They tended to be concentrated at one end of the vacuole and not distributed evenly within the vacuole. They were not surrounded by any membrane. AVIs in unfixed samples showed slight Brownian motion. AVI formation linked to the presence of cyanidin 3-*O*-(6″ coumaroyl) glucoside could be due to loss of the rhamnosyl group from cyanidin 3-*O*-rutinoside. To further understand this effect root hairs of line expressing 2x35S::*Del*/2x35S::*Ros1*/2x35S::*Sl3AT* were studied and AVI formation was clearly evident [Fig 4.18c]. Purified AVIs from these lines showed the presence of only cyanidin 3-*O*-(4‴ coumaroyl) rutinoside although cyanidin 3-*O*-rutinoside was present in the soluble contents of the vacuole of the same cells. This study showed that coumaroylation can induce AVI formation, irrespective of the position of acylation.

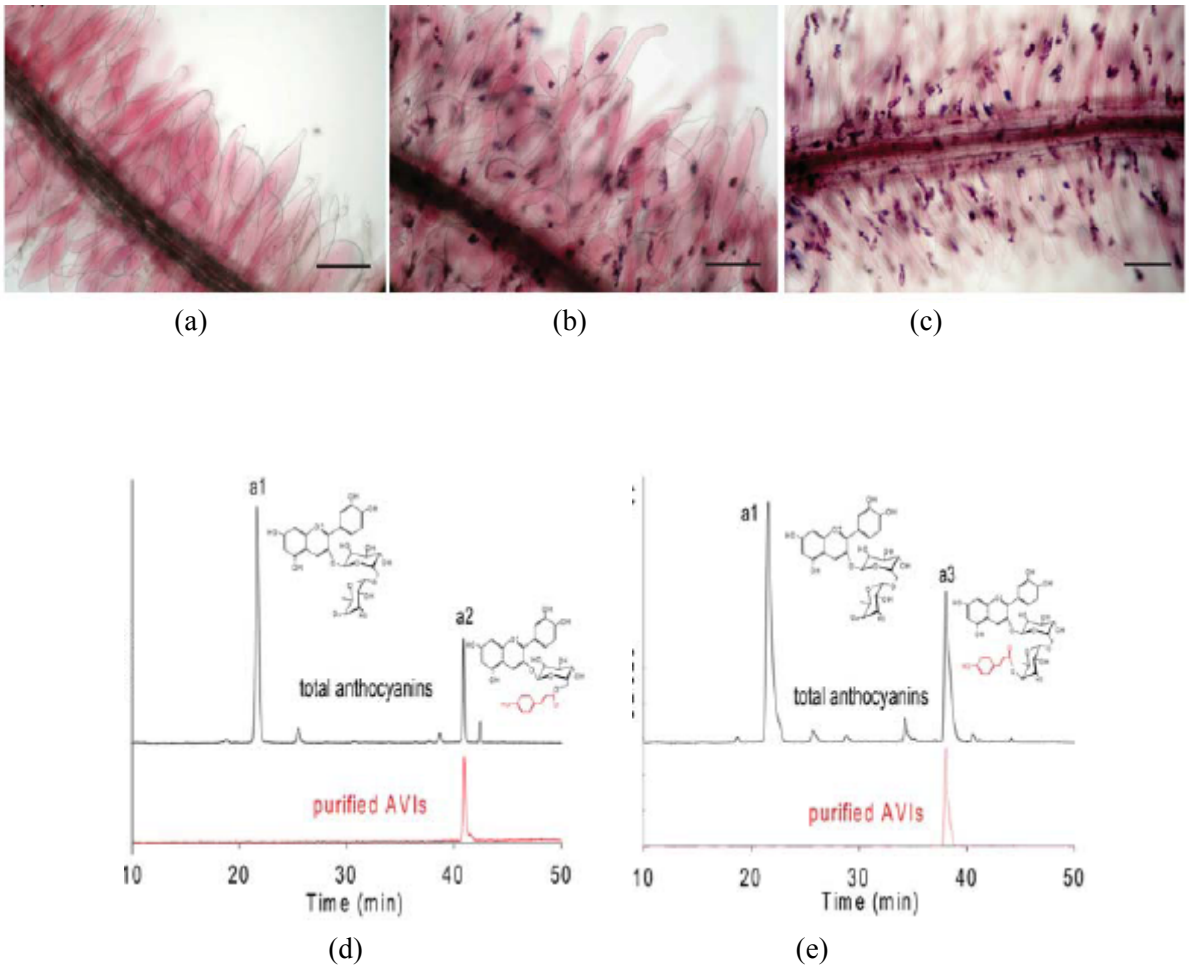

Figure | 4.18 AVI studies in root hairs of 2X35S::*Del*/2x35S::*Ros1*, 2X35S::*Del*/2x35S::*Ros*/2X35S::*At3AT* and 2X35S::*Del*/2x35S::*Ros*/2X35S::*Sl3AT* tobacco lines. (a) Root hairs of 2X35S::*Del*/2x35S::*Ros1* seedling showing accumulation of high levels of soluble anthocyanins.

(b) Root hairs of 2X35S::*Del*/2x35S::*Ros*/2X35S::*At3AT* seedling showing the accumulation of soluble anthocyanins and anthocyanic vacuolar inclusions (AVIs) as dense pigmented bodies.

(c) Root hairs of 2X35S::*Del*/2x35S::*Ros*/2X35S::*Sl3AT* seedling showing AVIs.

(d) HPLC profiles of total anthocyanins (top) and anthocyanins extracted from AVIs (bottom) of 2X35S::*Del*/2x35S::*Ros*/2X35S::*At3AT* lines. Cyanidin 3-(6″ coumaroyl) glucoside was detected in AVIs.

(e) HPLC profiles of total anthocyanins (top) and anthocyanins extracted from AVIs (bottom) of 2X35S::*Del*/2x35S::*Ros*/2X35S::*Sl3AT* lines. Cyanidin 3-(6″ coumaroyl) rutinoside was detected in AVIs. [This experiment performed by Jie Luo].

Figure 4.19 | Tobacco callus generated from stable transgenic lines accumulating high levels of cyanidin 3-*O*-rutinoside along with different modified anthocyanins (shown with chemical structure).

(a) Callus from 2x35S::*Del*/2x35S::*Ros* line accumulating high levels of cyanidin 3-*O*-rutinoside do not form AVIs.

(b) Callus from 2x35S::*Del*/2x35S::*Ros*/2x35S::*At3AT* line accumulating cyanidin 3-*O*-rutinoside and cyanidin 3-*O*-(6″ coumaroyl) glucoside do form AVIs.

(c) Callus from 2x35S::*Del*/2x35S::*Ros*/2X35S::*Ch3MAT* line accumulating cyanidin 3-*O*-(6″ malonyl) glucoside and cyanidin 3-*O*-rutinoside do not form AVIs.

(d) 2x35S::*Del*/2x35S::*Ros*/2x35S::*At5GT* line callus accumulating cyanidin 3-*O*-rutinoside 5-glucoside and cyanidin 3-*O*-rutinoside do not form AVIs.

(e) Callus form 2x35S::*Del*/2x35S::*Ros*/2x35S::*At3AT*/2x35S::*At5GT* producing cyanidin 3-*O*-(6″ coumaroyl) 5-diglucoside and cyanidin 3-*O*-rutinoside forms AVIs. The AVIs formed in the line mentioned above appear to not be membrane bound.

(a)

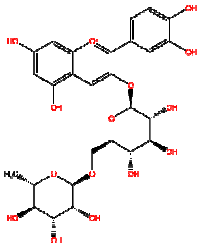

Cyanidin 3-*O*-rutinoside

(b)

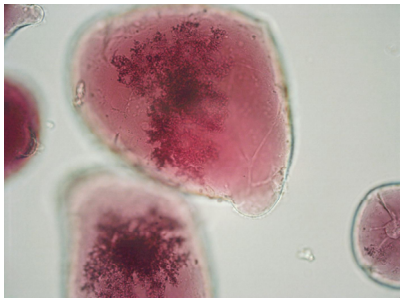

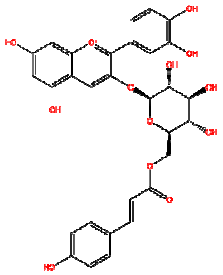

Cyanidin 3-*O (6"* coumaroyl) glucoside

(c)

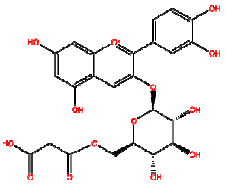

Cyanidin 3-*O*-(malonyl) glucoside

(d)

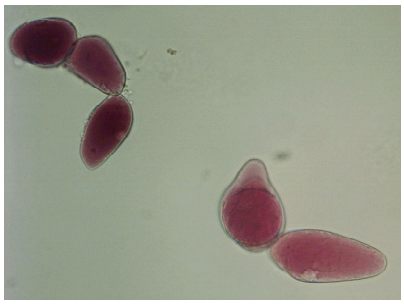

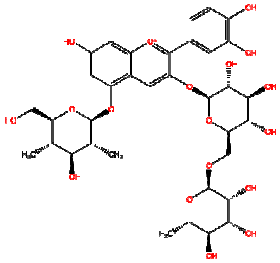

Cyanidin 3-*O*-rutinoside 5-glucoside

(e)

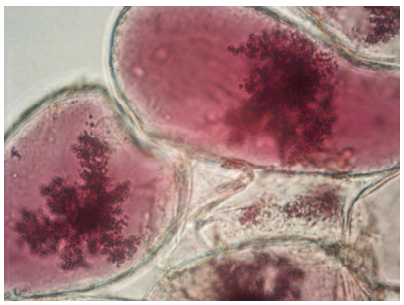

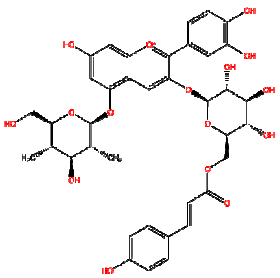

Cyanidin 3-(6" coumaroyl)-5-diglucoside

Tobacco flowers expressing 2x35S::*Ch3MaT* did not show AVI formation as observed in protoplasts [Fig 4.20]. To see if high levels of anthocyanin can trigger AVI formation callus produced from the lines expressing 2x35S::*Del*/2x35S::*Ros1*/ 2x35S::*Ch3MaT* and accumulating a mixture of cyanidin 3-*O*-rutinoside and cyanidin 3-*O*-(6″ malonyl) glucoside were studied [Fig 4.19c]. No AVI formation was observed in this callus. These experiments established that only aromatic acylation could trigger AVI formation in tobacco cells. Aliphatic acylation under similar conditions did not elicit any AVI formation. The formation of AVIs therefore could be due to intra molecular stacking of the anthocyanins with the additional ring structure of the aromatic acyl moieties in the high anthocyanin environment.

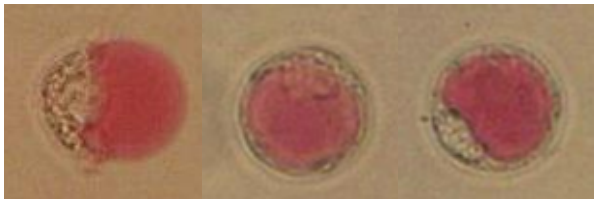

Figure 4.20 | Protoplasts isolated from petals of 2X35S::Ch3MAT showing no AVIs

4.3.5 Effect of 5-glucosylation on formation of AVIs

Markham et al., (2000) reported AVI selectivity for 3,5-diglucosidic anthocyanins in Lisianthus with a preference for cyanidin- over delphinidin-based anthocyanins. To understand the influence of 5-glucosylation in AVI formation in a high anthocyanin environment, cyanidin 3-*O*-rutinoside 5-*O*-glucoside was engineered in tobacco. The callus generated from lines expressing 2x35S::*Del*/2x35S::*Ros1*/2x35S::*At5GT* accumulating cyanidin 3-*O*-rutinoside 5-*O*-glucoside (~2-6%) along with cyanidin 3-*O*-rutinoside (~80%) showed no AVI formation [Fig 4.19d]. This study contradicts the observations of Markham et al.,(2000) in Lisianthus. These differences could be due to the low amounts of cyanidin 3-*O*-rutinoside 5-*O*-glucoside produced in

2x35S::*Del*/2x35S::*Ros1*/2x35S::*At5GT* tobacco lines or that 5-glucosylation cannot induce AVIs.

Since 5-glucosylation has been reported to reduce the stability of anthocyanins in solution (Luo et al., 2007) its effect on resilience of AVIs formed from coumaroylated anthocyanins was studied. To understand this, callus cells from tobacco leaves accumulating cyanidin 3-*O*-(6″ coumaroyl) 5-diglucoside obtained by the expression of 2x35S::*Del*/2x35S::*Ros1*/2x35S::*At3AT*/2x35S::*At5GT* were studied. AVI formation was observed in each and every cell [Fig 4.19e]. The AVIs appeared to be larger than those observed in callus of 2x35S::*Del*/2x35S::*Ros1*/2x35S::*At3AT* lines accumulating cyanidin 3-*O*-(6″ coumaroyl) glucoside but otherwise they appeared very similar. AVIs were formed in almost every cell observed in callus from 2x35S::*Del*/2x35S::*Ros1*/2x35S::*At3AT*/2x35S::*At5GT*. This indicated that 5-glucosylation did not destabilise the anthocyanins to an extent that affects AVI formation.

4.3.6 Relationship of AVIs: side-chain decoration and amount of anthocyanins

While AVI formation was associated to aromatic acylation coupled with high amounts of anthocyanins, I tried to understand whether the trigger in such cells is due to high anthocyanin concentration. For which the AVI formation and amount of anthocyanin produced in different lines: 2x35S::*Del*/2x35S::*Ros1* (DR), 2x35S::*Del*/2x35S::*Ros*/2x35S::*At5GT* (DRG), 2x35S::*Del*/2x35S::*Ros*/2x35S::*At3AT* (DRA), 2x35S::*Del*/2x35S::*Ros*/2x35S::*Ch3MAT* (DRM) and 2x35S::*Del*/2x35S::*Ros*/2x35S::*At3AT*/2x35S::*At5GT* (DRAG) were studied. The amount of anthocyanin produced in the callus lines was varying which, could be due to the level of Delila and Rosea1 expression. However, AVI formation was not altered with the amount of anthocyanin produced. DR-2 line which has similar amounts as DRA-1 line (~40 μM) did not show AVIs [Fig 4.21]. Similarly DRM-2 which produces >100 μM of anthocyanin compared to DRA-2 and DRAG-2 line do not show AVIs [Fig 4.21]. Therefore, from this study it is evident that acylation is the trigger for forming AVIs.

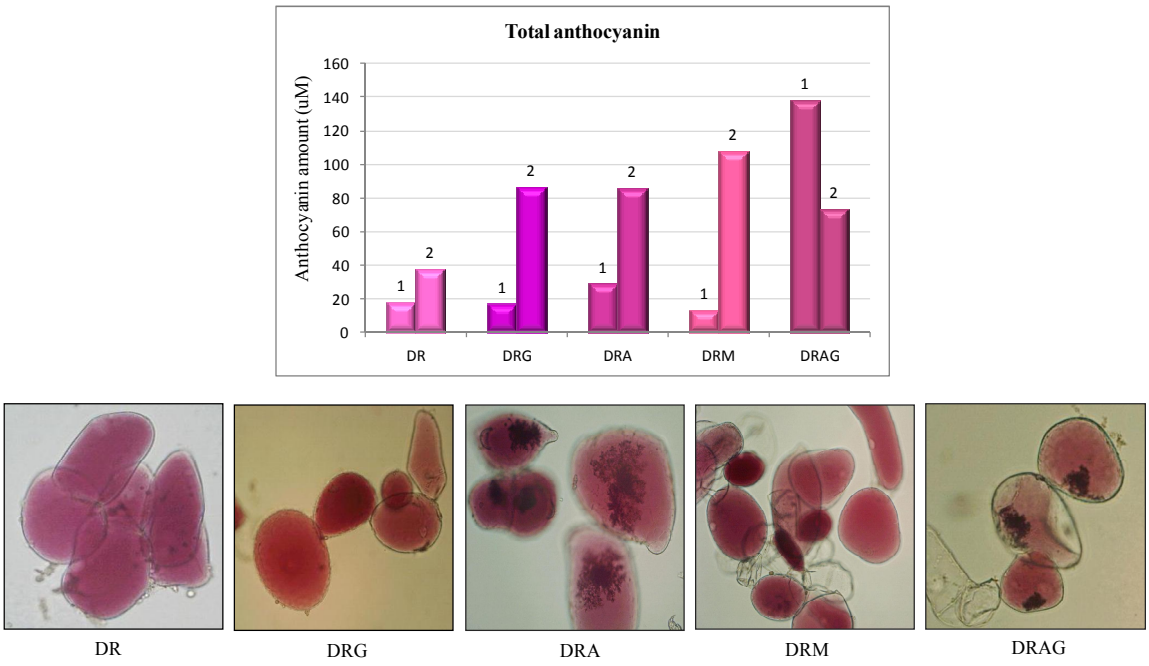

Figure 4.21 | Comparison of total anthocyanins extracted from the callus generated from different tobacco lines. Anthocyanins were extracted from two lines each of: DR; *Del/Ros1*, DRG; *Del*/*Ros*/*At5GT*, DRA; *Del*/*Ros*/*At3AT*, DRM; *Del*/*Ros*/*Ch3MAT* and DRAG; *Del*/*Ros*/*At3AT*/*At5GT* which are under 2x35S promoter. The amount of anthocyanin production was compared to AVI formation. Similar result was observed in the callus of the both lines of all genotypes though; here line 2 of each is shown. It was observed that AVI formation was independent of anthocyanin accumulation.

4.3.7 Influence of other factors in AVI formation

4.3.7.1 Effect of light

Environmental factors influence anthocyanin production and one such factor that has been widely studied is light (Irani et al., 2003). Maize BMS cells accumulating high levels of anthocyanins through constitutive expression of R and Cl regulators when coupled to light exposure induced the formation of AVI-like structures (Irani and Grotewold, 2005). So, I investigated whether light has any effect on 2x35S::*Del*/2x35S::*Ros1* expressing lines in inducing AVIs. Leaf material from these lines were grown on callus inducing medium in light and dark at 25 ºC temperature. The cells grown in light appeared to be darker than the cells grown in dark although there was no change in the anthocyanin profiles under either condition. The callus cells grown in

light did not show AVI formation indicating that light does not have any effect in triggering AVIs. But the callus growing in light could not be used for sub-culturing as high anthocyanin production became toxic to the cells. The lines expressing 2x35S::*Del*/2x35S::*Ros1*/2x35S::*At5GT*, 2x35S::*Del*/2x35S::*Ros1*/2x35S::*At3AT*, 2x35S::*Del*/2x35S::*Ros1*/2x35S::*Ch3MAT* and 2x35S::*Del*/2x35S::*Ros1*/2x35S::*At3AT*/ 2x35S::*At5GT* accumulating cyanidin 3-*O*-rutinoside 5-glucoside, cyanidin 3-*O*-(6″ coumaroyl) glucoside, cyanidin 3-*O*-(6″ malonyl) glucoside and cyanidin 3-*O*-(6″ coumaroyl) 5-diglucoside respectively along with cyanidin 3-*O*-rutinoside were also studied for the effects of light and dark. Light did not have any effect on the numbers of cells forming AVIs.

These experiments show that coumaroylation is the main factor determining AVI formation in tobacco and environment has little or no influence on their formation. Perhaps under natural conditions where exposure to light induces anthocyanin biosynthesis very significantly (as compared to conditions when transcription factors controlling anthocyanin accumulation are being expressed constitutively) light exposure may enhance AVI formation by inducing greater anthocyanin formation. The fact that AVI like structures were observed by Irani and Grotewold (2005) could also be due to the type of anthocyanin (with respect to decoration) present in BMS cells when exposed to light, which was not reported by these authors.

4.3.7.2 Effect of plant organs on AVI formation

To date, AVIs have been studied in flowers (Lisianthus) or fruits (grapes) both of which are sinks rather than source organs. Three forms of AVIs were shown to co-exist in the same Lisianthus petals differing dependent on the type of epidermal cell (Zhang et al., 2006) indicating that the form of AVIs can vary based on the cell type in which they are produced. So the shape of the cell, pH of the vacuoles or presence of other compounds or the whole morphology of cells can vary greatly. In our studies, callus from leaves showed formation of irregular AVIs with no specific shape. To understand further the organ/ origin relationship, callus was produced from roots of lines accumulating cyanidin 3-*O*-rutinoside 5-glucoside, cyanidin 3-*O*-(6″ coumaroyl) glucoside, cyanidin 3-*O*-(6″ malonyl) glucoside and cyanidin 3-*O*-(6″ coumaroyl) 5-diglucoside. The results were the same as in the respective callus cells produced from leaves [Fig 4.22]. The only difference was that roots produced callus faster than leaves and had many vacuoles. This

experiment showed that the origin of the cell does not have any effect on the formation of AVIs.

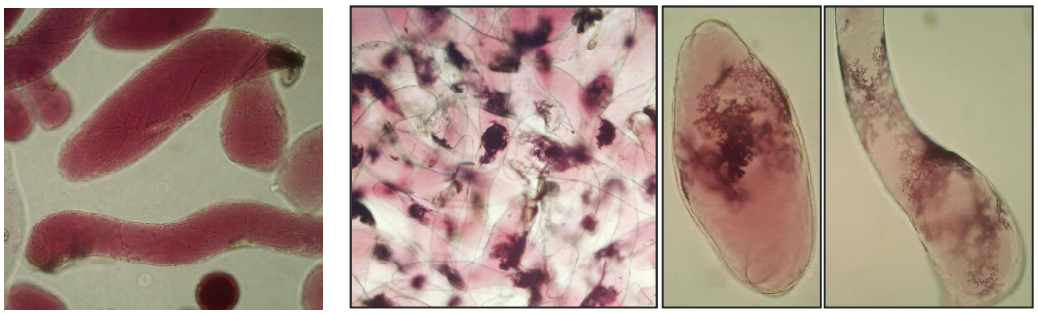

(a) (b)

Figure 4.22 | Callus produced from the roots. (a) 2x35S::*Del*/2x35S::*Ros1* line root callus accumulating soluble anthocyanins. (b) 2x35S::*Del*/2x35S::*Ros*/2x35S::*At3AT* line root callus showing anthocyanin accumulation as both soluble and AVIs. This result is similar to that found in the callus of respective lines produced from leaf [Fig 4.19].

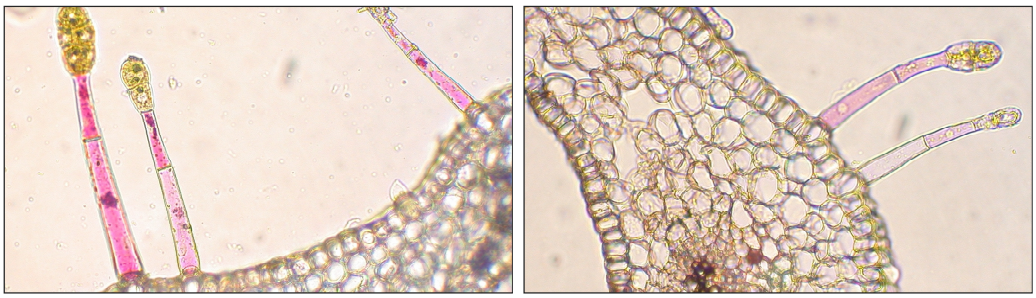

Del/Ros/At3AT Del/Ros/Myb12

Figure 4.23 | AVI study in high flavonol environment. Section of a 2x35S::*Del*/2x35S::*Ros*/2x35S::*At3AT* flower (Del/Ros/At3AT; on left) showing AVIs in trichomes. Flower section of 2x35S::*Del*/2x35S::*Ros*/2x35S::*Myb12* (Del/Ros/Myb12; on right) showing no AVIs in trichomes. Photo by Steve Mackay.

4.3.7.3 Effect of other metabolites on AVI formation

Purified AVIs from grape suspension cells have been shown to be enriched with long-chain proanthocyanidins mainly tannins (Conn et al., 2010). Tannins are secondary metabolites present in grapes apart from anthocyanins. However, Markham et al., (2000) showed no association of AVIs with flavonols in Lisianthus petals. So there is no clear

understanding whether the formation of AVIs is associated with other metabolites. I studied tobacco line 2x35S::*Del*/2x35S::Ros/2x35S::*Myb12* (generated by Jie Luo) accumulating anthocyanins and flavonols. Myb12 was studied to enhance flavonols levels in tobacco (Luo et al., 2008). Formation of AVIs was not observed under both anthocyanin and flavonol accumulation [Fig 4.23] suggesting that the chemistry of anthocyanins alone determine AVI formation.

4.3.7.4 Do AVIs form preferentially with cyanindin-based anthocyanins?

Earlier observations in other species showed different morphology/forms (vesicle like, rod like and irregular shaped) of AVIs (Zhang et al., 2006). In a tomato line expressing *Del/Ros*1 and producing delphinidin 3-*O*-(6″ coumaroyl) rutinoside 5-glucoside; AVIs were observed but were round structures [Fig 4.24] [Luo, personal communication]. AVIs in tobacco callus lines accumulating cyanidin 3-*O*-(6″ coumaroyl) glucoside and cyanidin 3-*O*-(6″ coumaroyl) 5-diglucoside resembled inter twined thread like structures. It is unclear what causes this variation in AVI morphology. To see if the type of anthocyanidin is causing this difference in AVI morphology I generated a line expressing 2x35S::*Del*/2x35S::*Ros1*/2x35S::*PeF3'5'H* accumulating delphinidin 3-*O*-rutinoside and cyanidin 3-*O*-rutinoside. Experiments are in progress to understand whether these lines form AVIs.

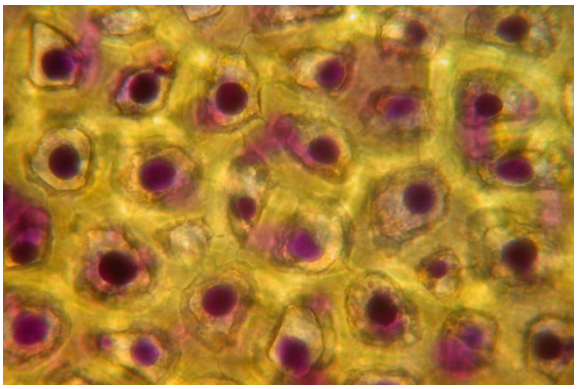

Figure 4.24 | Skin cells of tomato fruit expressing Del/Ros1 and accumulating delphinidin/petunidin 3-(p-coumaroyl) rutinoside, 5-glucoside forming globular AVIs. Photo by Steve Mackay.

4.4 Discussion

Previous studies in Lisianthus, grapes, maize etc., provided different theories about anthocyanic vacuolar inclusion formation. Many factors could be playing a role as these studies come from the observations in different species. A detailed approach based on the chemistry of anthocyanins using a common system was undertaken to determine the factors effecting anthocyanic vacuolar inclusion formation which, we think is the crucial process in understanding AVIs.

Tobacco was chosen for these studies due to presence of simple anthocyanins and for the ease with which stable transgenic plants can be produced. Transient expression studies could be used to understand AVI formation which might have speeded up experimentation (Irani and Grotewold, 2005), but the results obtained could be ambiguous making interpretation complicated. Hence stable transgenics were developed which could also be used for other studies. Different lines of tobacco accumulating high levels of anthocyanins (under the regulation of Delila and Rosea1 transcription factors) with modified profiles for aromatic acylation (coumaroylation), aliphatic acylation (malonylation) and glucosylation were generated. AVI formation was not observed in cells accumulating high amounts of cyanidin 3-*O*-rutinoside suggesting that high levels of anthocyanins per se do not determine AVI formation. Formation of AVIs was strongly correlated with coumaroylation coupled with enhanced anthocyanin accumulation. 5-glucosylated anthocyanins in a high anthocyanin environment did not trigger AVI formation but at the same time did not have any effect on the formation of existing AVIs in lines producing coumaroylated anthocyanins. And AVIs are formed in all the cells in lines producing cyanidin 3-*O*-(6″ coumaroyl) 5-diglucoside; similar to lines producing cyanidin 3-*O*-(6″ coumaroyl) glucoside. AVIs isolated from the line producing cyanidin 3-*O*-(6″ coumaroyl) glucoside contained only coumaroylated species whereas the non-coumaroylated anthocyanins in the vacuoles of the same cells were not incorporated into AVIs. This observation can be attributed to the ring structure of the coumaroylated anthocyanin molecule; the coumaroylation may be involved in intra molecular stacking of anthocyanins leading to AVI formation. Aromatic acylation stabilises anthocyanins (Goto and Kondo, 1991, Brouillard and Dangles, 1994). So in conditions of anthocyanin excess, species with coumaroylation may get stacked and there is a possibility of precipitation when these species are present above solubility levels within vacuoles in a manner similar to the precipitation of salts above saturation limit. However, this

phenomenon is possible only when anthocyanins are produced in large amounts, possibly excessive for easy storage within vacuoles.

This hypothesis is further strengthened by the observation of lines producing cyanidin 3-*O*-(6″ malonyl) glucoside. The malonyl residue is an open structure, and does not contribute to the intramolecular stacking of anthocyanins and hence no AVIs are seen. Malonylation is a modification affecting mainly the solubility of anthocyanins in water, stabilizing anthocyanin structure and for uptake into vacuoles (Heller and Forkmann, 1994). Hence no AVIs are formed with this modification as they are more soluble in the aqueous environment of the vacuole. Conn et al., (2010) suggested that the correlation of acylated anthocyanins with AVIs might be due to incorporation of specific acylated anthocyanin transporters in the AVI membrane. However, this hypothesis seems unlikely as AVIs in tobacco callus do not have a surrounding membrane.

Pigmented structures isolated from sweet potato suspension cells showed intense staining with neutral red indicating they are high density insoluble globules (Nozue et al., 1993) and in Lisianthus, AVIs stained red with Ponceau 2R stain indicating the presence of protein (Markham et al., 2000). A possible involvement of protein matrix with AVIs was also studied when VP24 was isolated from sweet potato AVIs (Nozue et al., 1997). To understand the physical nature of AVIs and a possible association with protein; callus cells of lines expressing 2x35S::*Del*/2x35S::*Ros1* and 2x35S::*Del*/2x35S::*Ros1*/ 2x35S::*At3AT* line showing AVIs were subjected to freeze fracture SEM. No internal structure was observed and AVIs appeared as dense blobs [Fig 4.25]. To study further the nature of AVIs, callus of 2x35S::*Del*/2x35S::*Ros1* and 2x35S::*Del*/2x35S::*Ros1*/ 2x35S::*At3AT* lines was observed under TEM. Preliminary observations showed intensely stained globular structures within vacuoles in both the lines (with and without AVIs). But 2x35S::*Del*/2x35S::*Ros1*/2x35S::*At3AT* line showed a different phenotype with intensely stained irregular ridged structures which stained even with toluidine blue. Osmium tetraoxide used to the fix samples for TEM studies can stain lipids. So we think the round structures seen in control sample and AVI samples could be oil bodies present in vacuoles of all plant species. The dark stained irregular ridged structures could be coumaroylated anthocyanins associated with a particular kind of lipids. Further staining test and studies on purified AVIs are under way to fully understand lipid interaction with AVIs. Lipid involvement with AVIs was earlier suggested in grape AVIs (Conn et al., 2010, Jasik and Vancova, 1992) red cabbage, radish (Yasuda and Kumagai, 1984) and in Arabidopsis (Poustka et al., 2007).

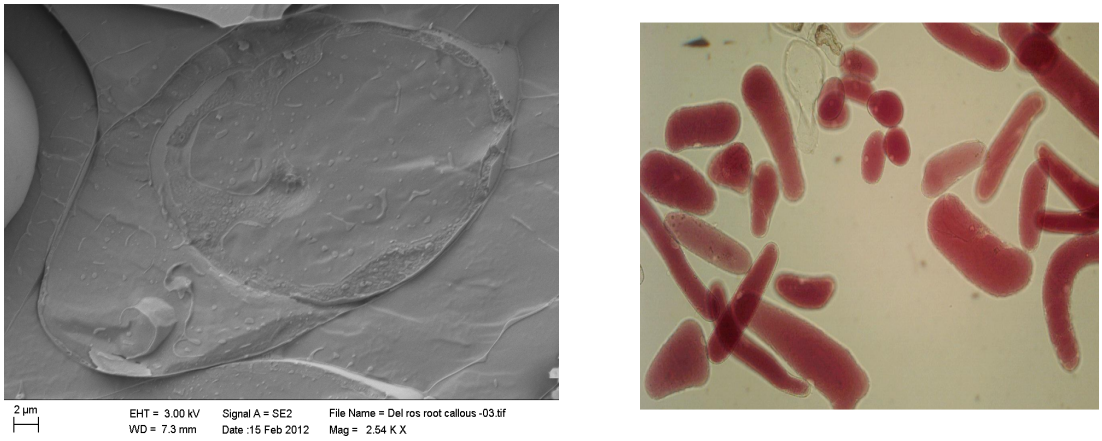

(a)

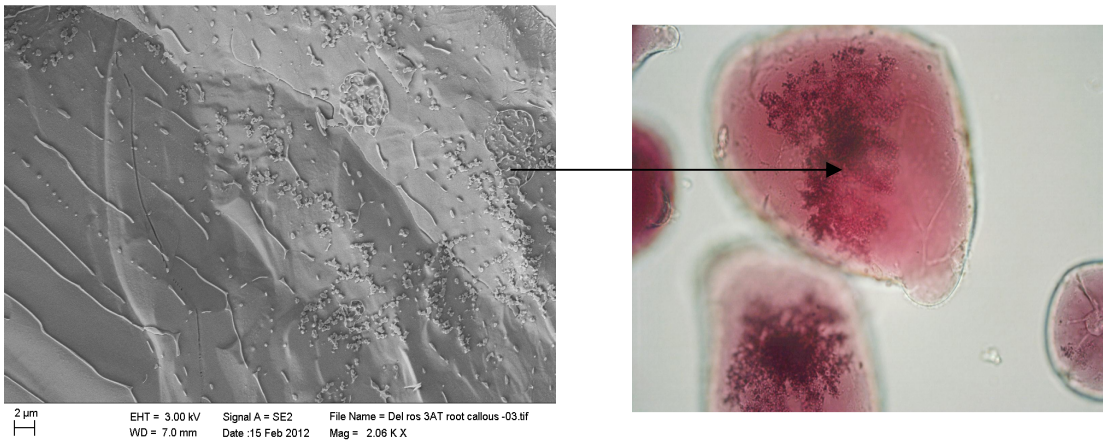

(b)

Figure 4.25 Freeze fractured callus cells observed under SEM. (a) callus of 2x35S::*Del*/2x35S::*Ros1* line (b) callus of 2x35S::*Del*/2x35S::*Ros1*/2x35S::*At3AT* line. AVIs are observed as coarse structures under the SEM and a comparative view of AVI as observed under high resolution light microscopy is shown indicated with an arrow.

The idea of AVIs and anthocyanoplasts consisting of NADES (Natural Deep Eutectic Solvents) was proposed by (Choi et al., 2011) which may form when the level of anthocyanins is higher than their solubility in water (Markham et al., 2000). They hypothesized that to protect the membranes and the contents of various cellular compartments, antioxidants like ascorbate, glutathione, flavonoids, and anthocyanins could concentrate at high levels into sheets of NADES mainly for protection against

oxidation and light damage. This proposal would be supported by my data if AVIs were formed in high anthocyanin environments. But my data show that AVIs do not form in high anthocyanin environment in the absence of coumaroylated anthocyanins. Conn et al., (2010) also emphasised AVIs as dynamic structures which can respond or influence their anthocyanin environment. My study shows that specific anthocyanin chemistry contributes significantly to the formation of AVIs. Possibly coumaroylation contributes to NADES type behaviour of anthocyanins when they accumulate at levels higher than their solubility in water and is a means of concentrating compounds. But this might be responsible for the appearance of 'soft AVIs' which appear like those observed in purple tomato fruit and which cannot be purified. AVI formation could be a mechanism of protection developed by plants to overcome the adverse effects of certain kind of anthocyanins or a mechanism evolved to enhance the pigmentation of flowers to attract pollinators and probably could be a reason why many plant species, that accumulate both acylated and non-acylated anthocyanins, form AVIs. Alternatively, AVI formation could simply be due to precipitation of coumaroylated anthocyanins.

To date only complex anthocyanins have been shown to be involved in AVI formation (in Lisianthus and grape) leading to conclusions that trapping of anthocyanins occurs within vacuoles by concentrating anthocyanins above certain level (Conn et al., 2010). However, I have shown that AVI formation is related to the chemistry of anthocyanins in combination with high concentrations of anthocyanins, and no other factors are involved.

Anthocyanin biosynthesis is one of the most widely studied metabolic pathways in plants but the later stages of their sequestration are not fully understood. Understanding how the secondary metabolites get stored or modified is very useful for harnessing many of their useful properties. The results in this chapter suggest that aromatic acylation of anthocyanins leads to a modified form of storage in plant vacuoles.

CHAPTER V

Effects of Side-chain Decoration on the properties of Anthocyanins

5.1 Introduction

Anthocyanins, with their enormous health beneficial properties for humans and offering attractive colours from orange through red and purple to blue, are of great interest for use as natural colourants. But their variable colour properties and stability in solution hinder their wide applications. Various factors including structure (chemistry), concentration, pH, temperature, light, interaction with copigments, metallic ions, sugars contribute to the different properties of anthocyanins (Mazza and E.Miniati, 1993, Francis and Markakis, 1989). In acid medium anthocyanins exist as four different forms in equilibrium: flavylium cation, quinonoidal base, carbinol pseudobase and chalcone. pH influences greatly the relative amounts of these forms at equilibrium (Mazza and E.Miniati, 1993). Interconversion of the different forms involves changes in their colour. At lower pH 1-2 flavylium cations which offers red colour exist and at higher pH values, the quinoidal bases which are blue forms exist. Carbinol pseudobase and chalcone forms which are colourless exist and at pH values 4-5 and >7 respectively [Fig 5.1].

Side chain decoration of anthocyanins such as glycosylation, acylation (aromatic and aliphatic) improves stability and solubility of anthocyanins in solution. Particularly aromatic acylation with planar aromatic substituents offers remarkable stability in mildly acidic conditions due to formation of hydrated species unlike mono and di-glucosylated anthocyanins that are colourless in similar conditions (Brouillard et al., 1978). Also anthocyanin colour stability is achieved by acylated molecules due to intramolecular copigmentation by the interaction of aromatic moiety with planar pyrylium core protecting anthocyanin against nucleophilic water attack known to occur at 2 and 4 positions of the anthocyanidin (Kurtin and Song, 1968). Glucosylated molecules at higher concentration offer stability from self association. Intermolecular copigmentation stabilises anthocyanins with their interaction with flavonoids such as flavones and flavonols and particular this type of stacking offers stability to quinoidal bases [Fig 5.1b].

Inspite of an understanding of the mechanisms of stability anthocyanin are not yet widely used in the food industry due to their relative instability. Several, more stable colourants are available in nature, although natural blue colours are not widely available. Identification and characterization of the chemical attributes of different anthocyanins and determination of how side chain decorations influence these attributes is indispensable. However, a series of systematically decorated anthocyanins from a common source are not available commercially, and so these attributes have not been

analysed comparatively. In this chapter I aimed to understand some of the physical properties of anthocyanins in solution to facilitate the development of of anthocyanins as health-promoting natural colourants. For this purpose, I used anthocyanins purified from one of the tobacco lines I generated for my studies on AVI formation.

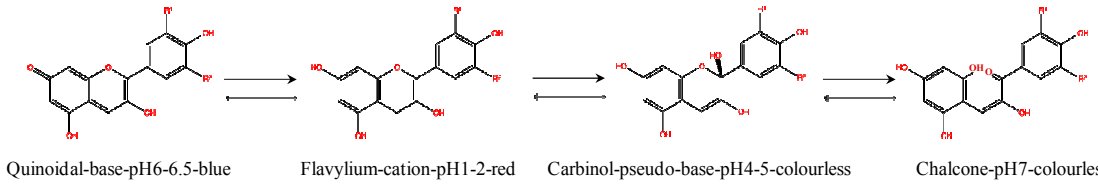

Figure 5.1a | Schematic showing anthocyanin chemical forms at various pH. Flavylium cation predominates at pH 1-2 giving red colour to anthocyanin in solution and at pH 4-5 anthocyanin converts to carbinol pseudo base which is colourless. Blue coloured quinoidal base is formed at pH 6-6.5 and is converted to colourless chalcone structure when the pH is 7 (alkaline).

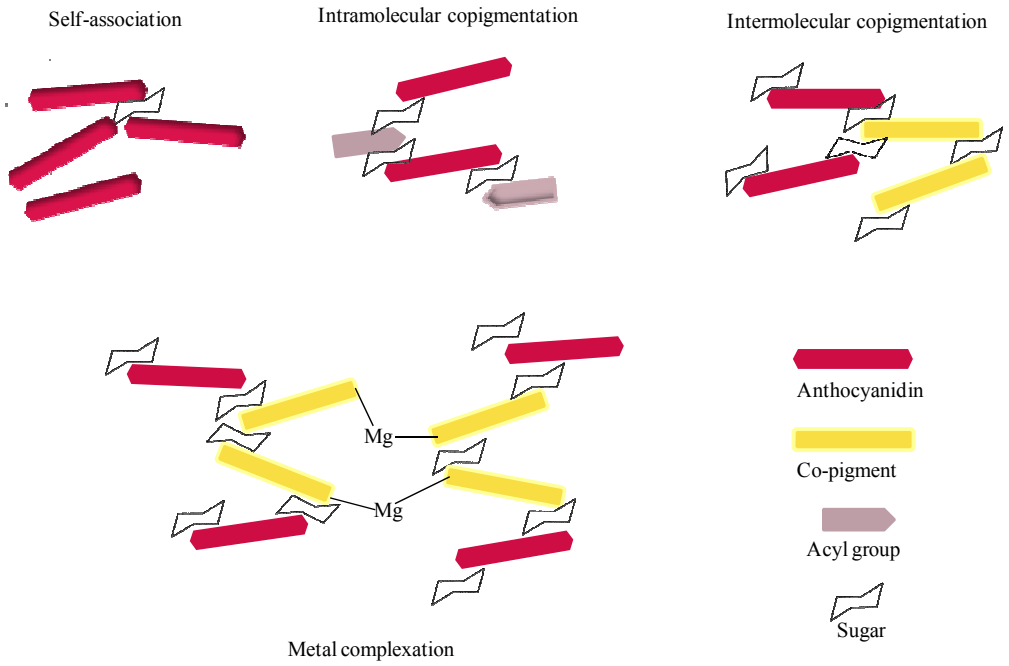

Figure 5.1b | Different modes of copigmentation observed in nature. Self-association, intramolecular copigmentation, intermolecular copigmentation, metal complexation are shown. Different molecules used for the depiction are presented.

5.2 Experimental procedures

5.2.1 Anthocyanin extraction

Extraction, isolation and purification of anthocyanins from the leaves of tobacco TCU 33-1 line (2x35S::*Del*/2x35S::*Ros1*/2x35S::*At5GT*/2x35S::*At3AT*) was performed based on the protocol on anthocyanins extraction (Rodriguez-Saona and Wrolstad, 2001) with a few modifications. Finely powdered leaf material (50 g) was mixed with 70% aqueous acetone and 0.01% HCl. The anthocyanin extract (filtrate) was separated from the insoluble plant material by filtering the slurry through a Whatmann no. 1 filter paper using vacuum suction with a Buchner funnel. Two volumes of chloroform were added to the filtrate and gently mixed by inverting the vessel, a few times. The sample was stored overnight at 4 ° C or until a clear partition between the two phases was obtained. The aqueous phase (upper portion) was transferred to a 500 mL boiling flask and the residual acetone/chloroform was removed in a rotary evaporator at 40°C under vacuum. Acidified water was added to the remaining aqueous extract and the sample was stored at -20 °C.

5.2.2 Anthocyanin purification

5.2.2.1 Primary purification

Extracted anthocyanins in acidified water were passed through a preconditioned C18 mini cartridge (Sep-Pak Cartidge 500 mg sorbent, Waters Chromotography®). The C18 cartridge was conditioned by passing two column volumes of methanol through the sorbent bed followed by three column volumes of acidified deionized milliQ water to remove the remaining methanol. The sample was loaded onto the column until excess colour passed through the cartridge. The cartridge was washed with two column volumes of acidified water to remove compounds not adsorbed (e.g., sugars, acids) followed by two column volumes of ethyl acetate to remove polyphenolic compounds such as phenolic acids and flavonols. Anthocyanin pigments were eluted with acidified methanol and collected in a 50 to 100 mL round-bottomed glass flask. Methanol was removed from the extract in a rotary evaporator at 40 °C under vacuum and the anthocyanins were re-dissolved in acidified milliQ water and stored at -20 °C until further use.

5.2.2.2 Preparative HPLC purification

Anthocyanins were purified using Gilson Preparative High Pressure Liquid Chromatography (Prep HPLC) System. Partially purified and filtered (using a 0.2 μm polyfluortetraethylene filter, Sartorius) extracts were applied onto a 250 x 21.2 mm C18 column (Phenomenex) fitted with a guard column (Phenomenex Prodigy). The column was pre-equilibrated with water containing 0.5% Triflouroacetic Acid (TFA). The sample was injected onto the column, developed by a wash with 96% solvent A (0.5% TFA in water) and 4% solvent B (0.5% TFA in 50% acetonitrile (ACN)). Anthocyanins were eluted with a linear gradient of increasing solvent B at a flow rate of 1 ml/ min: from 20% to 40% over 10 min, 40% to 60% over 5 min, 60% to 80% over 13 min, 80% to 100% over 7 min and 100% for 10 min. The elution products were monitored with a UV detector. This protocol was developed for separation of all the compounds. The desired fractions were collected and the residual ACN from the fractions was removed using a rotary evaporator. Acidified water was added to the samples and they were freeze dried. Freeze dried powdered anthocyanin samples were stored at -80 °C in an air tight container or dissolved in the desired solvent for further studies.

5.2.3 Anthocyanin quantification

Freeze dried anthocyanin fractions were dissolved in methanol and the separation carried out using analytical HPLC (protocol described in chapter 4, section 4.2.10) except that a 45 minute gradient was run. Commercial anthocyanins: cyanidin 3-*O*-rutinoside and cyanidin 3-*O*-glucoside (Extrasynthase, France) were used as standards. Standards (5 mg) were dissolved in methanol with 0.1% HCl and stored at -80 °C. The concentrations of the anthocyanins in samples were calculated based on the peak areas in the chromatograms and compared to external standards using a standard curve. Five concentrations of standards (10 μM, 20 μM, 40 μM, 80 μM and 160 μM) were prepared with 70% methanol and used to generate the standard curve.

5.2.4 Preparation of copigments

Two types of copigments: phenolic acids and flavonols were studied in this thesis. Phenolic acids viz., chlorogenic acid, *p*-coumaric acid, caffeic acid are purchased from Sigma (USA). Flavonols: quercetin 3-*O*-rutinoside (rutin) was purchased from Sigma and kaempferol 3-*O*-rutinoside was from Extrasynthase (France). Stocks of the copigments were made with different solvents; 10% DMSO (chlorogenic acid), DMSO

(quercetin 3-*O*-rutinoside) and ethanol (p-coumaric acid, caffeic acid and kaempferol 3-*O*-rutinoside) depending on their solubility properties.

5.2.5 McIlvaine's buffer preparation

McIlvaine's buffer (McIlvaine, 1921) was prepared using different volumes of two buffers; 0.1 M citric acid and 0.2 M Na_2HPO_4. The stock solutions of these buffers were prepared by taking a precise amount of the buffer and filtering it using a 0.2 µm filter. Calculated amounts of 0.1 M citric acid and 0.2 M Na_2HPO_4 buffers were combined according to the protocol of McIlvaine to obtain solutions in the pH range from 2.6 to 7.6.

5.2.6 Spectrophotometric measurements

The absorption spectra of samples were monitored in the visible range from 400-700 nm using a Spectra max 340PC384 (Molecular devices) spectrophotometer. Readings were analysed using Softmax$^{(R)}$ Pro software version 4.8.

5.2.7 Measurement of anthocyanin stability

Purified and freeze dried anthocyanins: cyanidin 3-*O*-rutinoside, cyanidin 3-*O*-rutinoside 5-*O*-glucoside, cyanidin 3-(*6″* coumaroyl) glucoside and cyanidin 3-(*6″* coumaroyl) 5-diglucoside were dissolved in methanol to obtain the desired stock concentrations. Solutions of each of these anthocyanins and cyanidin 3-*O*-glucoside (commercial standard) were prepared in different buffers (pH 2.6, 3.0, 3.6, 4, 5, 6, 7 and 7.6) to obtain a 50 µM working solution for each anthocyanin at a range of pH values. The reactions were prepared at room temperature (25-27 °C) and used for spectrophotometric analysis within 15 min to 1 hr of preparation. Two independent experiments (n=1) were performed for each anthocyanin and at each pH value. Anthocyanin stocks and buffers were prepared fresh for each experiment to include variation in buffer preparation. The absorption spectra of the stability reactions were monitored from 400-650 nm at several intervals over 2 days. The half-life time ($t_{1/2}$) of the samples under constant light and room temperature was calculated from the absorbance readings at the absorption maximum (λmax). The relative amounts of anthocyanins present were calculated from: % retention = (A_t/A_0) x 100 where A_t = final absorbance at time't' and A_0 = absorbance at time zero. The data was analysed using EXCEL 2007 (Micorsoft® Corp) and presented as the decline in the amount of anthocyanin in solution, over time. The equations used to calculate $t_{1/2}$ of all the anthocyanins at different pH values are shown in table 5.1.

Table 5.1 | Equations used to calculate $t_{1/2}$ of anthocyanins

pH	cyanidin 3-*O*-rutinoside	cyanidin 3-*O*-rutinoside 5-*O*-glucoside	cyanidin 3-*O*-glucoside	cyanidin 3-*O*-(6″-coumaroyl) glucoside	cyanidin 3-*O*-(6″-coumaroyl) 5-diglucoside
2.6	y = -3.6679x + 366.21	y = -3.0138x + 308.61	y = -3.1541x + 315.34	y = -2.2914x + 229.78	y = -3.1515x + 327.6
3.0	y = -3.0686x + 305.89	y = -2.7492x + 278.38	y = -1.7817x + 182.32	y = -2.6897x + 267.7	y = -3.8505x + 393.39
3.6	y = -3.0923x + 303.59	y = -2.673x + 270.08	y = -3.1057x + 309.67	y = -2.6453x + 276.7	y = -4.4963x + 453.05
4.0	y = -0.387x + 93.569	y = -2.1091x + 212.15	y = -0.3546x + 94.298	y = 0.0196x + 83.9	y = -2.396x + 240.13
5.0	y = 0.1398x2 - 26.919x + 1295.2	y = 0.0908x2 - 18.305x + 921.58	y = 0.0441x2 - 9.7317x + 528.29	y = -0.2784x2 + 50.029x - 2217.5	y = 0.0698x2 - 14.214x + 721.93
6.0	y = 0.0285x2 - 4.5754x + 172.23	y = 0.0043x2 - 0.9267x + 50.913	y = 0.0045x2 - 0.8594x + 39.433	y = 0.0158x2 - 2.3932x + 81.777	y = 0.0254x2 - 4.6999x + 214.98
7.0	y = 0.0091x2 - 1.4684x + 58.858	y = 0.0137x2 - 2.2866x + 93.64	y = 0.0081x2 - 1.2377x + 45.518	y = 0.0085x2 - 1.381x + 55.93	y = 0.0183x2 - 3.095x + 128.68
7.6	y = 0.0046x2 - 0.9832x + 53.673	y = 0.0082x2 - 1.3712x + 58.08	y = 0.0052x2 - 0.9834x + 47.616	y = 0.0048x2 - 1.087x + 60.196	y = 0.0083x2 - 1.4989x + 68.632

In the equation y= time taken for anthocyanins to reach half the amount; defined as t1/2 in hours, x= 50

5.2.8 Analysis of copigmentation

Anthocyanins and potential copigments were combined in buffered solution to obtain a final concentration of 50 µM anthocyanin and 50 µM, 0.5 mM, 1.25 mM, 5 mM of each co-pigment to attain a molar ratio of 1:1, 1:10, 1:25 and 1:100 respectively. The maximum molar ratio studied for kaempferol 3-O-rutinoside was 1:25 due to precipitation of the co-pigment at higher stock concentrations. Quercetin 3-*O*-rutinoside was precipitated at a high anthocyanin:co-pigment ratio. Copigmentation reactions were carried at pH 3.6; McIlvaine's buffer (McIlvaine, 1921) at 25-27 °C and the absorbance readings were monitored within 15 min to 1 h of preparation. Anthocyanin and copigments together were kept to less than 20% of the total reaction volume to avoid losing the buffering capacity of the buffer. Two independent experiments (n=2 or 3 depending on sample availability) were performed for each anthocyanin and co-pigment combination. For cyanidin 3-rutinoside 5-glucoside n=1 due to low compound availability. Anthocyanin stocks and buffers were prepared fresh for each experiment to

compensate for any variations in buffer preparation. Absorption spectra were recorded in visible range from 400-650 nm. A hyperchromic effect following addition of the co-pigment was recorded from the absorption reading at the absorption maximum (λmax) and compared to the reading from non co-pigmented samples. Colour enhancement due to addition of co-pigment was calculated from: CE (%) = $[(AC_{\lambda max}) - A_{\lambda max})/A_{\lambda max}] \times 100$ where CE = colour enhancement; $AC_{\lambda max}$ = absorbance reading of anthocyanin:co-pigment at λmax ; $A_{\lambda max}$ = absorbance reading of anthocyanin at λmax.

5.2.9 NMR spectroscopy

NMR spectroscopy was performed by Dr. Shirley Fairhurst (John Innes Centre). 1 H NMR spectra and gs-DQF-COSY (Double-quantum filtered correlation spectroscopy) (1024 3 128 points and 200 scans) were obtained at 300K using a Bruker Avance 600 MHz NMR spectrometer fitted with a Bruker TCI cryoprobe. Through these measurements it is possible to assign all the protons of the rhamnose and/or additional glucose units of the anthocyanin. The DQF-COSY spectrum shows couplings between neighboring protons which are revealed as cross-peaks in the spectrum (Andersen and Fossen, 2003). >1 mg of freeze dried anthocyanin samples were dissolved in 600 µL (approximately) of methanol-*d3* with 5 % TFA-*d3* and transferred to a 2-mm NMR tube. NMR spectra were referenced with respect to the residual protons. As limited sample was available several scans were performed to obtain the spectra for anthocyanins. Full NMR assignments were performed using a combination of TOCSY (Total correlation spectroscopy), NOESY (Nuclear overhauser enhancement spectroscopy), ROESY (Rotational nuclear overhauser effect spectroscopy), 13C, HSQC (Heteronuclear single quantum coherence spectroscopy), and HMBC (Heteronuclear multiple bond coherence spectroscopy) spectra and based on information from the literature. Protons that are close to each other in space can be observed as cross-peaks in NOESY. Similar to NOESY; using ROESY signals from the protons which are close in space but not connected by chemical bonds can be detected. 1H-13C correlations can be observed in HSQC and proton nuclei correlated with carbon nuclei that are separated by more than one bond can be studied (Andersen and Fossen, 2003).

5.3 Results

5.3.1 Isolation of anthocyanins

The anthocyanins from line TCU33-1 (2x35S::*Del*/2x35S::*Ros1*/2x35S::*At5GT*/ 2x35S::*At3AT*) (Refer to Chapter IV section 4.3.2.1.4 for description of this transgenic line) were purified for use in different studies. Analytical HPLC analysis of unpurified extract from this line showed four different anthocyanins [Fig 5.2a] which were cyanidin 3-*O*-rutinoside (hereafter referred to as C3R), cyanidin 3-*O*-rutinoside 5-*O*-glucoside (hereafter referred to as C3R5G), cyanidin 3-*O*-(6″-coumaroyl) glucoside (hereafter referred to as C3couG) and cyanidin 3-*O*-(6″-coumaroyl) 5-diglucoside (here after referred to as C3cou5G). The accumulation of these compounds was confirmed by mass fragmentation except for C3cou5G; the product obtained at 22.7 min. Based on the retention time this compound was expected to be a coumaroylated diglucoside but its molecular mass (m/z 757) and fragmentation pattern was similar to C3R5G (m/z 757). Hence the anthocyanins were further studied by NMR (as described in the next section).

All four anthocyanins from the TCU 33-1 line were isolated using preparative HPLC. Purified fractions were examined by analytical HPLC and all fractions showed relatively high purity [Fig 5.2a] which was established by comparison of fractions at 280 nm [Fig 5.1b]. The purified anthocyanins dissolved in methanol were quantified based on the area of peaks obtained from analytical HPLC in comparison to standards. 3R and C3R5G were quantified using the commercial standard cyanidin 3-*O*-rutinoside by plotting the standard curve and using the equation y = 2E-05x - 4.1459 (R^2 = 0.9973). C3couG and C3cou5G were quantified using the commercial standard cyanidin 3-*O*-glucoside from the equation y = 3E-05x - 1.4624 (R^2 = 0.9994). NMR analysis of fractions (peaks 2-4) confirmed their purity.

Figure 5.2 | Analytical HPLC chromatogram traces of purified anthocyanins.
(a) Traces of C3R (18.5 min), C3R5G (14.4 min), C3couG (25 min) and C3cou5G (22.7 min) at 520 nm absorption are shown in comparison to unpurified anthocyanin trace (on top).
(b) Traces of the purified anthocyanins absorbing at 280 nm to detect contaminating compounds are shown. Pure compounds were isolated using preparative HPLC technique.


At 520 nm
18.5 m
14.4 m
22.7 m
25.0 m
At 520 nm
Peak 1 at 14.4 min
At 520 nm
Peak 2 at 18.5 m
At 520 nm
Peak 3 at 22.7 m
At 520 nm
Peak4 at 25.0m
AU
Minutes

(a)

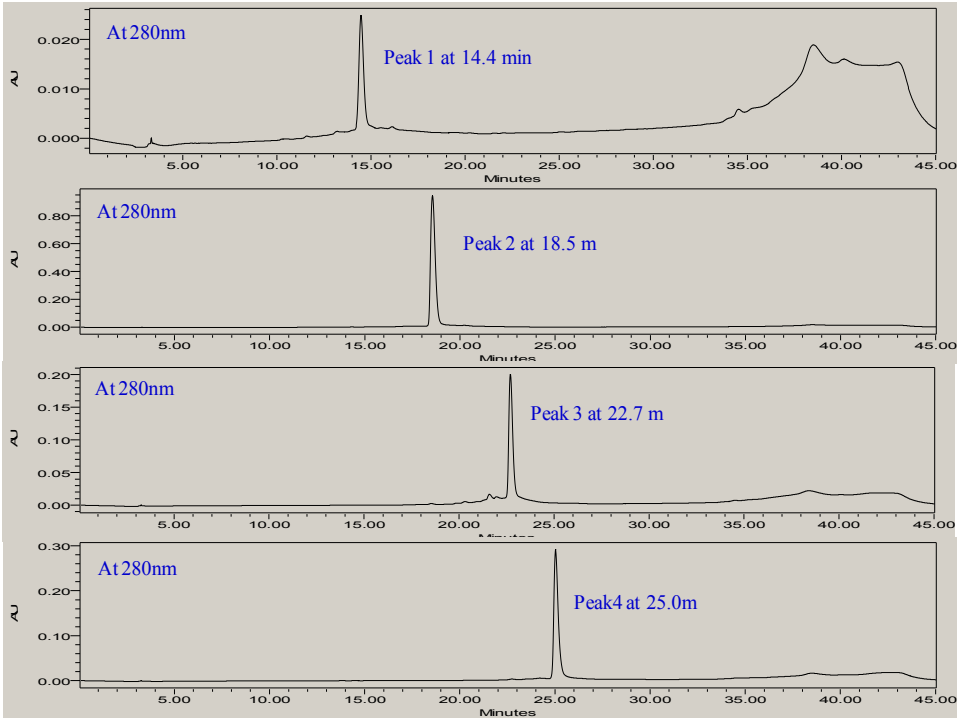
At 280nm
Peak 1 at 14.4 min
At 280nm
Peak 2 at 18.5 m
At 280nm
Peak 3 at 22.7 m
At 280nm
Peak4 at 25.0m
AU
Minutes

(b)

5.3.2 Structural elucidation of anthocyanins; C3R, C3couG and C3cou5G

Three purified anthocyanins of ~1 mg/mL; cyanidin 3-*O*-rutinoside, cyanidin 3-*O*-(6″-coumaroyl) glucoside and the compound obtained at 22.7 min (during HPLC separation) [Fig 5.2] which was expected to be cyanidin 3-*O*-(6″-coumaroyl) 5-diglucoside were subjected to NMR analysis. C3R and C3couG were studied as controls for the compound isolated at 22.7 min. The down field part of the ^{1}H-NMR spectra of C3R, C3couG and C3cou5G [Fig 5.3b, 5.4b and 5.5b respectively] showed six resonances in accordance with the aglycone of cyanidin [Table 5.2, 5a, 5b; appendix] having a singlet at 8.9 ppm for H-4 of cyanidin. Glucose attached at the 3-hydroxyl position of the anthocyanidin ring of all compounds was observed to be a *β*-D-glucose based on the coupling constant (*J*= 7.7). The linkage of glucose at the 3-position of cyanidin was determined as a cross-peak in the NOESY spectrum. The proton chemical shifts obtained by ^{1}H-NMR spectra and the relationships supported by COSY and TOCSY cross-peaks were used to assign the protons of the compounds.

^{1}H-NMR spectra of C3R identifies a methyl group of rhamnose as a signal at 1.19 ppm. Signals from all the protons of rhamnose were observed in δ 1.19 to 4.68 region. The glycosidic linkage of the 6″ –proton (δ4.4-4.5) to rhamnose was established from the HSQC spectrum [Fig 5.3].

Analysis of ^{1}H-NMR spectra of C3couG and C3cou5G indicated the presence of a coumaroyl moiety [Table 5b; appendix and table 5.2]. In C3couG and C3cou5G the 8″ - and 9″ –protons of the coumaroyl moiety had large coupling constants (*J*= 15.8 and 15.9 respectively). Ester linkages in these compounds were established from the HSQC (H-C correlation) spectra. Correlations between the 6″ –proton (δ4.4-4.5) and the carbon (δ 115.2) of coumaroyl moiety were observed in C3couG and C3cou5G indicating that the acylating position was the 6-OH of the glucose present on the C-3 of cyanidin [Fig 5.4 and 5.5]. s the 7″ –proton was a quaternary carbon, no hydrogen peaks were assigned. No hydrogen peaks were present for quaternary carbons and quaternary carbons were not detected in the HSQC spectra. All the samples were too weak for standard carbon experiments. In C3cou5G, the 4-1″ and 4-12″ –proton linkages were determined by ROESY. The cross-peaks identified at δ 3.97-4.02 and δ 4.49-4.52 at 65 ppm in the HSCQ spectrum together with the integration data identifies the presence of two sugars in C3cou5G [Fig 5.5]. The chemical shifts of the carbon atoms [Table 5.2] were assigned from the HSQC experiment and together with the sequential walk through the cross-

peaks in the COSY and TOCSY experiments coupled with the ^{1}H-NMR spectra C3cou5G was confirmed to be a 5-glucosylated cyanidin 3-(6″ coumaroyl) glucoside.

Table 5.2 | ^{1}H-NMR and ^{13}C NMR spectra of C3cou5G in MeOH-*d4* containing 5% TFA-*d*.

Position	^{1}H (ppm)	J (Hz)	^{13}C (ppm)
Aglycone(cyanidin)			
4	8.99 (s)		136.3
6	7.04 (s)		106.5
8	6.96 (s)		97.9
2’	8.05 (d)	2.3	118.8
5’	7.05 (d)	8.7	118.0
6’	8.31 (d,d)	2.3, 8.7	129.4
3-*O*-glucose			
1” (beta)	5.43 (d)	7.7	103.4
2”	3.74-3.78 (m)		*
3”	**		*
4”	**		*
5”	**		*
6” (2H)	4.49-4.52 (m)		64.6
Aromatic acyl moeity			
7”	-		Quat
8”	7.41 (d)	15.8	147.5
9”	6.26	15.8	115.2
10”	-		Quat
11”	7.32	8.6	117.2
12”	6.80	8.6	131.9
13”	-		Quat
5-*O*-glucose			
1’”	5.18 (d)	7.82	103.5
2’”	3.74-3.78 (m)		*
3’”	**		*
4’”	**		*
5’”	**		*
6’”	3.97-4.02 (m)		63.2
6’”	3.71-3.77 (m)		

Abbreviations: s=singlet; d=doublet; m=multiplet; quat= quaternary carbon. * 64.5, 71.7, 72.4, 72.8, 75.1, 78.3, 79.0 overlapping carbon from glucoses. ** hydrogens in range 3.4-3.9 ppm from overlapping glucoses. NMR referenced to CH_3OH-d4 at 3.34 ppm (^{1}H) and 49.8 ppm (^{13}C)

Figure 5.3 | Structural elucidation of anthocyanin; cyanidin 3-*O*-rutinoside (C3R) by NMR.
(a) Structure of C3R as studied by NMR spectroscopy.
(b) ^{1}H-NMR spectrum of C3R.
(c) CH_2 peak of 6″ –proton is shown as green contour (shown with red circle) in HSQC (H-C correlation) spectra.
(d) 4-1″ linkage shown by NOESY correlation; lines were drawn to represent their position and the protons were numbered in ^{1}H-NMR spectra that is represented as horizontal and vertical axis.
(e) On page 144

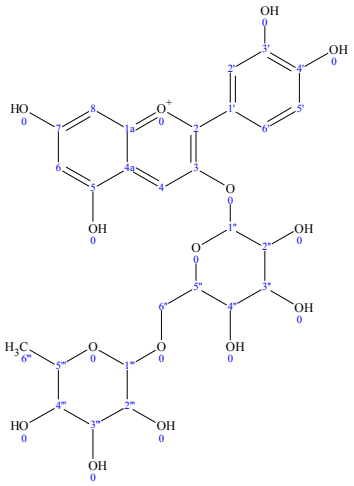

(a)

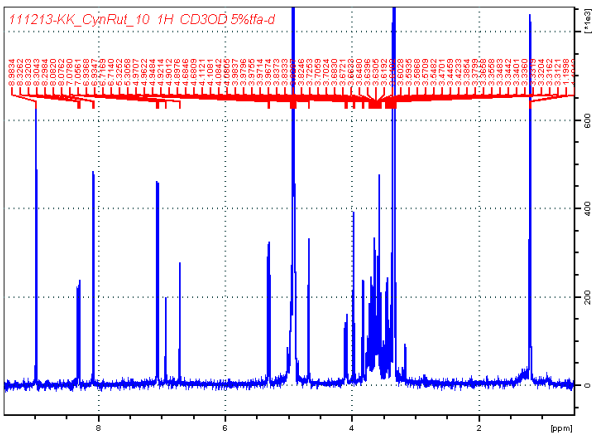
111213-KK_CynRut_10 1H CD3OD 5%tfa-d
[ppm]

(b)

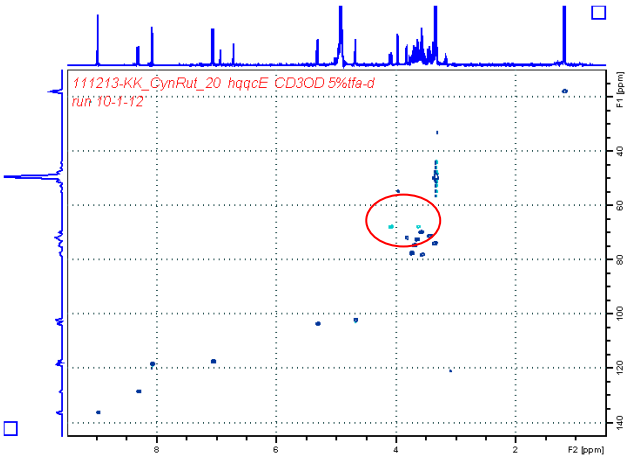
111213-KK_CynRut_20 hqqcE CD3OD 5%tfa-d
run 10-1-12
F1 [ppm]
F2 [ppm]

(c)

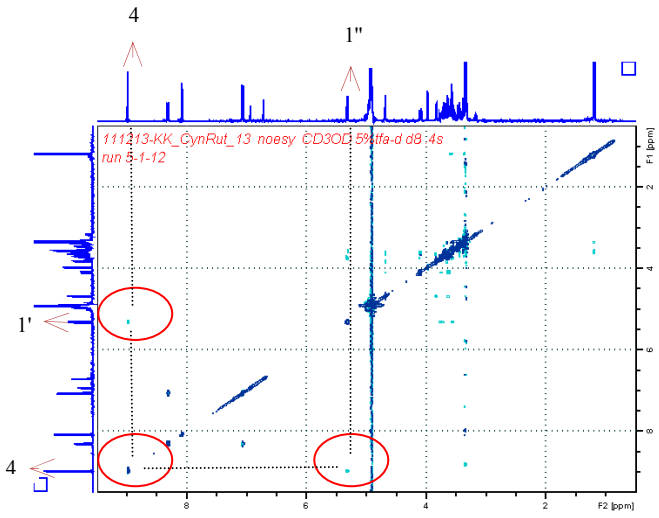
4
1"
111213-KK_CynRut_13 noesy CD3OD 5%tfa-d d8 4s
run 5-1-12
1'
4
F1 [ppm]
F2 [ppm]

(d)

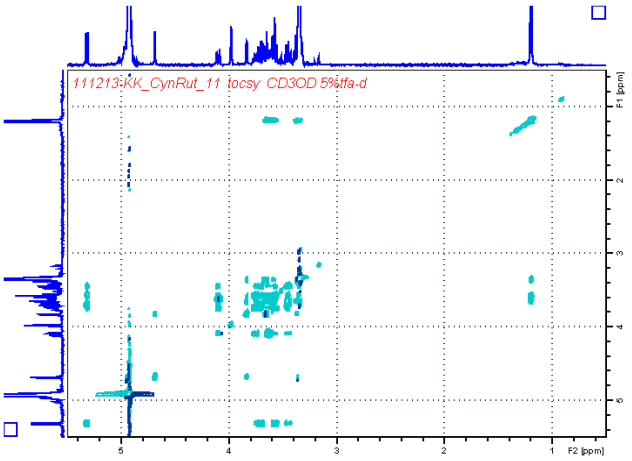

(e)

Figure 5.3 | Structural elucidation of anthocyanin; cyanidin 3-*O*-rutinoside (C3R) by NMR (e) TOCSY NMR spectrum of C3R.

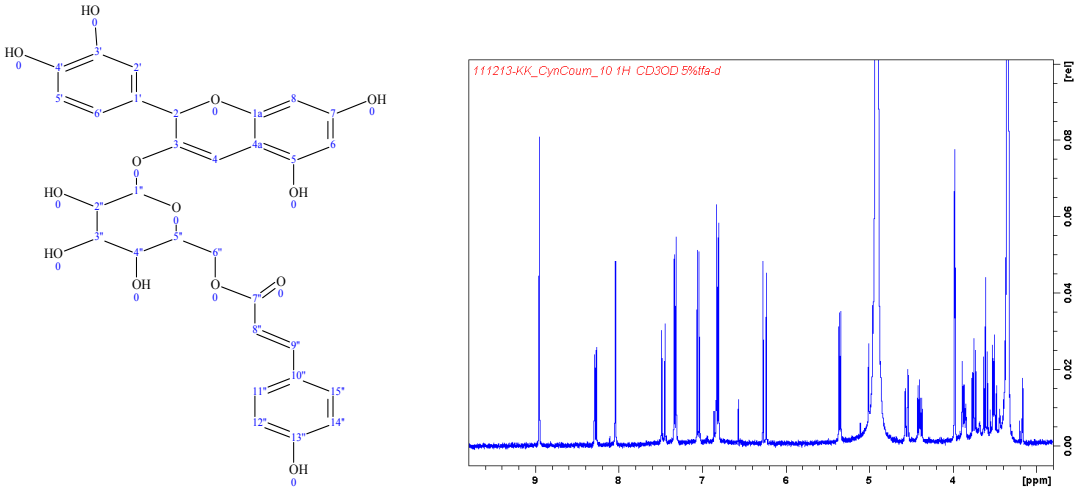

(a) (b)

Figure 5.4 | Structural elucidation of anthocyanin; cyanidin 3-*O*-(6″ coumaroyl) glucoside (C3couG) by NMR. (a) Structure of C3couG as studied by NMR spectroscopy. (b) ^{1}H-NMR spectrum of C3couG. (c) and (d) are presented on next page.

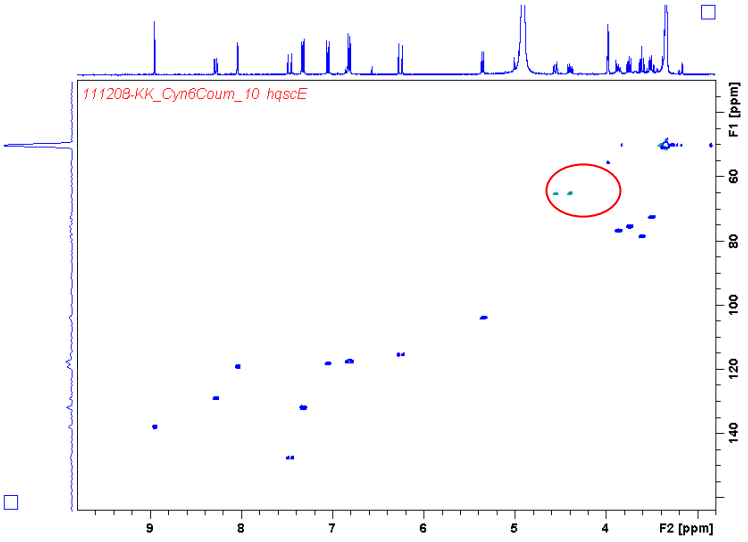

(c)

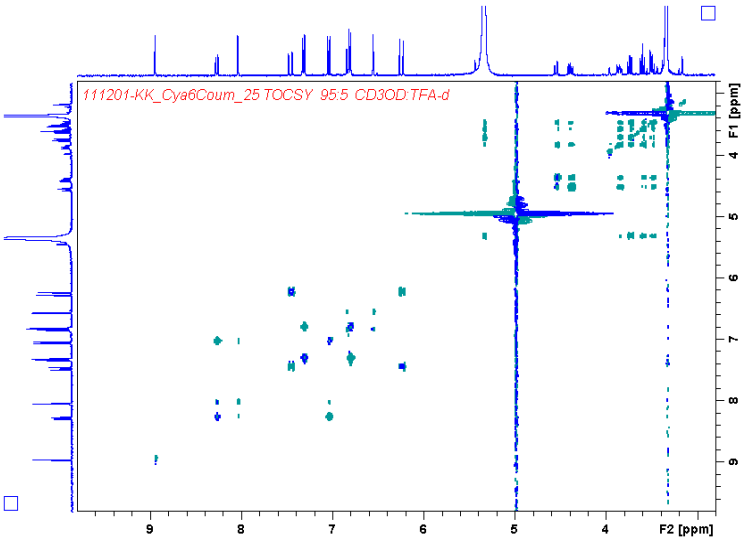

(d)

Figure 5.4 | Structural elucidation of anthocyanin; cyanidin 3-*O*-(6″ coumaroyl) glucoside (C3couG) by NMR. (c) CH_2 peak of 6″ –proton is shown as green contour (shown with red circle) in HSQC (H-C correlation) spectra. (d) TOCSY NMR spectrum of C3couG.

Figure 5.5 | Structural elucidation of anthocyanin; cyanidin 3-*O*-(6″ coumaroyl) 5-diglucoside (C3cou5G) by NMR.

(a) Structure of C3cou5G as studied by NMR spectroscopy.

(b) ^{1}H-NMR spectrum of C3cou5G.

(c) CH_2 peaks of 6″ –proton and 6‴ -protons is shown as green contour at about 65 ppm (shown with red circle) in HSQC (H-C correlation) spectra.

(d) 4-1″ and 4-12″ linkage shown by ROESY correlation; lines were drawn to represent their position and the protons were numbered in ^{1}H-NMR spectra that is represented as horizontal and vertical axis.

(e) presented on page 148.

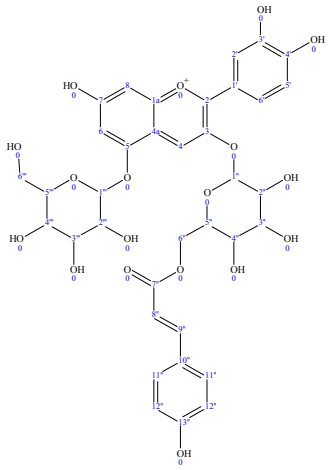

(a)

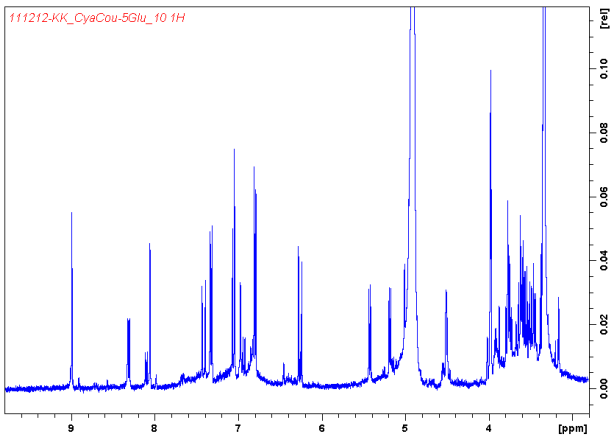
111212-KK_CyaCou-5Glu_10 1H
[rel]
[ppm]

(b)

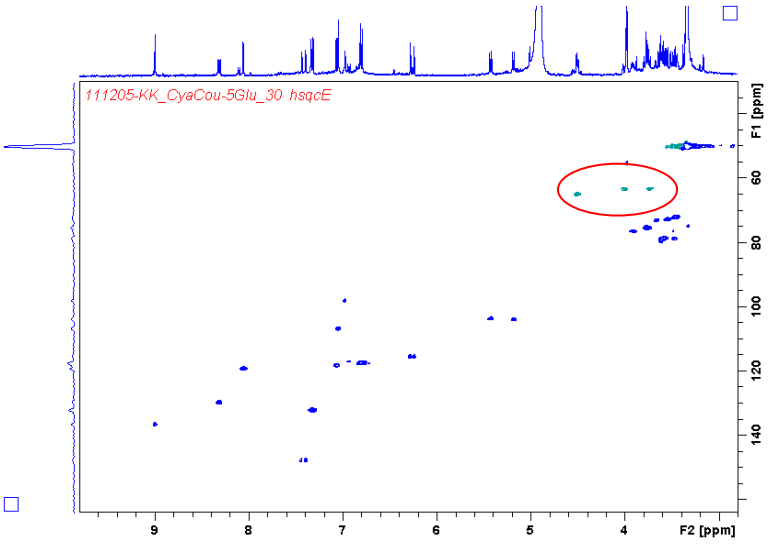
111205-KK_CyaCou-5Glu_30 hsqcE
F1 [ppm]
F2 [ppm]

(c)

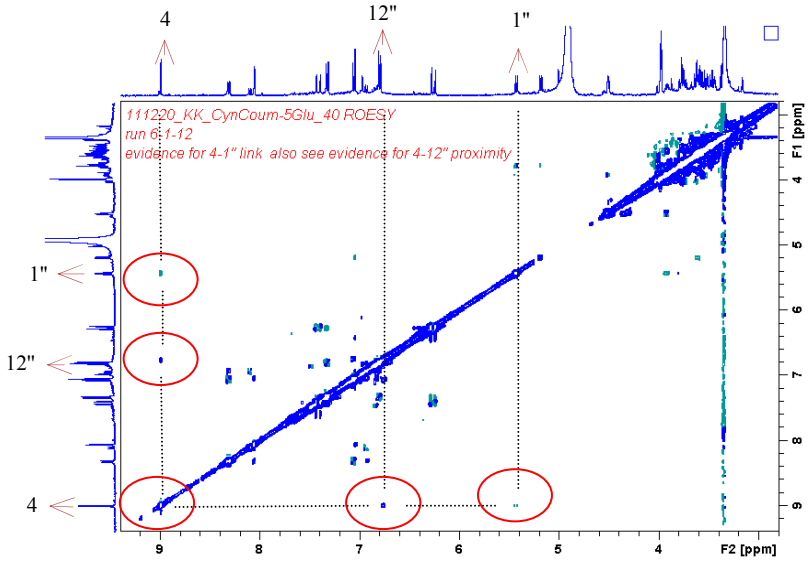
4
12"
1"
111220_KK_CynCoum-5Glu_40 ROESY
run 6: 1-12
evidence for 4-1" link also see evidence for 4-12" proximity
F1 [ppm]
F2 [ppm]

(d)

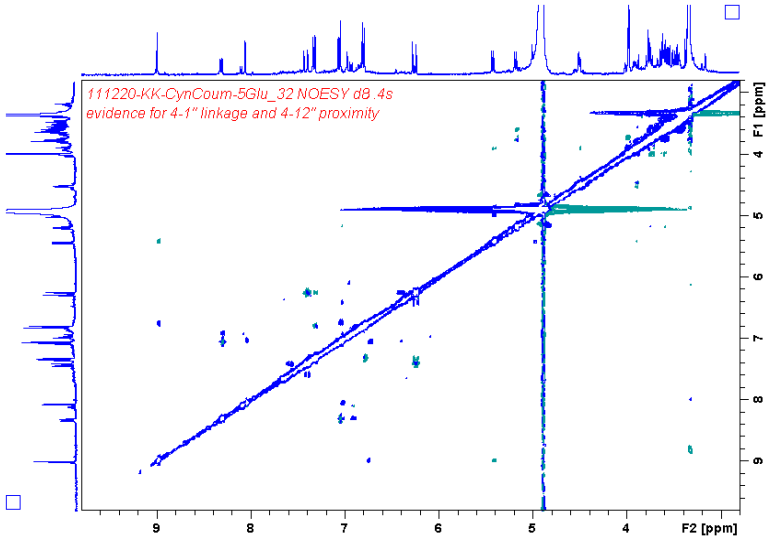

(e)

Figure 5.5 | Structural elucidation of anthocyanin; cyanidin 3-*O*-(6″ coumaroyl) 5-diglucoside (C3cou5G) by NMR. (e) ROESY NMR spectrum of C3cou5G for a clear evidence of 4-1″ and 4-12″ linkage proximity.

5.3.3 Influence of side chain decoration on anthocyanin colour

Studies on synthetic flavylium salts (FVs) have shown changes in colour depending on the solvent (acetonitrile:water, ethanol, propilenglycol, diocane etc.,) and FV concentration in solution (Ito et al., 2002). In protic solvents the FVs are red whereas in aprotic solvents they are yellow. With the purified anthocyanins in my study the flavylium ring being the same (ie., cyanidin) the effects of different side chain modifications on the colour of anthocyanins were observed. C3R, C3R5G, C3couG and C3cou5G each of ~1mM concentration in methanol showed varying colours [Fig 5.6]. C3R appeared as red colour solution and addition of glucose at the 5-OH position of C3R shifted the colour to blue from reddish pink (hypsochromic shift). C3couG appeared pink in colour whereas; addition of 5-glucose to a coumaroylated cyanidin 3-*O*-glucoside resulted in a pinkish red coloured anthocyanin solution. So the spatial orientation and interaction of different side chains of anthocyanins in solution in combination with the flavylium structure have effects on the absorption or the reflection of light by anthocyanins.

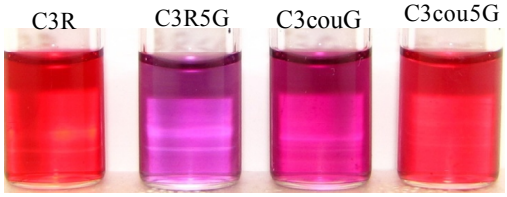

(a)

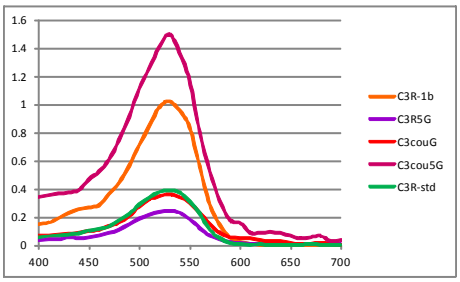

(b)

Figure 5.6 | Visible characteristics of purified anthocyanins with additional side chain decoration. (a) Colour differences between C3R, C3R5G, C3couG and C3cou5G dissolved in methanol are shown. (b) Absorbance shift of anthocyanins in the visible range is shown. C3couG showed a slighter bathochromic shift compared to C3R standard (C3R-std) and C3R5G. C3cou5G showed greater bathochromic shift. C3R purified (C3R-1b) also showed a slight bathochromic shift which could be due to flavonol contamination.

5.3.4 Effect of concentration on anthocyanin stability

Anthocyanin stability depends largely on the concentration of pigment in solution and this effect is studied by observing the colour of the solution. Anthocyanin stability increases with concentration through the mechanism of self-association (Gakh et al., 1998). Concentrated samples appear to be more stable as the anthocyanin molecules are more in number. To determine whether the stability of differently decorated anthocyanins is impacted by their concentration, I studied standard compounds (obtained commercially); cyanidin 3-*O*-rutinoside (C3R) and cyanidin 3-*O*-glucoside (C3G) at four different concentrations: 50 µM, 100 µM, 150 µM and 200 µM at pH 2.6 to pH 7.6. To determine the effect of pH, standard compounds were dissolved in methanol without addition of acid. The degradation curve obtained from two independent experiments (by measuring the amount of anthocyanin over time) was similar for all the concentrations of C3R and C3G at pH 2.6, 3, 6 and 7 [Fig 5.7]. Hence no differences in stability were observed with increasing concentration at these pH values. This observation suggests that anthocyanins in their flavylium cation form which is responsible for red colour at pH 1-2 are stable irrespective of concentration. And quinoidal base forms that attain blue colour at pH 6-6.5 also have less concentration effect on stability. However, stability changed very significantly at pH 4 to 5 and >7 where anthocyanins are colourless in carbinol pseudo-base and chalcone forms respectively. Particularly, deviation of the degradation curve was observed at 50 µM and 150 µM concentrations indicating stability at higher concentrations [Appendix].

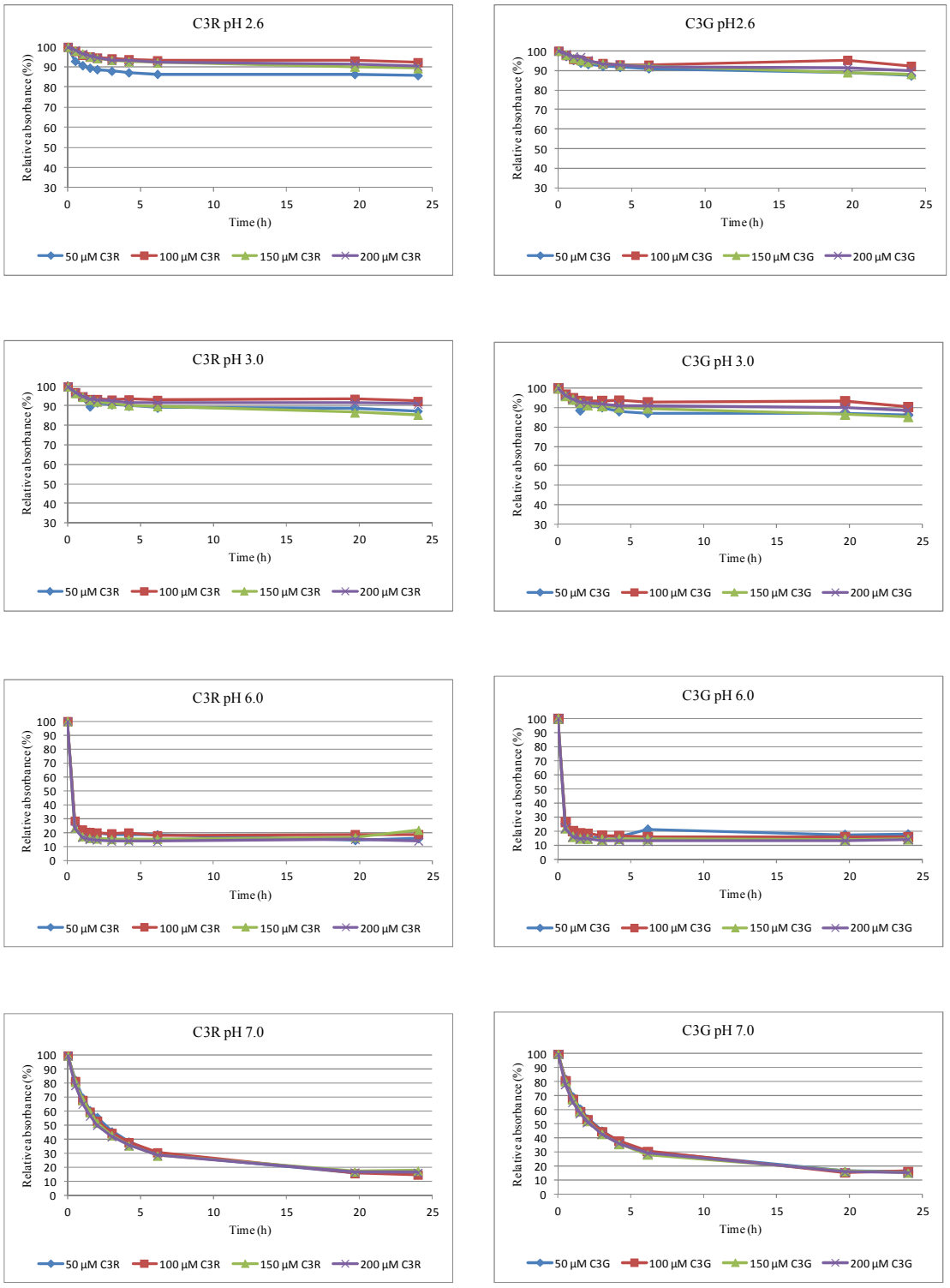

Figure 5.7 | Changes in anthocyanin stability as a result of concentration

Stability of C3R and C3G were studied at 50 µM, 100 µM, 150 µM and 200 µM concentration under eight pH conditions (2.6 to 7.6). *The data represents mean values (± SD) of two independent experiments. Error bars are not shown for clarity. The graphs at other pH are presented in appendix

5.3.5 Anthocyanin stability

It is well established that anthocyanins are stable in acidic conditions due to the predominant red flavylium species (Cooper-Driver, 2001). And anthocyanidin stability is influenced by the ring B substituents and by additional hydroxyl or methoxyl groups (Fleschhut et al., 2006). Acylation of anthocyanins contributes largely to their stability and solubility in solution and even enhances their stability at neutral pH solutions (Luo et al., 2007). However it is very important to understand the stability of anthocyanins at various pH conditions for identifying novel compounds that can be used in different foods such as dairy products that need alkaline conditions. Here the stability of five anthocyanins: C3R, C3R5G, C3G, C3couG and C3cou5G with different modifications [Fig 5.11] was studied in the pH range 2.6 to 7.6 at 50 μM concentration each. pH range above 7.6 and below 2.6 was not studied as such pH related foods cannot be consumed.

5.3.5.1 Effect of pH on stability

All the compounds (C3R, C3R5G, C3G, C3couG and C3cou5G) studied showed a decrease in absorbance reading at their respective λmax from pH 2.6 to 5.0 and bathochromic shifts were observed from λmax at pH 7.0 when solutions were initially prepared in the different buffers. All anthocyanins became redder at lower pH values. [Fig 5.8a]. The relative absorption of C3R, C3G and C3couG dropped more precipitously between pH 4 to 6 than C3R5G and C3cou5G [Fig 5.8b], suggesting that the presence of the 5-glucoside reduces the shift between the flavinium cation and the hemiacetal/chalcone forms at lower pH. The decrease in absorption at λmax for C3G and C3R was greater than for C3couG suggesting that acylation reduces the shift to the carbinol form. The intramolecular stacking attributed by acyl-moieties stabilises the anthocyanins in mildly acidic conditions by protecting the chromophore from nucleophillic attack (Brouillard et al., 1978, Brouillard, 1982). C3R5G and C3cou5G showed slightly less discoloration at pH 4 to 6 compared to the other anthocyanins, and again, this could be attributed to the presence of 5-glucoside. From pH 4 to 6 anthocyanins are colourless as the red flavylium cation hydrates to yield the colourless carbinol (Mazza and E.Miniati, 1993). All samples showed higher absorption between 570 and 600nm in the pH range 6.0 to 7.6. This shift is due to the presence of unstable quinonoidal structures which give bluer colours. The increase in absorption at pH6.0 to 7.6 was greater for C3R5G and C3cou5G, suggesting that the presence of the 5 glucoside promotes the formation of quinoidal bases. Table 5.3 shows the shift in λmax of all the

anthocyanins at various pH values studied. Anthocyanins have a bluer tone as the pH rises above pH5.0. The additional groups decorating the anthocyanins also contribute to their colour. At pH 7.0 and 7.6 both C3R5G and C3cou5G showed much bluer colour compared to the others due to presence of the 5-glucosyl moiety [Fig 5.9].

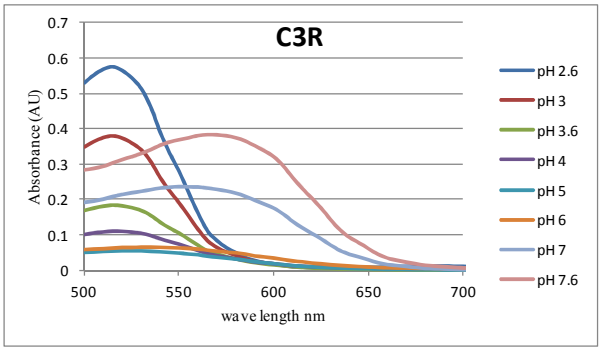

(a)

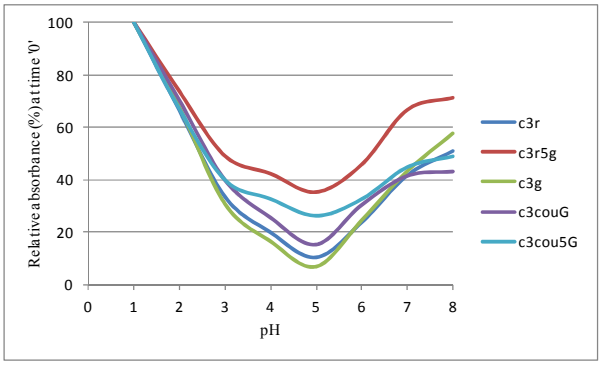

(b)

Fig 5.8 Characteristics of absorption spectra of anthocyanins (50 µM) at different pH solutions (2.6 to 7.6)

(a) A bathochromic shift C3R as the pH is raised was observed in the spectra from 500 to 700 nm. (b) Relative decrease in absorption maxima at pH 4 to 6 is shown. This decrease was more prominent for C3R, C3R and C3couG.

In general all compounds were stable for several days in acidic conditions (pH < 4) irrespective of the groups attached [Fig 5.10]. At pH 5 and 6 the data obtained showed huge variations due to low detection levels of anthocyanin as it exists as colourless chalcone structure at those pH values. At neutral pH the stability of compounds was decreased to hours [Fig 5.10]. The $t_{1/2}$ of anthocyanins is presented in table 5.4. Variability was observed at higher pH conditions where the additional groups contributed to different stabilities (discussed in detail in next section).

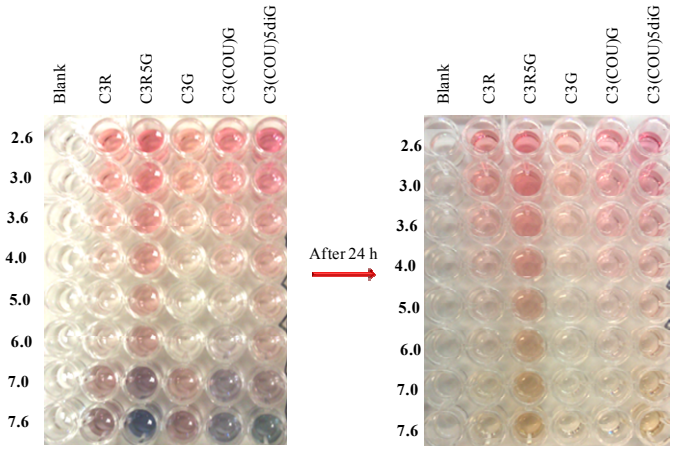

Figure 5.9 | Colour changes of different anthocyanins with pH. The change to blue colour at neutral pH (7 and 7.6) was prominently seen at the start of the reaction particularly for 5-glucosylated anthocyanins. The degradation of anthocyanin after 24 hr was noticed mainly at pH 5 to 7.6.

Table 5.3 | Shift in the absorption maxima of anthocyanins at various pH values

pH	cyanidin 3-*O*-rutinoside (nm)	cyanidin 3-*O*-rutinoside 5-*O*-glucoside (nm)	cyanidin 3-*O*-glucoside (nm)	cyanidin 3-*O*-(6″-coumaroyl) glucoside (nm)	cyanidin 3-*O*-(6″-coumaroyl) 5-diglucoside (nm)
2.6	515	515-520	510	515-520	520-525
3.0	515	520	510	515-520	525
3.6	515	520-525	515	520	525
4.0	515	525	515	520	525
5.0	525	525-530	520-530	525-530	525-530
6.0	530-535	535	530-535	555-560	540
7.0	550	565	545-550	575	560-565
7.6	565	590	565	585-590	590-595

Table 5.4 | Stability of anthocyanins studied from pH range 2.6 to 7.6. Half-life ($t_{1/2}$) of each anthocyanin is shown.

pH	cyanidin 3-*O*-rutinoside	cyanidin 3-*O*-rutinoside 5-*O*-glucoside	cyanidin 3-*O*-glucoside	cyanidin 3-*O*-(6″-coumaroyl) glucoside	cyanidin 3-*O*-(6″-coumaroyl) 5-diglucoside
2.6	7.6 d	6.58 d	6.57 d	4.8 d	7.01 d
3.0	6.35 d	5.87 d	3.88 d	5.55 d	8.36 d
3.6	6.2 d	5.68 d	6.43 d	6.02 d	9.51 d
4.0	5.76 d	4.45 d	7.45 d	9.11 d	5.01 d
5.0	*12.48 h	*9.72 h	*6.33 h	*17.19 h	*7.74 h
6.0	*14.71 h	*15.33 h	*7.71 h	*1.62 h	*43.46 h
7.0	8.19 h	13.56 h	3.88 h	8.13 h	19.68 h
7.6	16.01 h	10.02 h	11.44 h	17.84 h	14.13 h

* Data not significant due to large standard deviation of the replicates

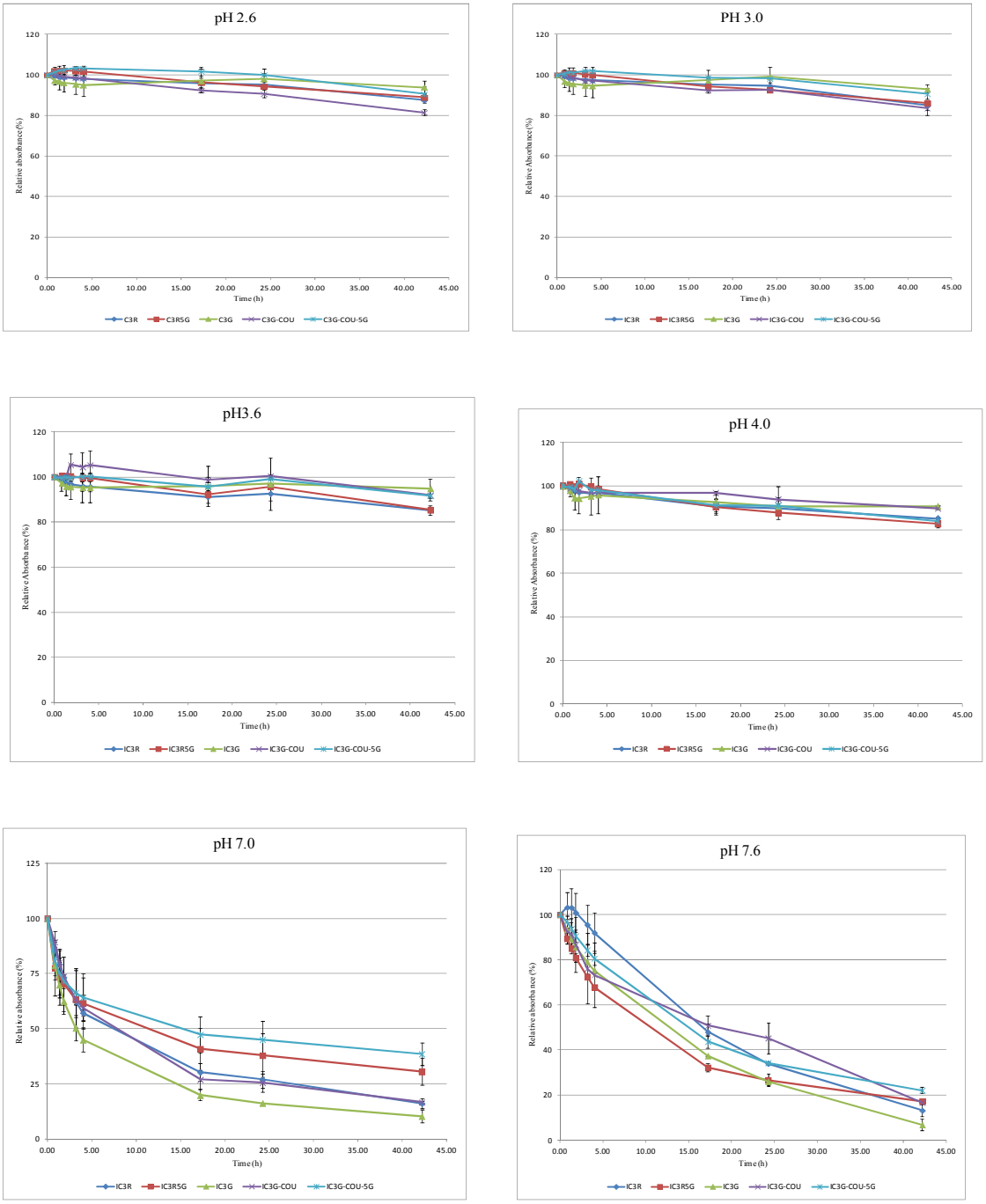

Figure 5.10 | Stability of anthocyanins studied at different pH conditions. Stabilities of different purified anthocyanins (C3R, C3R5G, C3G, C3couG and C3cou5G; 50 µM each) in several pH conditions (McIlvaine's buffer pH 2.6 to 7.6) at 25-27 °C are shown. *The data represent mean values (± SD) of two independent experiments. Stability data at pH 6.0 is presented in appendix.

5.3.5.2 Effect of side chain decoration on stability

Fleschhut et al., (2006) showed that anthocyanin monoglycosides and diglycosides are more stable under neutral pH conditions than the aglycones. Luo et al., (2007) showed that cyanidin 3,5-diglcuoside was less stable than cyanidin -3-*O*-glucoside in neutral conditions. My study was undertaken to have a more complete understanding of how each additional group contributes to the stability of anthocyanins at different pH conditions.

In acidic conditions all anthocyanins C3R, C3R5G, C3G, C3couG and C3cou5G showed relatively similar stabilities due to presence of anthocyanins in flavylium cation form. At pH 5 and 6 anthocyanins exist as colourless carbinol pseudo bases and chalcones (Castañeda-Ovando et al., 2009). Hence, accurate stability studies were not possible under these conditions. Because the standard deviations of the replicates were large, this reduced the significance of measurements. However at these conditions C3R5G and C3cou5G showed slight blue colour due to 5-glycoside, as 5-glucose tend to give bluer tones to anthocyanins [Fig 5.9]. At neutral pH (7.0) where a transition state from quinoidal base (which offers blue colour) to colourless chalcone occurs, the stability of anthocyanins depended on the number of additional groups. And at this pH (pH 7) 5-glycosidic (C3cou5G and C3R5G) anthocyanins showed the highest stability. This could be due to the significant self association found with anthocyanidin 3,5-diglucoside (Gakh et al., 1998, Tsutomu, 1992). Coumaroylated anthocyanins showed more stability followed by non-acylated anthocyanins. Although the stability of all the anthocyanins was greatly reduced at neutral pH compared to acidic pH. Fleschhut et al., (2006) suggested that 5-glycosylation provides stability at pH7. Similar to this finding, in this study C3R5G ($t_{1/2}$ 13.56 h) was observed to be more stable than C3couG ($t_{1/2}$ 8.13 h) at pH 7. Coumaroylation with and an additional 5-glucoside provided more stability ($t_{1/2}$ 19.68 h) at pH 7 among the anthocyanins studied probably due to both intramolecular stacking and self-association.

Interestingly, at slightly higher pH (7.6) there was a destabilising effect of 5-glycosylation similar to observations made by Luo et al., (2007). The half life of C3R5G ($t_{1/2}$ 10.02 h) was lower than that of C3R ($t_{1/2}$ 16.01 h) and C3cou5G ($t_{1/2}$ 14.13 h) was lower than C3couG ($t_{1/2}$ 17.84 h) at pH 7.6. But C3cou5G ($t_{1/2}$ 14.13 h) is more stable than C3G ($t_{1/2}$ 11.44 h) suggesting that coumaroylation plays a major role in protecting

the chromophore at this pH. Comparison of C3R and C3G at different pH studied shows that C3R is more stable suggesting stability is offered by additional rhamnose to anthocyanins than a glucose molecule alone. However C3couG is stable compared to C3R5G indicating that the stability offered by coumaroylation is greater than 5-glycosylation.

5.3.6 Intermolecular copigmentation of anthocyanins

Five copigments: chlorogenic acid (from here after referred to as CGA), p-coumaric acid (referred to as couA), caffeic acid (referred to as caffA) which are phenolic acids and quercetin 3-*O*-rutinoside (rutin, referred to as Q3R), kaempferol 3-*O*-rutinoside (referred to as K3R) which are flavonols were studied for their different copigmentation effects on the isolated anthocyanins: C3R, C3R5G, C3G, C3couG and C3cou5G at pH 3.6. Structures of all the copigments and anthocyanins studied were presented in Fig 5.11. At pH 3.6 copigmentation effects have been reported to be maximal (Mazza and Brouillard, 1990) and hence pH 3.6 was chosen for this study.

5.3.6.1 Effect of pigment: co-pigment concentration

Immediate intermolecular copigmentation; studied as an increase in colour was observed with all the anthocyanins (50 μM each) and copigments at 1:100 molar ratio and no copigmentation was noticed by eye at 1:1 and 1:10 molar ratio. However a slight bathocromic shift (~1 nm) was observed in the absorbance spectrum at 1:1 and 1:10 molar ratios [Table 5.6]. Among the five copigments studied kaempferol 3-*O*-rutinoside (K3R) showed strong copigmentation at a 1:25 molar ratio with all the anthocyanins [Fig 5.13]. The increase in colour intensity with K3R was more profound with C3couG and C3R compared to other anthocyanins. The effect of K3R at higher molar concentrations could not be studied due to precipitation of the compound in the reaction and also due to its low solubility.

The individual effect of each co-pigment on anthocyanins at 1:25 molar ratio is very variable [Fig 5.13]. Chlorogenic acid (CGA) showed colour enhancement at 1:25 with C3R, C3G and C3couG compared to anthocyanins (without copigment). Whereas, at 1:25 molar ratio C3cou5G did not show copigmentation with CGA suggesting that 5-glucosylated anthocyanins copigment with CGA at higher molar concentration. CaffA, couA and Q3R did not show copigmentation with anthocyanins at 1:25 molar ratio.

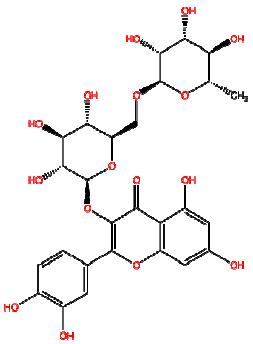

Quercitin-3-*O*-rutinoside

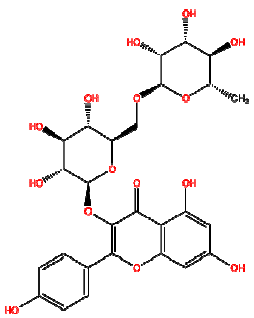

Kaempferol-3-*O*-rutinoside

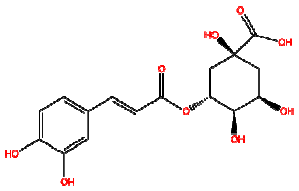

Chlorogenic-acid

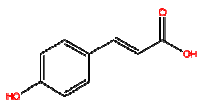

p-Coumaric-acid

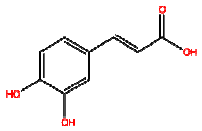

Caffeic-acid

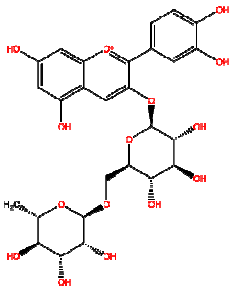

Cyanidin3-*O*-rutinoside

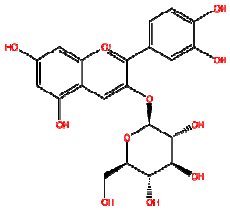

Cyanidin3-*O*-glucoside

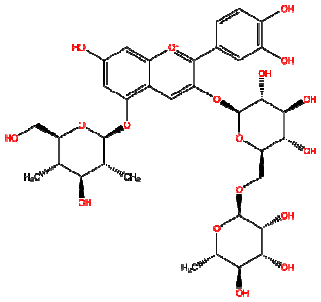

Cyanidin3-*O*-rutinoside-5-glucoside

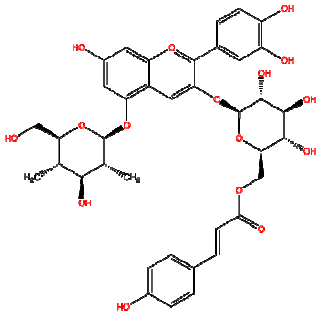

Cyanidin3-(6”-coumaroyl)5-diglucoside

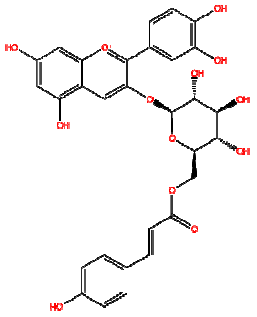

Cyanidin3-(6”coumaroyl)glucoside

Figure 5.11 | Structures of copigments and purified anthocyanins used in this study

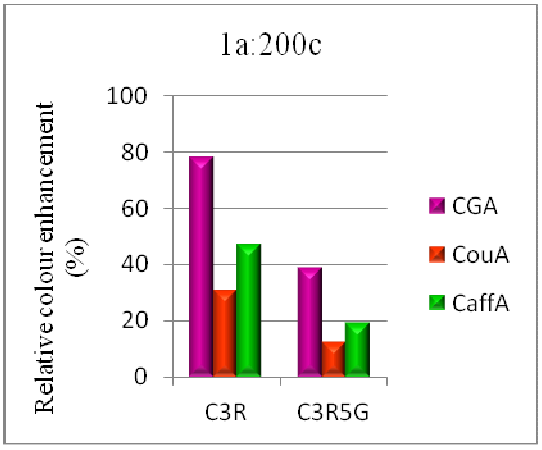

Figure 5.12 | Relative percent increase of copigmentation of C3R and C3R5G with different copigments (CGA, CouA, CaffA) at 1a:200c molar ratio. A bathochromic shift in absorbance spectrum of C3R and C3R5G is observed due to addition of copigments. The data represent relative percentage of two independent experiments.

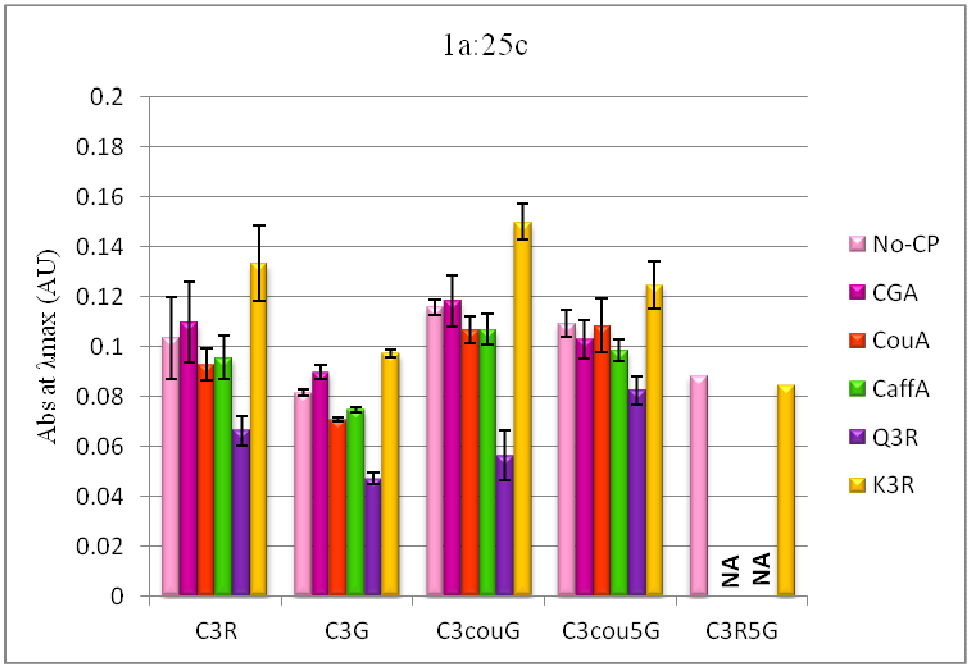

Figure 5.13 | Comparison of hyperchromic effects of different anthocyanins (50 µM each) to copigments (1.25 mM each) at 1a:25c molar ratio at pH 3.6. *The data represents mean values (± SE) of two independent experiments.

The colour enhancement of C3R5G with other copigments apart from K3R could not be studied due to less pigment/compound availability. Hence, copigmentation ability of C3R5G was compared with C3R at a molar ratio of 1:200 to understand 5-glycosylation effect. The relative percent of colour enhancement was observed with CGA, caffA and

couA [Fig 5.12]. C3R showed higher co-pigmentation than C3R5G which again proves the inability of 5-glucosylation in co-pigmentation. And so self-association does not have a role in copigmentation like in stability. Thus this study shows that certain kinds of flavonols can copigment at lower molar ratios whereas phenolic acids copigment only at higher molar ratios. However, in this study the effect of different concentrations of anthocyanin with copigments was not studied. Since it was obvious that colour intensity increases with increase in anthocyanin concentration.

5.3.6.2 Effect of type of co-pigment in increasing blueness (bathochromic shift)

Blue colour is particularly desirable with very few flower species producing this colour. Copigmentation offers a means to provide such blue-purple tones for use in food industry and for producing rare coloured flowers. In my study copigmentation at 1:100 molar ratio was observed as both a hyperchromic effect (detected as an increase in absorbance at λmax) and bathochromic shift (a shift of λmax towards higher wavelength) [Fig 5. 14]; a result in agreement with earlier studies (Asen et al., 1972, Dangles et al., 1993). Bathochromic shift was more prominently seen with Q3R at 1:100 molar ratio [Table 5.6]. Although, the shift with K3R was more when studied at a lower molar ratio of 1:25 [Table 5.5]. Copigmentation through bathochromic shift also depends largely on the decoration of anthocyanins. Coumaroylation of anthocyanins potentiated co-pigmentation especially in presence of flavonols. C3cou5G exhibited higher bathochromic shift when compared to C3couG; without the addition of copigment. However, in presence of copigments C3couG showed higher bathochromic shift than C3cou5G.

Table 5.5| Bathochromic shift observed due to copigmentation at 1:25 molar.

Δmax (nm) of 50 µM anthocyanin and 1250 µM copigment was presented in this table.

co-pigment	cyanidin 3-*O*-rutinoside	cyanidin 3-*O*-glucoside	cyanidin 3-*O*-(6″-coumaroyl) glucoside	cyanidin 3-*O*-(6″-coumaroyl) 5-diglucoside
No copigment	515-516	512-514	517-520	522-524
CGA	517-519	515	519-523	522-527
CouA	517-520	516-517	522-524	523
CaffA	518-520	517-518	520-523	523-528
Q3R	526-529	524-529	529	529
K3R	527-528	524-526	532-533	531-533

Table 5.6 | Bathochromic shift observed due to copigmentation. Δmax (nm) of 50 µM anthocyanin and 50 µM, 500 µM, 1250 µM, 5 mM and 10mM of copigment combination was presented in this table.

Ratio of pigment to co-pigment	cyanidin 3-*O*-rutinoside	cyanidin 3-*O*-rutinoside 5-*O*-glucoside	cyanidin 3-*O*-glucoside	cyanidin 3-*O*-(6″-coumaroyl) glucoside	cyanidin 3-*O*-(6″-coumaroyl) 5-diglucoside
1:O	515-516	515-519	512-514	517-520	522-524
1:1 CGA	515-517	Nd	512-513	520	524-526
1:10 CGA	517	Nd	513-514	517-520	526-528
1:25 CGA	517-519	Nd	515	519-523	522-527
1:100 CGA	523-525	Nd	519-520	525-526	530-531
1:200 CGA	521	525-526	nd	Nd	Nd
1:1 couA	516-517	Nd	514-516	517-522	524-525
1:10 couA	516-518	Nd	515-516	520-522	522-524
1:25 couA	517-520	Nd	516-517	522-524	523
1:100 couA	520-522	Nd	517-519	522-523	520-529
1:200 couA	521	526-530	nd	Nd	Nd
1:1 caffA	516-518	Nd	513-516	520-522	521-524
1:10 caffA	515-518	Nd	514-515	522	524-525
1:25 caffA	518-520	Nd	517-518	520-523	523-528
1:100 caffA	522	Nd	519-520	523-524	527-530
1:200 caffA	521	525-529	nd	Nd	Nd
1:1 Q3R	517	Nd	516-517	520	529-530
1:10 Q3R	523	Nd	520-521	525	530
1:25 Q3R	526-529	527	524-529	529	529
1:100 Q3R	Na	Nd	na	546	530-539
1:1 K3R	518-519	Nd	516-518	524	520-526
1:10 K3R	521-525	Nd	517-521	524-530	529-530
1:25 K3R	527-528	529	524-526	532-533	531-533

Abbreviation: nm = wave length at maximum absorbance reading (λ max); nd = not determined.
Note: due to low availability of C3R5G, it was studied only at the maximum molar ratio

5.3.6.3 Effect of type of co-pigment on pigment intensity (hyperchromic shift)

Flavonols were observed to have higher copigmentation effect than phenolic acids with all the anthocyanins studied since at lower molar ratios they showed an enhanced hyperchromic effect. When the colour enhancement obtained due to addition of copigments was studied; K3R provided the best enhancement with all the anthocyanins at 1:25 molar ratio [Fig 5.13]. The relative percent of colour enhancement at 1:100 molar ratio of each anthocyanin was studied [Fig 5.15]. The variation in hyperchromic shift attributed by slight concentration differences in anthocyanins can be nullified by studying the relative percent of colour enhancement (% CE). Thus an understanding of the effect of side chain modification of anthocyanins in associating with the copigments can be achieved. C3R showed highest copigmentation with CGA (57%) and had least enhancement with couA (16.8%). CGA also had strong copigmenting properties (in terms of intensifying pigmentation) with C3G (68.23% at 1:100) and C3R5G (38.7% at 1:200). For C3couG, flavonols Q3R, (64% at 1:100) and K3R (36.7% at 1:25) enhanced the hyperchromic shift best, followed by phenolic acids (CGA, 40%; couA, 26.2% and caffA, 21.6%). Q3R showed a remarkable enhancement of pigment intensity for C3cou5G (69.5%) compared to other copigments. Over all, flavonols were better copigments compared to phenolics as monitored by their percent enhancement of colour intensity of the different anthocyanins.

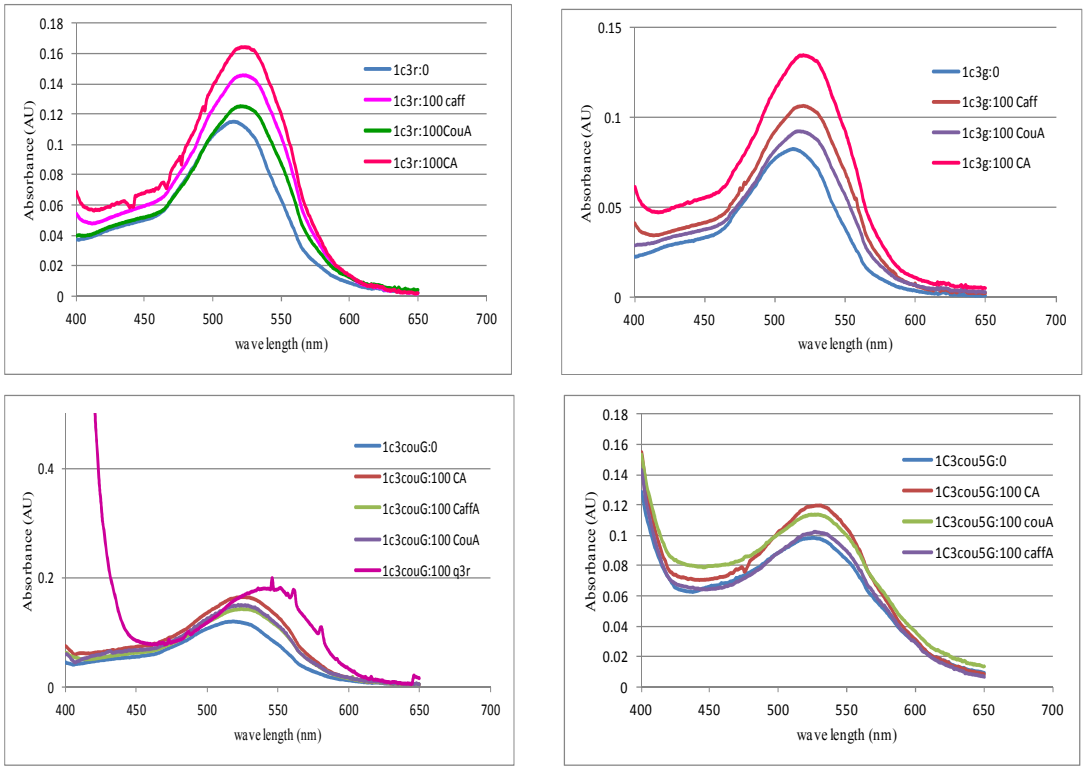

Figure 5.14 | Absorption spectra of anthocyanins with and without copigments. Hyperchromic effects and bathochromic shifts observed as a result of addition of copigments as studied at 1:100 molar ratio of different anthocyanins; 50 µM/ copigment (5 mM) are shown.

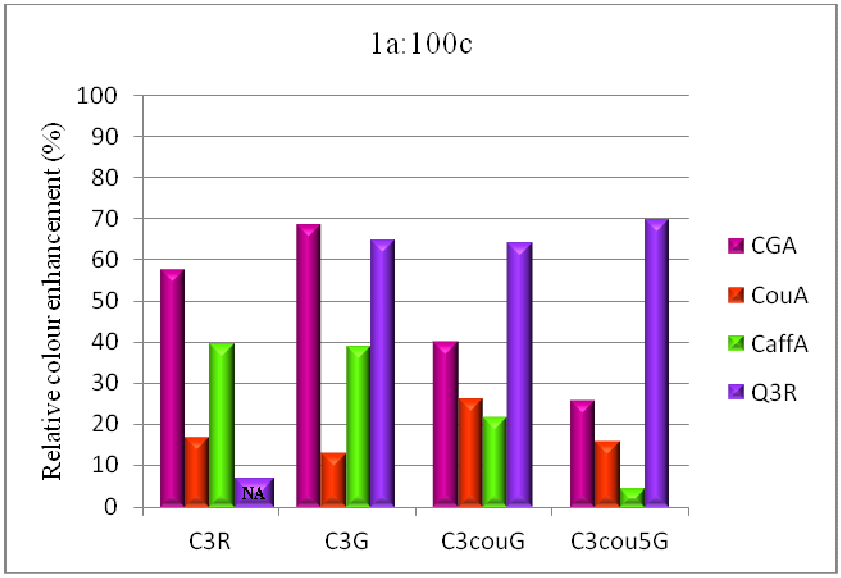

Figure 5.15 | Relative colour enhancement (in terms of % increase) of different anthocyanins at pH 3.6 and at 1:100 molar ratio of anthocyanin (1a; mentioned in figure) to copigment (100c; mentioned in figure) was shown.

5.3.6.4 Effect of side-chain decoration

The increase in colour intensity of anthocyanins offered by the copigments at pH 3.6 was studied for each anthocyanin at all molar ratios to understand the contributions of additional groups to copigmentation properties. By using anthocyanins with common flavylium ring structure the effects offered by the decorations could be identified clearly. Earlier studies had shown that all anthocyanins are capable of copigmentation but the influence of side chain decoration on copigmentation has not been studied. Here I studied the influence of 5-glucosylation on copigmentation by comparing with C3R and C3R5G. As C3R5G was available in limited quantities I studied 1:200 molar ratio with CGA, couA, caffA and at 1:20 and 1:25 with Q3R and K3R (due to a solubility problem with these copigments) respectively. C3R showed relatively stronger copigmentation compared to C3R5G with all copigments [Fig 5.12]. This shows that trisaccharidic anthocyanins inhibit copigmentation compared to disaccharidic anthocyanins, supporting earlier studies by Eiro and Heinone (2002) claiming that three sugar moieties are enough to prevent intermolecular copigmentation. In my study flavonols showed stronger copigmentation than phenolics. Among phenolic acids; CGA copigments more followed by caffA and couA being the least [Fig 5.16]. However with C3couG compared to caffA and couA; couA showed higher colour enhancement. C3G showed better colour enhancement with CGA compared to C3R with CGA and Q3R. Figure 5.16 shows the changes in absorption of C3R, C3G, C3couG and C3cou5G in association with different copigments. Coumaroylation of anthocyanins offered better colour enhancement than other non-coumaroylated anthocyanins when compared at 1:100 anthocyanin/copigment ratio [Fig 5.17]. C3couG showed enhancement even when compared to C3cou5G. This decrease in colour enhancement associated with 5-glucosylation may be due to self association catalysed by 5-glucose and altering the availability of coumaroyl group for a complete intermolecular copigmentation.

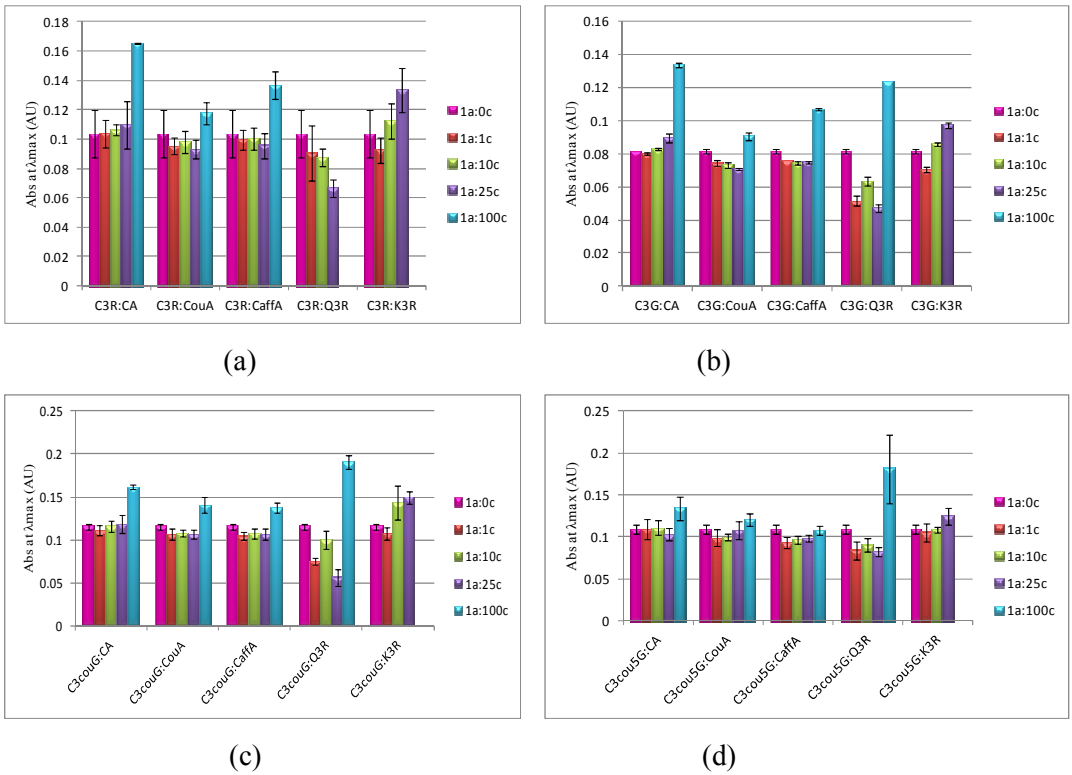

Figure 5.16 | Intermolecular copigmentation effect of different anthocyanins caused by copigments (a) C3R, (b) C3G, (c) C3couG and (d) C3cou5G at 50 µM/ copigments: CGA, couA, caffA, Q3R and K3R at 1:1, 1:10, 1:25, 1:100 molar ratios in pH 3.6 McIlvaines buffer.
*The data represents mean values (± SD) of two independent experiments.

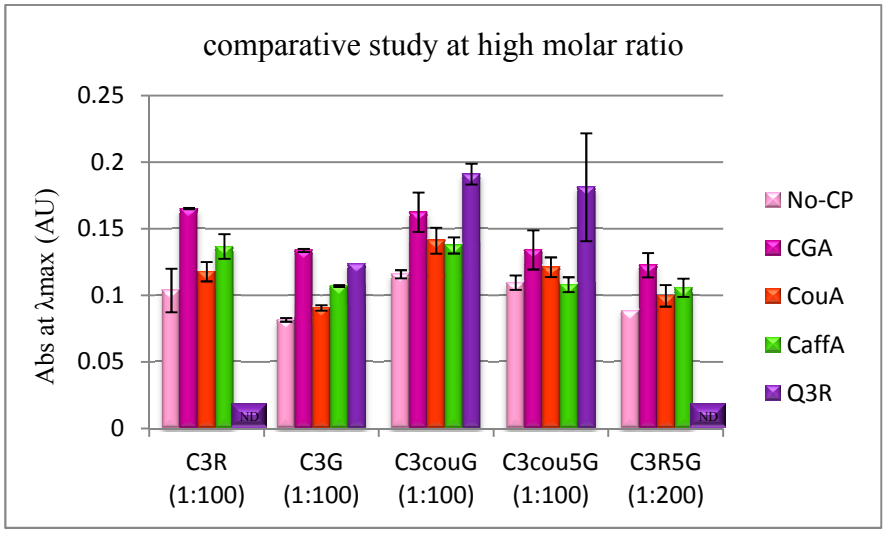

Figure 5.17 | Comparative intermolecular copigmentation of different anthocyanins with four copigments at 1:100 molar ratio studied. C3R5G was studied at 1:200 molar ratio. *The data represent mean values (± SD) of two independent experiments. ND – Not determined.

5.4 Discussion

Anthocyanin properties are dictated by several factors in solution. Understanding these is crucial for their use. To characterise some of the physical properties of different anthocyanins in solution, I purified C3R, C3R5G, C3couG and C3cou5G from one of the transgenic tobacco lines generated as a part of this thesis. The stability and intermolecular copigmentation properties of these anthocyanins were compared.

All anthocyanins showed greater stability at low pH (2.6 to 4.0). At higher pH, 5-glycosylated and coumaroylated anthocyanins showed greater stability than non 5-glycosylated and non-acylated anthocyanins. Acylation offers stability to anthocyanins through intramolecular copigmentation mainly by protecting the molecules from nucleophilic attack by water (Figueiredo et al., 1999). Similar results were obtained in this study however acylated and 5-glycosylated anthocyanin (C3cou5G) was more stable than acylated anthocyanin (C3couG) alone. This behaviour probably could be due to sugar molecules avoiding the degradation of instable intermediaries into phenolic acid and aldehyde compounds (Fleschhut et al., 2006). Also self-association offers stability to 5-glucosylated anthocyanins (Tsutomu, 1992). Garzon and Wrolstad (2001) showed that the stability of acylated pelargonidin 3-sophoroside-5-glucoside was weaker than that of pelargonidin 3-glucoside. But my work showed that C3cou5G which is both acylated and 5-glucosylation; is more stable than C3G and C3couG at pH 7. This could be due to different anthocyanidin ring indicating that the type of anthocyanidin ring can influence stability. Additionally, both intramolecular stacking and self-association could add to the stability. C3R5G was observed to have higher stability compared to C3R alone suggesting that the sterical conditions created by glycosylation can stabilize anthocyanins along with self-association of flavylium offered by 5-glycosylation. Whereas, at pH7.6 acylated anthocyanins were more stable and followed by rhamnosylated anthocyanins. And at this pH 5-glycosylation contributed to destabilizing effect of anthocyanins. However 5-glucosides retained better colour at pH 5 to 7 compared to acylated and non-acylated anthocyanins. Such anthocyanins could be a good source for foods where mild pH is maintained. But for foods requiring a wider range of conditions coumaroylated anthocyanins should be preferred.

Copigmentation is one of the factors contributing stability to pigments in plants (Davies and Mazza, 1993). Copigments with rich π- electron content interact with the flavylium ions of anthocyanins which are rather poor in electrons and this offers protection to the anthocyanins from nucleophilic attack by water (Matsufuji et al., 2003).

The type of interaction varies with both the anthocyanin and the copigment. With less anthocyanin copigmentation greatly improves the appearance of colour and also enhances the stability of anthocyanins. In this study I characterised purified anthocyanins for their abilities to copigment. By using a common anthocyanidin ring structure the colour enhancement offered by different anthocyanin side chain decoration and co-pigments can be understood.

I studied three phenolic acids (CGA, caffA and couA) and two flavonols (K3R and Q3R) for their copigmenting properties with five anthocyanins. Flavonols were shown to confer enhanced co-pigmentation both by hyperchromic and bathochromic shift compared to phenolic acids. Among flavonols K3R showed the highest copigmentation effects even at 1:25 molar ratio. And at 1:100 ratio Q3R showed higher bathochromic shift as studied with C3cou5G. However, acylated anthocyanins are better in their copigmentation ability relative to other anthocyanins. This probably could be due to acylation having intramolecular bonding as well. Hence it is evident that acylated anthocyanins are capable of intra and inter molecular copigmentation. Glycosylation also played a role in enhancing the colour. However the role of 5-glucosylation in copigmentation was not significantly higher compared to its role in anthocyanin stability. This suggests that self-association does not contribute to copigmentation but it offers more stability. Among phenolic acids; chlorogenic acid copigmented anthocyanins better particularly non-acylated anthocyanins. A similar *in-vivo* observation was in Del/Ros tobacco plants where the plants appeared darker (pinkish purple) where C3R is the major anthocyanin and CGA accumulating in tobacco. But higher copigmentation is achieved when flavonol containing tomato extracts were added to extracts from Del/Ros tomatoes (Cathie Martin, personal communication). It is thus evident that flavonols offer better copigmentation than phenolics.

So with every modification of anthocyanins the spatial structure and interaction within the group changes and offers varied protection. And every anthocyanin has a different property to offer and physical characterisation of anthocyanins is desirable to identify new compounds. Future studies looking into the role of anthocyanins in copigmentation at different pH and their stability can provide valuable information for creating novel colours. A thorough understanding of how different modifications of anthocyanins contribute to their varied physical properties is also useful in engineering new horticultural plant species and in designing varied but optimised natural food colours.

CHAPTER VI

General Discussion

6.1 General discussion of the project

"*Side chain decoration of anthocyanins; mechanisms and effects on functionality*"

Anthocyanins are some of the most widely studied flavonoids and much is known about the biosynthesis and their biological functions. In this project I aimed to further the understanding of the molecular mechanisms leading to different side chain decorations of anthocyanins and the effects of such decorations on both *in-vivo* and *in-vitro* functions. Various properties of anthocyanins such as colour, stability and solubility are largely dictated by the addition of side groups such as sugars, methyl and acyl moieties at several positions on the anthocyanidin core structure.

Acyltransferases are modifying enzymes that catalyze the addition of acyl-groups onto the sugar moieties of anthocyanins. Anthocyanin acyltransferases (AATs) are classified based on their acyl donor specificities, and are capable of acting on aromatic acyl-CoAs and aliphatic acyl-CoAs, and have regio-specificity of acyl transfer on to 3-glucoside or 5-glucoside. Several acyltransferases have been isolated and characterised to date. A start to understanding the molecular basis of their specificity was possible only with the crystal structure of an aliphatic AAT; anthocyanidin 3-*O*-glucoside-6″-*O*-malonyltransferase (Unno et al., 2007). However, as AATs have a strict acyl-donor specificity it is imperative to study aromatic AATs for a full understanding of the determinants of their preferences. Through mutagenesis studies based on primary sequence comparison and homology modelling, I showed that phenylalanine at position 181 of anthocyanidin 3- *O*-glucoside-6″-*O*-coumaroyltransferase from Arabidopsis (At3AT) is crucial for its specificity for an aromatic acyl donor. This was shown as a complete loss of coumaroylation by At3AT as studied in tobacco. The loss of coumaroylation can be attributed to the structural change of enzyme due to replacement of Phe^{181}; a phenyl ringed aromatic amino acid to arginine; an open chained amino acid. Malonylation ability was gained by F181RAt3AT enzyme while still retaining the coumaroylation property in the recombinant protein from *E.coli*. The fact that malonylation was not observed in tobacco flowers may reflect non-optimum availability of malonyl CoA in the petal cells.

Residues interacting with the CoA moiety of the acyl donor are essential in guiding the acyl-CoA molecule in the active site of the enzyme. This conclusion was

drawn from a comparative mutagenesis study of anthocyanidin 3-*O*-glucoside-6″-*O*-malonyltransferase from chrysanthemum (Ch3MAT). Replacing Arg^{181} with Phe^{181} in Ch3MAT resulted in loss of malonylation ability of the enzyme although it retained its aliphatic acylation activity. R181FCh3MAT gained acetylation specificity and cyanidin 3-(6″ acetyl) glucoside was accumulated in tobacco along with cyanidin 3-*O*-rutinoside which is a major anthocyanin accumulated in tobacco flowers. These results showed that the CoA binding residues might have been conserved in aliphatic AATs and the ability to accept acyl moieties is determined by particular aminoacids. Site-directed mutagenesis of Ch3MAT showed that arginine at position 181 is crucial for malonylation (ie the specific recognition of malonyl-CoA). An anthocyanidin 5-*O*-glucose-6‴-*O*-malonyltransferase from Arabidopsis (At5MAT) had strict substrate specificity accepting only malonyl-CoA (Luo et al., 2007) and arginine is present near motif1 in this enzyme. So the arginine residue is responsible for malonyl-CoA specificity of AATs. Replacement of this arginine by aromatic amino acids in aliphatic AATs leads to modification of the enzyme pocket suitable for catalysis. Future site-directed mutation studies in the CoA binding region particularly the amino acids that are not conserved could add to an in-depth understanding of the determinants of acyl donor specificity.

Another important question which still needs to be addressed with respect to AATs is how their anthocyanin acceptor preferences are achieved. Although primary sequence and homology modelling studies alone cannot address this question, a crystal structure of an aromatic AAT could provide clues about their evolution. However, with the limited understanding that has emerged from the results of this study, AATs could be engineered to change the colour of flowers through genetic manipulation, thus producing novel malonylated anthocyanins.

I also studied whether aromatic and aliphatic acylation of anthocyanins can alter the function of anthocyanins in plant vacuoles. The relationship between the amount of anthocyanin and different side chain modifications in the formation of anthocyanic vacuolar inclusions (AVIs) was investigated. In nature, anthocyanins associate into globular bodies in the vacuoles of some plant species. These are known as AVIs (Markham et al., 2000). Through studies in tobacco callus over-expressing Delila and Rosea1, I showed that AVI formation is not a result of anthocyanin aggregation in a high anthocyanin environment. I also showed enhanced levels of anthocyanin accumulation controlled by Delila and Rosea1 transcription factors when the sugar levels were increased in the growth medium, but this had no effect on AVI formation.

The presence of different kinds of anthocyanidins does not have any role in AVI formation as was shown by comparison of two lines of tobacco producing cyanidin 3-*O*-rutinoside and delphinidin 3-*O*-rutinoside. It has been suggested that recruitment of anthocyanins into AVIs is influenced heavily by the degree of glycosylation of the anthocyanins, (Markham et al., 2000) although no AVIs were observed in tobacco cells producing high levels of cyanidin 3-rutinoside. By producing 5-glucosylated cyanidin 3-rutinoside in high anthocyanin tobacco I showed that presence of additional glucose does not contribute to AVI formation. I also established that AVI formation is specific to anthocyanins decorated with aromatic acyl groups. The presence of 5-glucose on cyanidin 3-(6″ coumaroyl) glucoside does not alter the degree of AVI formation.

5-glucosylation was shown to have a destabilising effect on anthocyanins at neutral pH (Luo et al., 2007). Tobacco callus producing cyanidin 3-(6″ coumaroyl) 5-diglucoside showed bigger AVIs when observed under the microscope by visual comparison with AVIs in callus producing cyanidin 3-(6″ coumaroyl) glucoside. Isolation of AVIs from 2x35S::*Del*/2x35S::*Ros*1/2x35S::*At3AT* callus showed only cyanidin 3-(6″ coumaroyl) glucoside present in these structures, underlining the importance of aromatic acylation to AVI formation. Round AVI-like structures were observed in tomato skin producing delphinidin 3-(coumaroyl) 5-glucoside; however these ‘AVIs’ could not be isolated suggesting that these globular AVIs had a different form to the ‘hard AVIs’ that could be purified from tobacco cells expressing Delila, Rosea1 and an anthocyanin aromatic acyltransferase. These ‘hard AVIs’ observed in tobacco appeared to be scattered with no particular shape, suggesting that they are not membrane bound.

VP24 protein was suggested to be associated with AVIs in sweet potato (Nozue et al., 1997). However no such association with protein was observed in AVIs that formed in tobacco (Jie Luo personal communication). It is clearly evident from these experiments that aromatic acylation can trigger AVI formation, supporting earlier observations (Conn et al., 2003). However, to date no studies had been undertaken to understand the role of aliphatic acylation in AVI formation. By producing cyanidin 3-(6″ malonyl) glucoside in a high anthocyanin environment I showed for the first time that aliphatic acylation cannot trigger AVI formation. From my experiments it is evident that aromatic acylation along with high anthocyanin accumulation are prerequisites for formation of AVIs, at least in most cells of tobacco.

The mechanisms which lead to AVI formation can be postulated having established the importance of aromatic acylation in AVI formation. Aromatic acylated anthocyanin has the property of intramolecular stacking resulting from interaction of the aromatic rings of the acyl molecules with each other (intermolecular stacking) and with the anthocyanidin ring (intramolecular stacking). Such stacking contributes to the stability of aromatic acylated anthocyanins, by avoiding degradation by nucleophillic attack. In a high anthocyanin environment it can be hypothesised that stacking is triggered by aromatic acylation and leads to AVI formation. However, hard AVIs that can be isolated from tobacco contain no non-acylated anthocyanins (although they are present in the vacuole of the tobacco cells in large amounts) suggesting that intramolecular stacking is of particular importance in AVI formation.

AVI formation could be a means of accommodating more anthocyanin in vacuoles. However, aliphatic acylated molecules without a ring structure are not involved in stacking and AVIs are not formed with aliphatic acylation of anthocyanins. Aliphatic acylation enhances the solubility of anthocyanins in water and therefore accommodates excess compound in the vacuole by a different mechanism.

I also studied the role of light and the effect of the origin of the tissues on AVI formation and showed that only the chemistry of the anthocyanins contributes significantly to AVI formation. In nature, formation of AVIs could be a method of storing particular anthocyanins and enhancing tissue pigmentation. In Lisianthus (*Eustomia grandiflora*) AVIs are formed in the dark basal region of the petals but not in the paler pigmented petal tips. Producing AVIs in ornamental plants and flowers could be a novel way of attaining bright colours for aesthetic use. Additionally, isolated AVIs could be used as an alternative to synthetic colours in yogurts, drinks and foods providing bright, natural and healthy colours with greater stability than soluble anthocyanins.

I purified four different anthocyanins from a single tobacco line with additional decorating activities; cyanidin 3-*O*-rutinoside, cyanidin 3-*O*-rutinoside 5-*O*-glucoside, cyanidin 3-*O*-(6″-coumaroyl) glucoside and cyanidin 3-*O*-(6″-coumaroyl) 5-diglucoside for use in NMR studies. A consequence of working on the formation of AVIs, with the objective of developing novel and healthy natural colours was that I realized the importance of studying anthocyanin properties in solution influenced by various decorations. I used the purified anthocyanins to study some of the properties of these differently decorated anthocyanins in solution in a quest to identify potential new

applications. The stereo chemistry and spatial arrangement of different molecules of anthocyanins and their interactions dictates their properties. In my studies the anthocyanidin ring was common in all the different anthocyanin species, so any additional properties could be attributed to the side-chain decorations. As the concentration of anthocyanins increases, self-association has been considered to be the mechanism of stabilization (Gakh et al., 1998). I studied the degradation pattern for cyanidin 3-*O*-rutinoside and cyanidin 3-*O*-glucoside at four different concentrations 50, 100, 150 and 200 μM. The degradation curve was similar for all concentrations at pH 2.6, 3, 6 and 7. This observation suggested that the flavylium cation (responsible for red colour at pH 1-2) and the quinoidal base forms (for attaining blue colour at pH 6-6.5) of anthocyanin are stable, irrespective of their concentration. At pH 4 to 5 and >7 where anthocyanins are colourless as carbinol pseudo-bases and chalcone forms, respectively, the degradation curve deviated, showing stability at higher concentrations. In such cases self association may restore stability. The anthocyanins were stable at lower pH for long periods of time irrespective of their decorations. However at neutral pH (7.0) the stability of anthocyanins depended on the number of additional groups. Acylation along with 5-glucosylation (C3(cou)5G) favoured more stability, probably due to the occurrence of both intramolecular stacking and self-association. This was followed by 5-glucosylated anthocyanins (C3R5G) where self-association of the flavylium cation contributes to stability. Significant self association has been found with anthocyanidin 3,5-diglucoside with an increase in concentration (Gakh et al., 1998, Tsutomu, 1992). However, at pH7.6 where only intramolecular stacking prevails, acylated anthocyanin (C3(cou)G) was the most stable, followed by C3R. Across the entire range of pH values, coumaroylated anthocyanin showed stability. However for visual appearance anthocyanins with 5-glucosides retained better their colour at pH 5 to 7 compared to others. Such anthocyanins might be useful in food colourants where stability over a wide range of pH is preferred.

Co-pigmentation is a phenomenon responsible for the diverse colours of anthocyanins seen at different pH conditions. This property could be very advantageous for food industry in obtaining stable natural food colourants. In co-pigmentation, inter-molecular stacking of anthocyanins and co-pigments is likely to be the mechanism of stabilization (Gakh et al., 1998). In a comparative co-pigmentation study of anthocyanins with phenolic acids and flavonols at pH 3.6, I found flavonols to be better co-pigments than phenolic acids. In flavonols, kaempferol 3-*O*-rutinoside offered a hyperchromic

effect even at a 1:25 molar ratio whereas quercetin 3-*O*-rutinoside offered a greater hypsochromic effect. So when a blue or bluer colour is desired, co-pigmentation with quercetin 3-*O*-rutinoside should be considered. When much more intense colours are required, kaempferol 3-*O*-rutinoside would be a more effective co-pigment.

Among the anthocyanins, coumaroylated anthocyanin, C3(cou)G, co-pigmented the best with kaempferol 3-*O*-rutinoside followed by cyanidin 3-rutinoside. However, the relative colour enhancement (hypochromic shift) was greater with C3R and kaempferol 3-*O*-rutinoside than with C3(cou)G and kaempferol 3-*O*-rutinoside. C3(cou)5G showed more colour enhancement with quercetin 3-*O*-rutinoside than C3(cou)G. In general, 5-glucosylation played a role in stabilising anthocyanins but had less of an effect on co-pigmentation. When co-pigmentation ability of anthocyanins with phenolic acids was compared, chlorogenic acid showed higher relative colour enhancement (hypochromic shift) followed by caffeic acid and coumaric acid. For coumaroylated anthocyanins, chorogenic acid showed the greatest degree of co-pigmentation followed by coumaric acid and then caffeic acid. Cyanidin 3-*O*-glucoside showed higher colour enhancement with chlorogenic acid compared to cyanidin 3-*O*-rutinoside.

For co-pigmentation to occur naturally several factors influence the degree of colour enhancement and colour shift (bathochromic shift). Important are the pigment to co-pigment ratios, the nature of co-pigments available, the presence of other compounds such as sugars, metals, proteins etc. These all contribute to colour development. *In-vitro* studies, of the type undertaken by me, allow to analyse the influence of individual factors and to predict the combinations that may be most effective in achieving desired colours of appropriate stability. And this study can contribute to assess the potential of anthocyanin-co-pigment combinations for use as food colours. The results from this study show how each additional decoration of an anthocyanin contributes to colour development based on intra and inter molecular interactions.

Though much is known about anthocyanins, their use for nutritional and aesthetic value is limited due to their complex behaviour in solution. Their sensitivity to changes in pH and their interaction with other metabolites can lead to change in their properties. An understanding of how their properties change with each chemical modification, affecting *in-vivo* and *in-vitro* properties can provide a clue for harnessing their useful properties. The property of anthocyanins to form AVIs can be best used for developing natural stable colours. Purified AVIs can be used to create stable and bright coloured healthy drinks, confectionary foods and yogurts. The property of AVI formation when

further investigated can be used in creating different and novel patterns in flowers. The results presented in this thesis thus offers an insight into these simple and yet complex natural pigments that could be used for benifical applications.

7 References

Abdulrazzak N, Pollet B, Ehlting Jr, Larsen K, Asnaghi C, Ronseau S, Proux C, Erhardt M, Seltzer V, Renou J-P, Ullmann P, Pauly M, Lapierre C, Werck-Reichhart Dl. 2006. A coumaroyl-ester-3-hydroxylase Insertion Mutant Reveals the Existence of Nonredundant meta-Hydroxylation Pathways and Essential Roles for Phenolic Precursors in Cell Expansion and Plant Growth. *Plant Physiology,* **140**: 30-48.

Abrahams S, Tanner GJ, Larkin PJ, Ashton AR. 2002. Identification and biochemical characterization of mutants in the proanthocyanidin pathway in Arabidopsis. *Plant Physiology,* **130**: 561-76.

Aharoni A, De Vos CH, Wein M, Sun Z, Greco R, Kroon A, Mol JN, O'Connell AP. 2001. The strawberry FaMYB1 transcription factor suppresses anthocyanin and flavonol accumulation in transgenic tobacco. *The Plant Journal,* **28**: 319-32.

Albert NW, Lewis DH, Zhang H, Schwinn KE, Jameson PE, Davies KM. 2011. Members of an R2R3-MYB transcription factor family in Petunia are developmentally and environmentally regulated to control complex floral and vegetative pigmentation patterning. *The Plant Journal,* **65**: 771-784.

Alfenito MR, Souer E, Goodman CD, Buell R, Mol J, Koes R, Walbot V. 1998. Functional complementation of anthocyanin sequestration in the vacuole by widely divergent glutathione S-transferases. *The Plant Cell,* **10**: 1135-49.

Almeida J, Carpenter R, Robbins PT, Martin C, Coen SE. 1989. Genetic interactions underlying flower color patterns in *Antirrhinum majus*. *Genes & Development,* **3**: 1758-1767.

Andersen MØ, Fossen T. 2003. Characterization of Anthocyanins by NMR. *Current Protocols in Food Analytical Chemistry* F1.4.1-F1.4.23.

Andersen ØA, Jordheim M. 2006. The anthocyanins In: Anderson O.M., Markham K.R.,. *Flavonoids, Chemistry, biochemistry and applications*: 471-530.

Asen S, Stewart RN, Norris KH. 1972. Co-pigmentation of anthocyanins in plant tissues and its effect on color. *Phytochemistry,* **11**: 1139-1144.

Bassham DC. 2007. Plant autophagy-more than a starvation response. *Current Opinion in Plant Biology,* **10**: 587-593.

Baudry A, Heim MA, Dubreucq B, Caboche M, Weisshaar B, Lepiniec L. 2004. TT2, TT8, and TTG1 synergistically specify the expression of BANYULS and proanthocyanidin biosynthesis in Arabidopsis thaliana. *The Plant Journal,* **39**: 366-80.

Bayer A, Ma XY, Stockigt J. 2004. Acetyltransfer in natural product biosynthesis - functional cloning and molecular analysis of vinorine synthase. *Bioorganic & medicinal chemistry,* **12**: 2787-2795.

Bloor SJ, Abrahams S. 2002. The structure of the major anthocyanin in Arabidopsis thaliana. *Phytochemistry,* **59**: 343-346.

Borevitz JO, Xia Y, Blount J, Dixon RA, Lamb C. 2000. Activation tagging identifies a conserved MYB regulator of phenylpropanoid biosynthesis. *The Plant Cell,* **12**: 2383-2394.

Boss PK, Davies C, Robinson SP. 1996. Expression of anthocyanin biosynthesis pathway genes in red and white grapes. *Plant Molecular Biology,* **32**: 565-569.

Bradshaw HD, Schemske DW. 2003. Allele substitution at a flower colour locus produces a pollinator shift in monkeyflowers. *Nature,* **426**: 176-178.

Brink RA. 1973. Paramutation. *Annual Review of Genetics,* **7**: 129-52.

Brouillard R. 1982. Chemical structure of anthocyanins. *In Anthocyanins as food colors (P. Markakis,Ed)*: 1-40.

Brouillard R, Dangles O. 1994. Flavonoids and flower colour. In: Harborne JB ed. *The Flavonoids: Advances in Research since 1986.* London, Chapman & Hall.

Brouillard R, Delaporte B, Dubois JE. 1978. Chemistry of anthocyanin pigments. 3. Relaxation amplitudes in pH-jump experiments. *Journal of the American Chemical Society,* **100**: 6202-6205.

Brouillard R, Dubois J-E. 1977. Mechanism of the structural transformations of anthocyanins in acidic media. *Journal of the American Chemical Society,* **99**: 1359-1364.

Burhenne K, Kristensen BK, Rasmussen SrK. 2003. A New Class of N-Hydroxycinnamoyltransferases. *Journal of Biological Chemistry,* **278**: 13919-13927.

Busso D, Delagoutte-Busso Bnd, Moras D. 2005. Construction of a set Gateway-based destination vectors for high-throughput cloning and expression screening in Escherichia coli. *Analytical Biochemistry,* **343**: 313-321.

Butelli E, Titta L, Giorgio M, Mock HP, Matros A, Peterek S, Schijlen EG, Hall RD, Bovy AG, Luo J, Martin C. 2008. Enrichment of tomato fruit with health-promoting anthocyanins by expression of select transcription factors. *Nature Biotechnology,* **26**: 1301-8.

Callebaut A, Terahara N, Decleire M. 1996. Anthocyanin acyltransferases in cell cultures of Ajuga reptans. *Plant Science,* **118**: 109-118.

Castañeda-Ovando A, Pacheco-Hernández MdL, Páez-Hernández ME, Rodríguez JA, Galán-Vidal CA. 2009. Chemical studies of anthocyanins: A review. *Food Chemistry,* **113**: 859-871.

Chiu L-W, Zhou X, Burke S, Wu X, Prior RL, Li L. 2010. The Purple Cauliflower Arises from Activation of a MYB Transcription Factor. *Plant Physiology,* **154**: 1470-1480.

Choi YH, van Spronsen J, Dai Y, Verberne M, Hollmann F, Arends IW, Witkamp GJ, Verpoorte R. 2011. Are natural deep eutectic solvents the missing link in understanding cellular metabolism and physiology? *Plant Physiology,* **156**: 1701-5.

Christie PJ, Alfenito MR, Walbot V. 1994. Impact of low-temperature stress on general phenylpropanoid and anthocyanin pathways: Enhancement of transcript abundance and anthocyanin pigmentation in maize seedlings. *Planta,* **194**: 541-549.

Conn S, Franco C, Zhang W. 2010. Characterization of anthocyanic vacuolar inclusions in *Vitis vinifera* L. cell suspension cultures. *Planta,* **231**: 1343-1360.

Conn S, Zhang W, Franco C. 2003. Anthocyanic vacuolar inclusions (AVIs) selectively bind acylated anthocyanins in *Vitis vinifera* L. (grapevine) suspension culture. *Biotechnology Letters,* **25**: 835-9.

Cooper-Driver GA. 2001. Contributions of Jeffrey Harborne and co-workers to the study of anthocyanins. *Phytochemistry,* **56**: 229-236.

Cutanda-Perez M-C, Ageorges A, Gomez C, Vialet S, Terrier N, Romieu C, Torregrosa L. 2009. Ectopic expression of VlmybA1 in grapevine activates a narrow set of genes involved in anthocyanin synthesis and transport. *Plant Molecular Biology,* **69**: 633-648.

D'Auria JC. 2006. Acyltransferases in plants: a good time to be BAHD. *Current Opinion in Plant Biology,* **9**: 331-340.

D'Auria JC, Reichelt M, Luck K, Svatos A, Gershenzon J. 2007. Identification and characterization of the BAHD acyltransferase malonyl CoA: anthocyanidin 5-O-glucoside-6″-O-malonyltransferase (At5MAT) in Arabidopsis thaliana. *FEBS Letters,* **581**: 872-8.

Dangles O, Saito N, Brouillard R. 1993. Anthocyanin intramolecular copigment effect. *Phytochemistry,* **34**: 119-124.

Davies AJ, Mazza G. 1993. Copigmentation of simple and acylated anthocyanins with colorless phenolic compounds. *Journal of Agricultural and Food Chemistry,* **41**: 716-720.

Deluc L, Barrieu F, Marchive C, Lauvergeat V, Decendit A, Richard T, Carde J-P, Mérillon J-M, Hamdi S. 2006. Characterization of a Grapevine R2R3-MYB Transcription Factor That Regulates the Phenylpropanoid Pathway. *Plant Physiology,* **140**: 499-511.

Dey PM, Harborne JB. 1993. Plant phenolics methods in plant biochemistry. *(2nd printing). London: Academic Press Limited*: 326-341.

Dooner HK, Robbins TP, Jorgensen RA. 1991. Genetic and Developmental Control of Anthocyanin Biosynthesis. *Annual Review of Genetics,* **25**: 173-199.

Downey MO, Dokoozlian NK, Krstic MP. 2006. Cultural Practice and Environmental Impacts on the Flavonoid Composition of Grapes and Wine: A Review of Recent Research. *American Journal of Enology and Viticulture,* **57**: 257-268.

Dubos C, Le Gourrierec J, Baudry A, Huep G, Lanet E, Debeaujon I, Routaboul JM, Alboresi A, Weisshaar B, Lepiniec L. 2008. MYBL2 is a new regulator of flavonoid biosynthesis in Arabidopsis thaliana. *The Plant Journal,* **55**: 940-53.

Edwards R, Gatehouse JA. 1999. Secondary metabolism. *Plant Biochemistry and Molecular Biology*: 193-218. .

Eiro MJ, Heinonen M. 2002. Anthocyanin Color Behavior and Stability during Storage: Effect of Intermolecular Copigmentation. *Journal of Agricultural and Food Chemistry,* **50**: 7461-7466.

Espley RV, Hellens RP, Putterill J, Stevenson DE, Kutty-Amma S, Allan AC. 2007. Red colouration in apple fruit is due to the activity of the MYB transcription factor, MdMYB10. *The Plant Journal,* **49**: 414-427.

Fedoroff N. 2001. How jumping genes were discovered. *Nature Structural & Molecular Biology,* **8**: 300-301.

Ferrer JL, Austin MB, Stewart Jr C, Noel JP. 2008. Structure and function of enzymes involved in the biosynthesis of phenylpropanoids. *Plant Physiology and Biochemistry,* **46**: 356-370.

Figueiredo P, George F, Tatsuzawa F, Toki K, Saito N, Brouillard R. 1999. New features of intramolecular copigmentation byacylated anthocyanins. *Phytochemistry,* **51**: 125-132.

Fleschhut J, Kratzer F, Rechkemmer G, Kulling S. 2006. Stability and biotransformation of various dietary anthocyanins *in vitro*. *European Journal of Nutrition,* **45**: 7-18.

Florigene Pty L. 2006. Inclusion of dealing with GM carnation lines, modified for flower colour, on the GMO register.

Ford CM, Boss PK, Hoj PB. 1998. Cloning and characterization of Vitis vinifera UDP-glucose:flavonoid 3-O-glucosyltransferase, a homologue of the enzyme encoded by the maize Bronze-1 locus that may primarily serve to glucosylate anthocyanidins in vivo. *Journal of Biological Chemistry,* **273**: 9224-33.

Forkmann G, Heller W, Editors-in-Chief:, Otto M-C, Sir Derek B, Koji N. 1999. Biosynthesis of Flavonoids. *Comprehensive Natural Products Chemistry.* Oxford, Pergamon.

Forkmann G, Martens S. 2001. Metabolic engineering and applications of flavonoids. *Current Opinion in Biotechnology,* **12**: 155-160.

Fournier-Level A, Hugueney P, Verries C, This P, Ageorges A. 2011. Genetic mechanisms underlying the methylation level of anthocyanins in grape (*Vitis vinifera* L.). *BMC Plant Biology,* **11**: 179.

Francis FJ, Markakis PC. 1989. Food colorants: Anthocyanins. *Critical Reviews in Food Science and Nutrition,* **28**: 273-314.

Fraser CM, Thompson MG, Shirley AM, Ralph J, Schoenherr JA, Sinlapadech T, Hall MC, Chapple C. 2007. Related Arabidopsis Serine Carboxypeptidase-Like Sinapoylglucose Acyltransferases Display Distinct But Overlapping Substrate Specificities. *Plant Physiology,* **144**: 1986-1999.

Fujiwara H, Tanaka Y, Fukui Y, Nakao M, Ashikari T, Kusumi T. 1997. Anthocyanin 5-Aromatic Acyltransferase from Gentiana Triflora. *European Journal of Biochemistry,* **249**: 45-51.

Fujiwara H, Tanaka Y, Yonekura-Sakakibara K, Fukuchi-Mizutani M, Nakao M, Fukui Y, Yamaguchi M, Ashikari T, Kusumi T. 1998. cDNA cloning, gene expression and subcellular localization of anthocyanin 5-aromatic acyltransferase from Gentiana triflora. *The Plant Journal,* **16**: 421-31.

Fukui Y, Nomoto K, Iwashita T, Masuda K, Tanaka Y, Kusumi T. 2006. Two novel blue pigments with ellagitannin moiety, rosacyanins A1 and A2, isolated from the petals of Rosa hybrida. *Tetrahedron,* **62**: 9661-9670.

Gachon CMM, Langlois-Meurinne M, Saindrenan P. 2005. Plant secondary metabolism glycosyltransferases: the emerging functional analysis. *Trends in Plant Science,* **10**: 542-549.

Gakh EG, Dougall DK, Baker DC. 1998. Proton nuclear magnetic resonance studies of monoacylated anthocyanins from the wild carrot: Part 1. Inter- and intra-molecular interactions in solution. *Phytochemical Analysis,* **9**: 28-34.

Galvano F, La Fauci L, Lazzarino G, Fogliano V, Ritieni A, Ciappellano S, Battistini NC, Tavazzi B, Galvano G. 2004. Cyanidins: metabolism and biological properties. *The Journal of nutritional biochemistry,* **15**: 2-11.

Garzon GA, Wrolstad RE. 2001. The stability of pelargonidin-based anthocyanins at varying water activity. *Food Chemistry,* **75**: 185-196.

Gauche C, Malagoli EdS, Bordignon Luiz MT. 2010. Effect of pH on the copigmentation of anthocyanins from Cabernet Sauvignon grape extracts with organic acids. *Scientia Agricola,* **67**: 41-46.

Gomez C, Conejero G, Torregrosa L, Cheynier V, Terrier N, Ageorges A. 2011. In vivo grapevine anthocyanin transport involves vesicle-mediated trafficking and the contribution of anthoMATE transporters and GST. *The Plant Journal,* **67**: 960-970.

Gomez C, Terrier N, Torregrosa L, Vialet S, Fournier-Level A, Verries C, Souquet JM, Mazauric JP, Klein M, Cheynier V, Ageorges A. 2009. Grapevine MATE-Type Proteins Act as Vacuolar H+-Dependent Acylated Anthocyanin Transporters. *Plant Physiology,* **150**: 402-415.

Gonnet JF. 2003. Origin of the color of Cv. rhapsody in blue rose and some other so-called "blue" roses. *Journal of agricultural and food chemistry,* **51**: 4990-4.

Goodman CD, Casati P, Walbot V. 2004. A multidrug resistance-associated protein involved in anthocyanin transport in Zea mays. *The Plant Cell,* **16**: 1812-26.

Goodrich J, Carpenter R, Coen ES. 1992. A common gene regulates pigmentation pattern in diverse plant species. *Cell,* **68**: 955-964.

Goto T, Kondo T. 1991. Structure and Molecular Stacking of Anthocyanins—Flower Color Variation. *Angewandte Chemie International Edition in English,* **30**: 17-33.

Goto T, Kondo T, Kawai T, Tamura H. 1984. Structure of cinerarin, a tetra-acylated anthocyanin isolated from the blue garden cineraria, Senecio cruentus. *Tetrahedron Letters,* **25**: 6021-6024.

Gray J, Caparrós-Ruiz D, Grotewold E. 2012. Grass phenylpropanoids: Regulate before using! *Plant Science,* **184**: 112-120.

Grotewold E, Davies K. 2008. Trafficking and sequestration of anthocyanins. *Natural Product Communications,* **3**: 1251-1258.

Guerineau F, Mullineaux P. 1993. Plant transformation and expression vectors *Plant Molecular Biology Labfax*: 121–147.

Gutterson NC, Napoli C, Lemieux C, Morgan A, Firoozabady E, Robinson EPK. 1994. Modification of flower color in florist's chrysanthemum: production of a white-flowering variety through molecular genetics. *Nature Biotechnology,* **12**: 268-271.

Harborne JB. 1957. Spectral methods of characterizing anthocyanins. *The Biochemical journal,* **70**: 22-28.

Harborne JB. 1986. Nature, distribution and function of plant flavonoids. *Progress in Clinical & Biological Research,* **213**: 15-24.

Harborne JB. 1988. Flavonoids in the environment: structure-activity relationships. *Progress in Clinical & Biological Research,* **280**: 17-27.

Harborne JB, Grayer RJ. 1988. The anthocyanins. *In The Flavonoids: Advances in Research since 1980*: 1-20.

Harborne JB, Williams CA. 2000. Advances in flavonoid research since 1992. *Phytochemistry,* **55**: 481-504.

Hause B, Meyer K, Viitanen P, Chapple C, Strack D. 2002. Immunolocalization of 1-O-sinapoylglucose: malate sinapoyltransferase in Arabidopsis thaliana. *Planta,* **215**: 26-32.

Heller W, Forkmann G. 1994. Biosynthesis of Flavonoids. In: Harborne JB ed. *The Flavonoids: Advances in Research since 1986.* London, Chapman and Hall.

Herrmann KM. 1995. The Shikimate Pathway as an Entry to Aromatic Secondary Metabolism. *Plant Physiology,* **107**: 7-12.

Holton TA, Brugliera F, Lester DR, Tanaka Y, Hyland CD, Menting JGT, Lu C-Y, Farcy E, Stevenson TW, Cornish EC. 1993a. Cloning and expression of cytochrome P450 genes controlling flower colour. *Nature,* **366**: 276-279.

Holton TA, Brugliera F, Tanaka Y. 1993b. Cloning and expression of flavonol synthase from Petunia hybrida. *The Plant Journal,* **4**: 1003-1010.

Honda T, Saito N. 2002. Recent progress in the chemistry of polyacylated anthocyanins as flower color pigments. *Heterocycles,* **56**: 633-692.

Hopp W, Seitz HU. 1987. The uptake of acylated anthocyanin into isolated vacuoles from a cell suspension culture of *Daucus carota*. *Planta,* **170**: 74-85.

Horsch RB, Fry JE, Hoffmann NL, Eichholtz D, Rogers SG, Fraley RT. 1985. A simple and general method for transferring genes into plants. *Science,* **227**: 1229-1231.

Hrazdina G, Wagner GJ. 1985. Metabolic pathways as enzyme complexes: Evidence for the synthesis of phenylpropanoids and flavonoids on membrane associated enzyme complexes. *Archives of Biochemistry and Biophysics,* **237**: 88-100.

Hugo DK, Oliver NE. 1977. Genetic control of UDPglucose:flavonol 3-O-glucosyltransferase in the endosperm of maize. *Biochemical Genetics,* **15**: 509-519.

Hugueney P, Provenzano S, Verries C, Ferrandino A, Meudec E, Batelli G, Merdinoglu D, Cheynier V, Schubert A, Ageorges A. 2009. A novel cation-dependent O-methyltransferase involved in anthocyanin methylation in grapevine. *Plant Physiology,* **150**: 2057-70.

Ino I, Nishiyama H, Yamaguchi M-a. 1993. Malonylation of anthocyanins by extracts of flower buds in Dendranthema morifolium cultivars. *Phytochemistry,* **32**: 1425-1426.

Ino I, Yamaguchi M-A. 1993. Acetyl-coenzyme A: Anthocyanidin 3-glucoside acetyltransferase from flowers of Zinnia elegans. *Phytochemistry,* **33**: 1415-1417.

Irani N, Grotewold E. 2005. Light-induced morphological alteration in anthocyanin-accumulating vacuoles of maize cells. *BMC Plant Biology,* **5**: 7.

Irani NG, Hernandez JM, Grotewold E. 2003. Regulation of anthocyanin pigmentation. *Recent Advances in Phytochemistry,* **38**: 59 - 78.

Ito F, Tanaka N, Katsuki A, Fujii T. 2002. Why do flavylium salts show so various colors in solution? - Effect of concentration and water on the flavylium's color changes. *Journal of Photochemistry and Photobiology A: Chemistry,* **150**: 153-157.

Jackson D, Culianez-Macia F, Prescott AG, Roberts K, Martin C. 1991. Expression patterns of myb genes from Antirrhinum flowers. *The Plant Cell,* **3**: 115-25.

Jackson D, Roberts K, Martin C. 1992. Temporal and spatial control of expression of anthocyanin biosynthetic genes in developing flowers of *Antirrhinum majus*. *The Plant Journal,* **2**: 425-434.

Jang YP, Zhou J, Nakanishi K, Sparrow JR. 2005. Anthocyanins protect against A2E photooxidation and membrane permeabilization in retinal pigment epithelial cells. *Photochemistry and photobiology,* **81**: 529-36.

Jasik J, Vancova B. 1992. Cytological study of anthocyanin production in grapevine (*Vitis vinifera* L.) callus cultures. *Acta Botanica Hungarica,* **37**: 251-259.

Johnson ET, Ryu S, Yi H, Shin B, Cheong H, Choi G. 2001. Alteration of a single amino acid changes the substrate specificity of dihydroflavonol 4-reductase. *The Plant Journal,* **25**: 325-333.

Jones P, Vogt T. 2001. Glycosyltransferases in secondary plant metabolism: tranquilizers and stimulant controllers. *Planta,* **213**: 164-174.

Jonsson LMV, Donker-Koopman WE, Uitslager P, Schram AW. 1983. Subcellular Localization of Anthocyanin Methyltransferase in Flowers of Petunia hybrida. *Plant Physiology,* **72**: 287-290.

Jorgensen K, Rasmussen AV, Morant M, Nielsen AH, Bjarnholt N, Zagrobelny M, Bak S, Moller BL. 2005. Metabolon formation and metabolic channeling in the biosynthesis of plant natural products. *Current Opinion in Plant Biology,* **8**: 280-291.

Kamsteeg J, Van Brederode J, Hommels CH, Van Nigtevecht G. 1980. Identification, properties and genetic control of hydroxycinnamoyl-coenzyme A: Anthocyanidin. 3-rhamnosyl (1- 6) glucoside, 4´-hydroxycinnamoyl transfersae isolated from petals of *Silene dioica*. *Biochemie und Physiologie der Pflanzen,* **175**: 403-411.

Katsumoto Y, Fukuchi-Mizutani M, Fukui Y, Brugliera F, Holton TA, Karan M, Nakamura N, Yonekura-Sakakibara K, Togami J, Pigeaire A, Tao GQ, Nehra NS, Lu CY, Dyson BK, Tsuda S, Ashikari T, Kusumi T, Mason JG, Tanaka Y. 2007. Engineering of the rose flavonoid biosynthetic pathway successfully generated blue-hued flowers accumulating delphinidin. *Plant and Cell Physiology,* **48**: 1589-1600.

Kitamura S. 2006. Transport of flavonoids:from cytosolic synthesis to vacuolar accumulation. *In The Science of Flavonoids*: 123 - 146.

Kitamura S, Shikazono N, Tanaka A. 2004. TRANSPARENT TESTA 19 is involved in the accumulation of both anthocyanins and proanthocyanidins in Arabidopsis. *The Plant Journal,* **37**: 104 - 114.

Kliebenstein DJ, Kroymann J, Mitchell-Olds T. 2005. The glucosinolate myrosinase system in an ecological and evolutionary context. *Current Opinion in Plant Biology,* **8**: 264-271.

Konczak I, Zhang W. 2004. Anthocyanins-More Than Nature's Colours. *Journal of Biomedicine & Biotechnology,* **2004**: 239-240.

Kondo T, Ueda M, Goto T. 1990. Structure of ternatin B1, a pentaacylated anthocyanin substituted on the B-ring asymmetrically with two long chains. *Tetrahedron,* **46**: 4749-4756.

Kuc J. 1995. Phytoalexins, Stress Metabolism, and Disease Resistance in Plants. *Annual Review of Phytopathology,* **33**: 275-297.

Kurtin WE, Song P-S. 1968. Electronic structures and spectra of some natural products of theoretical interest: Molecular orbital studies of anthocyanidins. *Tetrahedron,* **24**: 2255-2267.

Li J, Ou-Lee TM, Raba R, Amundson RG, Last RL. 1993. Arabidopsis Flavonoid Mutants Are Hypersensitive to UV-B Irradiation. *The Plant Cell,* **5**: 171-179.

Lin-Wang KUI, Micheletti D, Palmer J, Volz R, Lozano L, Espley R, Hellens RP, Chagnè D, Rowan DD, Troggio M, Iglesias I, Allan AC. 2011. High temperature reduces apple fruit colour via modulation of the anthocyanin regulatory complex. *Plant Cell & Environment,* **34**: 1176-1190.

Lloyd JC, Zakhleniuk OV. 2004. Responses of primary and secondary metabolism to sugar accumulation revealed by microarray expression analysis of the Arabidopsis mutant, pho3. *Journal of Experimental Botany,* **55**: 1221-1230.

Lucker J, Martens S, Lund ST. 2010. Characterization of a Vitis vinifera cv. Cabernet Sauvignon 3',5'-O-methyltransferase showing strong preference for anthocyanins and glycosylated flavonols. *Phytochemistry,* **71**: 1474-84.

Ludwig SR, Wessler SR. 1990. Maize R gene family: Tissue-specific helix-loop-helix proteins. *Cell,* **62**: 849-851.

Luo J, Butelli E, Hill L, Parr A, Niggeweg R, Bailey P, Weisshaar B, Martin C. 2008. AtMYB12 regulates caffeoyl quinic acid and flavonol synthesis in tomato: expression in fruit results in very high levels of both types of polyphenol. *The Plant Journal,* **56**: 316-326.

Luo J, Fuell C, Parr A, Hill L, Bailey P, Elliott K, Fairhurst SA, Martin C, Michael AJ. 2009. A novel polyamine acyltransferase responsible for the accumulation of spermidine conjugates in Arabidopsis seed. *The Plant Cell,* **21**: 318-33.

Luo J, Nishiyama Y, Fuell C, Taguchi G, Elliott K, Hill L, Tanaka Y, Kitayama M, Yamazaki M, Bailey P, Parr A, Michael AJ, Saito K, Martin C. 2007. Convergent evolution in the BAHD family of acyl transferases: identification and characterization of anthocyanin acyl transferases from Arabidopsis thaliana. *The Plant Journal,* **50**: 678-695.

Ma XY, Koepke J, Panjikar S, Fritzsch G, Stockigt J. 2005. Crystal structure of vinorine synthase, the first representative of the BAHD superfamily. *Journal of Biological Chemistry,* **280**: 13576-13583.

Marinova K, Pourcel L, Weder B, Schwarz M, Barron D, Routaboul JM, Debeaujon I, Klein M. 2007. The Arabidopsis MATE transporter TT12 acts as a vacuolar flavonoid/H+ -antiporter active in proanthocyanidin-accumulating cells of the seed coat. *The Plant Cell,* **19**: 2023-38.

Markham KR, Gould KS, Winefield CS, Mitchell KA, Bloor SJ, Boase MR. 2000. Anthocyanic vacuolar inclusions-their nature and significance in flower colouration. *Phytochemistry,* **55**: 327-36.

Marrs KA, Alfenito MR, Lloyd AM, Walbot V. 1995. A glutathione S-transferase involved in vacuolar transfer encoded by the maize gene Bronze-2. *Nature,* **375**: 397-400.

Martin C, Paz-Ares J. 1997. MYB transcription factors in plants. *Trends in Genetics,* **13**: 67-73.

Martin C, Prescott A, Mackay S, Bartlett J, Vrijlandt E. 1991. Control of anthocyanin biosynthesis in flowers of *Antirrhinum majus*. *The Plant Journal,* **1**: 37-49.

Matsuba Y, Sasaki N, Tera M, Okamura M, Abe Y, Okamoto E, Nakamura H, Funabashi H, Takatsu M, Saito M, Matsuoka H, Nagasawa K, Ozeki Y. 2010. A Novel Glucosylation Reaction on Anthocyanins Catalyzed by Acyl-Glucose-Dependent Glucosyltransferase in the Petals of Carnation and Delphinium. *The Plant Cell,* **22**: 3374-3389.

Matsufuji H, Otsuki T, Takeda T, Chino M, Takeda M. 2003. Identification of Reaction Products of Acylated Anthocyanins from Red Radish with Peroxyl Radicals. *Journal of Agricultural and Food Chemistry,* **51**: 3157-3161.

Matsui K, Umemura Y, Ohme-Takagi M. 2008. AtMYBL2, a protein with a single MYB domain, acts as a negative regulator of anthocyanin biosynthesis in Arabidopsis. *The Plant Journal,* **55**: 954-67.

Matus J, Poupin M, Cañón P, Bordeu E, Alcalde J, Arce-Johnson P. 2010. Isolation of WDR and bHLH genes related to flavonoid synthesis in grapevine (*Vitis vinifera* L.). *Plant Molecular Biology,* **72**: 607-620.

Mazza G, Brouillard R. 1990. The mechanism of co-pigmentation of anthocyanins in aqueous solutions. *Phytochemistry,* **29**: 1097-1102.

Mazza G, E.Miniati. 1993. Anthocyanins in Fruits, Vegetables and Grains. *Molecular Nutrition and Food Research,* **38**: 343.

McClintock B. 1950. The origin and behavior of mutable loci in maize. *Proceedigs of the National Academy of Sciences,* **36**: 344-55.

McIlvaine TC. 1921. A buffer solution for colorimetric comparision. *Journal of Biological Chemistry,* **49**: 183-186.

Mendel G. 1895. Verhandlungen des Naturforschenden Vereins in. *Brunn,* **4**.

Milkowski C, Strack D. 2004. Serine carboxypeptidase-like acyltransferases. *Phytochemistry,* **65**: 517-524.

Mizuno H, Hirano K, Okamoto G. 2006. Effect of anthocyanin composition in grape skin on anthocyanic vacuolar inclusion development and skin coloration. *Vitis,* **45**: 173-177.

Mol J, Grotewold E, Koes R. 1998. How genes paint flowers and seeds. *Trends in plant science,* **3**: 212-217.

Molish H. 1905. *Bot. Zeitung,,* **63**: 145-162

Mooney M, Desnos T, Harrison K, Jones J, Carpenter R, Coen E. 1995. Altered regulation of tomato and tobacco pigmentation genes caused by the delila gene of Antirrhinum. *The Plant Journal,* **7**: 333-339.

Moyer RA, Hummer KE, Finn CE, Frei B, Wrolstad RE. 2002. Anthocyanins, phenolics, and antioxidant capacity in diverse small fruits: vaccinium, rubus, and ribes. *Journal of agricultural and food chemistry,* **50**: 519-25.

Mueller LA, Goodman CD, Silady RA, Walbot V. 2000. AN9, a petunia glutathione S-transferase required for anthocyanin sequestration, is a flavonoid-binding protein. *Plant Physiology,* **123**: 1561-70.

Nakaishi H, Matsumoto H, Tominaga S, Hirayama M. 2000. Effects of black current anthocyanoside intake on dark adaptation and VDT work-induced transient refractive alteration in healthy humans. *Alternative medicine review,* **5**: 553-62.

Nakatsuka T, Haruta KS, Pitaksutheepong C, Abe Y, Kakizaki Y, Yamamoto K, Shimada N, Yamamura S, Nishihara M. 2008. Identification and Characterization of R2R3-MYB and bHLH Transcription Factors Regulating Anthocyanin Biosynthesis in Gentian Flowers. *Plant and Cell Physiology,* **49**: 1818-1829.

Nakayama T, Suzuki H, Nishino T. 2003. Anthocyanin acyltransferases: specificities, mechanism, phylogenetics, and applications. *Journal of Molecular Catalysis B: Enzymatic,* **23**: 117-132.

Napoli C, Lemieux C, Jorgensen R. 1990. Introduction of a Chimeric Chalcone Synthase Gene into Petunia Results in Reversible Co-Suppression of Homologous Genes in trans. *The Plant Cell,* **2**: 279-289.

Nerdal W, Andersen ØM. 1992. Intermolecular aromatic acid association of an anthocyanin (petanin) evidenced by two-dimensional nuclear overhauser enhancement nuclear magnetic resonance experiments and distance geometry calculations. *Phytochemical Analysis,* **3**: 182-189.

Nozue M, Kubo H, Nishimura M, Katou A, Hattori C, Usuda N, Nagata T, Yasuda H. 1993. Characterization of Intravacuolar Pigmented Structures in Anthocyanin-Containing Cells of Sweet-Potato Suspension-Cultures. *Plant and Cell Physiology,* **34**: 803 - 808.

Nozue M, Yamada K, Nakamura T, Kubo H, Kondo M, Nishimura M. 1997. Expression of a vacuolar protein (VP24) in anthocyanin-producing cells of sweet potato in suspension culture. *Plant Physiology,* **115**: 1065-72.

Nozzolillo C, Ishikura N. 1988. An investigation of the intracellular site of anthocyanoplasts using isolated protoplasts and vacuoles. *Plant Cell Reports,* **7**: 389 - 392.

OllÉ D, Guiraud JL, Souquet JM, Terrier N, Ageorges A, Cheynier V, Verries C. 2011. Effect of pre- and post-veraison water deficit on proanthocyanidin and anthocyanin accumulation during Shiraz berry development. *Australian Journal of Grape and Wine Research,* **17**: 90-100.

Ono E, Fukuchi-Mizutani M, Nakamura N, Fukui Y, Yonekura-Sakakibara K, Yamaguchi M, Nakayama T, Tanaka T, Kusumi T, Tanaka Y. 2006. Yellow flowers generated by expression of the aurone biosynthetic pathway. *Proceedings of the National Academy of Sciences,* **103**: 11075-11080.

Pauling L. 1939. Recent work on the configuration and electronic structure of molecules. *Fortschritte der Chemie Organischer Naturstoffe,* **3**: 203–235.

Paz-Ares J, Ghosal D, Wienand U, Peterson PA, Saedler H. 1987. The regulatory c1 locus of *Zea mays* encodes a protein with homology to myb proto-oncogene products and with structural similarities to transcriptional activators. *EMBO Journal,* **6**: 3553-8.

Pecket RC, Small CJ. 1980. Occurrence, location and development of anthocyanoplasts. *Phytochemistry,* **19**: 2571 - 2576.

Pichersky E, Noel JP, Dudareva N. 2006. Biosynthesis of Plant Volatiles: Nature's Diversity and Ingenuity. *Science,* **311**: 808-811.

Pourcel L, Irani NG, Lu Y, Riedl K, Schwartz S, Grotewold E. 2010. The Formation of Anthocyanic Vacuolar Inclusions in Arabidopsis thaliana and Implications for the Sequestration of Anthocyanin Pigments. *Molecular Plant,* **3**: 78-90.

Poustka F, Irani NG, Feller A, Lu Y, Pourcel L, Frame K, Grotewold E. 2007. A trafficking pathway for anthocyanins overlaps with the endoplasmic reticulum-to-vacuole protein-sorting route in Arabidopsis and contributes to the formation of vacuolar inclusions. *Plant Physiology,* **145**: 1323-35.

Procissi A, Dolfini S, Ronchi A, Tonelli C. 1997. Light-Dependent Spatial and Temporal Expression of Pigment Regulatory Genes in Developing Maize Seeds. *The Plant Cell,* **9**: 1547-1557.

Quattrocchio F, Verweij W, Kroon A, Spelt C, Mol J, Koes R. 2006. PH4 of Petunia is an R2R3 MYB protein that activates vacuolar acidification through interactions with basic-helix-loop-helix transcription factors of the anthocyanin pathway. *The Plant Cell,* **18**: 1274-91.

Quattrocchio F, Wing JF, Va K, De, Woude, Mol JNM, Koes R. 1998. Analysis of bHLH and MYB domain proteins: species-specific regulatory differences are caused by divergent evolution of target anthocyanin genes. *The Plant Journal,* **13**: 475-488.

Rechner AR, Kroner C. 2005. Anthocyanins and colonic metabolites of dietary polyphenols inhibit platelet function. *Thrombosis research,* **116**: 327-34.

Robinson GM, Robinson R. 1931. A survey of anthocyanins. I. *Biochemical Journal,* **25**: 1687-705.

Rodriguez-Saona LE, Wrolstad RE. 2001. Extraction, Isolation, and Purification of Anthocyanins. *Current Protocols in Food Analytical Chemistry*. John Wiley & Sons, Inc.

Rolland F, Baena-Gonzalez E, Sheen J. 2006. Sugar sensing and signaling in plants: conserved and novel mechanisms. *Annual Review of Plant Biology,* **57**: 675-709.

Ronchi A, Petroni K, Tonelli C. 1995. The reduced expression of endogenous duplications (REED) in the maize R gene family is mediated by DNA methylation. *EMBO Journal,* **14**: 5318-28.

Rowan DD, Cao M, Lin-Wang K, Cooney JM, Jensen DJ, Austin PT, Hunt MB, Norling C, Hellens RP, Schaffer RJ, Allan AC. 2009. Environmental regulation of leaf colour in red 35S:PAP1 Arabidopsis thaliana. *The New phytologist,* **182**: 102-15.

Saito N, Tatsuzawa F, Miyoshi K, Shigihara A, Honda T. 2003. The first isolation of C-glycosylanthocyanin from the flowers of *Tricyrtis formosana*. *Tetrahedron Letters,* **44**: 6821-6823.

Saito N, Toki K, Honda T, Kawase K. 1988. Cyanidin 3-malonylglucuronylglucoside in Bellis and cyanidin 3-malonylglucoside in Dendranthema. *Phytochemistry,* **27**: 2963-2966.

Sambrook J, Russell DW. 2001. Molecular cloning : a laboratory manual. *Cold Spring Harbor, N.Y : Cold Spring Harbor Laboratory,* **3rd. ed**.

Sarma AD, Sharma R. 1999. Anthocyanin-DNA copigmentation complex: mutual protection against oxidative damage. *Phytochemistry,* **52**: 1313-1318.

Sarni P, Fulcrand H, Souillol V, Souquet J-M, Cheynier V. 1995. Mechanisms of anthocyanin degradation in grape must-like model solutions. *Journal of the Science of Food and Agriculture,* **69**: 385-391.

Schijlen EG, Ric de Vos CH, van Tunen AJ, Bovy AG. 2004. Modification of flavonoid biosynthesis in crop plants. *Phytochemistry,* **65**: 2631-48.

Schoch G, Morant M, Abdulrazzak N, Asnaghi C, Goepfert S, Petersen M, Ullmann P, Werck-Reichhart D, le. 2006. The meta-hydroxylation step in the phenylpropanoid pathway: a new level of complexity in the pathway and its regulation. *Environmental Chemistry Letters,* **4**: 127-136.

Schwinn K, Venail J, Shang Y, Mackay S, Alm V, Butelli E, Oyama R, Bailey P, Davies K, Martin C. 2006. A Small Family of MYB-Regulatory Genes Controls Floral Pigmentation Intensity and Patterning in the Genus Antirrhinum. *The Plant Cell,* **18**: 831-851.

Shang Y, Venail J, Mackay S, Bailey PC, Schwinn KE, Jameson PE, Martin CR, Davies KM. 2011. The molecular basis for venation patterning of pigmentation and its effect on pollinator attraction in flowers of Antirrhinum. *New Phytologist,* **189**: 602-15.

Shaw WV, Leslie AG. 1991. Chloramphenicol acetyltransferase. *Annual Review of Biophysics and Biophysical Chemistry,* **20**: 363-86.

Solfanelli C, Poggi A, Loreti E, Alpi A, Perata P. 2006. Sucrose-specific induction of the anthocyanin biosynthetic pathway in Arabidopsis. *Plant Physiology,* **140**: 637-46.

Spelt C, Quattrocchio F, Mol JN, Koes R. 2000. Anthocyanin1 of petunia encodes a basic helix-loop-helix protein that directly activates transcription of structural anthocyanin genes. *The Plant Cell,* **12**: 1619-32.

Springob K, Nakajima J-i, Yamazaki M, Saito K. 2003. Recent advances in the biosynthesis and accumulation of anthocyanins. *Natural Product Reports,* **20**: 288-303.

Stintzing FC, Stintzing AS, Carle R, Frei B, Wrolstad RE. 2002. Color and antioxidant properties of cyanidin-based anthocyanin pigments. *Journal of agricultural and food chemistry,* **50**: 6172-81.

Strack D, Wray V. 1994. The anthocyanins. *In The Flavonoids: Advances in Research Since 1986,* **J.B. Harborne, ed. Chapman and Hall**.

Strack D, Wray V, Metzger JrW, Grosse W. 1992. Two anthocyanins acylated with gallic acid from the leaves of Victoria amazonica. *Phytochemistry,* **31**: 989-991.

Sun J, Cao X, Bai w, Liao X, Hu X. 2010. Comparative analyses of copigmentation of cyanidin 3-glucoside and cyanidin 3-sophoroside from red raspberry fruits. *Food Chemistry,* **120**: 1131-1137.

Sun Y, Li H, Huang J-R. 2011. Arabidopsis TT19 Functions as a Carrier to Transport Anthocyanin from the Cytosol to Tonoplasts. *Molecular Plant,* **5**: 387-400.

Suzuki H, Nakayama T, Nishino T. 2003a. Proposed mechanism and functional amino acid residues of malonyl-CoA : anthocyanin 5-O-glucoside-6 ‴-O-malonyltransferase from flowers of Salvia splendens, a member of the versatile plant acyltransferase family. *Biochemistry,* **42**: 1764-1771.

Suzuki H, Nakayama T, Yamaguchi MA, Nishino T. 2004a. cDNA cloning and characterization of two Dendranthema x morifolium anthocyanin malonyltransferases with different functional activities. *Plant Science,* **166**: 89-96.

Suzuki H, Nakayama T, Yonekura-Sakakibara K, Fukui Y, Nakamura N, Nakao M, Tanaka Y, Yamaguchi M, Kusumi T, Nishino T. 2001. Malonyl-CoA : anthocyanin 5-O-glucoside-6 '''-O-malonyltransferase from scarlet sage (*Salvia splendens*) flowers - Enzyme purification, gene cloning, expression, and characterization. *Journal of Biological Chemistry,* **276**: 49013-49019.

Suzuki H, Nakayama T, Yonekura-Sakakibara K, Fukui Y, Nakamura N, Yamaguchi M, Tanaka Y, Kusumi T, Nishino T. 2002. cDNA cloning, heterologous expressions, and functional characterization of malonyl-coenzyme A : anthocyanidin 3-O-glucoside-6 "-O-malonyltransferase from dahlia flowers. *Plant Physiology,* **130**: 2142-2151.

Suzuki H, Nishino T, Nakayama T. 2007. cDNA cloning of a BAHD acyltransferase from soybean (*Glycine max*): Isoflavone 7-O-glucoside-6"-O-malonyltransferase. *Phytochemistry,* **68**: 2035-2042.

Suzuki H, Sawada S, Watanabe K, Nagae S, Yamaguchi M, Nakayama T, Nishino T. 2004b. Identification and characterization of a novel anthocyanin malonyltransferase from scarlet sage (*Salvia splendens*) flowers: an enzyme that is phylogenetically separated from other anthocyanin acyltransferases. *The Plant Journal,* **38**: 994-1003.

Suzuki H, Sawada S, Yonekurasakakibara K, Nakayama T, Yamaguchi M-a, Nishino T. 2003b. ldentification of a cDNA Encoding Malonyl CoenZymeA: Anthocyanidin 3-O-Glucoside 6"-O-Malonyltransferase from Cineraria (*Senecio cruentus*) Flowers. *Plant Biotechnology,* **20**: 229-234.

Takos AM, Jaffe FW, Jacob SR, Bogs J, Robinson SP, Walker AR. 2006. Light-Induced Expression of a MYB Gene Regulates Anthocyanin Biosynthesis in Red Apples. *Plant Physiology,* **142**: 1216-1232.

Tanaka Y, Brugliera F. 2007. Flower Colour: Flowering and its Manipulation. *Annual Plant Reviews* Blackwell Publishing Ltd.

Tanaka Y, Yonekura K, Fukuchi-Mizutani M, Fukui Y, Fujiwara H, Ashikari T, Kusumi T. 1996. Molecular and biochemical characterization of three anthocyanin synthetic enzymes from *Gentiana triflora*. *Plant Cell Physiology,* **37**: 711-6.

Taylor LP, Grotewold E. 2005. Flavonoids as developmental regulators. *Current Opinion in Plant Biology,* **8**: 317-323.

Teng S, Keurentjes J, Bentsink L, Koornneef M, Smeekens S. 2005. Sucrose-specific induction of anthocyanin biosynthesis in Arabidopsis requires the MYB75/PAP1 gene. *Plant Physiology,* **139**: 1840-52.

Teusch M, Forkmann G. 1987. Malonyl-coenzyme A: Anthocyanidin 3-glucoside malonyltransferase from flowers of *Callistephus chinensis*. *Phytochemistry,* **26**: 2181-2183.

Teusch M, Forkmann G, Seyffert W. 1987. Genetic control of hydroxycinnamoyl-coenzyme a: Anthocyanidin 3-glycoside-hydroxycinnamoyltransferase from petals of *Matthiola incana*. *Phytochemistry,* **26**: 991-994.

Timberlake CF, Bridle P. 1966. Spectral studies of anthocyanin and anthocyanidin equilibria in aqueous solution. *Nature,* **212**: 158-9.

Timberlake CF, Bridle P. 1975. The anthocyanins. *The flavonoids, Harborne, J.B., Mabry,H.(eds),* **Chapman and Hall, London**.

Tohge T, Nishiyama Y, Hirai MY, Yano M, Nakajima J-i, Awazuhara M, Inoue E, Takahashi H, Goodenowe DB, Kitayama M, Noji M, Yamazaki M, Saito K. 2005. Functional genomics by integrated analysis of metabolome and transcriptome of

Arabidopsis plants over-expressing an MYB transcription factor. *The Plant Journal,* **42**: 218-235.

Tsutomu H. 1992. Self-association of flavylium cations of anthocyanidin 3,5-diglucosides studied by circular dichroism and 1H NMR. *Phytochemistry,* **31**: 647-653.

Unno H, Ichimaida F, Suzuki H, Takahashi S, Tanaka Y, Saito A, Nishino T, Kusunoki M, Nakayama T. 2007. Structural and mutational studies of anthocyanin malonyltransferases establish the features of BAHD enzyme catalysis. *The Journal of biological chemistry,* **282**: 15812-22.

Verweij W, Spelt C, Di Sansebastiano G-P, Vermeer J, Reale L, Ferranti F, Koes R, Quattrocchio F. 2008. An H+ P-ATPase on the tonoplast determines vacuolar pH and flower colour. *Nature Cell Biology,* **10**: 1456-1462.

Vetten Nd, Quattrocchio F, Mol J, Koes R. 1997. The an11 locus controlling flower pigmentation in petunia encodes a novel WD-repeat protein conserved in yeast, plants, and animals. *Genes and Development,* **11**: 1422-1434.

Vogt T. 2010. Phenylpropanoid Biosynthesis. *Molecular Plant,* **3**: 2-20.

Vom Endt Db, Kijne JW, Memelink J. 2002. Transcription factors controlling plant secondary metabolism: what regulates the regulators? *Phytochemistry,* **61**: 107-114.

Wade HK, Sohal AK, Jenkins GI. 2003. Arabidopsis ICX1 Is a Negative Regulator of Several Pathways Regulating Flavonoid Biosynthesis Genes. *Plant Physiology,* **131**: 707-715.

Wajant H, Mundry K-W, Pfizenmaier K. 1994. Molecular cloning of hydroxynitrile lyase from *Sorghum bicolor* (L.). Homologies to serine carboxypeptidases. *Plant Molecular Biology,* **26**: 735-746.

Walker AR, Davison PA, Bolognesi-Winfield AC, James CM, Srinivasan N, Blundell TL, Esch JJ, Marks MD, Gray JC. 1999. The TRANSPARENT TESTA GLABRA1 Locus, Which Regulates Trichome Differentiation and Anthocyanin Biosynthesis in Arabidopsis, Encodes a WD40 Repeat Protein. *The Plant Cell,* **11**: 1337-1349.

Wang J, Pichersky E. 1999. Identification of specific residues involved in substrate discrimination in two plant O-methyltransferases. *Archives of Biochemistry & Biophysics,* **368**: 172-80.

Weisshaar B, Jenkins GI. 1998. Phenylpropanoid biosynthesis and its regulation. *Current Opinion in Plant Biology,* **1**: 251-257.

Willstätter R, Everest AE. 1913. Untersuchungen über die Anthocyane. I. Über den Farbstoff der Kornblume. *Justus Liebigs Annalen der Chemie,* **401**: 189-232.

Willstätter R, Zollinger EH. 1916. Uber die Farbstoffe der Weintraube und der Heidelbeere, II. *Justus Liebigs Annalen der Chemie,* **412**: 195-216.

Winkel-Shirley B. 1999. Evidence for enzyme complexes in the phenylpropanoid and flavonoid pathways. *Physiologia Plantarum,* **107**: 142-149.

Winkel-Shirley B. 2001. It Takes a Garden. How Work on Diverse Plant Species Has Contributed to an Understanding of Flavonoid Metabolism. *Plant Physiology,* **127**: 1399-1404.

Winkel BSJ. 2004. Metabolic channeling in plants. *Annual Review of Plant Biology,* **55**: 85-107.

Yamaguchi MA, Maki T, Kawanobu S, Ino I. 1996. Cyanidin 3-malonylglucoside and malonyl-coenzyme A: anthocyanidin malonyltransferase in *Lactuca sativa* leaves. *Phytochemistry,* **42**: 661-663.

Yamaguchi MA, Maki T, Ohishi T, Ino I. 1995. Succinyl-coenzyme A: anthocyanidin 3-glucoside succinyltransferase in flowers of *Centaurea cyanus*. *Phytochemistry,* **39**: 311-313.

Yamaguchi MA, Oshida N, Nakayama M, Koshioka M, Yamaguchi Y, Ino I. 1999. Anthocyanidin 3-glucoside malonyltransferase from *Dahlia variabilis*. *Phytochemistry,* **52**: 15-18.

Yamazaki M, Gong Z, Fukuchi-Mizutani M, Fukui Y, Tanaka Y, Kusumi T, Saito K. 1999. Molecular cloning and biochemical characterization of a novel anthocyanin 5-O-glucosyltransferase by mRNA differential display for plant forms regarding anthocyanin. *Journal of Biological Chemistry,* **274**: 7405-11.

Yamazaki M, Yamagishi E, Gong Z, Fukuchi-Mizutani M, Fukui Y, Tanaka Y, Kusumi T, Yamaguchi M, Saito K. 2002. Two flavonoid glucosyltransferases from *Petunia*

hybrida: molecular cloning, biochemical properties and developmentally regulated expression. *Plant Molecular Biology,* **48**: 401-11.

Yasuda H, Kumagai T. 1984. Electron microscopic observations on the anthocyanoplasts in the radish seedlings. *Proceedings of the Annual Meeting 24th Symposium, Japaneese Society of Plant Physiology,* **206**: 1.

Yonekura-Sakakibara K, Tanaka Y, Fukuchi-Mizutani M, Fujiwara H, Fukui Y, Ashikari T, Murakami Y, Yamaguchi M, Kusumi T. 2000. Molecular and biochemical characterization of a novel hydroxycinnamoyl-CoA: Anthocyanin 3-O-glucoside-6 "-O-acyltransferase from *Perilla frutescens*. *Plant and Cell Physiology,* **41**: 495-502.

Yoshida K, Kitahara S, Ito D, Kondo T. 2006. Ferric ions involved in the flower color development of the Himalayan blue poppy, *Meconopsis grandis*. *Phytochemistry,* **67**: 992-998.

Yoshida K, Kondo T, Goto T. 1992. Intramolecular stacking conformation of gentiodelphin, a diacylated anthocyanin from *Gentiana makinoi*. *Tetrahedron,* **48**: 4313-4326.

Yoshida K, Mori M, Kondo T. 2009. Blue flower color development by anthocyanins: from chemical structure to cell physiology. *Natural Product Reports,* **26**: 884-915.

Zhang H, Wang L, Deroles S, Bennett R, Davies K. 2006. New insight into the structures and formation of anthocyanic vacuolar inclusions in flower petals. *BMC plant biology,* **6**: 29.

Zhao J, Dixon RA. 2009. The 'ins' and 'outs' of flavonoid transport. *Trends in Plant Science,* **15**: 72-80.

Zimmermann IM, Heim MA, Weisshaar B, Uhrig JF. 2004. Comprehensive identification of *Arabidopsis thaliana* MYB transcription factors interacting with R/B-like BHLH proteins. *The Plant Journal,* **40**: 22-34.

APPENDIX

Chapter III related

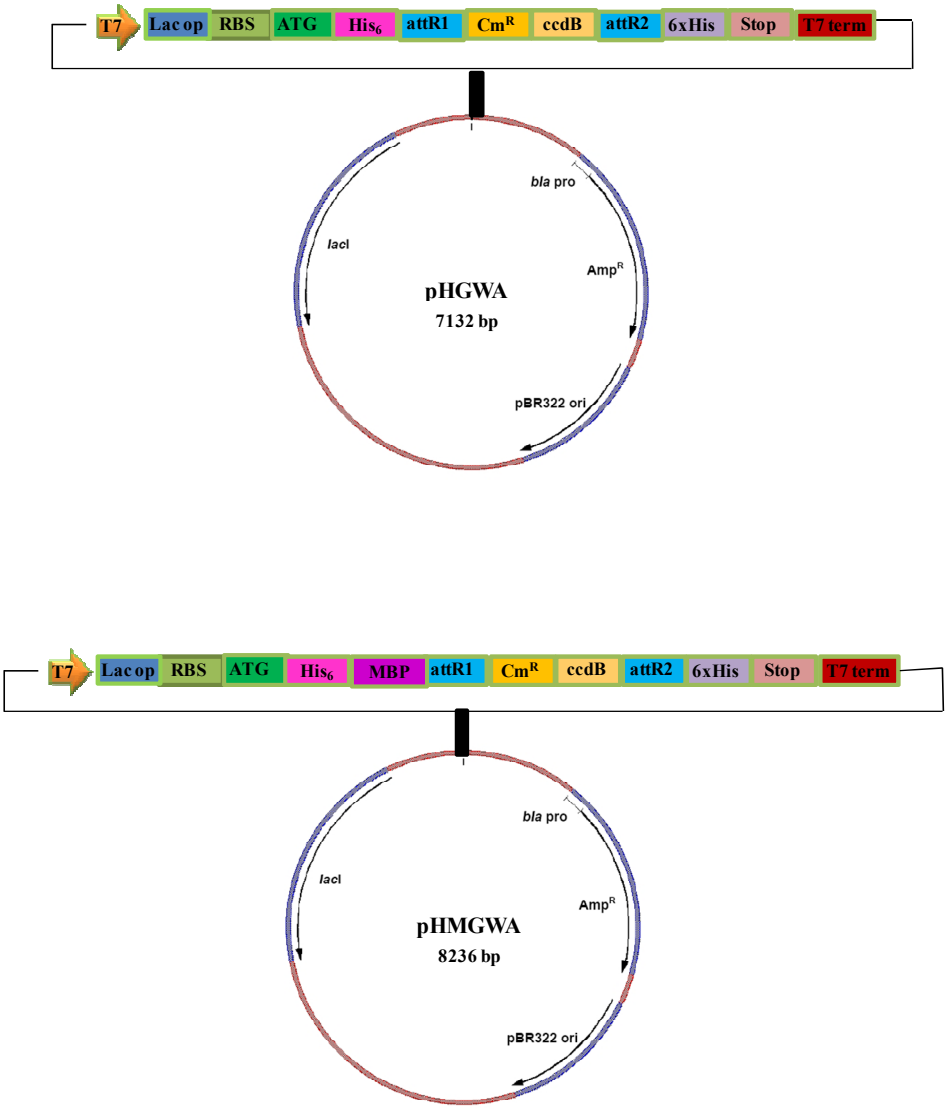

Figure 3a.i | Map showing vector features of pHGWA and pHMGWA used to construct *E.coli* expression vectors of *Sl3AT*, *At3AT* and *Gt5AT*. T7; T7 promoter, Lac op; lac operator, RBS; ribosome binding site, ATG; translation start site, MBP; maltose binding protein tag, attR1 and attR2; Gateway recombinant sites, CmR; chloramphenicol resistance gene, ccdB; lethal gene that targets DNA gyrase, 6xHis; six histidine tag, Stop; stop codon, T7 term; T7 terminator, bla pro; bla promoter, Amp^R; ampicillin resistance gene, pBR322 ori; pBR322 origin, lac*I*; lac*I* encoding sequence.

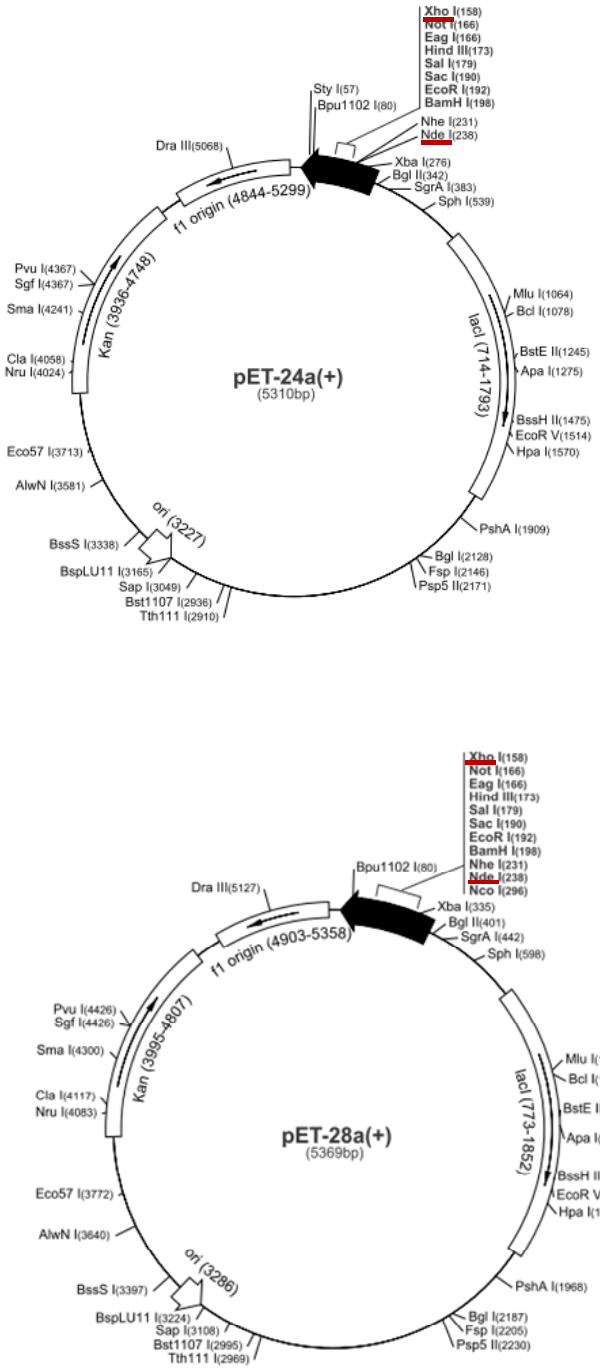

Figure 3a.ii | Map showing vector features of pET-24a and pET-28a used to construct *E.coli* expression vectors of *Sl3AT*, *At3AT* and *Gt5AT*. Map of pET-28b used for cloning is same as pET-28a. LacI; lac operator, kan; kanamycin resistance, ori; pBR322 origin, selected restriction enzyme sites are shown.

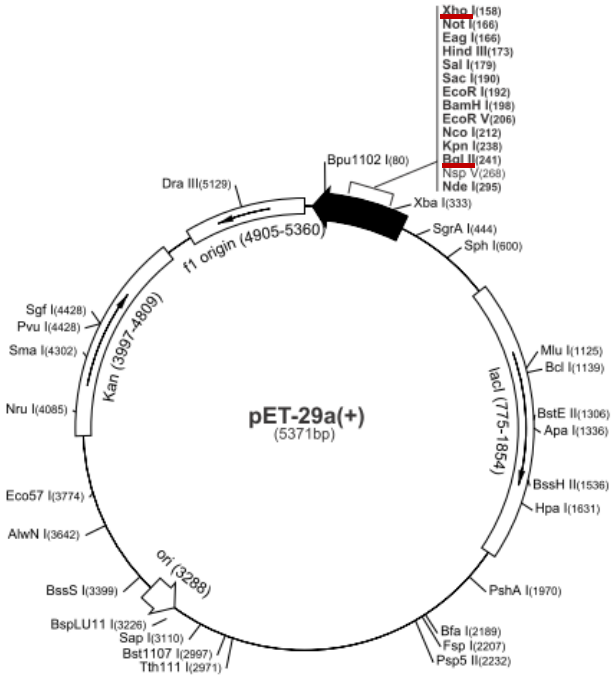

Figure 3b | Map showing vector features of pET-29a used to construct *E.coli* expression vectors of *Sl3AT*, *At3AT* and *Ch3MAT*. LacI; lac operator, kan; kanamycin resistance, ori; pBR322 origin, selected restriction sites are shown.

Table 3a | Sequences of all the primers used for cloning and sequencing

Primer name	Primer sequence
Sl24aF	5’ GGAATTCCATATGAGCCAAATTACAACACA 3’
Sl24aR	5’ CCGCTCGAGCTTTGGCACATAACTAAACT 3’
Sl21aR	5’ CCGCTCGAGCTACTTTGGCACATAACTAAACT 3’
B1 F	5’ GGGGACAAGTTTGTACAAAAAAGCAGGCTGGATGAGCC AAATTACAACACAAAA 3’
B2 R	5’ GGGGACCACTTTGTACAAGAAAGCTGGGTCCTACTACTTT GGCACATAACTA 3’
B1tevSAT	5’ GGGGACAAGTTTGTACAAAAAAGCAGGCTGGGAAAATCTG TACTTTCAGGGCATGAGCCAAATTACAACACAAA 3’
B2SAT	5’GGGGACCACTTTGTACAAGAAAGCTGGGTCCTTTGGCACAT AACTAAACTC 3’
Sl998F	5’CAGAATTACATGAAATTGTAACCTTA 3’
Sl242R	5’ CTTGGTTAGAACTTCAGACA 3’
Sl804R	5’ GTCACAACTTCAACTCTTGATGAA 3’
28GatF	5’ GGAATTCCATATGATGGAACAA ATTCAGATGGTT 3’

28GatNS R	5’ CCGCTCGAGTTAGCTCAGGCTGCAAAAG 3’
B1GAT	5’ GGGGACAAGTTTGTACAAAAAAGCAGGCTGGATGGA ACAAATTCAGATGGTTAA 3’
B2GAT’	5’ GGGGACCACTTTGTACAAGAAAGCTGGGTCTTAGCTC AGGCTGCAAAAGC 3’
B1tevGAT	5’ GGGGACAAGTTTGTACAAAAAAGCAGGCTGGGAAAAT CTGTACTTTCAGGGCATGGAACAAATTCAGATGGTTAA 3’
B2GAT	5’ GGGGACCACTTTGTACAAGAAAGCTGGGTCGCTCAGGCT GCAAAAGCCT 3’
GAT651F	5’GATCTGTATGGCCTGGAAGAA 3’
GAT1051F	5’ GTTGGTGATAAAGGTCTGCTG 3’
GAT851R	5’ GGTCCAAACATAACCACAGGT 3’
GAT251R	5’ CACCGCTTTTAATCGGCATCA 3’
At24aF	5’ GGAATTCCATATGGAAAATCTGTACTTTCAGGGCATGGT GGCTCATCTTCAACCT 3’
At24aR	5’ CCGCTCGAGCGTTGCGAATTTCTTGATCCC 3’
AtATsR	5’ CCGCTCGAGCTACGTTGCGAATTTCTTGATC 3’
B1AAT	5’ GGGGACAAGTTTGTACAAAAAAGCAGGCTGGATGGTGG CTCATCTTCAACCT 3’
B1tevAAT	5’ GGGGACAAGTTTGTACAAAAAAGCAGGCTGGGAAAATC TGTACTTTCAGGGCATGGTGGCTCATCTTCAACCT3’
B2AAT	5’ GGGGACCACTTTGTACAAGAAAGCTGGGTCCGTTGCGAAT TTCTTGATCCC 3’
B2AATs	5’ GGGGACCACTTTGTACAAGAAAGCTGGGTCCTACGTTGCG AATTTCTTGATC 3’
ArAcSF	5’ GGAGTACGTAAATGGGTCATG 3’
ArAcSR1	5’ GTTTCACTGTCTTGTACAAGTG 3’
ArAcSR2	5’ GCCATCGTTGTAGTGTAAATATGG 3’
ArAcS F2	5' ACGGTTCTTCTACCCTCTCTGCCT 3'
174HsatN F	5’ GCGCTAGCCGTGCAAATTGTCAACACAACAGGTGATGGA TTCTC3’
174HsatN R	5’ GAGAATCCATCACCTGTTGTGTTGACAATTTGCACGGCTA GCGC 3’
SAT29aFnew	5’ GAAGATCTGATGAGCCAAATTACAACACA 3’
181FsatR F	5’ GTCCACACAACAGGTGATGGACGTTCTGGCTGCGCGATC ACCGAT 3’
181FsatR R	5’ ATCGGTGATCGCGCAGCCAGAACGTCCATCACCTGTTGT GTGGAC 3’
AAt29Fnew	5’ GAAGATCTGATGGTGGCTCATCTTCAACCT 3’
AtF181Rf	5’ GTTGTAGCAGATGGAGTCACCCGCAGTCATTTCATGAAGT ATTG 3’
AtF181Rr	5’ CAATACTTCATGAAATGACTGCGGGTGACTCCATCTG CTACAAC 3’
CMat29Fnew	5’ GAAGATCTGATGGCTTCCAATTCCATTGTTAC 3’
C3MaR	5’ CCGCTCGAGTTATATCTCACTCTCTAATCCGTG 3’
ChR183Ff	5’ GCCTAGGTGACGCTAGCACATTCCTTGGTTTTTTGAAGGC GTGG 3’
ChR183Fr	5’ CCACGCCTTCAAAAAACCAAGGAATGTGCTAGCGTCACC TAGGC 3’

Figure 3c | Characteristics of the anthocyanin products obtained in enzyme catalysed reactions of wild type and mutated proteins of At3AT and Ch3MAT as studied through ESI-LC-MS

Fig 3c.1 | C3Gcou-29vector

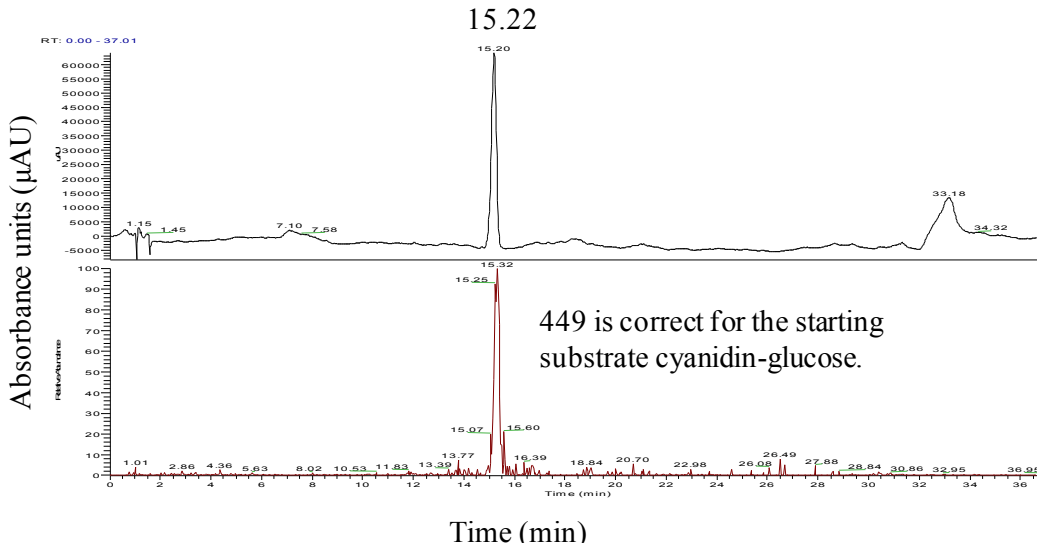

Fig 3c. 2 | At3AT-C3Gcou

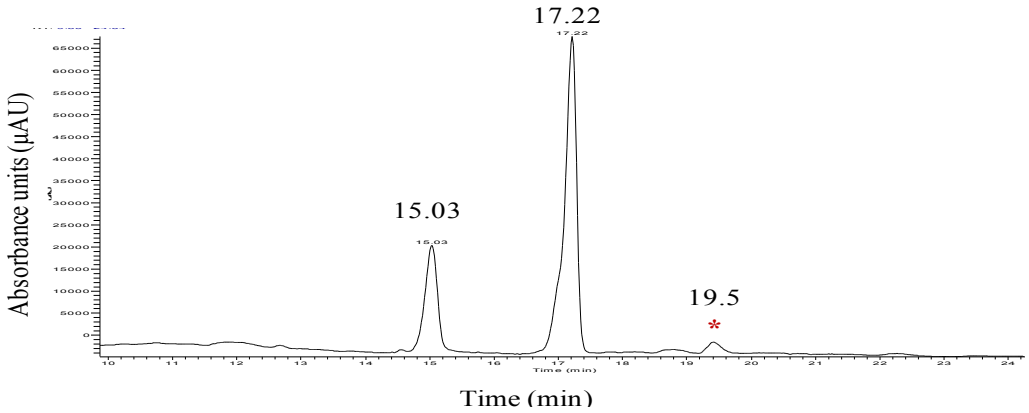

MS of product at 19.5 min correspond to Cyanidin 3-(6″ coumaroyl) glucoside

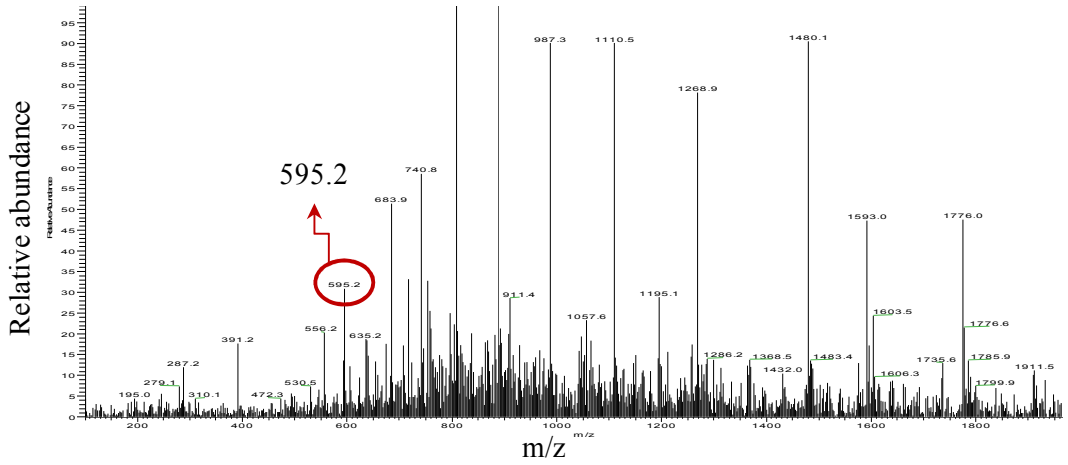

Full MS of averaged spectra (top) and MS of product at 17.22 min.

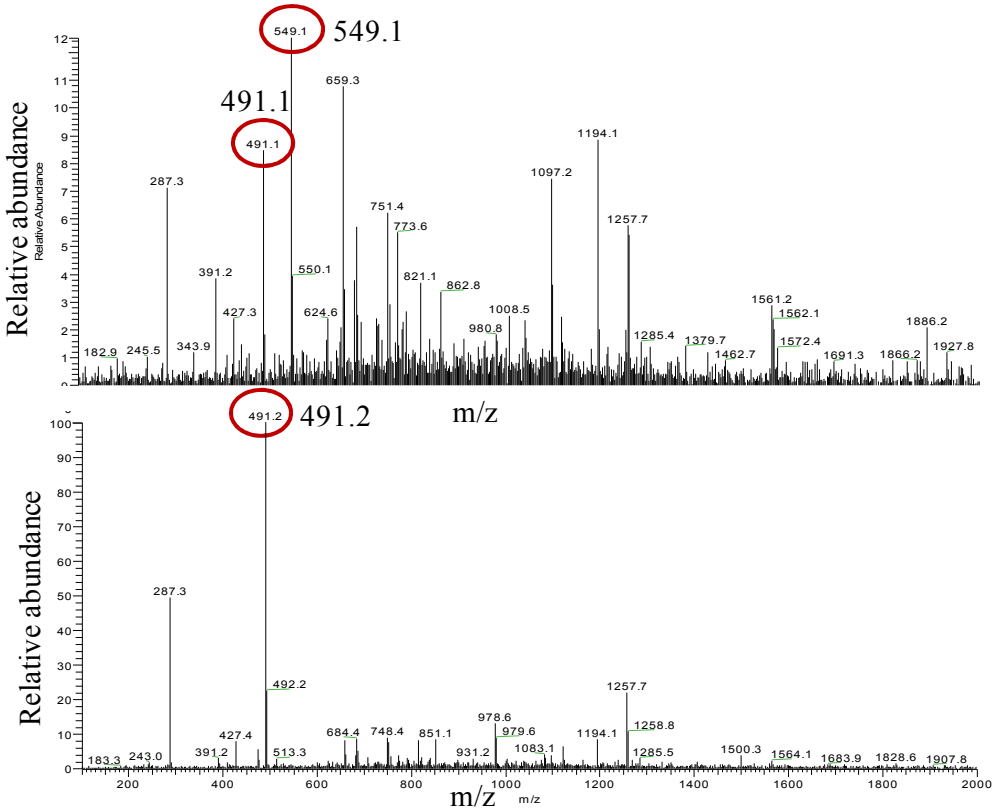

MS2 spectra of 549 and 449 indicates presence of cyanidin (m/z 287); hence addition of sodium fluoroacetate (m/z 100) and acetate respectively to cyanidin 3-*O*-glucoside was predicted.

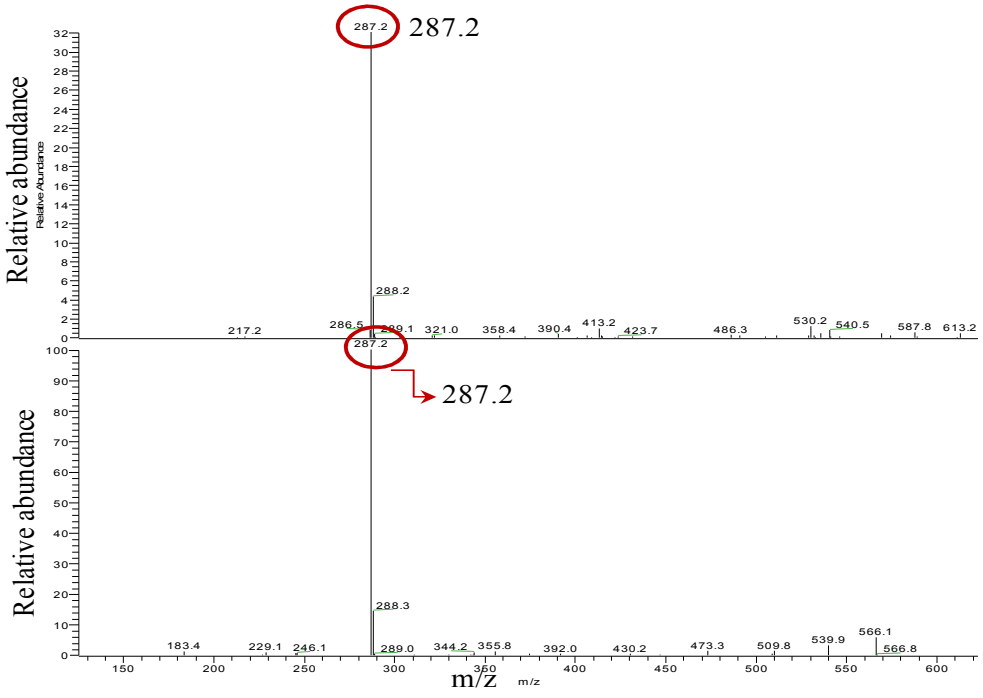

Fig 3c. 3 | At3AT-C3GMal

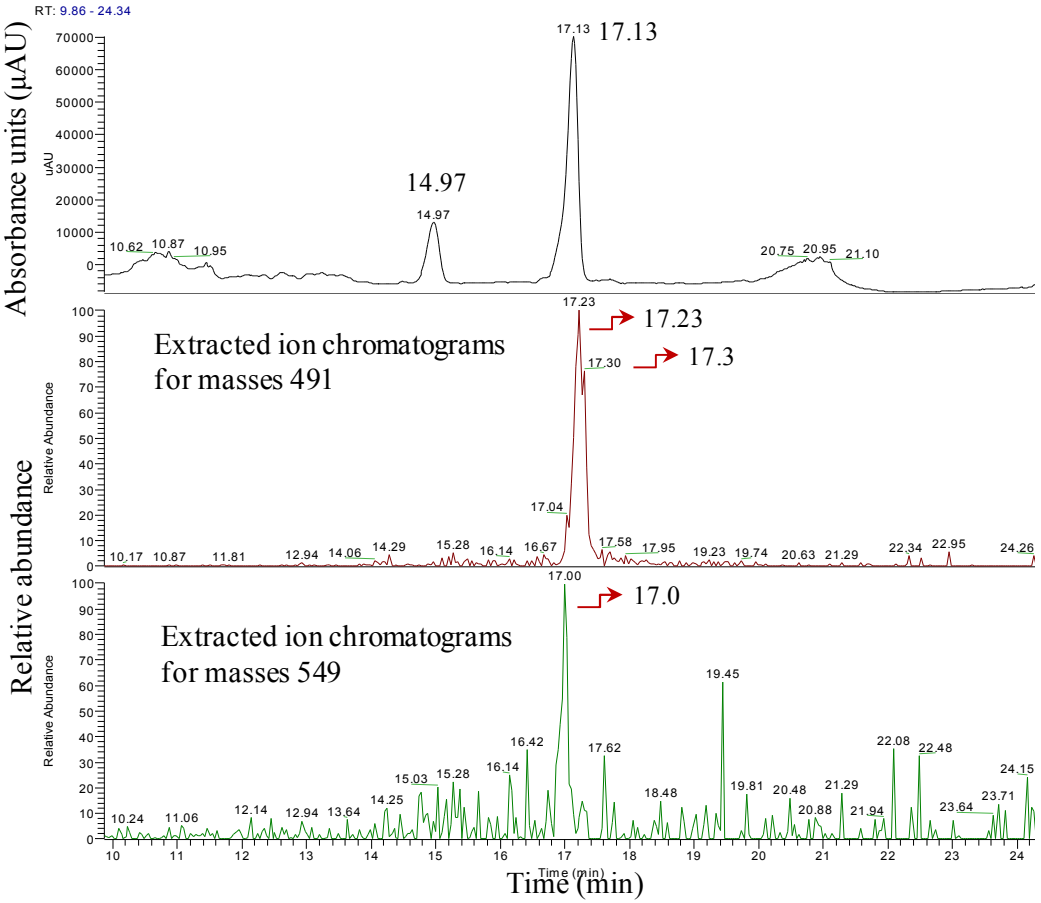

Fig 3c.4 | F181R-At3AT- C3Gcou

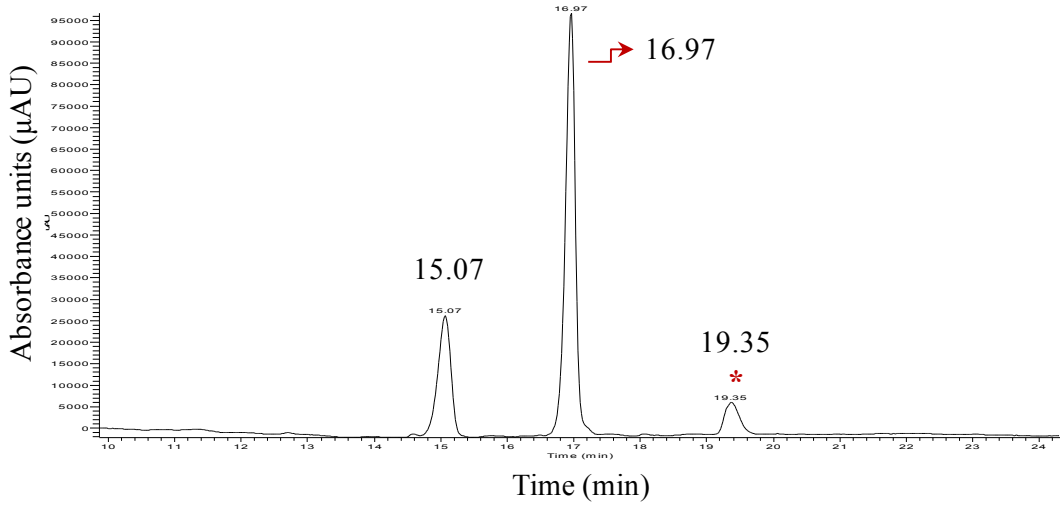

MS of product at 16.97 min

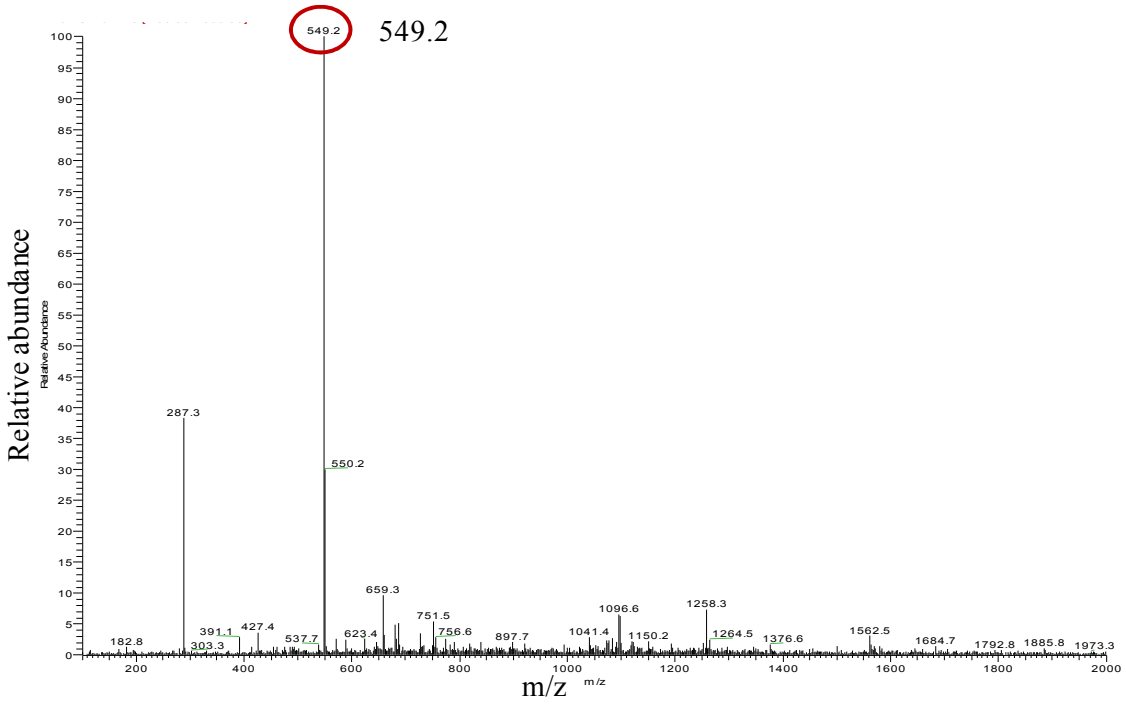

MS of product at 19.35 min correspond to Cyanidin 3-(6″ coumaroyl) glucoside

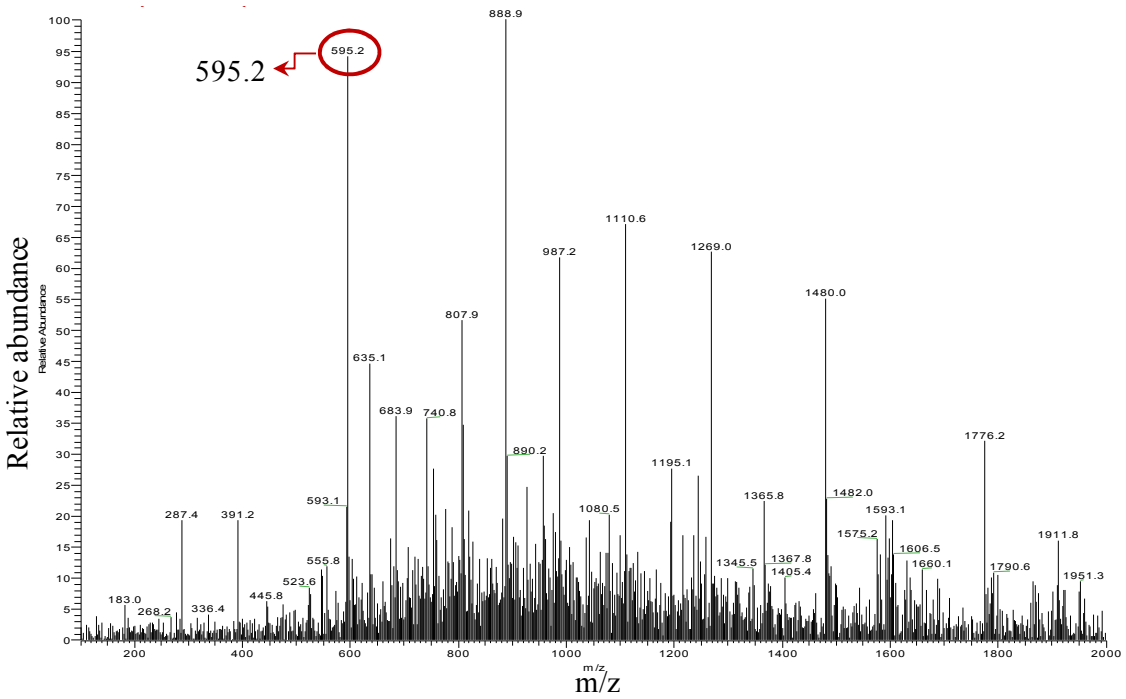

Fig 3c. 5 | F181R-At3AT- C3GMal

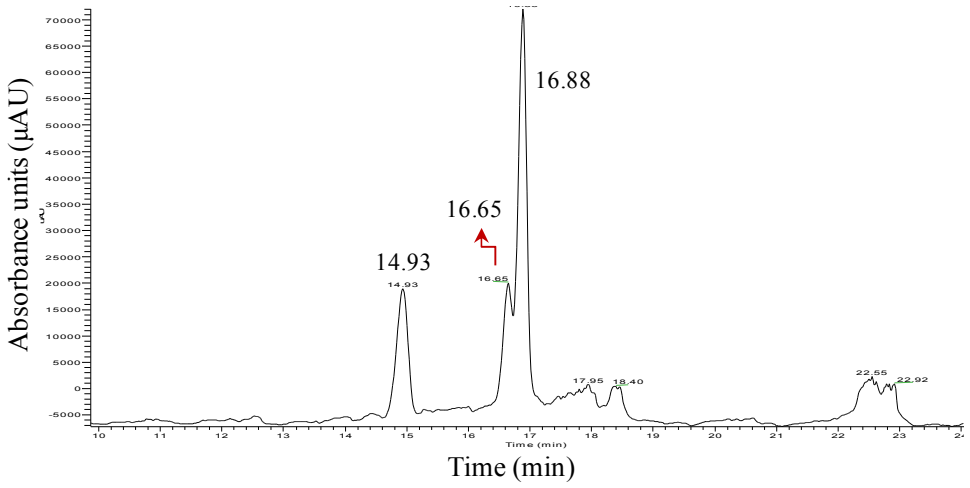

MS of product at 16.65 min correspond to Cyanidin 3-(6″ malonyl) glucoside (m/z 535.2)

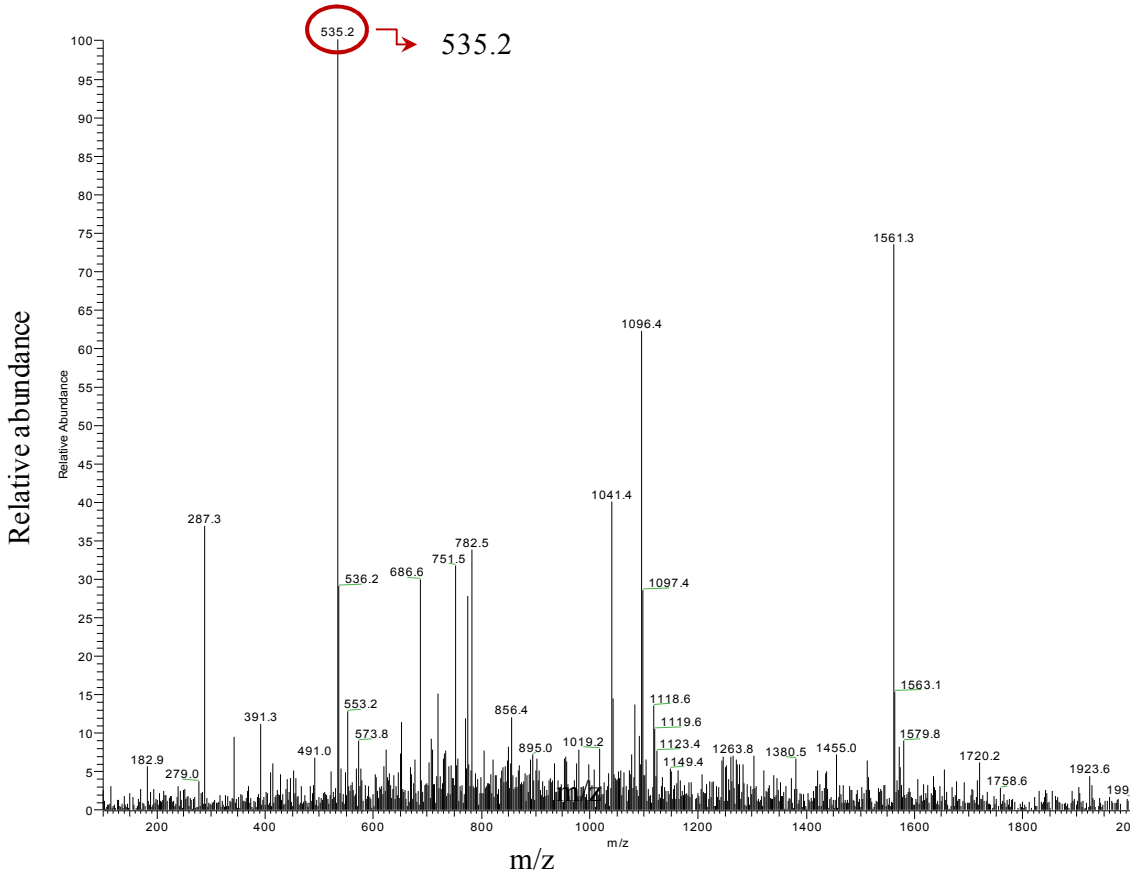

MS2 of product at 16.65 min shows the presence of cyanidin 3-*O*-glucoside (m/z 449.2) and cyanidin (m/z 287)

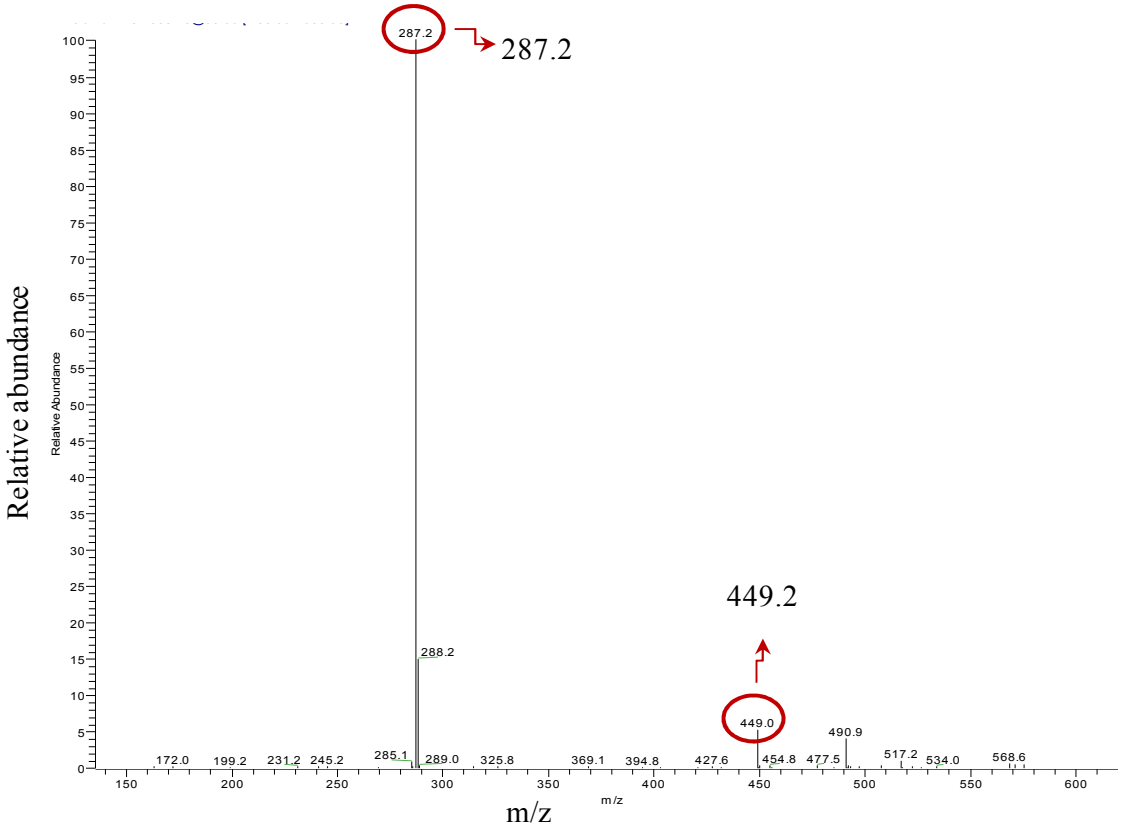

MS of product at 16.88 min

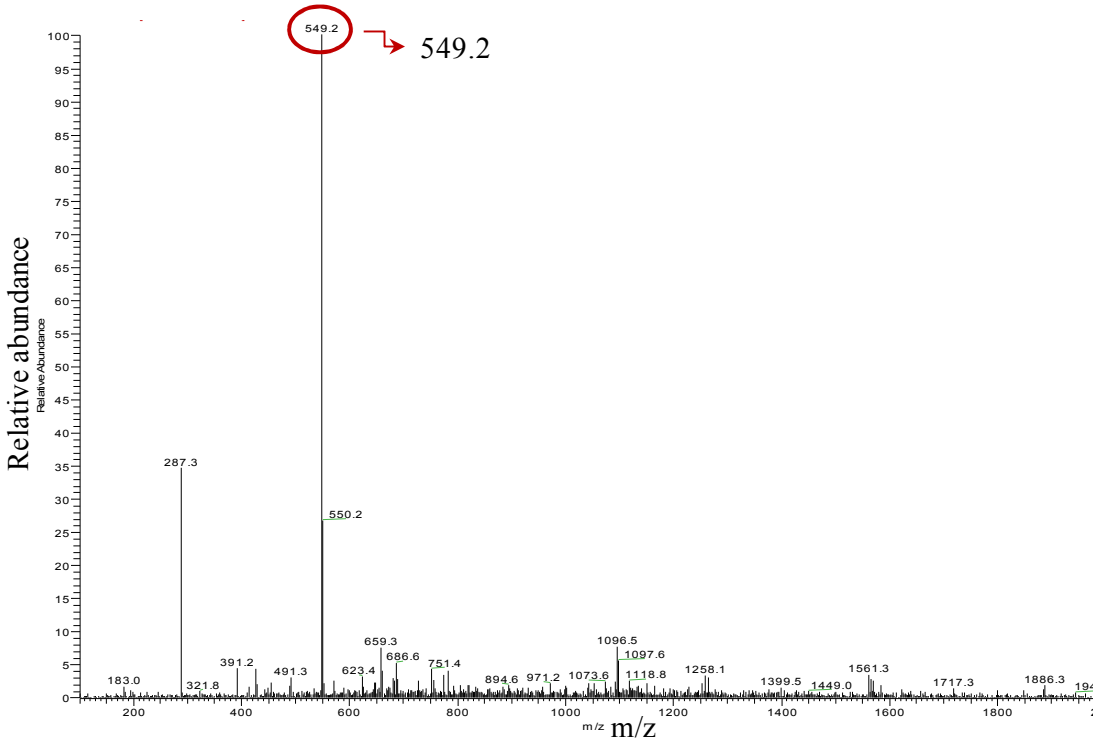

Fig 3c.6 | C3Gmal-29vector

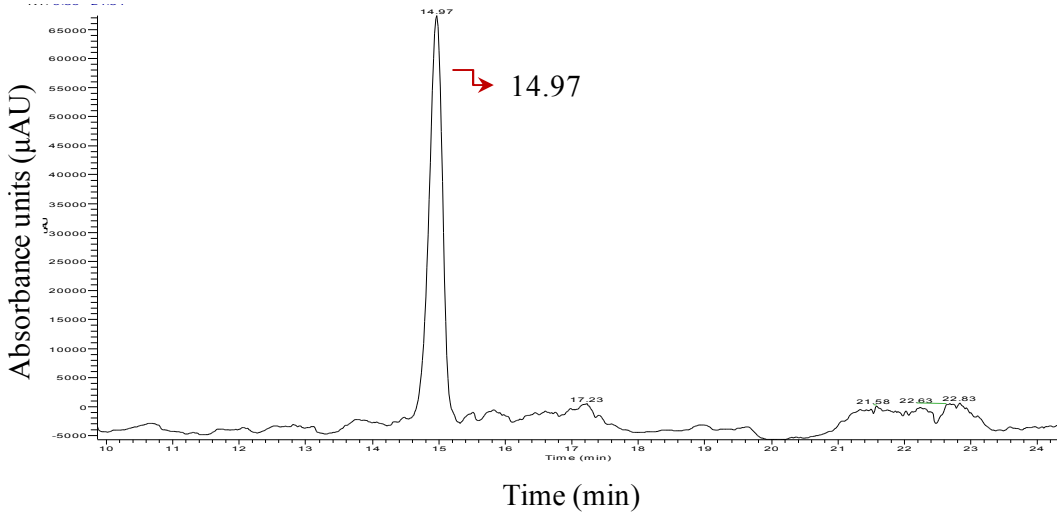

Fig 3c.7 | Ch3MAT- C3GMal

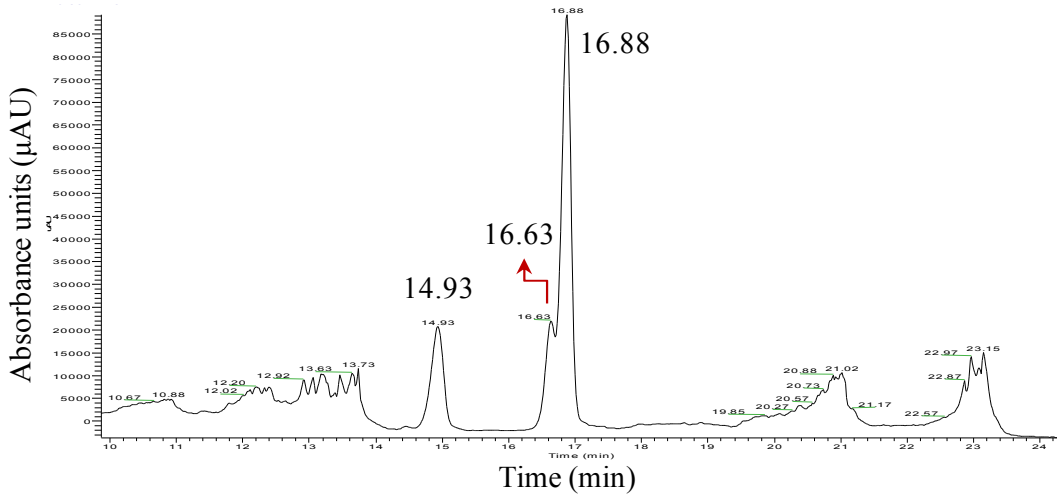

MS of product at 16.63 min correspond to Cyanidin 3-(6″ malonyl) glucoside

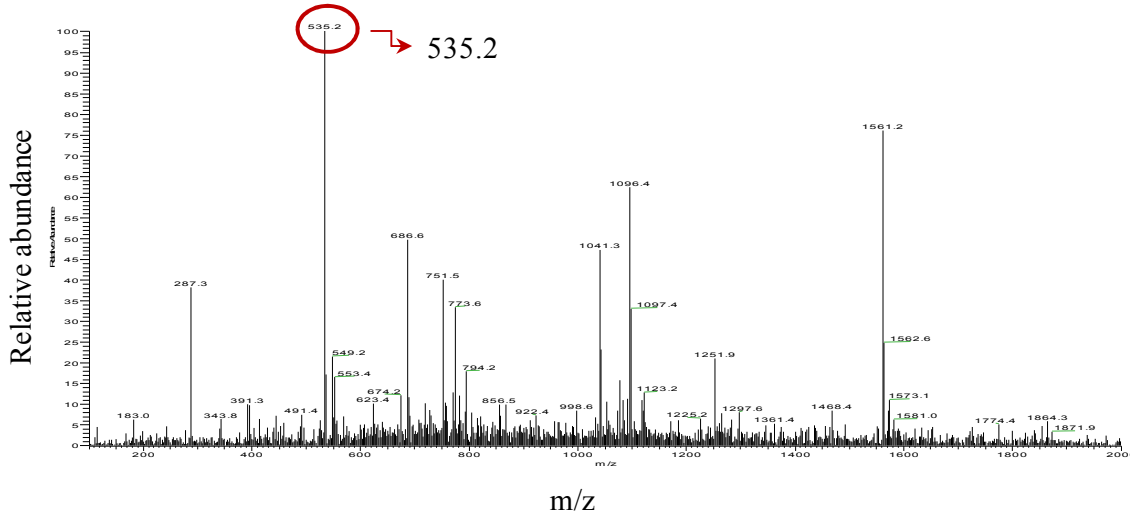

Fig 3c.8 | Ch3MAT- C3Gcou

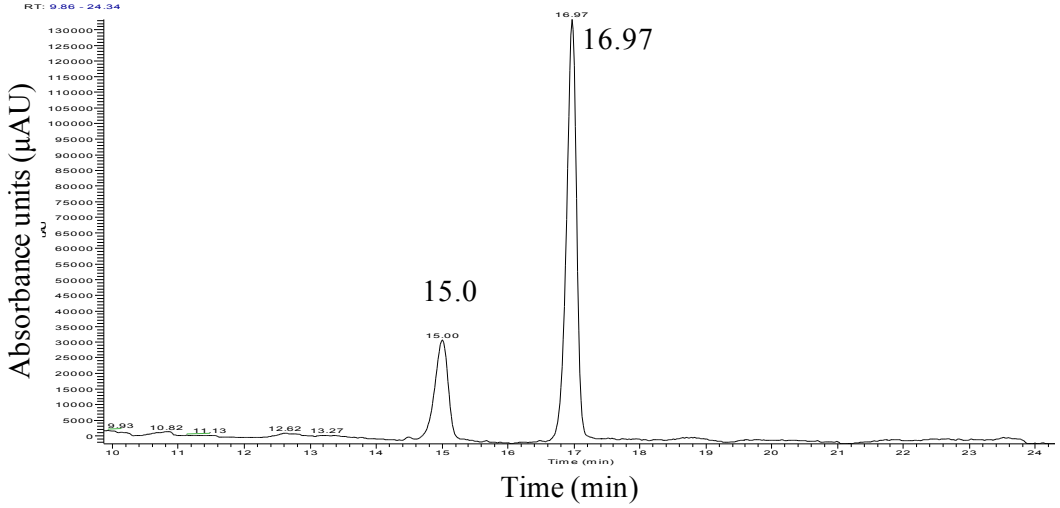

MS of product at 16.97 min

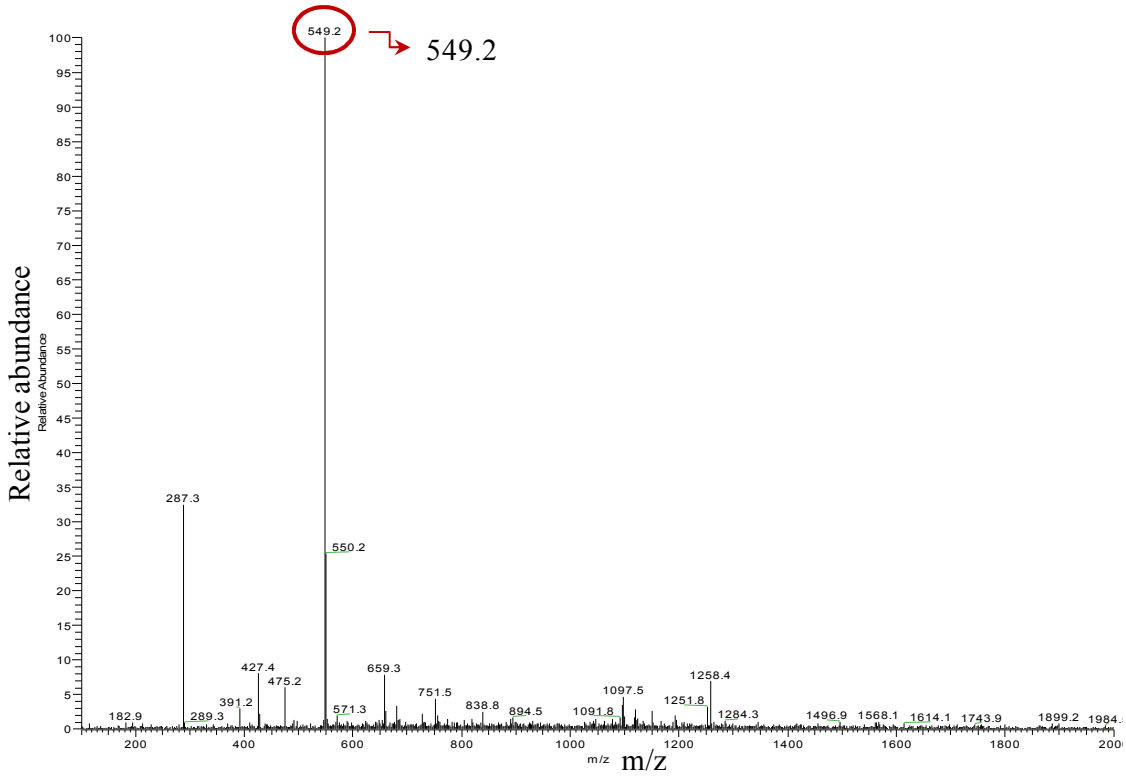

Fig 3c.9 | R183FCh3MAT- C3GMal

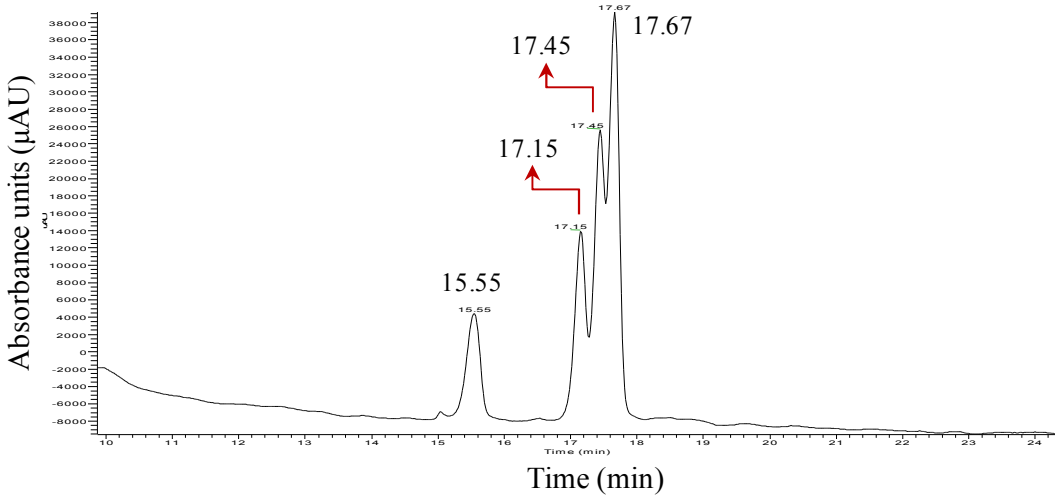

MS of product at 17.15 min correspond to Cyanidin 3-(6″ malonyl) glucoside (m/z 535.2)

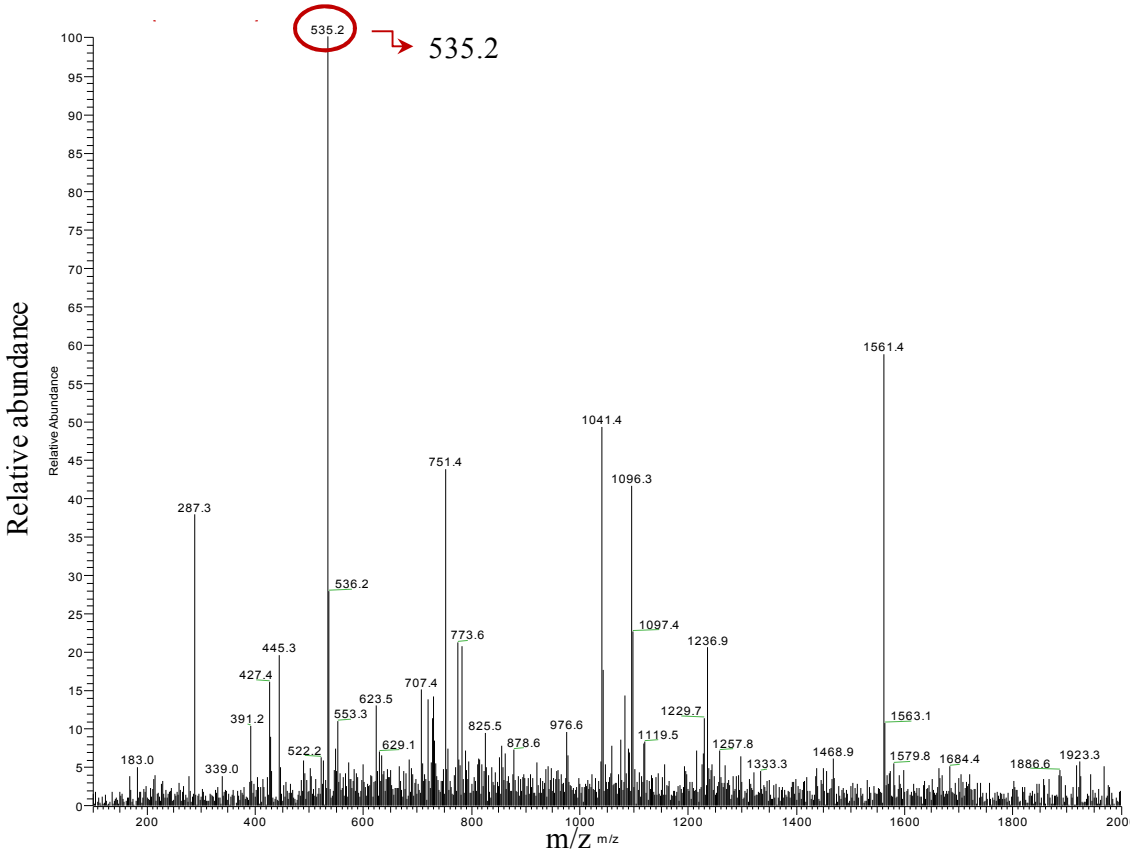

MS of product at 17.45 min

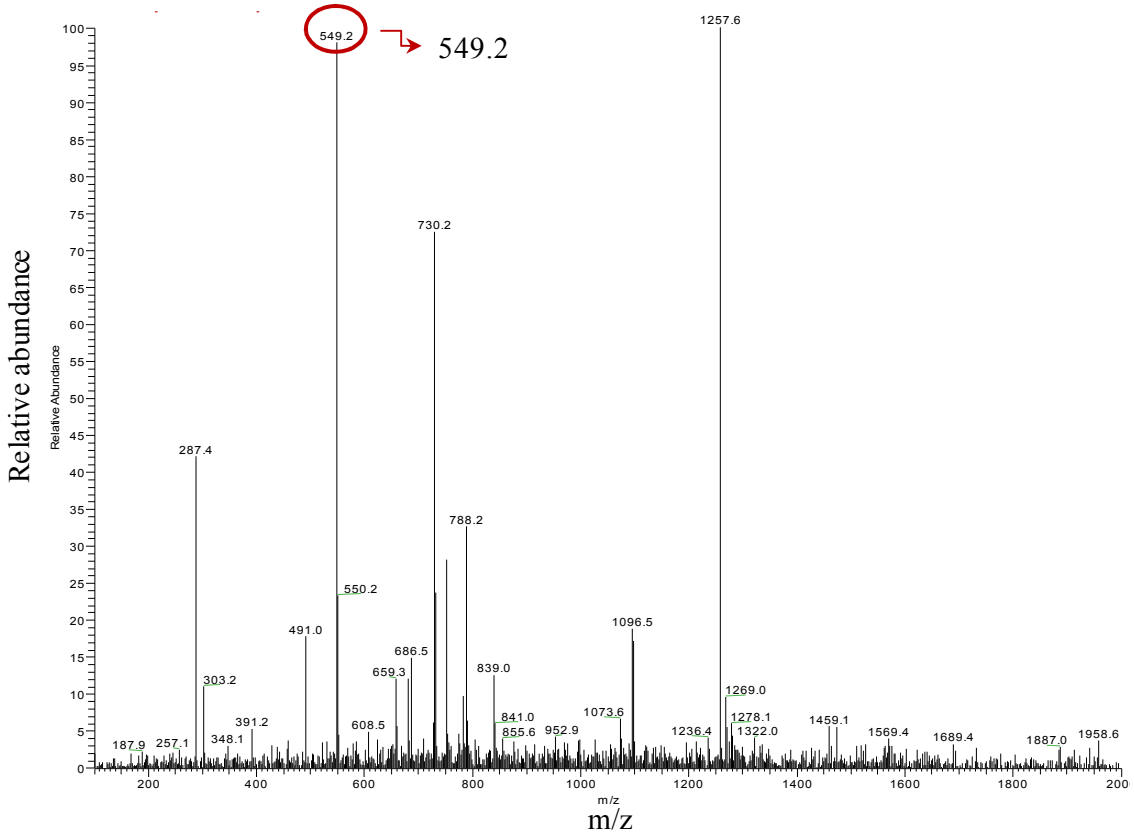

MS of product at 17.67 min correspond to Cyanidin 3-(6″ acetyl) glucoside (m/z; 491.2)

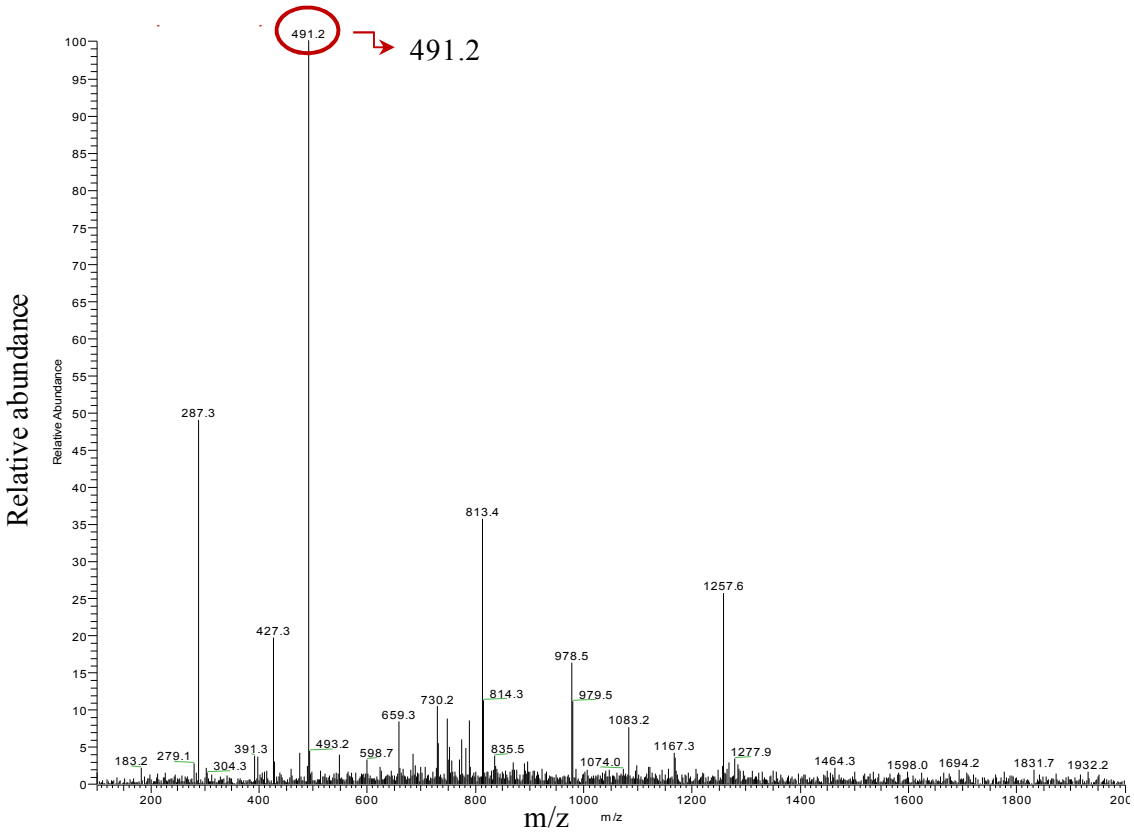

Fig 3c.10 | R183FCh3MAT- C3Gcou

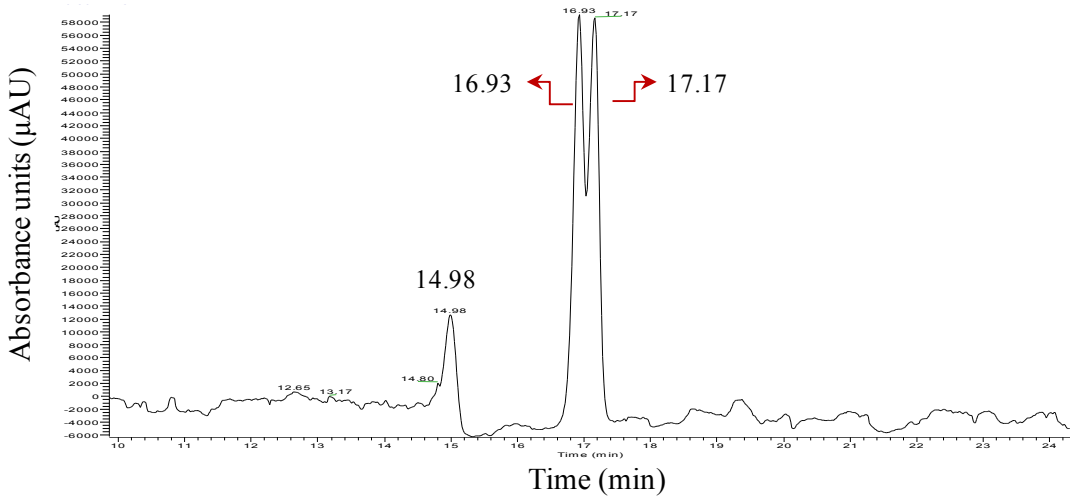

MS of product at 16.93 min

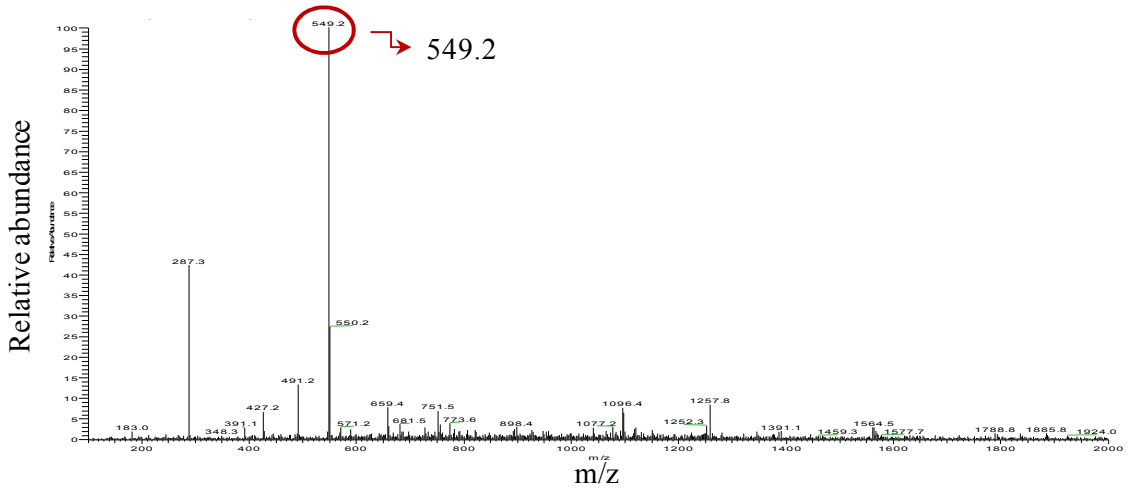

MS of product at 17.17 min

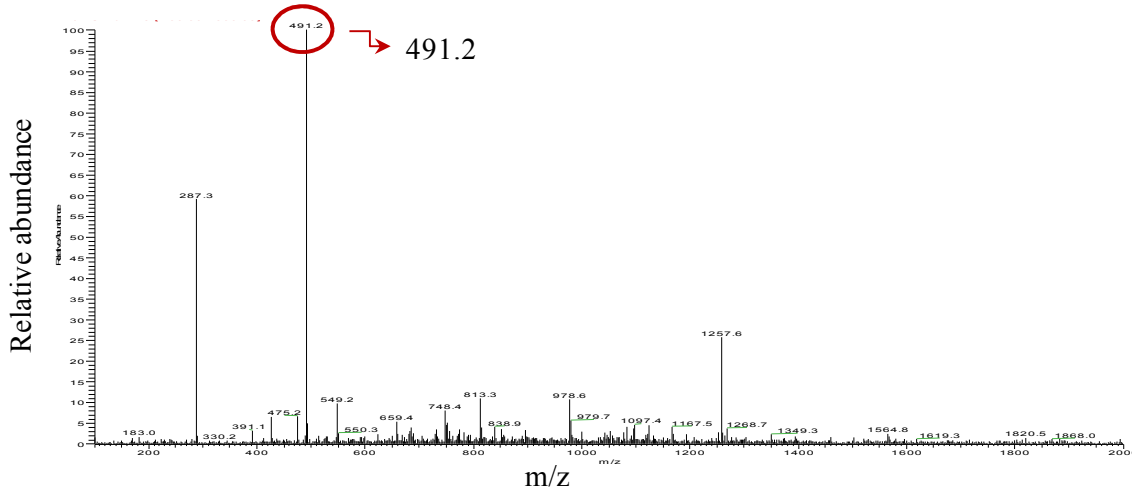

Chapter IV related

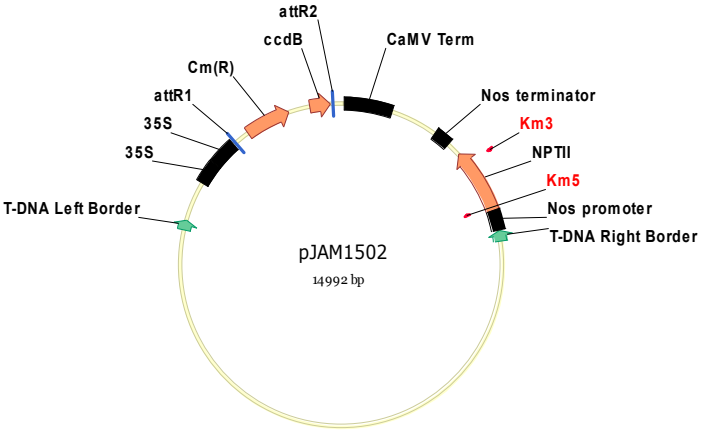

Figure 4a | Map showing features of pJAM1502 used to construct plant expression vectors. 35S; double 35S promoter from cauliflower mosaic virus (CaMV) to drive the transgene expression, attR1 and attR2; Gateway recombinant sites, Cm(R); chloramphenicol resistance gene, ccdB; lethal gene that targets DNA gyrase, CaMV Term; terminator of CaMV, NPTII; kanamycin resistance gene.

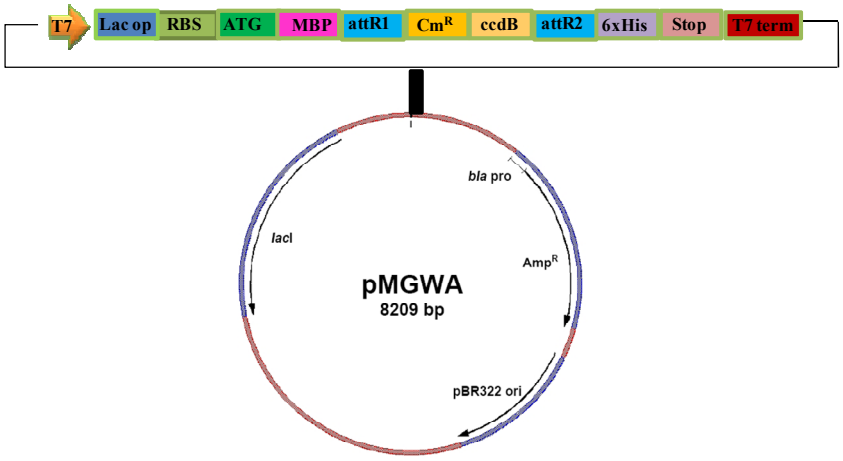

Figure 4b | Map showing vector features of pMGWA used to construct *E.coli* expression vector for *At5GT*. T7; T7 promoter, Lac op; lac operator, RBS; ribosome binding site, ATG; translation start site, MBP; maltose binding protein tag, attR1 and attR2; Gateway recombinant sites, CmR; chloramphenicol resistance gene, ccdB; lethal gene that targets DNA gyrase, 6xHis; six histidine tag, Stop; stop codon, T7 term; T7 terminator, bla pro; bla promoter, Amp^R; Ampicillin resistance gene, pBR322 ori; pBR322 origin, lac*I*; lac*I* encoding sequence.

Table 4a | Sequences of all the primers used in this chapter

Primer name	Primer sequence
B1Ptf35hF	5' GGGGACAAGTTTGTACAAAAAAGCAGGCTGGA CCATGATGCTACTTACTGAGCTTG 3'
B2 Ptf35hR	5' GGGGACCACTTTGTACAAGAAAGCTGGGTCCT ATGGTACATAAACATCCAATTGTAA 3'
PeFH 673F	5' CCTTGTTTAGCTTGGATGGATTTAC 3'
PeFH 1049F	5' CTTACCTCCGAGCAATTTGCAAAG 3'
PeFH 410R	5' AGCATATGCAAGTTGCTTAATTTC 3'
PeFH 809R	5' AATCTGGTTTCCCCTTACGTTCATA 3'
AtGF	5' GGGGACAAGTTTGTACAAAAAAGCAGGCTGGAT GGCCACTTCCGTCAATGG 3'
AtGR	5' GGGGACCACTTTGTACAAGAAAGCTGGGTCCTAC TCATCCTCGTCCACAAA 3'
B1TevAGT	5' GGGGACAAGTTTGTACAAAAAAGCAGGCTGGGAA AATCTGTACTTTCAGGGCATGGCCACTTCCGTCAATGG 3'
B2AGT	5' GGGGACCACTTTGTACAAGAAAGCTGGGTCCTC ATCCTCGTCCACAAAAC 3'
Gt401F	5' ACCTCCCAACTACACTTCTCTGGA 3'
Gt901F	5' TTTTTATGGATCGTGAGGGAGA 3'
Gt373R	5' ACGGGACGAGAACAGAGTAGATTAC 3'
GT700R	5' AACCAACGGTCCGATTGGGATCAT 3'
AgtF	5' ATGGCCACTTCCGTCAATGG 3'
AgtR	5' CTACTCATCCTCGTCCACAAA 3'
qA5gt R	5’ AGCTCTCGAAACGGAATCAAACC 3’
qA5gt F	5’ TCTCTGGTAAATCATCGGCGTGT 3’
Ch3MATB1 F	5' GGGGACAAGTTTGTACAAAAAAGCAGGCTGGAT GGCTTCCAATTCCATTGTTA 3'
Ch3MATB2 R	5' GGGGACCACTTTGTACAAGAAAGCTGGGTCT TATATCTCACTCTCTAATCCG 3'
3MAT 501F	5' CTCTATTGGAATGACAAATCATCAT 3'
3MAT 1001F	5' TCACAACCATAAAAAATGTTGTTTTG 3'
3MAT 901R	5' GCCCTTTTTTTCTCCCATTTTCACT 3'
3MAT 301R	5' AATTTCCGGTTTTCTAATGACGCCA 3'
qRos R	5’ GGTAACAAATGGTCGCTGATTGC 3'
qRos F	5’ ATCGGTTTTTCCGACTTCTCTCG 3'
qDel R	5’ ACCGTTCCCAAGATTCCCAACTA 3'
qDel F	5’ CATTGATGCCTTCTGCCAAATTC 3'
qAt3AT L	5’ ATGGCTCCTGGTATCGTATCAGTCA 3'
qAt3AT R	5’ AGGGCTTTCCTAATCCAAAATCCAT 3'
qCh3MAT L	5’ TTCGGGCAACATTTATATTGAGTCG 3'
qCh3MAT R	5’ AAGTAGGTTGATGGAATCGGTGGAT 3'
qPefh L	5’ ATCGGAGCACTTCCACTTTTAGGAG 3'
qPefh R	5’ ATCGTGGTCCATAATGTGCAAAAAC 3'

C3mC281Tf	5' CTAATGCTGATGATTTTGGCGTCATTAG AAAACCGGAAATTAG 3'
C3mC281Tr	5' CTAATTTCCGGTTTTCTAATGACGCCAAA ATCATCAGCATTAG 3'
C3mC566Tf	5'CGCTAGCACACGCCTTGGTTTTTTGAAGGTGTGGAC TTCAATTGCTAAATC 3'
C3mC566Tr	5' GATTTAGCAATTGAAGTCCACACCTTCAAAAAACC AAGGCGTGTGCTAGCG 3'

Chapter V related

Table 5a | ^{1}H-NMR and ^{13}C NMR spectral data of C3R in MeOH-*d4* containing 5% TFA-*d*.

position	^{1}H (ppm)	*J* (Hz)
Aglycone(cyanidin)		
4	8.99 (s)	-
6	6.93 (s)	-
8	6.7 (s)	-
2'	8.08 (d)	2.4
5'	7.07 (d)	8.7
6'	8.32 (d,d)	2.4, 8.7
3-*O*-glucose		
1" (beta)	5.33 (d)	7.7
2"	3.72 (d,d)	7.7, 9.0
3"	3.67 (d,d)	9.0
4"	3.59 (m)	
5"	3.82 (m)	
6" (2H)	4.40, 4.55 (m)	
6"-rhamnose		
1"'	4.68 (s)	
2"'	3.98 (s)	
3"'	3.83 (m)	
4"'	3.38 (s)	
5"'	3.47 (d)	
6"'	1.19 (d)	

Abbreviations: s-singlet; d-doublet; m=multiplet.
NMR referenced to CH_3OH-d4 at 3.34 ppm (^{1}H) and 49.8 ppm (^{13}C)

Table 5b | ^{1}H-NMR and ^{13}C NMR spectral data of C3couG in MeOH-*d4* containing 5% TFA-*d*.

position	^{1}H (ppm)	J (Hz)	^{13}C (ppm)
Aglycone(cyanidin)			
4	8.95 (s)	-	137.6
6	6.82 (s)	-	ND
8	6.57 (s)	-	ND
2’	8.04 (d)	2.4	118.9
5’	7.05 (d)	8.7	117.9
6’	8.28 (d,d)	2.4, 8.7	128.9
3-*O*-glucose			
1” (beta)	5.35 (d)	7.7	103.7
2”	3.75 (d,d)	7.7, 9.0	75.2
3”	3.60 (d,d)	9.0	78.3
4”	3.50 (m)	-	72.1
5”	3.87 (m)	-	76.5
6” (2H)	4.40, 4.55 (m)	-	65.0
Aromatic acyl moeity			
7”	-	-	quat
8”	7.47 (d)	15.9	147.3
9”	6.25	15.9	115.2
10”	-	-	quat
11”	6.82 (d)	8.3	117.4
12”	7.32 (d)	8.3	131.7
13”	-	-	quat

Abbreviations: s=singlet; d=doublet; m=multiplet; quat= quaternary carbon
NMR referenced to CH_3OH-d4 at 3.34 ppm (^{1}H) and 49.8 ppm (^{13}C)

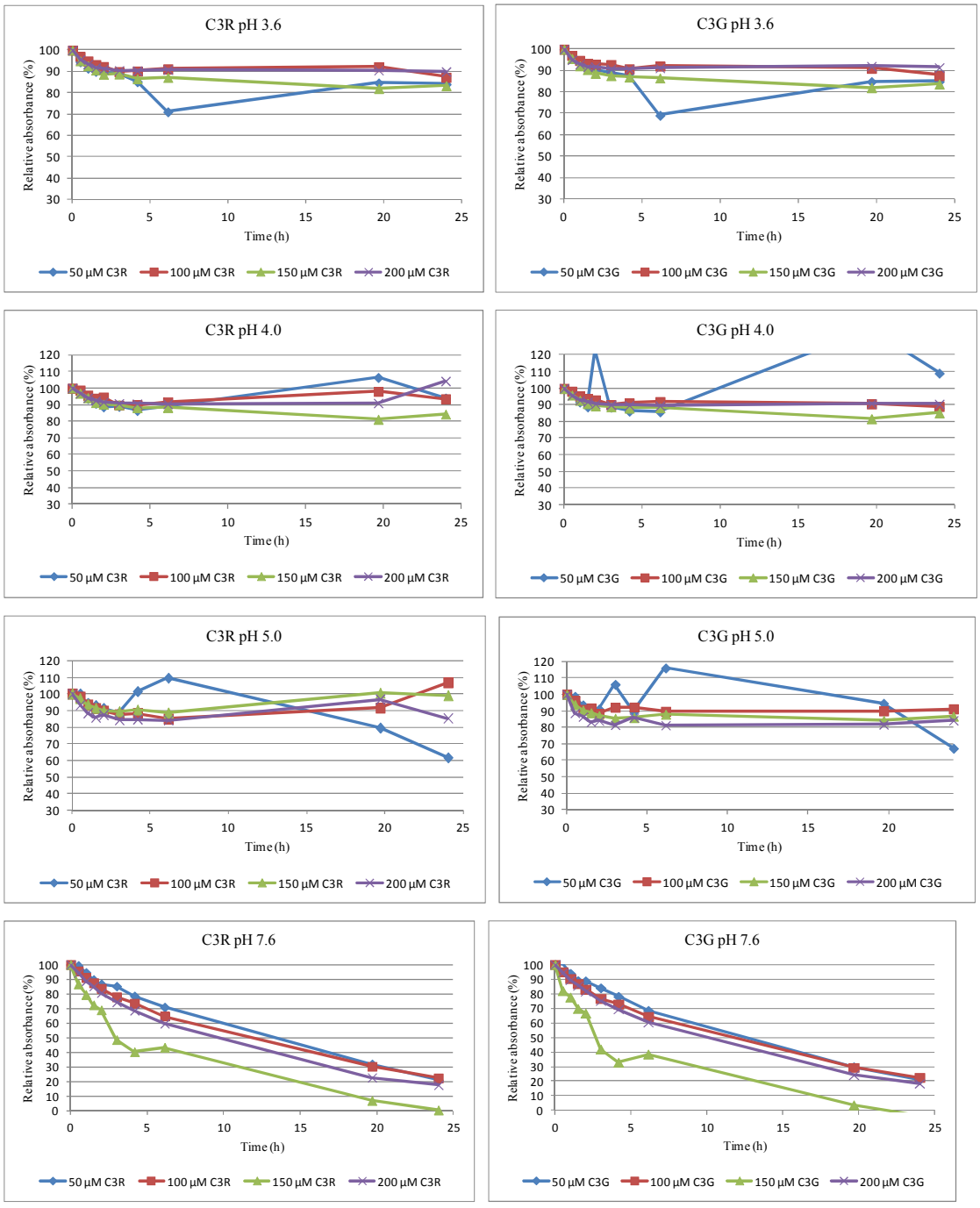

Figure 5.7 | Changes in anthocyanin stability as a result of concentration

Stability of C3R and C3G were studied at 50 µM, 100 µM, 150 µM and 200 µM concentration under eight pH conditions (2.6 to 7.6) and here data at pH 3.6, 4, 5 and 7.6 are shown . *The data represents mean values (± SD) of two independent experiments. Error bars are not shown for clarity.

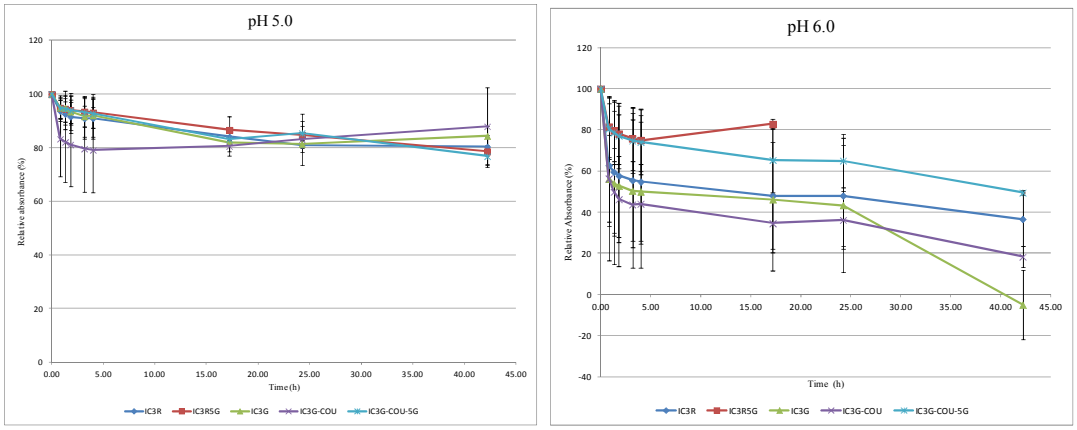

Figure 5.10 | Stability of different anthocyanins at different pH conditions. Stabilities of different purified anthocyanins (50 μM each) in several pH conditions (McIlvaine's buffer pH 5 and 6) at 25-27 °C are shown. *The data represents mean values (± SD) of two independent experiments.

Sequences of the genes (along with adjacent vector sequences) in various vectors constructed in this study are presented below.

(1) pE24aSl3AT

CATATG: NdeI site
CTCGAG: XhoI site
CACCACCACCACCACCAC: C-terminal His_6-tag

TGCGCCATTCGATGGTGTCCGGGATCTCGACGCTCTCCCTTATGCGACTCCTGCATTA
GGAAGCAGCCCAGTAGTAGGTTGAGGCCGTTGAGCACCGCCGCCGCAAGGAATGGT
GCATGCAAGGAGATGGCGCCCAACAGTCCCCCGGCCACGGGGCCTGCCACCATACC
CACGCCGAAACAAGCGCTCATGAGCCCGAAGTGGCGAGCCCGATCTTCCCCATCGGT
GATGTCGGCGATATAGGCGCCAGCAACCGCACCTGTGGCGCCGGTGATGCCGGCCA
CGATGCGTCCGGCGTAGAGGATCGAGATCTCGATCCCGCGAAATTAATACGACTCAC
TATAGGGGAATTGTGAGCGGATAACAATTCCCCTCTAGAAATAATTTTGTTTAACTTT
AAGAAGGAGATATACATATGAGCCAAATTACAACACAAAATTTGAATGGTACTTGT
ATTCAAATTGAAATCTTGAATGAAAAACTTATAAAACCATCGTTACCAACTCCAAAT
CATCTCAATTCCTACAAGTTATCATTTTTTGATCAAATTGCACCTAATTTTGCTGTACC
CCTTCTTTACTTCTACCCTCCAGTACCACCAGAAAACTCCCACCTACAACGCGTCGAA
GAAGTTCATAAACAACTACAAAACTCACTGTCTGAAGTTCTAACCAAGTTCTATCCA
CTTGCTGGAAGGTTGTCTGAAGATGGTACTTCCATTGAATGTCATGACCAAGGGGTT

ATTTACTTGGAAGCAAAGGTGAATTGTCAATTGAATGAATTTCTAGACAAAGCATAC
AAAGATAGTGACCTTGTTAAAATCTTTGTACCACCTATAAGAATTAGGCTAGCTGAA
TTGCCAAATAGACCAATGATGGCAATTCAGGCCACCATGTTTGAACATGGTGGCCTG
GCGCTAGCCGTGCAAATTGTCCACACAACAGGTGATGGATTCTCTGGCTGCGCGATC
ACCGATGAGTGGGCTAAAGTTAGTCGAATGGAGAAAGGGAATGTGAGAAATTTACA
ATTTCGTTCGGATTTAGTGGAAGTATTTCCACCTAGGGATAATATTTTGGAGATGATT
AAAAAAGGTAGGCCTAGAGGATATGAAATGAAAATTGCTACAAGAATTTTCATGTTT
GATGAAATTGCAATATCTAAGTTGAAGGAAAATGTGAACAAGTTTATGAGTTATTCA
TCAAGAGTTGAAGTTGTGACTGCACTTATTTGGAGAAGCCTTATGCGTGTGGTGAGG
TTGAGACATGGTCACAATAGGCCATCCATGCTACAATTTGCCATAAATTTAAGAGGA
AGAGGGTCTCCAAGAGTAGTTGGGGAAGATCAAAACTTTTTTGGGAACTTCTACCTT
GACATTCCAATCAAATATGTGTCATCTCGTAGCAATCAAGATCCAGAATTACATGAA
ATTGTAACCTTAATTAGGAATGCGAAGAACAAAATTCTATCAGAGATTGCAAATGCT
TCAAGTGAAGAGATTTTCTCAATATTAATTGAGTCATTGAATCAAATAAGAGAAGGG
TATAATGATGATGAAATTGACCTTTATCCAACTTCAAGTTTGTGTAAATTTCCACTAA
ATGAGTCTGATTTTGGATGGGCTAAACCAATTTGGGTGAGCAGAGTAAATGTGCCAT
TTCAAATGTTCTTCTTGATGGACTCAAAAAATGGGATTGAAGCTAGAGTTTGCTTGA
ATGAAGAGGATATGATGAAGTTGGAAAAGGATGTTGATATTGTGGAGTTTAGTTATG
TGCCAAAGCTCGAGCACCACCACCACCACCACTGAGATCCGGCTGCTAACAAAGCC
CGAAAGGAAGCTGAGTTGGCTGCTGCCACCGCTGAGCAATAACTAGCATAACCCCTT
GGGGCCTCTAAACGGGTCTTGAGGGGTTTTTTGCTGAAAGGAGGAACTATATCCGGA
TTGGCGAATGGGACGCGCCCTGTAGCGGCGCATTAAGCGCGGCGGGTGTGGTGGTTA
CGCGCAGCGTGACCGCTACACTTGCCAGCGCCCTA

(2) P530 Sl3AT- gene in blue colour and Gateway sites flank 5' and 3' of gene sequence. MBP sequence (partial) is present upstream to gene sequence.

GGATAAACTGGAAGAGAAATTCCCACAGGTTGCGGCAACTGGCGATGGCCCTGACA
TTATCTTCTGGGCACACGACCGCTTTGGTGGCTACGCTCAATCTGGCCTGTTGGCTGA
AATCACCCCGGACAAAGCGTTCCAGGACAAGCTGTATCCGTTTACCTGGGATGCCGT
ACGTTACAACGGCAAGCTGATTGCTTACCCGATCGCTGTTGAAGCGTTATCGCTGAT
TTATAACAAAGATCTGCTGCCGAACCCGCCAAAAACCTGGGAAGAGATCCCGGCGC
TGGATAAAGAACTGAAAGCGAAAGGTAAGAGCGCGCTGATGTTCAACCTGCAAGAA
CCGTACTTCACCTGGCCGCTGATTGCTGCTGACGGGGGTTATGCGTTCAAGTATGAA
AACGGCAAGTACGACATTAAAGACGTGGGCGTGGATAACGCTGGCGCGAAAGCGGG
TCTGACCTTCCTGGTTGACCTGATTAAAAACAAACACATGAATGCAGACACCGATTA
CTCCATCGCAGAAGCTGCCTTTAATAAAGGCGAAACAGCGATGACCATCAACGGCC
CGTGGGCATGGTCCAACATCGACACCAGCAAAGTGAATTATGGTGTAACGGTACTGC
CGACCTTCAAGGGTCAACCATCCAAACCGTTCGTTGGCGTGCTGAGCGCAGGTATTA
ACGCCGCCAGTCCGAACAAAGAGCTGGCAAAAGAGTTCCTCGAAAACTATCTGCTG
ACTGATGAAGGTCTGGAAGCGGTTAATAAAGACAAACCGCTGGGTGCCGTAGCGCT
GAAGTCTTACGAGGAAGAGTTGGCGAAAGATCCACGTATTGCCGCCACCATGGAAA
ACGCCCAGAAAGGTGAAATCATGCCGAACATCCCGCAGATGTCCGCTTTCTGGTATG
CCGTGCGTACTGCGGTGATCAACGCCGCCAGCGGTCGTCAGACTGTCGATGAAGCCC
TGAAAGACGCGCAGACTGGTACCGGATCTTACATCACAAGTTTGTACAAAAAAGCA
GGCTGGGAAAATCTGTACTTTCAGGGCATGAGCCAAATTACAACACAAAATTTGAAT
GGTACTTGTATTCAAATTGAAATCTTGAATGAAAAACTTATAAAACCATCGTTACCA
ACTCCAAATCATCTCAATTCCTACAAGTTATCATTTTTTGATCAAATTGCACCTAATT
TTGCTGTACCCCTTCTTTACTTCTACCCTCCAGTACCACCAGAAAACTCCCACCTACA
ACGCGTCGAAGAAGTTCATAAACAACTACAAAACTCACTGTCTGAAGTTCTAACCAA
GTTCTATCCACTTGCTGGAAGGTTGTCTGAAGATGGTACTTCCATTGAATGTCATGAC
CAAGGGGTTATTTACTTGGAAGCAAAGGTGAATTGTCAATTGAATGAATTTCTAGAC
AAAGCATACAAAGATAGTGACCTTGTTAAAATCTTTGTACCACCTATAAGAATTAGG

CTAGCTGAATTGCCAAATAGACCAATGATGGCAATTCAGGCCACCATGTTTGAACAT
GGTGGCCTGGCGCTAGCCGTGCAAATTGTCCACACAACAGGTGATGGATTCTCTGGC
TGCGCGATCACCGATGAGTGGGCTAAAGTTAGTCGAATGGAGAAAGGGAATGTGAG
AAATTTACAATTTCGTTCGGATTTAGTGGAAGTATTTCCACCTAGGGATAATATTTTG
GAGATGATTAAAAAAGGTAGGCCTAGAGGATATGAAATGAAAATTGCTACAAGAAT
TTTCATGTTTGATGAAATTGCAATATCTAAGTTGAAGGAAAATGTGAACAAGTTTAT
GAGTTATTCATCAAGAGTTGAAGTTGTGACTGCACTTATTTGGAGAAGCCTTATGCG
TGTGGTGAGGTTGAGACATGGTCACAATAGGCCATCCATGCTACAATTTGCCATAAA
TTTAAGAGGAAGAGGGTCTCCAAGAGTAGTTGGGGAAGATCAAAACTTTTTTGGGA
ACTTCTACCTTGACATTCCAATCAAATATGTGTCATCTCGTAGCAATCAAGATCCAGA
ATTACATGAAATTGTAACCTTAATTAGGAATGCGAAGAACAAAATTCTATCAGAGAT
TGCAAATGCTTCAAGTGAAGAGATTTTCTCAATATTAATTGAGTCATTGAATCAAAT
AAGAGAAGGGTATAATGATGATGAAATTGACCTTTATCCAACTTCAAGTTTGTGTAA
ATTTCCACTAAATGAGTCTGATTTTGGATGGGCTAAACCAATTTGGGTGAGCAGAGT
AAATGTGCCATTTCAAATGTTCTTCTTGATGGACTCAAAAAATGGGATTGAAGCTAG
AGTTTGCTTGAATGAAGAGGATATGATGAAGTTGGAAAAGGATGTTGATATTGTGGA
GTTTAGTTATGTGCCAAAGTAGGACCCAGCTTTCTTGTACAAAGTGGTTGATGTACCT
CGAGCACCACCACCACCACCACTGAGATCCGGCTGCTAACAAAGCCCGAAAGGAAG
CTGAGTTGGCTGCTGCCACCGCTGAGCAATAACTAGCATAACCCCTTGGGGCCTCTA
AACGGGTCTTGAGGGGTTTTTTGCTGAAAGGAGGAACTATATCCGGATTGGCGAATG
GGACGCGCCCTGTAGCGGCGCATTAAGCGCGGCGGGTGTGGTGGTTACGCGCAGCG
TGACCGCTACACTTGCCAGCGCCCTAGCGCCCGCTCCTTTCGCTTTCTTCCCTTCCTTT
CTCGCCACGTTCGCCGGCTTTCCCCGTCAAGCTCTAAATCGGGGGCTCCCTTTAGGGT
TCCGATTTAGTGCTTTACGGCACCTCGACCCCAAAAAACTTGATTAGGGTGATGGTT
CACGTAGTGGGCCATCGCCCTGATAGACGGTTTTTCGCCCTTTGACGTTGGAGTCCAC
GTTCTTTAATAGTGGACTCTTGTTCCAAACTGGAACAACACTCAACCCTATCTCGGTC
TATTCTT

(3) pMtevSlAT

GGCGTGCTGAGCGCAGGTATTAACGCCGCCAGTCCGAACAAAGAGCTGGCAAAAGA
GTTCCTCGAAAACTATCTGCTGACTGATGAAGGTCTGGAAGCGGTTAATAAAGACAA
ACCGCTGGGTGCCGTAGCGCTGAAGTCTTACGAGGAAGAGTTGGCGAAAGATCCAC
GTATTGCCGCCACTATGGAAAACGCCCAGAAAGGTGAAATCATGCCGAACATCCCG
CAGATGTCCGCTTTCTGGTATGCCGTGCGTACTGCGGTGATCAACGCCGCCAGCGGT
CGTCAGACTGTCGATGAAGCCCTGAAAGACGCGCAGACTAATTCGAGCTCGAACAA
CAACAACAATAACAATAACAACAACCTCGGGATCGAGGGAAGGATTTCAGAATTCG
AAAATCTTTATTTTCAAGGTGGCATGAGCCAAATTACAACACAAAATTTGAATGGTA
CTTGTATTCAAATTGAAATCTTGAATGAAAAACTTATAAAACCATCGTTACCAACTC
CAAATCATCTCAATTCCTACAAGTTATCATTTTTTGATCAAATTGCACCTAATTTTGC
TGTACCCCTTCTTTACTTCTACCCTCCAGTACCACCAGAAAACTCCCACCTACAACGC
GTCGAAGAAGTTCATAAACAACTACAAAACTCACTGTCTGAAGTTCTAACCAAGTTC
TATCCACTTGCTGGAAGGTTGTCTGAAGATGGTACTTCCATTGAATGTCATGACCAA
GGGGTTATTTACTTGGAAGCAAAGGTGAATTGTCAATTGAATGAATTTCTAGACAAA
GCATACAAAGATAGTGACCTTGTTAAAATCTTTGTACCACCTATAAGAATTAGGCTA
GCTGAATTGCCAAATAGACCAATGATGGCAATTCAGGCCACCATGTTTGAACATGGT
GGCCTGGCGCTAGCCGTGCAAATTGTCCACACAACAGGTGATGGATTCTCTGGCTGC
GCGATCACCGATGAGTGGGCTAAAGTTAGTCGAATGGAGAAAGGGAATGTGAGAAA
TTTACAATTTCGTTCGGATTTAGTGGAAGTATTTCCACCTAGGGATAATATTTTGGAG
ATGATTAAAAAAGGTAGGCCTAGAGGATATGAAATGAAAATTGCTACAAGAATTTT
CATGTTTGATGAAATTGCAATATCTAAGTTGAAGGAAAATGTGAACAAGTTTATGAG
TTATTCATCAAGAGTTGAAGTTGTGACTGCACTTATTTGGAGAAGCCTTATGCGTGTG
GTGAGGTTGAGACATGGTCACAATAGGCCATCCATGCTACAATTTGCCATAAATTTA
AGAGGAAGAGGGTCTCCAAGAGTAGTTGGGGAAGATCAAAACTTTTTTGGGAACTT
CTACCTTGACATTCCAATCAAATATGTGTCATCTCGTAGCAATCAAGATCCAGAATT

ACATGAAATTGTAACCTTAATTAGGAATGCGAAGAACAAAATTCTATCAGAGATTGC
AAATGCTTCAAGTGAAGAGATTTTCTCAATATTAATTGAGTCATTGAATCAAATAAG
AGAAGGGTATAATGATGATGAAATTGACCTTTATCCAACTTCAAGTTTGTGTAAATT
TCCACTAAATGAGTCTGATTTTGGATGGGCTAAACCAATTTGGGTGAGCAGAGTAAA
TGTGCCATTTCAAATGTTCTTCTTGATGGACTCAAAAAATGGGATTGAAGCTAGAGT
TTGCTTGAATGAAGAGGATATGATGAAGTTGGAAAAGGATGTTGATATTGTGGAGTT
TAGTTATGTGCCAAAGTAGTAGAAGCTTGGCACTGGCCGTCGTTTTACAACGTCGTG
ACTGGGAAAACCCTGGCGTTACCCAACTTAATCGCCTTGCAGCACATCCCCCTTTCG
CCAGCTGGCGTAATAGCGAAGAGGCCCGCACCGATCGCCCTTCCCAACAGTTGCGCA
GCCTGAATGGCGAATGGCAGCTTGGCTGTTTTGGCGGATGAGATAAGATTTTCAGCC
TGATACAGATTAAATCAGAACGCAGAAGCGGTCTGATAAAACAGAATTTGCCTGGC
GGCAGTAGCGCGGTGGTCCCACCTGA

(4) pE24Gt5AT

AGGAAGCAGCCCAGTAGTAGGTTGAGGCCGTTGAGCACCGCCGCCGCAAGGAATGG
TGCATGCAAGGAGATGGCGCCCAACAGTCCCCCGGCCACGGGGCCTGCCACCATAC
CCACGCCGAAACAAGCGCTCATGAGCCCGAAGTGGCGAGCCCGATCTTCCCCATCG
GTGATGTCGGCGATATAGGCGCCAGCAACCGCACCTGTGGCGCCGGTGATGCCGGC
CACGATGCGTCCGGCGTAGAGGATCGAGATCTCGATCCCGCGAAATTAATACGACTC
ACTATAGGGGAATTGTGAGCGGATAACAATTCCCCTCTAGAAATAATTTTGTTTAAC
TTTAAGAAGGAGATATACATATGCATCATCATCACCACCATGAAAATCTGTACTTTC
AGGGCATGGAACAAATTCAGATGGTTAAAGTGCTGGAAAAATGTCAGGTTACCCCTC
CGAGCGATACCACCGATGTTGAACTGAGCCTGCCGGTTACCTTTTTTGATATTCCGTG
GCTGCATCTGAATAAAATGCAGAGCCTGCTGTTTTATGATTTTCCGTATCCGCGTACC
CATTTTCTGGATACCGTTATTCCGAATCTGAAAGCAAGCCTGAGCCTGACCCTGAAA
CATTATGTTCCGCTGTCTGGTAATCTGCTGATGCCGATTAAAAGCGGTGAAATGCCG
AAATTTCAGTATAGCCGTGATGAAGGTGATAGCATTACCCTGATTGTTGCAGAAAGC
GATCAGGATTTTGATTATCTGAAAGGCCATCAGCTGGTTGATAGCAATGATCTGCAT
GGACTGTTTTATGTTATGCCACGTGTTATTCGTACCATGCAGGATTATAAAGTTATTC
CGCTGGTTGCAGTTCAGGTTACCGTGTTTCCGAATCGTGGTATTGCAGTTGCACTGAC
CGCACATCATAGCATTGCAGATGCGAAAAGCTTTGTGATGTTTATTAATGCCTGGGC
CTATATTAATAAATTTGGCAAAGATGCCGATCTGCTGTCTGCAAATTTACTGCCGAG
CTTTGATCGTAGCATTATTAAAGATCTGTATGGCCTGGAAGAAACCTTTTGGAATGA
AATGCAGGATGTGCTGGAAATGTTTAGCCGTTTTGGTAGCAAACCTCCGCGTTTTAA
TAAAGTTCGTGCCACCTATGTTCTGAGCCTGGCAGAAATTCAGAAACTGAAAAATAA
AGTGCTGAATCTGCGTGGTAGCGAACCGACCATTCGTGTTACCACCTTTACCATGAC
CTGTGGTTATGTTTGGACCTGTATGGTGAAAAGCAAAGATGATGTGGTTAGCGAAGA
AAGCAGCAATGATGAAAATGAACTGGAATATTTTAGCTTTACCGCAGATTGTCGTGG
TCTGCTGACCCCTCCGTGTCCTCCGAATTACTTTGGTAATTGTCTGGCAAGCTGTGTT
GCAAAAGCCACCCATAAAGAACTGGTTGGTGATAAAGGTCTGCTGGTTGCCGTTGCA
GCAATTGGTGAAGCCATTGAAAAACGCCTGCATAATGAAAAAGGTGTTCTGGCAGA
TGCAAAAACCTGGCTGTCTGAAAGCAATGGTATTCCGAGCAAACGTTTTCTGGGTAT
TACCGGTAGCCCGAAATTTGATAGCTATGGCGTGGATTTTGGTTGGGGTAAACCGGC
AAAATTTGATATTACCAGCGTGGATTATGCCGAACTGATTTATGTTATTCAGAGCCGT
GATTTTGAAAAAGGCGTGGAAATTGGTGTTAGCCTGCCGAAAATTCACATGGATGCC
TTTGCCAAAATTTTTGAAGAAGGCTTTTGCAGCCTGAGCTAATAACTCGAGCACCAC
CACCACCACCACTGAGATCCGGCTGCTAACAAAGCCCGAAAGGAAGCTGAGTTGGC
TGCTGCCACCGCTGAGCAATAACTAGCATAACCCCTTGGGGCCTCTAAACGGGTCTT
GAGGGGTTTTTTGCTGAAAGGAGGAACTATATCCGGATTGGCGAATGGGACGCGCCC
TGTAGCGGCGCATTAAGCGCGGCGGGTGTGGTGGTTACGCGCAGCGTGACCGCTACA
CTTGCCAGCGCCCTAGCGCCCGCTCCTTTCGCTTTCTT

(5) pE28(N)GtAT

GAAGTGGCGAGCCCGATCTTCCCCATCGGTGATGTCGGCGATATAGGCGCCAGCAAC
CGCACCTGTGGCGCCGGTGATGCCGGCCACGATGCGTCCGGCGTAGAGGATCGAGA
TCTCGATCCCGCGAAATTAATACGACTCACTATAGGGGAATTGTGAGCGGATAACAA
TTCCCCTCTAGAAATAATTTTGTTTAACTTTAAGAAGGAGATATACCATGGGCAGCA
GCCATCATCATCATCATCACAGCAGCGGCCTGGTGCCGCGCGGCAGCCATATGCATC
ATCATCACCACCATGAAAATCTGTACTTTCAGGGCATGGAACAAATTCAGATGGTTA
AAGTGCTGGAAAAATGTCAGGTTACCCCTCCGAGCGATACCACCGATGTTGAACTGA
GCCTGCCGGTTACCTTTTTTGATATTCCGTGGCTGCATCTGAATAAAATGCAGAGCCT
GCTGTTTTATGATTTTCCGTATCCGCGTACCCATTTTCTGGATACCGTTATTCCGAATC
TGAAAGCAAGCCTGAGCCTGACCCTGAAACATTATGTTCCGCTGTCTGGTAATCTGC
TGATGCCGATTAAAAGCGGTGAAATGCCGAAATTTCAGTATAGCCGTGATGAAGGTG
ATAGCATTACCCTGATTGTTGCAGAAAGCGATCAGGATTTTGATTATCTGAAAGGCC
ATCAGCTGGTTGATAGCAATGATCTGCATGGACTGTTTTATGTTATGCCACGTGTTAT
TCGTACCATGCAGGATTATAAAGTTATTCCGCTGGTTGCAGTTCAGGTTACCGTGTTT
CCGAATCGTGGTATTGCAGTTGCACTGACCGCACATCATAGCATTGCAGATGCGAAA
AGCTTTGTGATGTTTATTAATGCCTGGGCCTATATTAATAAATTTGGCAAAGATGCCG
ATCTGCTGTCTGCAAATTTACTGCCGAGCTTTGATCGTAGCATTATTAAAGATCTGTA
TGGCCTGGAAGAAACCTTTTGGAATGAAATGCAGGATGTGCTGGAAATGTTTAGCCG
TTTTGGTAGCAAACCTCCGCGTTTTAATAAAGTTCGTGCCACCTATGTTCTGAGCCTG
GCAGAAATTCAGAAACTGAAAAATAAAGTGCTGAATCTGCGTGGTAGCGAACCGAC
CATTCGTGTTACCACCTTTACCATGACCTGTGGTTATGTTTGGACCTGTATGGTGAAA
AGCAAAGATGATGTGGTTAGCGAAGAAAGCAGCAATGATGAAAATGAACTGGAATA
TTTTAGCTTTACCGCAGATTGTCGTGGTCTGCTGACCCCTCCGTGTCCTCCGAATTAC
TTTGGTAATTGTCTGGCAAGCTGTGTTGCAAAAGCCACCCATAAAGAACTGGTTGGT
GATAAAGGTCTGCTGGTTGCCGTTGCAGCAATTGGTGAAGCCATTGAAAAACGCCTG
CATAATGAAAAAGGTGTTCTGGCAGATGCAAAAACCTGGCTGTCTGAAAGCAATGG
TATTCCGAGCAAACGTTTTCTGGGTATTACCGGTAGCCCGAAATTTGATAGCTATGG
CGTGGATTTTGGTTGGGGTAAACCGGCAAAATTTGATATTACCAGCGTGGATTATGC
CGAACTGATTTATGTTATTCAGAGCCGTGATTTTGAAAAAGGCGTGGAAATTGGTGT
TAGCCTGCCGAAAATTCACATGGATGCCTTTGCCAAAATTTTTGAAGAAGGCTTTTG
CAGCCTGAGCTAATAACTCGAGCACCACCACCACCACCACTGAGATCCGGCTGCTAA
CAAAGCCCGAAAGGAAGCTGAGTTGGCTGCTGCCACCGCTGAGCAATAACTAGCAT
AACCCCTTGGGGCCTCTAAACGGGTCTTGAGGGGTTTTTTGCTGAAAGGAGGAACTA
TATCCGGAT

(6) pEnt207GtAT

TGGCCTTTTGCTCACATGTTCTTTCCTGCGTTATCCCCTGATTCTGTGGATAACCGTAT
TACCGCTAGCCAGGAAGAGTTTGTAGAAACGCAAAAAGGCCATCCGTCAGGATGGC
CTTCTGCTTAGTTTGATGCCTGGCAGTTTATGGCGGGCGTCCTGCCCGCCACCCCTCC
GGGCCGTTGCTTCACAACGTTCAAATCCGCTCCCGGCGGATTTGTCCTACTCAGGAG
AGCGTTCACCGACAAACAACAGATAAAACGAAAGGCCCAGTCTTCCGACTGAGCCT
TTCGTTTTATTTGATGCCTGGCAGTTCCCTACTCTCGCGTTAACGCTAGCATGGATCT
CGGGCCCCAAATAATGATTTTATTTTGACTGATAGTGACCTGTTCGTTGCAACAAATT
GATGAGCAATGCTTTTTTATAATGCCAACTTTGTACAAAAAAGCAGGCTGGATGGAA
CAAATTCAGATGGTTAAAGTGCTGGAAAAATGTCAGGTTACCCCTCCGAGCGATACC
ACCGATGTTGAACTGAGCCTGCCGGTTACCTTTTTTGATATTCCGTGGCTGCATCTGA
ATAAAATGCAGAGCCTGCTGTTTTATGATTTTCCGTATCCGCGTACCCATTTTCTGGA
TACCGTTATTCCGAATCTGAAAGCAAGCCTGAGCCTGACCCTGAAACATTATGTTCC
GCTGTCTGGTAATCTGCTGATGCCGATTAAAAGCGGTGAAATGCCGAAATTTCAGTA
TAGCCGTGATGAAGGTGATAGCATTACCCTGATTGTTGCAGAAAGCGATCAGGATTT
TGATTATCTGAAAGGCCATCAGCTGGTTGATAGCAATGATCTGCATGGACTGTTTTAT
GTTATGCCACGTGTTATTCGTACCATGCAGGATTATAAAGTTATTCCGCTGGTTGCAG

TTCAGGTTACCGTGTTTCCGAATCGTGGTATTGCAGTTGCACTGACCGCACATCATAG
CATTGCAGATGCGAAAAGCTTTGTGATGTTTATTAATGCCTGGGCCTATATTAATAA
ATTTGGCAAAGATGCCGATCTGCTGTCTGCAAATTTACTGCCGAGCTTTGATCGTAGC
ATTATTAAAGATCTGTATGGCCTGGAAGAAACCTTTTGGAATGAAATGCAGGATGTG
CTGGAAATGTTTAGCCGTTTTGGTAGCAAACCTCCGCGTTTTAATAAAGTTCGTGCCA
CCTATGTTCTGAGCCTGGCAGAAATTCAGAAACTGAAAAATAAAGTGCTGAATCTGC
GTGGTAGCGAACCGACCATTCGTGTTACCACCTTTACCATGACCTGTGGTTATGTTTG
GACCTGTATGGTGAAAAGCAAAGATGATGTGGTTAGCGAAGAAAGCAGCAATGATG
AAAATGAACTGGAATATTTTAGCTTTACCGCAGATTGTCGTGGTCTGCTGACCCCTCC
GTGTCCTCCGAATTACTTTGGTAATTGTCTGGCAAGCTGTGTTGCAAAAGCCACCCAT
AAAGAACTGGTTGGTGATAAAGGTCTGCTGGTTGCCGTTGCAGCAATTGGTGAAGCC
ATTGAAAAACGCCTGCATAATGAAAAAGGTGTTCTGGCAGATGCAAAAACCTGGCT
GTCTGAAAGCAATGGTATTCCGAGCAAACGTTTTCTGGGTATTACCGGTAGCCCGAA
ATTTGATAGCTATGGCGTGGATTTTGGTTGGGGTAAACCGGCAAAATTTGATATTAC
CAGCGTGGATTATGCCGAACTGATTTATGTTATTCAGAGCCGTGATTTTGAAAAAGG
CGTGGAAATTGGTGTTAGCCTGCCGAAAATTCACATGGATGCCTTTGCCAAAATTTTT
GAAGAAGGCTTTTGCAGCCTGAGCTAAGACCCAGCTTTCTTGTAC

(7) pJAt5AGT

CCAAAGATGGACCCCCACCCACGAGGAGCATCGTGGAAAAAGAAGACGTTCCAACC
ACGTCTTCAAAGCAAGTGGATTGATGTGACATCTCCACTGACGTAAGGGATGACGCA
CAATCCCACTATCCTTCGCAAGACCCTTCCTCTATATAAGGAAGTTCATTTCATTTGG
AGAGGACAGCCCAAGCTTGGCTGCAGGTCGACGGATCCCCATCAAACAAGTTTGTAC
AAAAAAGCAGGCTGGATGGCCACTTCCGTCAATGGTTCCCATCGTCGTCCACATTAC
TTGCTTGTAACATTCCCAGCGCAAGGTCACATCAACCCGGCGCTTCAACTAGCCAAC
CGCCTCATCCACCACGGTGCAACCGTCACATACTCCACCGCAGTCTCTGCTCACCGA
CGTATGGGCGAGCCACCTTCCACAAAAGGTCTATCCTTCGCTTGGTTCACCGATGGA
TTCGACGACGGTCTCAAGTCATTCGAAGACCAGAAAATCTACATGTCCGAACTCAAA
CGATGTGGTTCAAACGCCCTGAGAGACATCATCAAAGCCAATCTTGACGCCACCACC
GAAACAGAGCCTATCACCGGGGTAATCTACTCTGTTCTCGTCCCGTGGGTTTCTACG
GTAGCGCGTGAGTTTCACCTCCCAACTACACTTCTCTGGATTGAACCAGCTACTGTAC
TAGACATCTACTACTACTACTTCAACACCTCTTACAAACATCTCTTCGACGTTGAACC
GATTAAATTACCGAAACTGCCACTGATCACCACCGGTGACCTCCCGTCGTTTCTTCAA
CCTTCGAAGGCATTACCGTCAGCTCTTGTGACTCTAAGAGAACATATCGAAGCTCTC
GAAACGGAATCAAACCCTAAGATTCTTGTTAACACATTCTCTGCTTTGGAACACGAT
GCTTTAACCTCTGTTGAGAAACTCAAGATGATCCCAATCGGACCGTTGGTTTCTTCCT
CCGAGGGTAAAACCGATCTTTTCAAATCTTCCGACGAGGATTACACGAAATGGTTAG
ACTCGAAGCTCGAGAGATCAGTGATTTACATTTCCTTAGGCACACACGCCGATGATT
TACCAGAGAAACACATGGAAGCGCTTACTCACGGCGTGTTAGCTACAAACAGACCG
TTTTTATGGATCGTGAGGGAGAAAAATCCAGAAGAGAAGAAGAAGAATCGGTTTCT
TGAATTGATCAGAGGAAGTGATCGAGGATTGGTGGTGGGATGGTGTTCTCAGACAGC
TGTTTTGGCGCATTGTGCTGTGGGATGTTTTGTGACTCATTGTGGTTGGAATTCGACG
TTGGAGAGTTTAGAGAGTGGTGTTCCGGTGGTTGCGTTTCCGCAGTTTGCTGATCAGT
GTACAACGGCGAAGCTTGTGGAGGATACGTGGAGGATTGGAGTGAAGGTGAAGGTT
GGGGAGGAAGGAGATGTGGATGGGGAGGAGATTAGAAGGTGTTTGGAGAAGGTGA
TGAGTGGTGGAGAAGAGGCGGAGGAGATGAGAGAGAATGCAGAGAAGTGGAAGGC
GATGGCTGTTGATGCGGCAGCGGAAGGTGGACCGTCGGATTTGAATCTTAAAGGTTT
TGTGGACGAGGATGAGTAG

(8) pJ15AtGt 7.3

CATCGAAAGGACAGTAGAAAAGGAAGGTGGCTCCTACAAATGCCATCATTGCGATA
AAGGAAAGGCTATCATTCAAGATGCCTCTGCCGACAGTGGTCCCAAAGATGGACCCC
CACCCACGAGGAGCATCGTGGAAAAAGAAGACGTTCCAACCACGTCTTCAAAGCAA
GTGGATTGATGTGACATCTCCACTGACGTAAGGGATGACGCACAATCCCACTATCCT
TCGCAAGACCCTTCCTCTATATAAGGAAGTTCATTTCATTTGGAGAGGACAGCCCAA
GCTTGGCTGCAGGTCGACGGATCCCCATCAAACAAGTTTGTACAAAAAAGCAGGCTG
GATGGCCACTTCCGTCAATGGTTCCCATCGTCGTCCACATTACTTGCTTGTAACATTC
CCAGCGCAAGGTCACATCAACCCGGCGCTTCAACTAGCCAACCGCCTCATCCACCAC
GGTGCAACCGTCACATACTCCACCGCAGTCTCTGCTCACCGACGTATGGGCGAGCCA
CCTTCCACAAAAGGTCTATCCTTCGCTTGGTTCACCGATGGATTCGACGACGGTCTCA
AGTCATTCGAAGACCAGAAAATCTACATGTCCGAACTCAAACGATGTGGTTCAAACG
CCCTGAGAGACATCATCAAAGCCAATCTTGACGCCACCACCGAAACAGAGCCTATC
ACCGGGGTAATCTACTCTGTTCTCGTCCCGTGGGTTTCTACGGTAGCGCGTGAGTTTC
ACCTCCCAACTACACTTCTCTGGATTGAACCAGCTACTGTACTAGACATCTACTACTA
CTACTTCAACACCTCTTACAAACATCTCTTCGACGTTGAACCGATTAAATTACCGAAA
CTGCCACTGATCACCACCGGTGACCTCCCGTCGTTTCTTCAACCTTCGAAGGCATTAC
CGTCAGCTCTTGTGACTCTAAGAGAACATATCGAAGCTCTCGAAACGGAATCAAACC
CTAAGATTCTTGTTAACACATTCTCTGCTTTGGAACACGATGCTTTAACCTCTGTTGA
GAAACTCAAGATGATCCCAATCGGACCGTTGGTTTCTTCCTCCGAGGGTAAAACCGA
TCTTTTCAAATCTTCCGACGAGGATTACACGAAATGGTTAGACTCGAAGCTCGAGAG
ATCAGTGATTTACATTTCCTTAGGCACACACGCCGATGATTTACCAGAGAAACACAT
GGAAGCGCTTACTCACGGCGTGTTAGCTACAAACAGACCGTTTTTATGGATCGTGAG
GGAGAAAAATCCAGAAGAGAAGAAGAAGAATCGGTTTCTTGAATTGATCAGAGGAA
GTGATCGAGGATTGGTGGTGGGATGGTGTTCTCAGACAGCTGTTTTGGCGCATTGTG
CTGTGGGATGTTTTGTGACTCATTGTGGTTGGAATTCGACGTTGGAGAGTTTAGAGA
GTGGTGTTCCGGTGGTTGCGTTTCCGCAGTTTGCTGATCAGTGTACAACGGCGAAGC
TTGTGGAGGATACGTGGAGGATTGGAGTGAAGGTGAAGGTTGGGGAGGAAGGAGAT
GTGGATGGGGAGGAGATTAGAAGGTGTTTGGAGAAGGTGATGAGTGGTGGAGAAGA
GGCGGAGGAGATGAGAGAGAATGCA—

(9) pEnt207Ch3MAT

GCAGGCTGGATGGCTTCCAATTCCATTGTTACAATTCTTGAACAATCTCGAATATCCT
CACCACCAGGCACCATTGGTGAACGTTCATTGCCACTTACTTTTTTCGACATTGGATG
GGTACCTTTCCCTCCAGTCCACCATGTTTTCTTCTACCGCTTCCCGCACTCTAAATCA
CATTTCTTAGAAACCGTTGTCCCAAATCTTAAACACTCTTTATCACTCGCACTACAAC
ATTTTTTCCCATTCGCTAGCAATTTGTATGTATCTCCTAATGCTGATGATTTTGGCGTC
ATTAGAAAACCGGAAATTAGACACGTGGAAGGTGATTATGTTGCACTTACTTTTGCA
GAATGTTCTCTTGATTTTAATGATTTGACAGGAAATCATCCTCGAAAATGTGAAAAC
TTTTATCCACTTGTGCCTCCATTAGGTAATGTTGTTAAAATGGCTGATTGTGTCACAA
TCCCACTTTTTTCAGTCCAAGTGACGTACTTTAGGGACTCGGGTATCTCTATTGGAAT
GACAAATCATCATAGCCTAGGTGACGCTAGCACACGCCTTGGTTTTTTGAAGGTGTG
GACTTCAATTGCTAAATCGGGGGGGTGATCAATCACTTTTAATGAATGGATCACTCCC
GGTTTTAGATAGATTGATTGACGTTCCAAAACTAGATGAATACAGATTGAGGCACAC
AAGCCTTGAAACTTTTTATCAGCCTCCGAGCCTTGTTGGGCCTACAAAGAAAGTTCG
GGCAACATTTATATTGAGTCGAACCAATATCAATCAGTTAAAGAAAAGGGTCCTTAC
CCAAATCCCAACATTGGAATACATATCATCTTTTACGGTAACTTGTGGTTATATATGG
AGTTGCATTGCAAAATCACTAGTGAAAATGGGAGAAAAAAAGGGCGAGGATGAGTT
AGAACAATTCATTTGCACGGCTGATTGTCGCTCTCGTATGGATCCACCGATTCCATCA
ACCTACTTTGGTAATTGTGGTGCACCATGTGTCACAACCATAAAAAATGTTGTTTTGT
CGAGTGAAAATGGATTTGTATTCGCTGCTAAACTAATTGGCGAGGCTATAAATAAAA
TGGTAAAGAATAAGGAAGGAATCTTGAAAGATGCCGAGAGATGGCATGATGCTTTC
AAGATTCCAGCAAGGAAGATTGGTGTTGCGGGTACACCAAAGCTCAACTTCTATGAT
ATTGATTTTGGGTGGGGGAAGCCGCAAAAGAATGAAACTATTTCGATTGATTATAAC

GGTTCGGTTGCTATAAATGCAAGCAAAGAATCAACACAAGATTTTGAAATTGGATTG
TGTTTTTCAAATATGCAAATGGAGGCGTTTGCTGATATCTTTAATCACGGATTAGAGA
GTGAGATATAAGACCCAGCTTTCTTGTACAAAGTTGG

(10) pEnt207R183F-Ch3MAT

ATGGCTTCCAATTCCATTGTTACAATTCTTGAACAATCTCGAATATCCTCACCACCAG
GCACCATTGGTGAACGTTCATTGCCACTTACTTTTTTCGACATTGGATGGGTACCTTT
CCCTCCAGTCCACCATGTTTTCTTCTACCGCTTCCCGCACTCTAAATCACATTTCTTAG
AAACCGTTGTCCCAAATCTTAAACACTCTTTATCACTCGCACTACAACATTTTTTCCC
ATTCGCTAGCAATTTGTATGTATCTCCTAATGCTGATGATTTTGGCGTCATTAGAAAA
CCGGAAATTAGACACGTGGAAGGTGATTATGTTGCACTTACTTTTGCAGAATGTTCT
CTTGATTTTAATGATTTGACAGGAAATCATCCTCGAAAATGTGAAAACTTTTATCCAC
TTGTGCCTCCATTAGGTAATGTTGTTAAAATGGCTGATTGTGTCACAATCCCACTTTT
TTCAGTCCAAGTGACGTACTTTAGGGACTCGGGTATCTCTATTGGAATGACAAATCA
TCATAGCCTAGGTGACGCTAGCACATTCCTTGGTTTTTTGAAGGTGTGGACTTCAATT
GCTAAATCGGGGGGGTGATCAATCACTTTTAATGAATGGATCACTCCCGGTTTTAGAT
AGATTGATTGACGTTCCAAAACTAGATGAATACAGATTGAGGCACACAAGCCTTGAA
ACTTTTTATCAGCCTCCGAGCCTTGTTGGGCCTACAAAGAAAGTTCGGGCAACATTT
ATATTGAGTCGAACCAATATCAATCAGTTAAAGAAAAGGGTCCTTACCCAAATCCCA
ACATTGGAATACATATCATCTTTTACGGTAACTTGTGGTTATATATGGAGTTGCATTG
CAAAATCACTAGTGAAAATGGGAGAAAAAAAAGGGCGAGGATGAGTTAGAACAATTC
ATTTGCACGGCTGATTGTCGCTCTCGTATGGATCCACCGATTCCATCAACCTACTTTG
GTAATTGTGGTGCACCATGTGTCACAACCATAAAAAATGTTGTTTTGTCGAGTGAAA
ATGGATTTGTATTCGCTGCTAAACTAATTGGCGAGGCTATAAATAAAATGGTAAAGA
ATAAGGAAGGAATCTTGAAAGATGCCGAGAGATGGCATGATGCTTTCAAGATTCCA
GCAAGGAAGATTGGTGTTGCGGGTACACCAAAGCTCAACTTCTATGATATTGATTTT
GGGTGGGGGAAGCCGCAAAAGAATGAAACTATTTCGATTGATTATAACGGTTCGGTT
GCTATAAATGCAAGCAAAGAATCAACACAAGATTTTGAAATTGGATTGTGTTTTTCA
AATATGCAAATGGAGGCGTTTGCTGATATCTTTAATCACGGATTAGAGAGTGAGATA
TAAGACCCAGCTTTCTTGTACAAAGTTGGCATTATAA

(11) pEntPeF3’5’H

TCCGGGCCGTTGCTTCACAACGTTCAAATCCGCTCCCGGCGGATTTGTCCTACTCAGG
AGAGCGTTCACCGACAAACAACAGATAAAACGAAAGGCCCAGTCTTCCGACTGAGC
CTTTCGTTTTATTTGATGCCTGGCAGTTCCCTACTCTCGCGTTAACGCTAGCATGGAT
CTCGGGCCCCAAATAATGATTTTATTTTGACTGATAGTGACCTGTTCGTTGCAACAAA
TTGATGAGCAATGCTTTTTTATAATGCCAACTTTGTACAAAAAAGCAGGCTGGACCA
TGATGCTACTTACTGAGCTTGGTGCAGCAACTTCAATCTTTCTAATAGCACACATAAT
CATTTCAACTCTTATTTCAAAAACTACCGGCCGGCATCTACCGCCGGGGCCAAGAGG
GTGGCCGGTGATCGGAGCACTTCCACTTTTAGGAGCCATGCCACATGTTTCCTTAGCT
AAAATGGCAAAAAAATATGGAGCAATCATGTATCTCAAAGTTGGAACATGTGGCAT
GGCAGTTGCTTCTACCCCTGATGCTGCTAAAGCATTCTTGAAAACACTTGATATCAAC
TTCTCCAATCGTCCACCTAATGCAGGTGCCACTCACTTAGCTTATAATGCTCAAGACA
TGGTTTTTGCACATTATGGACCACGATGGAAGTTGCTAAGGAAATTAAGCAACTTGC
ATATGCTAGGGGGAAAAGCCTTAGAGAATTGGGCAAATGTTCGTGCCAATGAGCTA
GGGCACATGCTAAAATCAATGTCCGATATGAGTCGAGAGGGCCAGAGGGTTGTGGT
AGCGGAGATGTTGACATTTGCCATGGCCAATATGATCGGACAAGTGATGCTAAGCAA
AAGAGTATTTGTAGATAAAGGTGTTGAGGTAAATGAATTTAAGGACATGGTTGTAGA
GTTAATGACAATAGCAGGGTATTTCAACATTGGTGATTTTATTCCTTGTTTAGCTTGG
ATGGATTTACAAGGGATAGAAAAACGAATGAAACGTTTACATAAGAAGTTTGATGC
TTTATTGACAAAGATGTTTGATGAACACAAAGCAACTACCTATGAACGTAAGGGGAA
ACCAGATTTTCTTGATGTTGTTATGGAAAATGGGGACAATTCTGAAGGAGAAAGACT

CAGTACAACCAACATCAAAGCACTTTTGCTGAATTTGTTCACAGCTGGTACGGACAC
TTCTTCTAGTGCAATAGAATGGGCACTTGCAGAAATGATGAAGAACCCTGCCATTTT
GAAAAAAGCACAAGCAGAAATGGATCAAGTCATTGGAAGAAATAGGCGTTTACTCG
AATCCGATATCCCAAATCTCCCTTACCTCCGAGCAATTTGCAAAGAAACATTTCGAA
AACACCCTTCTACACCATTAAATCTTCCTAGGATCTCGAACGAACCATGCATAGTCG
ATGGTTATTACATACCAAAAAACACTAGGCTTAGTGTTAACATATGGGCAATTGGAA
GAGATCCCCAAGTTTGGGAAAATCCACTAGAGTTTAATCCCGAAAGATTCTTGAGTG
GAAGAAACTCCAAGATTGATCCTCGAGGGAACGATTTTGAATTGATACCATTTGGTG
CTGGACGAAGAATTTGTGCAGGAACAAGAATGGGAATTGTAATGGTGGAATATATA
TTAGGAACTTTGGTTCATTCATTTGATTGGAAATTACCAAGTGAAGTTATTGAGTTGA
ATATGGAAGAAGCTTTTGGCTTAGCTTTGCAGAAAGCTGTCCCTCTTGAAGCTATGG
TTACTCCAAGGTTACAATTGGATGTTTATGTACCATAGGACCCAGCTTTCTTGTACAA
AGTTGGCATTATAAGAAAGCATTG

(12) pE29AtAT

AGGAAGCAGCCCAGTAGTAGGTTGAGGCCGTTGAGCACCGCCGCCGCAAGGAATGG
TGCATGCAAGGAGATGGCGCCCAACAGTCCCCCGGCCACGGGGCCTGCCACCATAC
CCACGCCGAAACAAGCGCTCATGAGCCCGAAGTGGCGAGCCCGATCTTCCCCATCG
GTGATGTCGGCGATATAGGCGCCAGCAACCGCACCTGTGGCGCCGGTGATGCCGGC
CACGATGCGTCCGGCGTAGAGGATCGAGATCGATCTCGATCCCGCGAAATTAATACG
ACTCACTATAGGGGAATTGTGAGCGGATAACAATTCCCCTCTAGAAATAATTTTGTT
TAACTTTAAGAAGGAGATATACATATGAAAGAAACCGCTGCTGCTAAATTCGAACGC
CAGCACATGGACAGCCCAGATCTGATGGTGGCTCATCTTCAACCTCCTAAGATCATC
GAGACCTGTCACATCTCTCCCCCAAAGGGCACCGTTCCATCAACCACTCTTCCTCTCA
CCTTCTTCGATGCCCCCTGGCTCTCTCTCCCACTCGCCGATTCTCTCTTCTTCTTCTCT
TACCAAAACTCAACTGAATCTTTCCTCCAAGACTTTGTACCCAACCTCAAACATTCCC
TCTCCATCACTCTCCAACATTTCTTCCCTTACGCCGGTAAACTGATTATCCCGCCTCG
TCCCGACCCTCCATATTTACACTACAACGATGGCCAAGACTCTCTTGTTTTCACCGTA
GCAGAGTCTACTGAAACCGACTTCGACCAACTGAAGTCTGATTCCCCTAAAGATATC
AGTGTGTTGCATGGCGTCTTGCCCAAGTTACCTCCTCCTCACGTCTCTCCGGAAGGAA
TTCAGATGCGACCAATAATGGCTATGCAAGTCACCATCTTCCCTGGAGCTGGAATCT
GTATAGGCAACTCAGCTACACATGTTGTAGCAGATGGAGTCACCTTCAGTCATTTCA
TGAAGTATTGGATGTCATTGACCAAATCCAGCGGTAAAGATCCCGCCACGGTTCTTC
TACCCTCTCTGCCTATTCACAGCTGCAGAAACATGATCAAGGACCCAGGCGAGGTAG
GCGCAGGACATTTGGAGCGGTTTTGGAGCCAAAACTCTGCAAAACACAGTTCACATG
TTACGCCTGAGAACATGGTCAGAGCCACTTTTACATTGAGCCGGAAGCAGATAGATA
ATCTAAAAAGTTGGGTTACAGAGCAGTCTGAGAATCAATCTCCTGTTTCTACCTTCGT
GGTGACTCTAGCTTTCATTTGGGTAAGCTTGATCAAGACACTTGTACAAGACAGTGA
AACAAAGGCCAACGAGGAAGACAAGGATGAAGTATTTCACTTGATGATCAATGTGG
ATTGCAGGAATCGCCTCAAGTACACACAACCAATACCACAAACATACTTTGGCAACT
GTATGGCTCCTGGTATCGTATCAGTCAAGAAACACGATTTGCTAGGAGAAAAATGCG
TTTTGGCGGCTTCAGATGCAATCACAGCGAGAATCAAAGATATGTTATCAAGCGATC
TGTTGAAGACAGCACCAAGATGGGGACAAGGAGTACGTAAATGGGTCATGTCCCAT
TATCCAACCTCAATTGCAGGAGCTCCGAAATTGGGACTGTATGACATGGATTTTGGA
TTAGGAAAGCCCTGCAAAATGGAGATCGTGCACATAGAAACAGGTGGTTCTATCGC
ATTCTCAGAGTCCAGAGACGGCAGCAATGGAGTTGAGATTGGAATAGCACTAGAGA
AGAAGAAAATGGATGTGTTTGACTCAATTCTACAACAGGGGATCAAGAAATTCGCA
ACGTAGCTCGAGCACCACCACCACCACCACTGAGATCCGGCTGCTAACAAAGCCCG
AAAGGAAGCTGAGTTGGCTGCTGCCACCGCTGAGCAATAACTAGCATAACCCCTTGG
GGCCTCTAAACGGGTCTTGAGGGGTTTTTTGCTGAAAGGAGGAACTATATCCGGATT
GGCGAATGGGACGCGCCCTGTAGCGGCGCATTAAGCGCGGCGGGTGTGGTGGTTAC

GCGCAGCGTGACCGCTACACTTGCCAGCGCCCTAGCGCCCGCTCCTTTCGCTTTCTTC
CCTTCC

(13) pE29SlAT

GAGCACCGCCGCCGCAAGGAATGGTGCATGCAAGGAGATGGCGCCCAACAGTCCCC
CGGCCACGGGGCCTGCCACCATACCCACGCCGAAACAAGCGCTCATGAGCCCGAAG
TGGCGAGCCCGATCTTCCCCATCGGTGATGTCGGCGATATAGGCGCCAGCAACCGCA
CCTGTGGCGCCGGTGATGCCGGCCACGATGCGTCCGGCGTAGAGGATCGAGATCGAT
CTCGATCCCGCGAAATTAATACGACTCACTATAGGGGAATTGTGAGCGGATAACAAT
TCCCCTCTAGAAATAATTTTGTTTAACTTTAAGAAGGAGATATACATATGAAAGAAA
CCGCTGCTGCTAAATTCGAACGCCAGCACATGGACAGCCCAGATCTGATGAGCCAA
ATTACAACACAAAATTTGAATGGTACTTGTATTCAAATTGAAATCTTGAATGAAAAA
CTTATAAAACCATCGTTACCAACTCCAAATCATCTCAATTCCTACAAGTTATCATTTT
TTGATCAAATTGCACCTAATTTTGCTGTACCCCTTCTTTACTTCTACCCTCCAGTACCA
CCAGAAAACTCCCACCTACAACGCGTCGAAGAAGTTCATAAACAACTACAAAACTC
ACTGTCTGAAGTTCTAACCAAGTTCTATCCACTTGCTGGAAGGTTGTCTGAAGATGGT
ACTTCCATTGAATGTCATGACCAAGGGGTTATTTACTTGGAAGCAAAGGTGAATTGT
CAATTGAATGAATTTCTAGACAAAGCATACAAAGATAGTGACCTTGTTAAAATCTTT
GTACCACCTATAAGAATTAGGCTAGCTGAATTGCCAAATAGACCAATGATGGCAATT
CAGGCCACCATGTTTGAACATGGTGGCCTGGCGCTAGCCGTGCAAATTGTCCACACA
ACAGGTGATGGATTCTCTGGCTGCGCGATCACCGATGAGTGGGCTAAAGTTAGTCGA
ATGGAGAAAGGGAATGTGAGAAATTTACAATTTCGTTCGGATTTAGTGGAAGTATTT
CCACCTAGGGATAATATTTTGGAGATGATTAAAAAAGGTAGGCCTAGAGGATATGA
AATGAAAATTGCTACAAGAATTTTCATGTTTGATGAAATTGCAATATCTAAGTTGAA
GGAAAATGTGAACAAGTTTATGAGTTATTCATCAAGAGTTGAAGTTGTGACTGCACT
TATTTGGAGAAGCCTTATGCGTGTGGTGAGGTTGAGACATGGTCACAATAGGCCATC
CATGCTACAATTTGCCATAAATTTAAGAGGAAGAGGGTCTCCAAGAGTAGTTGGGGA
AGATCAAAACTTTTTTGGGAACTTCTACCTTGACATTCCAATCAAATATGTGTCATCT
CGTAGCAATCAAGATCCAGAATTACATGAAATTGTAACCTTAATTAGGAATGCGAAG
AACAAAATTCTATCAGAGATTGCAAATGCTTCAAGTGAAGAGATTTTCTCAATATTA
ATTGAGTCATTGAATCAAATAAGAGAAGGGTATAATGATGATGAAATTGACCTTTAT
CCAACTTCAAGTTTGTGTAAATTTCCACTAAATGAGTCTGATTTTGGATGGGCTAAAC
CAATTTGGGTGAGCAGAGTAAATGTGCCATTTCAAATGTTCTTCTTGATGGACTCAA
AAAATGGGATTGAAGCTAGAGTTTGCTTGAATGAAGAGGATATGATGAAGTTGGAA
AAGGATGTTGATATTGTGGAGTTTAGTTATGTGCCAAAGTAGCTCGAGCACCACCAC
CACCACCACTGAGATCCGGCTGCTAACAAAGCCCGAAAGGAAGCTGAGTTGGCTGC
TGCCACCGCTGAGCAATAACTAGCATAACCCCTTGGGGCCTCTAAACGGGTCTTGAG
GGGTTTTTTGCTGAAAGGAGGAACTATATCCGGATTGGCGAATG

(14) pE29Ch3MAT

GCAGCCCAGTAGTAGGTTGAGGCCGTTGAGCACCGCCGCCGCAAGGAATGGTGCAT
GCAAGGAGATGGCGCCCAACAGTCCCCCGGCCACGGGGCCTGCCACCATACCCACG
CCGAAACAAGCGCTCATGAGCCCGAAGTGGCGAGCCCGATCTTCCCCATCGGTGATG
TCGGCGATATAGGCGCCAGCAACCGCACCTGTGGCGCCGGTGATGCCGGCCACGAT
GCGTCCGGCGTAGAGGATCGAGATCGATCTCGATCCCGCGAAATTAATACGACTCAC
TATAGGGGAATTGTGAGCGGATAACAATTCCCCTCTAGAAATAATTTTGTTTAACTTT
AAGAAGGAGATATACATATGAAAGAAACCGCTGCTGCTAAATTCGAACGCCAGCAC
ATGGACAGCCCAGATCTGATGGCTTCCAATTCCATTGTTACAATTCTTGAACAATCTC
GAATATCCTCACCACCAGGCACCATTGGTGAACGTTCATTGCCACTTACTTTTTTCGA
CATTGGATGGGTACCTTTCCCTCCAGTCCACCATGTTTTCTTCTACCGCTTCCCGCACT
CTAAATCACATTTCTTAGAAACCGTTGTCCCAAATCTTAAACACTCTTTATCACTCGC
ACTACAACATTTTTTCCCATTCGCTAGCAATTTGTATGTATCTCCTAATGCTGATGAT

TTTGGCGTCATTAGAAAACCGGAAATTAGACACGTGGAAGGTGATTATGTTGCACTT
ACTTTTGCAGAATGTTCTCTTGATTTTAATGATTTGACAGGAAATCATCCTCGAAAAT
GTGAAAACTTTTATCCACTTGTGCCTCCATTAGGTAATGTTGTTAAAATGGCTGATTG
TGTCACAATCCCACTTTTTTCAGTCCAAGTGACGTACTTTAGGGACTCGGGTATCTCT
ATTGGAATGACAAATCATCATAGCCTAGGTGACGCTAGCACACGCCTTGGTTTTTTG
AAGGTGTGGACTTCAATTGCTAAATCGGGGGGTGATCAATCACTTTTAATGAATGGA
TCACTCCCGGTTTTAGATAGATTGATTGACGTTCCAAAACTAGATGAATACAGATTG
AGGCACACAAGCCTTGAAACTTTTTATCAGCCTCCGAGCCTTGTTGGGCCTACAAAG
AAAGTTCGGGCAACATTTATATTGAGTCGAACCAATATCAATCAGTTAAAGAAAAGG
GTCCTTACCCAAATCCCAACATTGGAATACATATCATCTTTTACGGTAACTTGTGGTT
ATATATGGAGTTGCATTGCAAAATCACTAGTGAAAATGGGAGAAAAAAAGGGCGAG
GATGAGTTAGAACAATTCATTTGCACGGCTGATTGTCGCTCTCGTATGGATCCACCG
ATTCCATCAACCTACTTTGGTAATTGTGGTGCACCATGTGTCACAACCATAAAAAAT
GTTGTTTTGTCGAGTGAAAATGGATTTGTATTCGCTGCTAAACTAATTGGCGAGGCTA
TAAATAAAATGGTAAAGAATAAGGAAGGAATCTTGAAAGATGCCGAGAGATGGCAT
GATGCTTTCAAGATTCCAGCAAGGAAGATTGGTGTTGCGGGTACACCAAAGCTCAAC
TTCTATGATATTGATTTTGGGTGGGGGAAGCCGCAAAAGAATGAAACTATTTCGATT
GATTATAACGGTTCGGTTGCTATAAATGCAAGCAAAGAATCAACACAAGATTTTGAA
ATTGGATTGTGTTTTTCAAATATGCAAATGGAGGCGTTTGCTGATATCTTTAATCACG
GATTAGAGAGTGAGATATAACTCGAGCACCACCACCACCACCACTGAGATCCGGCT
GCTAACAAAGCCCGAAAGGAAGCTGAGTTGGCTGCTGCCACCGCTGAGCAATAACT
AGCATAACCCCTTGGGGCCTCTAAACGGGTCTTGAGGGGTTTTTTGCTGAAAGGAGG
AACTATATCCGGATTGGCGAATGGGACGCGCCCTGTAGCGGCGCATTAA

(15) pE29F181RAtAT

AGCACCGCCGCCGCAAGGAATGGTGCATGCAAGGAGATGGCGCCCAACAGTCCCCC
GGCCACGGGGCCTGCCACCATACCCACGCCGAAACAAGCGCTCATGAGCCCGAAGT
GGCGAGCCCGATCTTCCCCATCGGTGATGTCGGCGATATAGGCGCCAGCAACCGCAC
CTGTGGCGCCGGTGATGCCGGCCACGATGCGTCCGGCGTAGAGGATCGAGATCGATC
TCGATCCCGCGAAATTAATACGACTCACTATAGGGGAATTGTGAGCGGATAACAATT
CCCCTCTAGAAATAATTTTGTTTAACTTTAAGAAGGAGATATACATATGAAAGAAAC
CGCTGCTGCTAAATTCGAACGCCAGCACATGGACAGCCCAGATCTGATGGTGGCTCA
TCTTCAACCTCCTAAGATCATCGAGACCTGTCACATCTCTCCCCCAAAGGGCACCGTT
CCATCAACCACTCTTCCTCTCACCTTCTTCGATGCCCCCTGGCTCTCTCTCCCACTCGC
CGATTCTCTCTTCTTCTTCTCTTACCAAAACTCAACTGAATCTTTCCTCCAAGACTTTG
TACCCAACCTCAAACATTCCCTCTCCATCACTCTCCAACATTTCTTCCCTTACGCCGG
TAAACTGATTATCCCGCCTCGTCCCGACCCTCCATATTTACACTACAACGATGGCCA
AGACTCTCTTGTTTTCACCGTAGCAGAGTCTACTGAAACCGACTTCGACCAACTGAA
GTCTGATTCCCCTAAAGATATCAGTGTGTTGCATGGCGTCTTGCCCAAGTTACCTCCT
CCTCACGTCTCTCCGGAAGGAATTCAGATGCGACCAATAATGGCTATGCAAGTCACC
ATCTTCCCTGGAGCTGGAATCTGTATAGGCAACTCAGCTACACATGTTGTAGCAGAT
GGAGTCACCCGCAGTCATTTCATGAAGTATTGGATGTCATTGACCAAATCCAGCGGT
AAAGATCCCGCCACGGTTCTTCTACCCTCTCTGCCTATTCACAGCTGCAGAAACATG
ATCAAGGACCCAGGCGAGGTAGGCGCAGGACATTTGGAGCGGTTTTGGAGCCAAAA
CTCTGCAAAACACAGTTCACATGTTACGCCTGAGAACATGGTCAGAGCCACTTTTAC
ATTGAGCCGGAAGCAGATAGATAATCTAAAAAGTTGGGTTACAGAGCAGTCTGAGA
ATCAATCTCCTGTTTCTACCTTCGTGGTGACTCTAGCTTTCATTTGGGTAAGCTTGATC
AAGACACTTGTACAAGACAGTGAAACAAAGGCCAACGAGGAAGACAAGGATGAAG
TATTTCACTTGATGATCAATGTGGATTGCAGGAATCGCCTCAAGTACACACAACCAA
TACCACAAACATACTTTGGCAACTGTATGGCTCCTGGTATCGTATCAGTCAAGAAAC

ACGATTTGCTAGGAGAAAAATGCGTTTTGGCGGCTTCAGATGCAATCACAGCGAGAA
TCAAAGATATGTTATCAAGCGATCTGTTGAAGACAGCACCAAGATGGGGACAAGGA
GTACGTAAATGGGTCATGTCCCATTATCCAACCTCAATTGCAGGAGCTCCGAAATTG
GGACTGTATGACATGGATTTTGGATTAGGAAAGCCCTGCAAAATGGAGATCGTGCAC
ATAGAAACAGGTGGTTCTATCGCATTCTCAGAGTCCAGAGACGGCAGCAATGGAGTT
GAGATTGGAATAGCACTAGAGAAGAAGAAAATGGATGTGTTTGACTCAATTCTACA
ACAGGGGATCAAGAAATTCGCAACGTAGCTCGAGCACCACCACCACCACCACTGAG
ATCCGGCTGCTAACAAAGCCCGAAAGGAAGCTGAGTTGGCTGCTGCCACCGCTGAG
CAATAACTAGCATAACCCCTTGGGGCCTCTAAACGGGTCTTGAGGGGTTTTTTGCTG
AAAGGAGGAACTATATCCGGATTGGCGAATGGGACGCGCCCTGT

(16) pE29F181RSlAT

GGTGTCCGGGATCTCGACGCTCTCCCTTATGCGACTCCTGCATTAGGAAGCAGCCCA
GTAGTAGGTTGAGGCCGTTGAGCACCGCCGCCGCAAGGAATGGTGCATGCAAGGAG
ATGGCGCCCAACAGTCCCCCGGCCACGGGGCCTGCCACCATACCCACGCCGAAACA
AGCGCTCATGAGCCCGAAGTGGCGAGCCCGATCTTCCCCATCGGTGATGTCGGCGAT
ATAGGCGCCAGCAACCGCACCTGTGGCGCCGGTGATGCCGGCCACGATGCGTCCGG
CGTAGAGGATCGAGATCGATCTCGATCCCGCGAAATTAATACGACTCACTATAGGGG
AATTGTGAGCGGATAACAATTCCCCTCTAGAAATAATTTTGTTTAACTTTAAGAAGG
AGATATACATATGAAAGAAACCGCTGCTGCTAAATTCGAACGCCAGCACATGGACA
GCCCAGATCTGATGAGCCAAATTACAACACAAAATTTGAATGGTACTTGTATTCAAA
TTGAAATCTTGAATGAAAAACTTATAAAACCATCGTTACCAACTCCAAATCATCTCA
ATTCCTACAAGTTATCATTTTTTGATCAAATTGCACCTAATTTTGCTGTACCCCTTCTT
TACTTCTACCCTCCAGTACCACCAGAAAACTCCCACCTACAACGCGTCGAAGAAGTT
CATAAACAACTACAAAACTCACTGTCTGAAGTTCTAACCAAGTTCTATCCACTTGCT
GGAAGGTTGTCTGAAGATGGTACTTCCATTGAATGTCATGACCAAGGGGTTATTTAC
TTGGAAGCAAAGGTGAATTGTCAATTGAATGAATTTCTAGACAAAGCATACAAAGAT
AGTGACCTTGTTAAAATCTTTGTACCACCTATAAGAATTAGGCTAGCTGAATTGCCA
AATAGACCAATGATGGCAATTCAGGCCACCATGTTTGAACATGGTGGCCTGGCGCTA
GCCGTGCAAATTGTCCACACAACAGGTGATGGACGTTCTGGCTGCGCGATCACCGAT
GAGTGGGCTAAAGTTAGTCGAATGGAGAAAGGGAATGTGAGAAATTTACAATTTCG
TTCGGATTTAGTGGAAGTATTTCCACCTAGGGATAATATTTTGGAGATGATTAAAAA
AGGTAGGCCTAGAGGATATGAAATGAAAATTGCTACAAGAATTTTCATGTTTGATGA
AATTGCAATATCTAAGTTGAAGGAAAATGTGAACAAGTTTATGAGTTATTCATCAAG
AGTTGAAGTTGTGACTGCACTTATTTGGAGAAGCCTTATGCGTGTGGTGAGGTTGAG
ACATGGTCACAATAGGCCATCCATGCTACAATTTGCCATAAATTTAAGAGGAAGAGG
GTCTCCAAGAGTAGTTGGGGAAGATCAAAACTTTTTTGGGAACTTCTACCTTGACAT
TCCAATCAAATATGTGTCATCTCGTAGCAATCAAGATCCAGAATTACATGAAATTGT
AACCTTAATTAGGAATGCGAAGAACAAAATTCTATCAGAGATTGCAAATGCTTCAAG
TGAAGAGATTTTCTCAATATTAATTGAGTCATTGAATCAAATAAGAGAAGGGTATAA
TGATGATGAAATTGACCTTTATCCAACTTCAAGTTTGTGTAAATTTCCACTAAATGAG
TCTGATTTTGGATGGGCTAAACCAATTTGGGTGAGCAGAGTAAATGTGCCATTTCAA
ATGTTCTTCTTGATGGACTCAAAAAATGGGATTGAAGCTAGAGTTTGCTTGAATGAA
GAGGATATGATGAAGTTGGAAAAGGATGTTGATATTGTGGAGTTTAGTTATGTGCCA
AAGTAGCTCGAGCACCACCACCACCACCACTGAGATCCGGCTGCTAACAAAGCCCG
AAAGGAAGCTGAGTTGGCTGCTGCCACCGCTGAGCAATAACTAGCATAACCCCTTGG
GGCCTCTAAACGGGTCTTGAGGGGTTTTTTGCTGAAAGGAGGAACTATATCCGGATT
GGCGAATGGGACGCGCCCTGTAGCGGCGCATTAAGCGCG

(17) pE29R183F-Ch3MAT

GAGCACCGCCGCCGCAAGGAATGGTGCATGCAAGGAGATGGCGCCCAACAGTCCCC
CGGCCACGGGGCCTGCCACCATACCCACGCCGAAACAAGCGCTCATGAGCCCGAAG
TGGCGAGCCCGATCTTCCCCATCGGTGATGTCGGCGATATAGGCGCCAGCAACCGCA

CCTGTGGCGCCGGTGATGCCGGCCACGATGCGTCCGGCGTAGAGGATCGAGATCGAT
CTCGATCCCGCGAAATTAATACGACTCACTATAGGGGAATTGTGAGCGGATAACAAT
TCCCCTCTAGAAATAATTTTGTTTAACTTTAAGAAGGAGATATACATATGAAAGAAA
CCGCTGCTGCTAAATTCGAACGCCAGCACATGGACAGCCCAGATCTGATGGCTTCCA
ATTCCATTGTTACAATTCTTGAACAATCTCGAATATCCTCACCACCAGGCACCATTGG
TGAACGTTCATTGCCACTTACTTTTTTCGACATTGGATGGGTACCTTTCCCTCCAGTC
CACCATGTTTTCTTCTACCGCTTCCCGCACTCTAAATCACATTTCTTAGAAACCGTTG
TCCCAAATCTTAAACACTCTTTATCACTCGCACTACAACATTTTTTCCCATTCGCTAG
CAATTTGTATGTATCTCCTAATGCTGATGATTTTGGCGTCATTAGAAAACCGGAAATT
AGACACGTGGAAGGTGATTATGTTGCACTTACTTTTGCAGAATGTTCTCTTGATTTTA
ATGATTTGACAGGAAATCATCCTCGAAAATGTGAAAACTTTTATCCACTTGTGCCTCC
ATTAGGTAATGTTGTTAAAATGGCTGATTGTGTCACAATCCCACTTTTTTCAGTCCAA
GTGACGTACTTTAGGGACTCGGGTATCTCTATTGGAATGACAAATCATCATAGCCTA
GGTGACGCTAGCACATTCCTTGGTTTTTTGAAGGTGTGGACTTCAATTGCTAAATCGG
GGGGTGATCAATCACTTTTAATGAATGGATCACTCCCGGTTTTAGATAGATTGATTG
ACGTTCCAAAACTAGATGAATACAGATTGAGGCACACAAGCCTTGAAACTTTTTATC
AGCCTCCGAGCCTTGTTGGGCCTACAAAGAAAGTTCGGGCAACATTTATATTGAGTC
GAACCAATATCAATCAGTTAAAGAAAAGGGTCCTTACCCAAATCCCAACATTGGAAT
ACATATCATCTTTTACGGTAACTTGTGGTTATATATGGAGTTGCATTGCAAAATCACT
AGTGAAAATGGGAGAAAAAAAGGGCGAGGATGAGTTAGAACAATTCATTTGCACGG
CTGATTGTCGCTCTCGTATGGATCCACCGATTCCATCAACCTACTTTGGTAATTGTGG
TGCACCATGTGTCACAACCATAAAAAATGTTGTTTTGTCGAGTGAAAATGGATTTGT
ATTCGCTGCTAAACTAATTGGCGAGGCTATAAATAAAATGGTAAAGAATAAGGAAG
GAATCTTGAAAGATGCCGAGAGATGGCATGATGCTTTCAAGATTCCAGCAAGGAAG
ATTGGTGTTGCGGGTACACCAAAGCTCAACTTCTATGATATTGATTTTGGGTGGGGG
AAGCCGCAAAAGAATGAAACTATTTCGATTGATTATAACGGTTCGGTTGCTATAAAT
GCAAGCAAAGAATCAACACAAGATTTTGAAATTGGATTGTGTTTTTCAAATATGCAA
ATGGAGGCGTTTGCTGATATCTTTAATCACGGATTAGAGAGTGAGATATAACTCGAG
CACCACCACCACCACCACTGAGATCCGGCTGCTAACAAAGCCCGAAAGGAAGCTGA
GTTGGCTGCTGCCACCGCTGAGCAATAACTAGCATAACCCCTTGGGGCCTCTAAACG
GGTCTTGAGGGGTTTTTTGCTGAAAGGAGGAACTATATCCGGATTGGCGAATGGGAC
GCGCCCTGTAGCGGCGCATTAAGCGCGGCGGGTGTGGTGGTTACGCGCAGCGTGACC
GCTA

The End